The cln-3 genes of Caenorhabditis elegans : making C. elegans models for Juvenile Neuronal Ceroid Lipofuscinosis.

Voer, G. de

The *cln-3* genes of *Caenorhabditis elegans*

Making *C. elegans* models for Juvenile Neuronal Ceroid Lipofuscinosis

The *cln-3* genes of *Caenorhabditis elegans*

Making *C. elegans* models for Juvenile Neuronal Ceroid Lipofuscinosis

Proefschrift

ter verkrijging van

de graad van Doctor aan de Universiteit Leiden,

op gezag van Rector Magnificus prof.mr. P.F. van der Heijden,

volgens besluit van het College voor Promoties

te verdedigen op donderdag 24 januari 2008

klokke 13:45 uur

door

Gert de Voer

geboren te Almelo

in 1973

PROMOTIECOMMISSIE

Promotor	Prof. Dr. G.J.B. van Ommen
Co-promotores	Dr. P.E.M. Taschner Dr. D.J.M. Peters
Referent	Dr. G. Jansen *Erasmus Medisch Centrum te Rotterdam*
Overige leden	Prof. Dr. L. Peltonen *University of Helsinki*

The printing of this thesis is financially supported
by De Jurriaanse Stichting and Genzyme Europe B.V.

"People demand freedom of speech to make up

for the freedom of thought which they avoid"

SOREN AABYE KIERKEGAARD *(1813-1855)*

Thesis design and lay-out Chubaloo, Voorburg
Print PrintPartners Ipskamp, Enschede

ISBN 978-90-9022642-2

The *cln-3* genes of *Caenorhabditis elegans*. Making *C. elegans* models for Juvenile Neuronal Ceroid Lipofuscinosis.

January 24, 2008

The *cln-3* genes of *Caenorhabditis elegans*

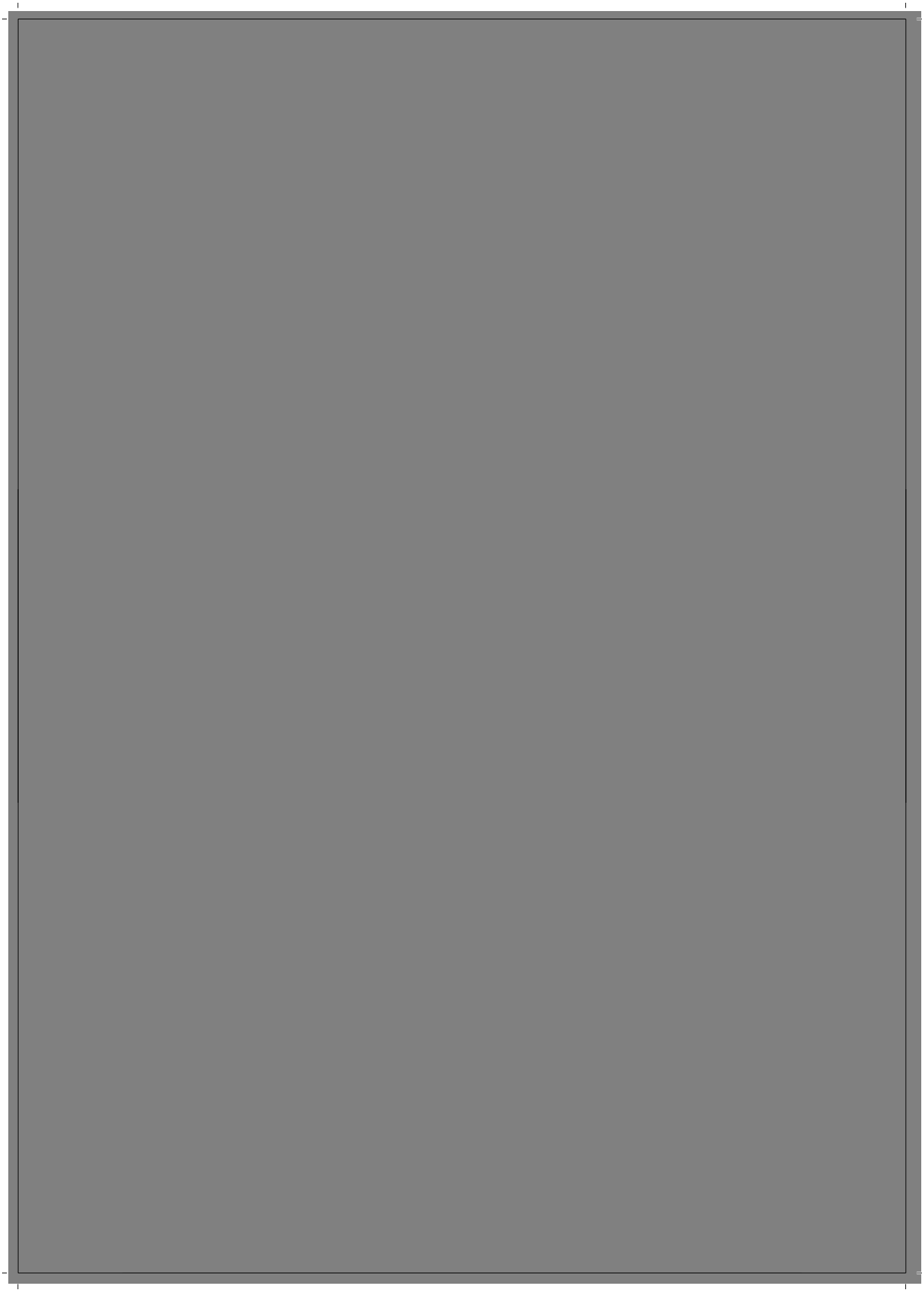

CHAPTER 1

Introduction

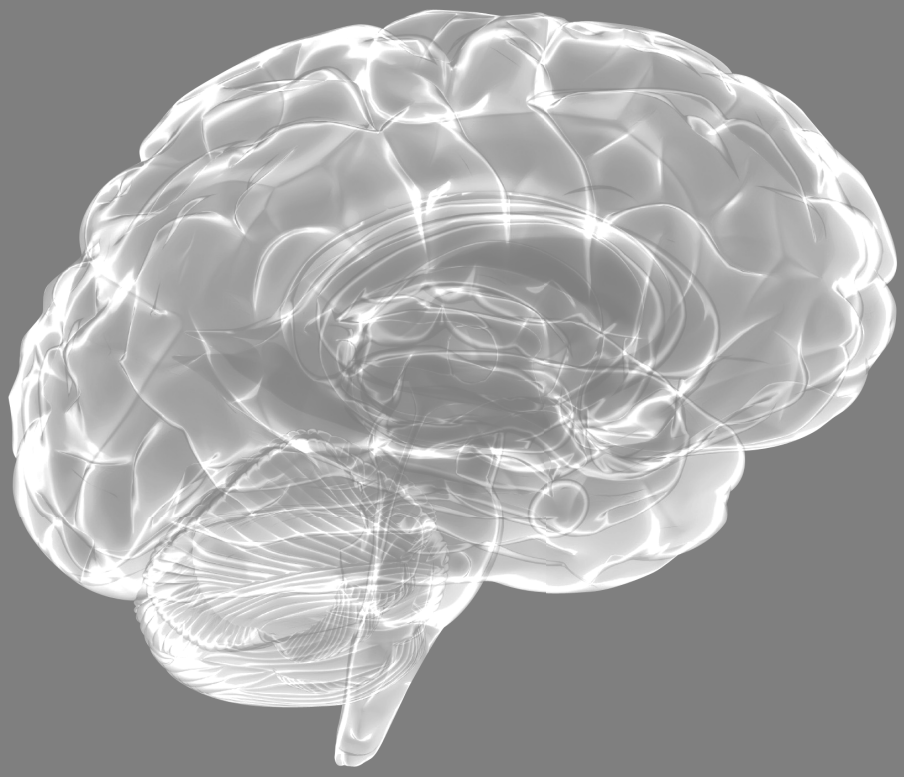

Table of Contents

1 Juvenile Neuronal Ceroid Lipofuscinosis

1.1 Clinical features

Juvenile Neuronal Ceroid Lipofuscinosis (JNCL, MIM 204200) is a severe autosomal recessive hereditary neurodegenerative disorder (reviewed in Rapola, 1993). It is the juvenile form of the most common lysosomal storage disorders of childhood, the neuronal ceroid lipofuscinoses (NCLs). This lysosomal storage disease (LSD) is also called Batten, Spielmeyer and Vogt disease, or Batten disease. Patients suffer from gradual decline of the nervous system, starting at an early age. The first symptom, loss of vision, becomes apparent between four and nine years of age. Ocular fundi show macular degeneration, optic atrophy, and retinal degeneration. Symptoms progress to generalized or complex partial type epileptic seizures, psychomotor deterioration, followed by dementia and a vegetative state, and patients eventually die usually between 20 and 40 years (Goebel *et al.*, 1999). This disease is distributed worldwide and has an incidence of 1,45 in 100 000 births. In patient cells accumulation of lipopigments can be found. These accumulations resemble the pathogenic pigment ceroid and the age pigment lipofuscin in their autofluorescent and staining characteristics, although chemically and ultrastructurally different. Stored materials can be found in lysosomes of a variety of cells and tissues, although only neurons appear to be pathologically affected. Most of the lipopigment accumulations have typical fingerprint profiles when observed using electron microscopy (Figure 1), and were found to mainly consist of Subunit c of the mitochondrial ATP synthase (Wisniewski *et al.*, 1988, Palmer *et al.*, 1992).

1.2 Positional cloning of the *CLN3* gene

Linkage analysis was used to map the JNCL locus to chromosome 16, by demonstration of linkage to the haptoglobin locus. A collaboration of researchers performed linkage analysis with microsatellite markers to define flanking markers. This was followed by haplotype analysis and cosmid walking, which resulted in identification of the cosmid that contained the microsatellite locus *D16S298* for which most JNCL disease chromosomes carry allele 6. Trapped exons of this cosmid were used to screen a fetal brain cDNA library for candidate transcripts, eventually yielding a clone of which the exons were found to flank the microsatellite locus. The cDNA was found to be a transcript of the *CLN3* gene, mutations in which are causative of JNCL (IBDC, 1995, MIM 607042). The most common mutation detected in the *CLN3* gene of Batten disease patients is a 1,02 kb deletion on genomic sequence level, which corresponds to 217 bp of cDNA sequence. Due to this deletion exons seven

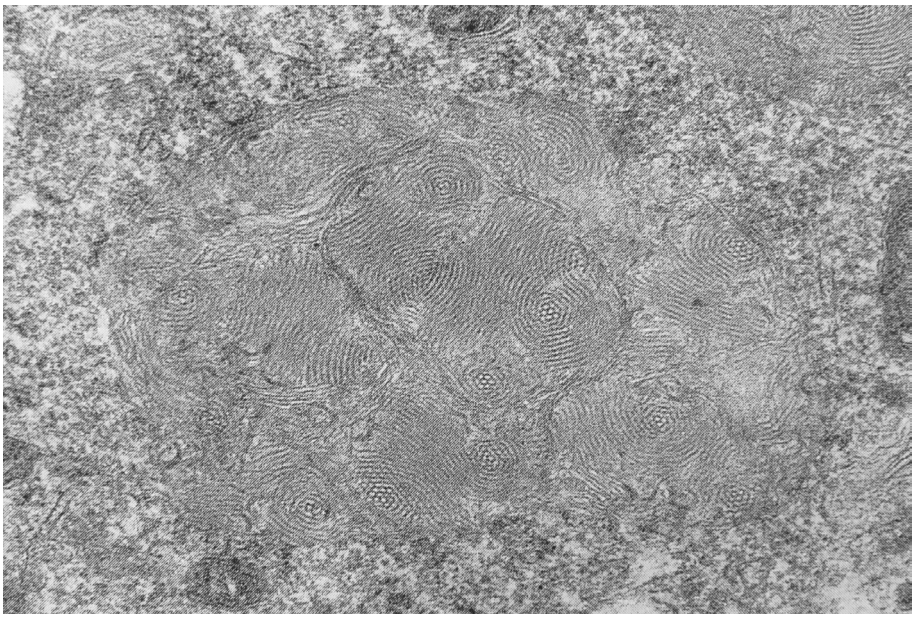

Figure 1 Pure fingerprint body, typical of juvenile NCL (*CLN3*), X 75000. Fingerprint bodies consist of alternating electron lucent, and dense paired parallel lines. The origin of this material is not certain, however, the frequent merging with the lysosomal matrix may indicate lysosomal origin, and this matrix may play a role in the typical fingerprint organization of the stored material. The intervening line may vary considerably in width, sometimes appearing as a mesh of unorganized single membranes that somewhat resemble fingerprint lamellae. Pure fingerprint bodies can be found in neurons of the peripheral nervous system in classic JNCL, Finnish variant NCL (*CLN5*), and in the variant late infantile/early juvenile NCL (*CLN6*). *(from The Neuronal Ceroid Lipofuscinosis (Batten disease); Biomedical and Health Research, Volume 33, H.H. Goebel, S.E. Mole, and B.D. Lake, IOS press)*

and eight are deleted, which probably leads to a truncated protein of 181 amino acids, consisting of the first 153 residues of the CLN3 protein and 28 novel amino acids (IBDC, 1995). 85% of JNCL disease chromosomes carry this mutation, which is in linkage disequilibrium with *D16S298* allele 6. Other mutations in the *CLN3* gene cause similar pathology, although a protracted disease course was observed for one mutation (Mole *et al.*, 2001). Delayed progression has been described for some genotypes, but on the other hand this might be caused by the common phenotypic variability that also is present in JNCL patients, and probably modulated by modifier genes and environmental influences (Mole *et al.*, 1999).

1.3 The *CLN3* gene and protein

The *CLN3* gene was mapped to locus 16p12.1, and contains 15 exons, spanning 15 kb of genomic sequence (IBDC, 1995). The cDNA sequence consists of 1689 bp and contains an open reading frame of 1314 bp, which is predicted to encode a 438 amino acid protein with a molecular mass of 48 kDa, with many post-translational modification sites, such as N-glycosylation sites, phosphorylation sites, and myristoylation sites, and has at least five transmembrane spanning domains (Phillips *et al.*, 2005).
The CLN3 protein is conserved throughout most eukaryotic organisms, suggesting that its function is of fundamental importance for the eukaryotic cell (Taschner *et al.*, 1997). Comparing protein sequences shows several nearly completely conserved regions throughout the eukayote phylogeny (De Voer *et al.*, 2001). The conservation of these regions suggests they are essential for protein function. In the CLN3 protein sequence no other domains could be recognized. All nine missense mutations found in *CLN3* affect residues conserved across species as dog, mouse, rabbit, the nematode *C. elegans*, the fruit fly *Drosophila melanogaster*, and yeast (NCL mutation database, http://www.ucl.ac.uk/ncl).

2 Lysosomes, operation/activity

2.1 Lysosomes and disease

Lysosomes, the cells degradation compartments, were first identified by De Duve in 1949 and in his review paper of 1963 lysosomes were already hypothesized to be involved in pathogenic mechanisms in a number of ways. Indeed, lysosomes were found to be involved in many disorders and in the future may be discovered to play a role, one way or another, in other diseases (Futerman and Van Meer, 2004, Vellodi *et al.*, 2005). Research into the etiology of lysosomal disease has elucidated mechanisms concerning formation, degradation and secretion and recycling of lysosomal compartments and components. This better understanding of common lysosomal processes may eventually lead to the development of treatments of diseases caused by lysosomal defects.

2.2 Lysosomes function in degradation

Lysosomes are dynamic membrane bound organelles essentially containing hydrolytic enzymes in an acidic internal environment in which digestion takes place (Bainton, 1981). After completion of the degradation process vesicles may bud off the lysosomes to secrete the left-over debris, recycle the lysosomal enzymes, or possibly take up the building blocks that result from the break-down process and use them in anabolism. It is the degradative activity of one of the lysosomal enzymes, acid phosphatase, that led to the discovery of lysosomes. Gentle homogenization of rat liver cells allowed the lysosomes to remain intact, thereby retaining all enzymes inside of the organelle. This caused a rather unexpected decrease of enzymatic acid phosphatase activity, compared to drastic homogenization that disrupted the lysosomal membrane thereby releasing the enzymes and permitting measurement of all acid phosphatase activity (De Duve, 1963). At that time the presence of many other enzymes had been established, altogether allowing degradation of proteins, nucleic acids, and polysaccharides in a slightly acidic environment. Due to the common lytic, or digestive, activities of the enzymes contained by the organelles, they were named “lysosomes”. Currently more than fifty lysosomal acid hydrolases are known, including phosphatases, nucleases, glycosidases, proteases, peptidases, sulfatases, and lipases, functioning in hydrolysis of biological compounds (Bainton, 1981).

2.3 Lysosomal enzymes are transported by multiple routes

The acid hydrolases are lysosomal enzymes that originate from the endoplasmic reticulum and move through the Golgi apparatus where they are glycosylated and prepared for the sorting process (see figure 2 for an overview of transport routes between compartments in the cell). In the *cis*-Golgi network, the mannose residues present on the lysosomal hydrolase precursors are provided with a phosphate completing the mannose 6-phosphate (M6P) marker (Brown *et al.*, 1986). The lysosomal hydrolase precursors with M6P groups progress through the Golgi apparatus and bind M6P receptors at pH 7, which permits M6P-receptor-ligand complex formation, in the *trans*-Golgi network. Multiple M6P receptors bound to their hydrolytic cargo gather in clathrin coated vesicles (CCV) that bud off from the Golgi apparatus and travel through the cytoplasm to engage other vesicles that contain material destined to be degraded. Upon fusion of these vesicles filled with hydrolases with an endosome, the internal pH of the resulting vesicle is lowered thereby releasing the hydrolytic enzymes from their receptors. The empty M6P receptors gather once

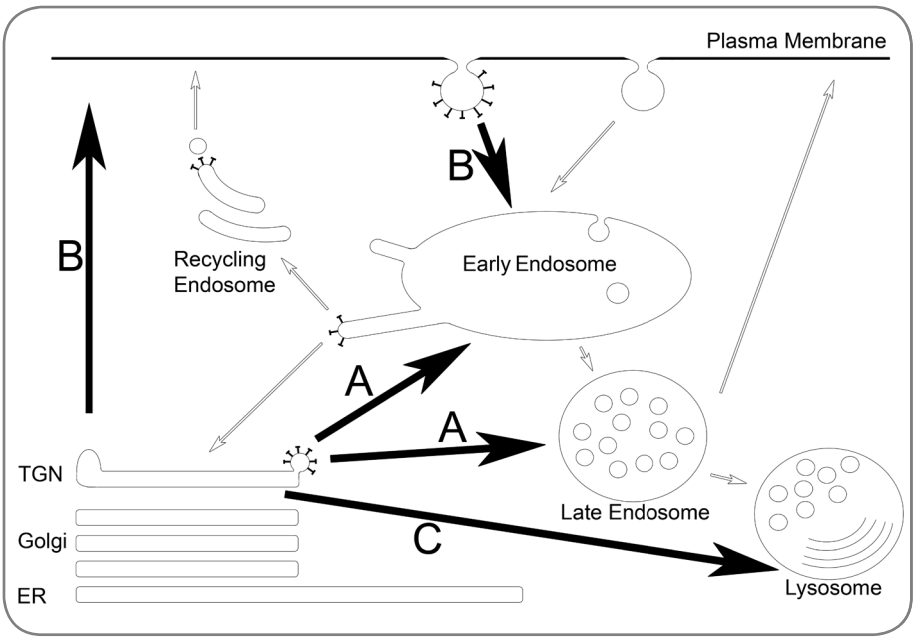

Figure 2 Trafficking pathways between different compartments in the cell

In this scheme the three known transport routes that lysosomal proteins use to reach the lysosome are depicted: A the 'direct' mannose-6-phosphate receptor mediated transport route, by which lysosomal proteins travel to the early or late endosome, B the 'indirect' pathway, by which lysosomal proteins first travel to the plasma membrane followed by their endocytosis, through which they reach the early endosome, C the 'direct' pathway independent of the mannose-6-phosphate receptor. (ER endoplasmic reticulum, TGN *trans*-Golgi network) Adapted from Sachse *et al.*, 2002.

more into a vesicle to bud off from the late endosome and recycle back to the Golgi apparatus where they can again bind the hydrolytic precursors. The late endosome, containing the hydrolytic precursors but not the M6P receptors, acidifies to about pH 5 allowing the hydrolytic enzymes to become active and start degradation, although some hydrolytic enzymes are expected to be at least partially active in late-endosomes. It should be noted however, that the M6P-receptor transport route is not the sole pathway by which hydrolytic enzymes are transported to lysosomes. The membrane-bound precursor of lysosomal acid phosphatase (LAP), for example, is transported to the plasma membrane. After endocytosis, the precursor is translocated to the lysosome, in which proteolysis cleaves the precursor from the membrane-bound part releasing the soluble LAP (Suter *et al.*, 2001). In addition, transport of the lysosomal aspartyl protease cathepsin D to lysosomes can be independent of M6P residues as was shown in hepatocytes (Rijnboutt *et al.*,1991). In cultured lymphoblastoid cells from I-cell disease patients phosphotransferase activity is absent, but cathepsin D can be identified in dense lysosomes (Glickman and Kornfeld, 1993). Mannose-6-phosphate deficient mice also have cathepsin D targeted to their lysosomes, although this was cell-type specific (Dittmer *et al.*, 1999). Thus, hydrolytic enzymes use multiple routes to travel to lysosomes in cell-type specific manner, and we can not exclude the existence of other yet undiscovered lysosomal transport routes.

2.4 The lysosome has a characteristic bounding membrane

Another striking characteristic of the lysosome is its degradation-resistant bounding membrane, separating and thereby controlling degradation and protecting the cytoplasm from the potentially deleterious lytic mixture of enzymes present inside. This unique membrane has a characteristic phospholipid composition, contains tremendous amounts of carbohydrates and is rich in lysosome-specific membrane proteins with which the lysosome maintains its internal environment (Eskelinen *et al.*, 2003).
Other functions of the resident proteins of the lysosomal membrane include the acidification of the lysosomal internal milieu, translocation of breakdown products for reuse, and vesicular fusion and fission. Lysosomal membrane proteins are transported from the *trans*-Golgi network to late-endosomes / lysosomes through either direct intracellular trafficking or indirectly via the plasma membrane. Adapter protein-3 (AP-3) is involved in direct trafficking of some lysosomal membrane proteins, whereas other heterotetrameric and monomeric adapter proteins are likely to play similar roles in the indirect pathway (Luzio *et al.*, 2003).

2.5 Lysosomes and endocytosis

Cells use endocytosis for uptake of extracellular macromolecules that subsequently will be transported to lysosomes for degradation. Phagocytosis, or cell eating, is mainly performed by specialized cells such as macrophages or neutrophils that aid in

neutralization of large pathogens and clear out cellular debris (Aderem and Underhill, 1999). In contrast, pinocytosis, or cell drinking, is a more general mechanism existing in different forms: macropinocytosis, caveolin- or clathrin-mediated endocytosis, or clathrin- and caveolin-independent endocytosis, in which lipid rafts presumably are involved and probably comprise more than one pathway (Conner and Schmid, 2003). The best understood form is clathrin-mediated endocytosis (CME), in which clathrin-coated vesicles with their receptor-bound macromolecular ligands form at the plasma membrane, and travel through cytoplasm to encounter and deliver their cargo to vesicles containing hydrolytic enzymes. Different hypotheses explain how material taken up by endocytosis eventually arrives in lysosomal compartments (Luzio *et al.*, 2003). For example, vesicle maturation presumably takes place in endosomes, as the receptors release their ligands destined to be degraded and return to the plasma membrane, and hydrolytic enzymes are introduced (Murphy 1991, Mellman and Warren, 2000). All proposed mechanisms may be intertwined. Vesicular traffic may carry the receptors back to the plasma membrane or *trans*-Golgi network (Mellman and Warren, 2000), and kiss-and-run occurrences may deliver hydrolytic enzymes to endosomes (Storrie and Desjardins, 1996, Bright *et al.*, 2005). Moreover, direct fusion between lysosome and endosome yielding a hybrid organelle also was shown to occur (Mullock 1998). The whole biological process of endocytosis may actually comprise a mixture of all proposed models with other complementary mechanisms to be discovered.

2.6 Secretion and recycling

Lysosomes are at the end of the endo-lysosomal pathway and a terminal degradative stage for most of the internalized materials, but these compartments should not be considered as dead-end organelles (Bainton, 1981). Most of the specific lysosomal components, e.g. hydrolytic enzymes, can be recycled and the breakdown products can be secreted or reused as building blocks (Luzio *et al.*, 2003). The recycling of endosomal markers, such as M6P receptors, to the *trans*-Golgi network is thought to occur mostly from endosomes as late-endosomes contain relatively small quantities of them. Other lysosomal transport routes certainly exist: cholesterol transport from late endosomes to the *trans*-Golgi network is modulated by the integral membrane protein NPC1 (Liscum, 2000). Transport of lysosomal contents can be studied in specialized cells, e.g., osteoclasts, cytotoxic T cells, and natural killer cells, which contain secretory lysosomes that are characterized by their dual function in degradation and secretion (Blott and Griffiths, 2002). Secretory lysosomes resemble conventional lysosomes in their structural diversity, acid hydrolytic contents, and ability to fuse with the plasma membrane, e.g. lysosomes are thought to be involved in membrane repair processes (Andrews, 2000). Regulated secretion by secretory lysosomes involves several distinct steps stimulated by a mostly external signal, causing the mobilization of the granules and transport to the site of stimulation, followed by docking and release of its contents.

3 Lysosomal storage diseases

3.1 Introduction

Genetic lesions affecting any aspect of the lysosomal processes described above may result in metabolic diseases caused by abnormal lysosomal function (Scriver *et al.*, 2001). Logically, when an acid hydrolase does not perform correctly the substrate will not be degraded, and will most likely accumulate and subsequently may disrupt the other processes that were proceeding in the organelle. Suboptimal performance of acid hydrolases can have various causes, e.g. mutations in the gene encoding the enzyme, incorrect trafficking of the enzyme or other requirements for degradation, such as co-enzymes or transporters, or suboptimal maintenance of the environment in which the enzyme is supposed to operate. Incorrect functioning of lysosomes may indirectly cause depletion of compounds used in anabolism, since lysosomes also play a role in recycling of cellular building blocks. Additional effects may arise when accumulated substances cause lysosomes to become enlarged and inflexible, possibly clogging the cell. Such a relatively small cellular defect may have devastating effects on the whole organism.

Review of the currently known LSDs and their causes makes clear that the majority is caused by lysosomal acid hydrolase defects, leading to the accumulation of their substrates. Therefore, enzyme replacement therapy (ERT) could be a possible approach to improve the quality of life of patients suffering from these diseases. Pompe and Gaucher disease patients, e.g., were shown to have significant improvements in quality of life during and after enzyme replacement therapy (Beck, 2007). The other group of LSDs consists of disorders that are caused by multiple different underlying defects: affected enzyme trafficking or enzyme regulation, abnormal transport of a substrate or reaction product, mutated cofactors leading to dysfunctional enzymes, aberrant vesicle trafficking or biogenesis, and still unknown mechanisms. Cellular metabolism involves many other genes and proteins, some of which may become associated with LSDs in the future. This group probably contains many essential genes and proteins, thus mutations in this group might never be found as they will cause lethality.

A comprehensive overview of detailed descriptions of all LSDs will not be provided in this dissertation, but can be found in Scriver *et al.* (2001). Here I will discuss a few examples of enzyme and alternative defects causative of lysosomal storage, and descriptive of basic lysosomal processes.

3.2 Enzyme defects leading to LSD

3.2.1 Glycogen storage disease

Many LSDs are caused by mutations in genes encoding lysosomal hydrolytic enzymes. The first LSD, in which defects in a degradative lysosomal enzyme were found, was glycogen storage disease type II, also known as acid α-glucosidase, acid maltase deficiency, or Pompe disease (Hers, 1963). This inherited disorder of glycogen metabolism is the result of reduced lysosomal hydrolase acid α-glucosidase activity, causing intralysosomal accumulation of normally structured glycogen in numerous tissues, most markedly in cardiac and skeletal muscle. Classical Pompe disease patients present with prominent cardiomegaly, hypotonia, hepatomegaly, and death due to cardiorespiratory failure, usually before the age of two (Pompe, 1932). After the genetic and metabolic defects were elucidated, varying clinical presentations could be diagnosed, revealing a highly variant disease progression, including degrees of myopathy, age of onset, and extent of organ involvement. Mild acid α-glucosidase deficiency presents as late as the sixth decade of life with slow progressive proximal myopathy, only in skeletal muscle. Enzyme activity is measured to confirm clinical diagnosis, and generally correlates to severity of the disease. Identification and characterization of the gene involved in this disease allowed DNA analysis for carrier detection and additional diagnostic means. The gene was designated acid alpha-1,4-glucosidase (GAA), and was found to encode an extensive posttranslationally modified 952 amino acid protein, in which multiple mutations have been identified (Hirschhorn and Reuser, 2001).

The effects of enzyme replacement therapy by intravenous infusion of recombinant human acid α-glucosidase were investigated. From an initial clinical trial could be concluded that the patients tolerated the infusions well, moreover, the patients heart size decreased, cardiac function could be maintained for more than one year, and the patients survived over the critical age of one year. In addition to the continued normal cardiac function, skeletal muscle function improved and muscle biopsies were used to show a dramatic decrease in glycogen accumulation in muscle cells (Amalfitano *et al.*, 2001). In another study recombinant human acid α-glucosidase that was isolated from milk from transgenic rabbits was intravenously injected in four classic infantile Pompe disease patients (Winkel *et al.*, 2003). After 72 weeks of treatment all patients had normal acid α-glucosidase activity in muscle cells, while the glycogen concentration decreased only in the least affected patient. Furthermore, after treatment all patients were in a better clinical condition, but only in the least affected patient substantial improvement of the muscle architecture was observed. All patients were alive after four years of treatment and the least affected patient achieved motor milestones comparable to a normal child (Van den Hout *et al.*, 2004). The variability of the response to acid α-glucosidase injection was suggested to depend on the degree of glycogen storage at the start of the treatment, thus for the treament to have optimal effect it has to be started as early as possible. A three year treatment of three patients suffering from juvenile Pompe's disease with infusion of acid α-glucosidase isolated from rabbit milk resulted in improved muscle strength, most prominently in the youngest patient that abandoned

his wheelchair after two years of treatment. Quality of life had increased for all three patients after treament (Winkel *et al.*, 2004). In overview of the ERTs can be stated that treatments with recombinant acid α-glucosidase have demonstrated the safety and efficacy for ameliorating the condition of infantile and juvenile Pompe's disease patients, indicating similar treatments might also be effective in other diseases caused by lysosomal hydrolytic enzyme defects.

3.2.2 Glycogen storage disease type IIb, Danon disease

Another form of glycogen storage disease is glycogen storage disease type IIb, a disorder characterized by prominent cardiac abnormalities, involvement of skeletal muscle, and variable mental retardation. This disease is also known as Danon disease, and was found to be caused by mutations in the *LAMP-2* gene, encoding the lysosome associated membrane protein-2 (Hirschhorn and Reuser, 2001). Although a definitive protein function has to be established, the protein is thought to be involved in protecting the lysosomal membrane from intralysosomal proteolytic enzymes, and in protein import into lysosomes, using its receptor function (Sugie *et al.*, 2002). Currently, no therapy is available but cardiac problems could be ameliorated by inserting pacemakers (Charron *et al.*, 2004).

3.2.3 Gaucher's disease

The lysosomal glycolipid storage disorder in which glucosylceramide or glucocerebroside is accumulated is called Gaucher's disease. There are three subtypes of this disorder (Beutler and Grabowski, 2001, Grabowski, 2005). Type 1 is the most common form, and type 1 patients have no primary nervous system symptoms, whereas the acute type 2 and subacute type 3 forms are neuronopathic. In Gaucher disease patients lysosomal accumulation of glucosylceramide leads to hepatosplenomegaly, anemia, and bone disease. Neurological symptoms, for the type 2 and 3 forms, at the onset of the disease include strabismus and other eye abnormalitites, for type 2 this starts early in life and progresses into severe neuronal disease and death usually before the patient is 2 years old. Whereas, type 3 patients have a later onset and neuronal symptoms may include progressive intellectual impairment, mental retardation, and myoclonic seizures. This disease is caused by mutations in the gene encoding acid β-glucosidase (Tsuji *et al.*, 1988). A possible therapy for this defective lysosomal hydrolase may be introduction of correct acid β-glucosidase or inhibition of the substrate of the hydrolase.
Gaucher disease type 1 patients can be treated with ERT. A patient that was treated with human placental glucocerebrosidase had increased hemoglobin levels and platelet counts, decreased phagocytic activity in the spleen and improved skeletal structure (Barton *et al.*, 1990). Recombinant forms of glucocerebrosidase, alglucerase or later imiglucerase, were produced by Genzyme corporation to enable production of sufficient enzyme to treat many more patients. Evaluation of long-term ERT indicates that imiglucerase infusions comprise a safe treatment of Gaucher disease (Starzyk *et al.*, 2007). Other therapies, such as gene therapy, chaperone therapy, substrate reduction therapy and bone marrow transplantation, are also under investigation to find a cure for all forms of the disease.

3.3 Affected cofactors, and coactivators of hydrolytic enzymes

3.3.1 Variant metachromatic leukodystrophy

Hydrolytic enzymes use coactivators and cofactors to proceed with degradation. Mutations in genes encoding the coactivators and cofactors were also found to be causative of LSDs. This is exemplified by the LSDs variant metachromatic leukodystrophy (MLD) and G_{M2} gangliosidoses, which can be caused by affected coactivator proteins. Variant MLD is caused by mutations in the gene encoding prosaposin, a sphingolipid activator protein (SAP) that exist in multiple forms (Rafi *et al.*, 1990). These non-enzymatic co-factors aid arysulfatase A in the lysosomal degradation of sphingolipids. Patients with defective prosaposin may have disease symptoms similar to juvenile MLD that present between 4 years of age and puberty, with gait disturbances and mental regression, while lysosomal hydrolase arysulfatase A activity, which is affected in MLD is normal (Wrobe *et al.*, 2000, Von Figura *et al.*, 2001). Additional clinical symptoms can be blindness, loss of speech and seizures. Retro-viral re-introduction of the correct prosaposin gene in cultured cells of a variant MLD patient restored SAP-1 protein levels and metabolism of endocytosed sulfatide (Rafi *et al.*, 1992). In a case report of a two year old patient that was treated with bone marrow transplantation and clinically followed for three years the patient initially transiently deteriorates, followed by improvement of peripheral nervous system functions, however, eventually the patient condition worsened, thus at present treatment of variant MLD is not possible (Landrieu *et al.*, 1998).

3.3.2 G_{M2} gangliosidoses

The G_{M2} gangliosidoses are caused by defective degradation of ganglioside G_{M2}, leading to its accumulation (Gravel *et al.*, 2001). This neurodegenerative disease is clinically variable: the most severe form, classical Tay-Sachs disease, presents with early developmental retardation, paralysis, dementia, and death usually in the second or third year of life. Other forms of this disease may display a protracted disease course of the neurological symptoms. Lysosomal G_{M2} ganglioside hydrolysis is modulated by β-hexosaminidase, which consists of two protein subunits encoded by the *HEXA* and *HEXB* genes (Neufeld, 1989). Another requirement for effective degradation is G_{M2} ganglioside binding to the G_{M2}/G_{M2} activator. Mutations in any of the genes encoding Hexosaminidase A (of HEXA), Hexosaminidase B, or the activator protein may lead to this disease. Treatment of this disease is not available, although the possibilities of enzyme replacement therapy, bone marrow transplantation, gene therapy and substrate deprivation therapy are currently being investigated.

3.4 Disorders of lysosomal enzyme localization, processing, and protection

3.4.1 I-cell disease and pseudo-Hurler polydystrophy

The mislocalization or misregulation of intact lysosomal enzymes may lead to impaired degradation of internalized compounds. I-cell disease (Mucolipidosis II, ML-II) and pseudo-Hurler polydystrophy (Mucolipidosis III, ML-III) are caused by abnormal transport of lysosomal enzymes due to defects in the *GNPTAB* gene encoding the N-acetylglucosamine-1-phosphotransferase alpha or beta subunit precursor, or *GNPTG* encoding the N-acetylglucosamine-1-phosphotransferase gamma subunit precursor, respectively (Kornfeld and Sly, 2001). After normal modification of lysosomal enzymes with M6P markers in the Golgi apparatus, these enzymes can become targeted to the lysosome by binding M6P-receptors. However, mutations in one of three genes encoding phosphotransferase complex subunits lead to a phosphotransferase that is catalytically active but unable to specifically recognize and bind its substrate, mannose residues of lysosomal enzymes. This results in mistargeting of lysosomal enzymes that can be found in the serum and body fluids of patients. Affected individuals present with progressive psychomotor retardation and premature death, usually in the first decade, although as in all LSDs clinical features may vary in age of onset and severity. Phase dense inclusions were detected in patient cells, which were called inclusion cells, hence the name I-cell disease. Although molecular diagnosis and carrier detection can be performed, definitive treatment is not available.

3.4.2 Multiple Sulfatase Deficiency

Affected sulfatase processing due to mutations in sulfatase-modifying factor-1, *SUMF1* can result in a deficiency of all twelve known sulfatases (Dierks *et al.*, 2003, Cosma *et al.*, 2003). Sulfatases require post-translational generation of α-formylglycine residues, which presumably have a function in sulfate ester cleavage and this modification step is partially mediated by sulfatase-modifying factor-1. Incomplete formation of α-formylglycine residues on sulfatases was found to affect sulfatase processing. Multiple sulfatase deficiency clinically resembles Metachromatic Leukodystrophy, which is caused by affected enzymatic activity of arylsulfatase A or non-enzymatic saposin B. The clinical presentation and disease progression are variable for both disorders. Patients generally first present themselves with gait disturbance and mental regression. Subsequently, childhood variants usually display blindness, loss of speech, and seizures, whereas adult variants present themselves with behavioral disturbance and dementia. Diagnosis is performed biochemically and prenatal diagnosis and carrier detection is reliable. There is no treatment for patients suffering from this disease.

3.4.3 Galactosialidosis

Transport of lysosomal enzymes β-galactosidase and neuraminidase to the lysosome and protection against intralysosomal degradation is mediated by normal protective protein/cathepsin A (CTSA) that is associates with these enzymes. Additional

CTSA functions comprise cathepsin A/deaminase/esterase activities on a subset of neuropeptides at both acidic and neutral pH. Mutations in the gene encoding CTSA were found to be involved with galactosialidosis, a lysosomal storage disorder in which sialyloligosaccharides accumulate in lysosomes and are excreted in body fluids (Zhou *et al.*, 1996, d'Azzo *et al.*, 2001). This disease is clinically heterogeneous, but most common features include dysmorphism, skeletal dysplasia, visceromegaly, cardiac and renal involvement, progressive neurologic manifestations, ocular abnormalities, angiokeratoma, and early death. Phenotypic variance and different age of onset distinguish three galactosialidosis subtypes, early infantile, late infantile, and juvenile/adult. Biochemical diagnosis, in patients and prenatal, is performed by demonstrating combined β-galactosidase/neuraminidase deficiency. Disease therapy is not present, but in *Ctsa* knockout mice systemic organ pathology can be fully corrected by bone marrow transplantation from mice overexpressing human CTSA in hematopoietic lineages (d'Azzo *et al.*, 2001), possibly providing for treatment of patients in the future.

3.5 Disorders caused by aberrant substrate or product transport

3.5.1 Niemann-Pick disease type C

Niemann-Pick disease type C is caused by defects in cellular trafficking of cholesterol (Schuchman and Desnick, 2001). Mutations in the *NPC1* gene, encoding a protein containing multiple transmembrane and a sterol-sensing domain, mostly cause progressive neurologic disease, occasionally accompanied by severely affected liver tissue and lethality. Age of onset and clinical presentation are highly variable. The diagnosis is based on the clinical presentations together with neurophysiological tests and tissue biopsies and can be confirmed by analyzing characteristic cholesterol staining patterns and measuring cholesterol esterification. Although symptomatic treatment of some of the accompanying clinical features is possible, disease progression can not be altered.

3.5.2 Nephropathic Cystinosis

Mutations in the *CTNS* gene, encoding cystinosin, which transports cystine out of lysosomes, leads to lysosomal accumulation of cystine in several tissues (Anikster *et al.*, 1999). The most affected organs are the kidneys, which malfunction and continuously waste water and nutrients. As a result, a failure to thrive, polyuria, dehydration, hypophosphatemic rickets, hypokalemia, and acidosis are observed as the earliest symptoms, with other symptoms appearing later in life. Patients can be treated with cysteamine, which enters the lysosomes and converts cystine thereby permitting depletion of 95% of the cells cystine content. This treatment preferably is initiated as early as possible in life of the patient, in order to minimalize kidney damage and to achieve normal growth rates (Gahl, 2003).

3.5.3 Infantile sialic acid storage disorder (ISSD) and Salla disease

Impaired sialic acid transport was found to be the cause for infantile sialic acid storage disorder and Salla disease (Wreden *et al.*, 2005). Both disorders share similar features, and differ in severity of clinical presentation. ISSD patients display intra-uterine hydrops, neonatal ascites, dysmorphic features, and death by 2 years of age. Salla disease is characterized by developmental delay with marked cognitive and motor impairment noticeable at 6–12 months of age, and patients usually reach adulthood. Mutations were identified in a gene, *SLC17A5*, encoding a transport protein that presumably acts as a symporter transporting protons and sialic acid (Verheijen *et al.*, 1999). Therapy for this disease is not available.

3.6 Disorders caused by affected lysosome biogenesis

3.6.1 Hermansky-Pudlak syndrome

The Hermansky-Pudlak syndromes 1-7 (HPS 1-7) is a group of diseases with characteristic symptoms, including oculocutaneous albinism, loss of visual acuity, prolonged bleeding times due to platelet storage pool deficiency, storage of ceroid, and premature death caused by fibrotic lung disease (Huizing *et al.*, 2001, Li *et al.*, 2004). Mutations in different genes are associated with the various forms of the disease. The *HPS1*and *HPS4* genes, involved in Hermansky-Pudlak syndrome 1 and 4, respectively, encode subunits of a complex, termed BLOC-3 for biogenesis of lysosome-related organelles complex–3 (Dell'Angelica, 2004). *HPS1* and *HPS4* gene products were shown to interact, and together were suggested to regulate late-endosome and lysosome localization, with possibly an additional role in melanosome biogenesis (Nazarian *et al.*, 2003). The *HPS2* gene encodes a subunit of the adaptor protein 3 complex, AP3β1, which is involved with protein transport to lysosomes (Dell'Angelica *et al.*, 1999). HPS3, HPS5, and HPS6 proteins were found to associate in the BLOC-2 complex (Di Pietro *et al.*, 2004), and HPS7 protein was reported to be a member of the BLOC-1 complex (Li *et al*, 2004). It is obvious to assign a function in vesicular biogenesis to each of the BLOC complexes due to the cellular defects observed in tissues from patients and knock-out mice, harboring mutations in *HPS* gene orthologues. Among the affected organelles are melanosomes, lysosomes, and platelet dense granules, suggesting particular common aspects in their biogenesis or function (Spritz, 1999B). Patients suffering from this disease can not be treated at present.

3.6.2 Chediak-Higashi syndrome

Chediak-Higashi syndrome (CHS) resembles HPS in the oculocutaneous albinism and platelet storage pool deficiency (Huizing *et al.*, 2001). However, CHS is distinct from HPS, and CHS patients also suffer from abnormally increased susceptibility to infections and a typical accelerated phase, in which patients develop a lymphoproliferative syndrome (Spritz, 1999A). Mutations in the *LYST* gene, lysosomal trafficking regulator, were found in CHS patients (Karim *et al.*, 1997). The LYST protein may be involved in the sorting of endosomal resident proteins into

late multivesicular endosomes (Introne *et al.*, 1999, Zarzour *et al.*, 2005). Patients can be treated with stem cell therapy before the accelerated phase has been reached, decreasing their susceptibility to infections. Neurological complications, however, can not be reversed.

3.6.3 Mucolipidosis type IV

Mucolipidosis type IV (MLIV) clinically presents with psychomotor deterioration, ophthalmological abnormalities, and premature death. Lysosomal hydrolase activity and trafficking appeared intact for this lysosomal storage disorder (Chen *et al.*, 1998). Markers for endocytosis were used to show that MLIV fibroblasts were affected in their rate of efflux from the lysosomes compared to wildtype cells, suggesting defects in late endosomal-lysosomal transport. In MLIV patients mutations in *MCONL1* were found as a cause for their disease (Bargal *et al.*, 2000). The MCOLN1 protein, mucolipin-1, was shown to be a Ca^{2+}-permeable cation channel that is transiently modulated by changes in intracellular calcium (LaPlante *et al.*, 2004). This suggests that calcium traffic and distribution in the cell is impaired, which could result in abnormal slow and inefficient late endosome-lysosome fusion in MLIV patients, leading to accumulation of lipids and other materials. A cure for this disease is not available at present.

4 The Neuronal Ceroid Lipofuscinoses

4.1 Historical description

The Neuronal Ceroid Lipofuscinoses originally belonged to a group of diseases collectively termed amaurotic familial idiocy (AFI) in 1896 (Rapola, 1993 and references therein). This cohort of diseases contained familial infantile neurological disorders that clinically presented with failure of psychomotor development, blindness, and early death. Although considerable clinical and pathological variance was present, this term has been used until far into the twentieth century and encompassed Tay-Sachs disease, a GM_2-gangliosidosis, besides the NCLs. Despite the important contributions of Batten, Spielmeyer, and Vogt, who described several NCL families early in the twentieth century and at that time made distinctions between NCL and Tay-Sachs, the definitive separation occurred only after description of the ultrastructure of the storage material and identification of GM_2-ganglioside. As the storage material in NCLs could be distinguished from stored materials found in other diseases and resembled ceroid and lipofuscin in staining characteristics, the term 'Neuronal Ceroid Lipofuscinosis' was introduced, obviously also bearing the neurological pathology in mind.

4.2 The different forms of NCL

The NCLs can be distinguished by age of onset of the first symptom, although for each form of NCL starting age can be variable, by ultrastructure of the stored material, and by causative gene (Goebel *et al.*, 1999, Wisniewski *et al.*, 2001b). An overview of the different forms of NCL and some of their characteristics is shown in Table 1 on the next page.

4.2.1 Infantile NCL, *CLN1*

Children suffering from the infantile form of NCL (INCL, Haltia-Santavuori disease) usually lose their eye-sight between six months and two years of age. Ultrastructural analysis, using electron micrographs, of INCL storage bodies revealed the so-called granular osmiophilic deposits (GRODs). INCL is caused by mutations in the *CLN1* gene, encoding a lysosomal enzyme, palmitoyl protein thioesterase (PPT). Dysfunctional PPT causes accumulations mainly consisting of the very hydrophobic saposins A and D.
In the other NCLs different ultrastructural storage patterns are observed and the main component of the stored material is Subunit c of the mitochondrial ATP synthase. The variability of the characteristic starting age of infantile NCL is demonstrated by the adult age of onset, 31 and 38 years, in two INCL patients that had mutations in the *CLN1* gene and had decreased palmitoyl-protein thioesterase activity (Van Diggelen *et al.*, 2001).

Table 1 An overview of the different NCL forms and some characteristics

Disease type	Gene symbol	Eponym	Genomic location	OMIM	Protein	Age of onset	EM storage profile	Inheritance
Infantile NCL	*CLN1*	Haltia-Santavuori	1p32	256730	Palmitoyl protein thioesterase I, lysosomal	0,1 - 38	GROD	autosomal recessive
Late infantile NCL	*CLN2*	Jansky-Bielschowsky	11p15	204500	Tripeptidyl peptidase I, lysosomal	2 - 8	CV, mixed	autosomal recessive
Juvenile NCL	*CLN3*	Batten-Spielmeyer-Vogt	16p12	204200	CLN3 lysosomal transmembrane protein	4 - 10	FP, mixed	autosomal recessive
Adult NCL	*CLN4*	Kufs	*not known*	204300	*not known*	11 - 55	FP, granular	autosomal recessive (1)
Finnish variant late infantile NCL	*CLN5*		13q31-32	256731	CLN5 lysosomal membrane protein	4 - 7	FP, CV, RL	autosomal recessive
Variant late infantile, early juvenile NCL	*CLN6*	Lake-Cavanagh	15q21-23	601780	CLN6 endoplasmic reticulum membrane protein	1,5 - 8	CV, FP, RL	autosomal recessive
Turkish variant late infantile NCL	*CLN7*		*not known*	600143	*not known*	1 - 6	RL, FP	autosomal recessive (2)
Turkish variant late infantile NCL, Northern epilepsy	*CLN8*		8p23	600143	CLN8 endoplasmic reticulum membrane protein	5 - 10	CV or GROD like	autosomal recessive
CLN9 deficiency	*CLN9*		*not known*	609055	unknown protein involved in dihydro-ceramide synthase pathway	4	FP, CV, GROD	autosomal recessive (2)
Congenital NCL	*CLN10*		11p15.5	610127	Cathepsin D, lysosomal	0	GROD	autosomal recessive (2)

Abbreviations: GROD: granular osmiophilic deposits, CV: curvilinear, FP: fingerprint, RL: rectilinear

(1) The majority of Adult NCL is autosomal recessively inherited, some cases of autosomal dominant inheritance have been described as Parry disease

(2) Most probable mode of inheritance as shown with pedigree, segregation or linkage analysis

4.2.2 Late infantile NCL, *CLN2*

The late infantile form of NCL (LINCL, Janský-Bielschowsky disease) has an average age of onset of seizures, ataxia and myoclonus between two and four years of age. Classical LINCL is caused by mutations in the *CLN2* gene, encoding the lysosomal enzyme tripeptidyl peptidase, and LINCL storage patterns mainly have curvilinear profiles. Three additional genetically distinct variant forms of LINCL are discussed below.

4.2.3 Adult NCL, *CLN4*

The adult form of NCL (ANCL, Kufs disease) is a rare form of NCL, for which the *CLN4* gene has not yet been identified. The diagnosis of ANCL is difficult due to the relatively low frequency of the disease combined with an overlap of clinical features with other diseases. In addition, autosomal dominant and recessive patterns of inheritance have been observed. This suggests that genetic heterogeneity underlies the phenotypical variation observed. The average age at which epilepsy or behavioral changes occur is 30 years, but cases with starting ages from 11 until 60 years have also been described. Consistent with genetic heterogeneity, the storage patterns in ANCL are also variable: all storage profiles observed in other types of NCL can be found in ANCL patient tissues.

4.2.4 Finnish variant late infantile NCL, *CLN5*

Three other variant forms of LINCL could be reclassified due to mapping to alternative loci or alternative disease characteristics. The first form, Finnish variant late infantile NCL (Finnish LINCL), is caused by mutations in the *CLN5* gene, which encodes a transmembrane protein with unknown function (Savukoski *et al.*, 1998). This variant form of NCL originally was described in patients from Finland and later also found in other countries (Santavuori *et al.*, 1991, Pineda-Trujillo *et al.*, 2005). The first symptoms, slight motor clumsiness and muscular hypotonia, become apparent between 4.5 and 6 years of age. Multiple storage pattern profiles are also found when performing ultrastructural analysis on tissues of Finnish LINCL patients.

4.2.5 Variant late infantile-early juvenile NCL, *CLN6*

Variant late infantile-early juvenile NCL patient tissues shared features of late infantile and juvenile NCLs, and could only be distinguished from other NCLs when the causative gene, *CLN6*, was mapped. Recently, the *CLN6* gene has been cloned and was found to encode a transmembrane protein (Gao *et al.*, 2002). Patients suffer from motor delay and seizures starting between 18 months and 8 years of age, and just less than half of the patients clinically appear similar to classic LINCL, although distinguishable using electron microscopy, since a mixture of fingerprint, curvilinear, and rectilinear profiles is present in patient lysosomes. This variant late infantile form differs subtly from classical late infantile NCL, in that the storage material also was present as fingerprint profiles, in addition to the curvilinear profiles predominantly found in classical LINCL (Williams, *et al.*, 1999).

4.2.6 Turkish variant late infantile NCL, *CLN7* - Northern Epilepsy, *CLN8*

Turkish variant late infantile NCL and Northern Epilepsy or progressive epilepsy with mental retardation (EPMR) initially were thought to be genetically distinct disorders, due to their predominance in different populations, Turkish and Finnish, respectively. However, mutations in *CLN8*, the gene involved in Northern Epilepsy, were also found in Turkish variant LINCL patients, although not all patients were homozygous for the used marker alleles (Ranta *et al.*, 2004, Ranta *et al.*, 1999). Clinically, both diseases can clearly be distinguished: Turkish variant LINCL patients display typical NCL symptoms, starting between one and six years of age with seizures, motor impairment, mental retardation and loss of vision. Storage patterns are either fingerprint or curvilinear-fingerprint mixture profiles in the Turkish variant. Northern Epilepsy, on the other hand, presents between five and ten years of age with seizures and mental retardation, while loss of vision is absent and clinical progression is slower. Mainly curvilinear storage patterns are detected by ultrastructural analysis. In the two distinct populations different mutations were found in the same gene (Ranta *et al.*, 2004). A clear genotype-phenotype correlation, however, could not be made, and the Turkish patients with *CLN8* mutations could clinically not be distinguished from Turkish LINCL patients without them. A subgroup of the latter patients is assumed to be linked to the unidentified CLN7 locus.

4.2.7 CLN9 deficiency, *CLN9*

The initial characterization of a small group of patients with typical NCL disease characteristics but without mutations in any of the earlier found NCL genes or in any of other lysosomal storage disease gene suggested the existence of another variant of juvenile NCL (Schulz *et al.*, 2004). Cultured patient cells used to analyse the defect underlying CLN9 had a decreased dihydroceramide synthase activity, which could be partially rescued by introducing other genes that increase the activity of the dihydroceramide synthase pathway (Schulz *et al.*, 2006). These results indicate that the CLN9 protein may be involved in the dihydroceramide synthase pathway, although the gene causing this disease has not been identified.

4.2.8 Congenital NCL, *CTSD*

The gene involved in congenital ovine NCL was identified more than five years ago as the sheep *CTSD* gene encoding Cathepsin D (Tyynela *et al.*, 2000). Its human counterpart, congenital NCL, is the very rare most severe form of the NCL and has been characterized genetically with CTSD mutations just recently (Siintola *et al.*, 2006). Congenital NCL patients clinically present with respiratory insufficiency, epileptic seizures and death occurs within hours to weeks after birth. The brain of patients is extremely small and show severe neuronal loss and accumulation of autofluorescent material that has granular osmiophilic nature at ultrastructural level. The severity of the pathology of congenital NCL depends on the mutation in the *CTSD* gene. In an individual in which residual cathepsin D activity could be measured the disease progressed slower than in patients without cathepsin D activity (Steinfeld *et al.*, 2006).

How mutations in the cathepsin D gene result in this pathology on a molecular level is unknown but the involvement of cathepsin D in NCL emphasizes the study of the naturally occurring sheep NCL and the artificially generated cathepsin D mutants in *Drosophila melanogaster* and *Mus musculus*, which allow for detailed investigation of the molecular mechanisms that underlie this disease.

4.3 Investigation of CLN protein function in cultured cells and model organisms

4.3.1 Infantile NCL, palmitoyl protein thioesterase

To understand how a reduced palmitoyl protein thioesterase (PPT) activity results in the clinical manifestation of INCL we need to know the normal function of the PPT protein. The presumed function of the PPT hydrolytic enzyme is to catalyze the cleavage of thioester bonds between target protein cysteine residues and their palmitoyl fatty acid side groups (Lu and Hofmann, 2006). The enzyme was found to facilitate the removal of palmitate from H-Ras *in vitro*, and may perform this activity on its natural substrates in the lysosome (Camp *et al.*, 1994, Kim *et al.*, 2006). The PPT protein localizes to lysosomes in non-neuronal cells, and enzyme activity could be measured at acidic pH, with the optimal activity at approximately pH 4 (Voznyi *et al.*, 1999), although activity at neutral pH was also reported (Verkruyse and Hofmann, 1996). PPT may also have an extracellular function, as the protein was found to be secreted (Camp *et al.*, 1994, Verkruyse and Hofmann, 1996). Since the disease manifests itself primarily in the nervous system, PPT may have a neuron-specific function. In neuronal cells, the enzyme is found in axons and presynaptic region localized to synaptic vesicles and synaptosomes (Ahtiainen *et al.*, 2003). In the brain, the expression is developmentally regulated, suggesting that PPT is involved in maturation and growth of neural networks (Isosomppi *et al.*, 1999). In addition, PPT may be involved in apoptosis, since PPT was found to exert an anti-apoptotic effect (Cho and Dawson, 2000). A second *PPT* gene, *PPT2,* was also detected in humans, but it was shown to encode a lysosomal thioesterase with a substrate specificity that was different from PPT1 (Soyombo and Hofmann, 1997). Furthermore, PPT2 could not complement the metabolic defect of PPT1 deficient cells. Despite these advances, our knowledge of the affected molecular mechanisms underlying INCL is limited. Therefore additional investigations in model organisms are required to elucidate the INCL etiology at the molecular level.

4.3.2 INCL mouse models

Several INCL mouse models are available to investigate PPT protein function and INCL pathogenesis. Knock-out strains of the murine *Ppt1* gene encoding the lysosomal palmitoyl protein thioesterase were generated (Gupta *et al.*, 2001, Jalanko *et al.*, 2005). The *Ppt1*$^{-/-}$ knock-out was shown to result in viable and fertile mice that developed spasticity. The *Ppt1*$^{-/-}$ mice showed progressive pathology, presenting as motor abnormalities and premature death at 10 months of age. Furthermore, in 6 months old *Ppt1*$^{-/-}$ mice autofluorescence levels were increased compared to 10 months old

wildtype mice, and granular osmiophilic deposits (GRODs) were easily identified in *Ppt1*$^{-/-}$ neurons while absent from wildtype mice. Neuronal degeneration was obvious in sections from 6 months old *Ppt1*$^{-/-}$ mice, of which apoptosis was suggested to be the underlying mechanism. Thus, the *Ppt1*$^{-/-}$ mouse represents an INCL model that displays several hallmarks of the disease and will provide a substrate for testing therapy (Gupta *et al.*, 2001). In addition, a mouse knock-out for *Ppt2* was generated. Mice, in which this lysosomal palmitoyl protein thioesterase activity was disrupted, were viable and fertile and spastic. Compared to the *Ppt1* knock-out, the *Ppt2* (-/-) mice displayed no other motor abnormalities and only slightly decreased survival, while autofluorescence levels were normal and GRODs were absent (Gupta *et al.*, 2001).
In another murine INCL model, *Ppt1*$^{\Delta ex4}$, exon 4 of *Ppt1* was eliminated, resulting in a frame-shift and premature stop codon in exon 3. This mutation deletes the active site of the Ppt1 enzyme and resembles the most common *Ppt1* mutation (Jalanko *et al.*, 2005). These mice were viable, fertile and gross morphology was normal. In the *Ppt1*$^{\Delta ex4}$ mice loss of vision was demonstrated to be significant at 14 weeks of age, the disease gradually progressed into seizures at four months and myoclonic jerks at six months of age, and the average age of death was 6.5 months, at which the brain was shown to be severely decreased in weight. In homozygous *Ppt1*$^{\Delta ex4}$ mutants no Ppt1 enzyme activity could be detected, and increased autofluorescence and GRODs were observed similar to the other INCL mouse model and human patients. Furthermore, in *Ppt1*$^{\Delta ex4}$ mutant mice prominent neuronal loss could be demonstrated. Expression profiling experiments performed on cerebra of 6 months old *Ppt1*$^{\Delta ex4}$ mutants indicate involvement of the immune system in neuronal degeneration. Inflammation was also reported in the *Cln3* knockout mouse and in other neurodegenerative diseases, such as Alzheimer's, and Parkinson's disease. Although these INCL mouse models display most of the disease characteristics, they may also be too complicated to unravel the molecular mechanisms that underlie the pathogenesis. Thus simpler model organisms, such as flies and worms, may be required to achieve this.

4.3.3 PPT1 genes of *Drosophila melanogaster* and *Caenorhabditis elegans*

PPT1 protein homologues were identified in the invertebrate fruitfly and nematode, to establish relatively simple models, in which molecular mechanisms underlying INCL could be elucidated. The homologous proteins were shown to exhibit an enzymatic activity that could be measured with the same assay as human PPT1 activity, indicating protein function conservation (Glaser *et al.*, 2003, Porter *et al.*, 2005, Van Diggelen *et al.*, 1999). Although *Drosophila Ppt1* knockouts are being generated, gene and protein function were mainly investigated in flies that overexpress *Ppt1* in the developing visual system (Korey and MacDonald, 2003). Overexpression of *Ppt1* leads to neuronal degeneration, manifested as black omatidia in the *Drosophila* eye presumably due to apoptosis. Identification of genetic modifiers of the observed phenotypes are expected to facilitate the unraveling of the pathways in which Ppt1 is involved.
In *C. elegans, ppt-1* knockouts were isolated and characterized (Porter *et al.*, 2005). Nematode *ppt-1* mutants displayed developmental and reproductive phenotypes:

development was delayed for four hours compared to wildtype, the number of embryos contained within the gonad consistently was higher compared to wildtype. The actual life span was similar to wildtype, but the animals were less motile and appeared aged earlier than wildtype. At the ultrastructural level, *ppt-1* nematodes were shown to contain abnormal mitochondria, already at day one of the adult life stage, indicating PPT1 has an influence on mitochondrial integrity. Further investigation of these models for INCL will be valuable to reveal the affected molecular mechanisms that cause this disease.

4.3.4 Late infantile NCL, tripeptidyl peptidase 1

The lysosomal serine protease, tripeptidyl peptidase 1 (TPP1), which when affected leads to late infantile NCL (LINCL) cleaves tripeptides of the amino terminus of small proteins (Lin *et al.*, 2001,Sleat *et al.*, 1997, Bernardini and Warburton, 2001). Although the natural substrates of TPP1 have not been identified, its enzymatic activity can be assayed *in vitro* (Wisniewski *et al.*, 2001). The enzyme appeared to have an acidic pH optimum and was found to be localized to lysosomes. To investigate the function of TPP1 and how changed function may lead to LINCL, a *Cln2*$^{-/-}$ mouse model was generated (Sleat *et al.*, 2004). This mouse model recapitulates the phenotype of the disease in humans, starting with body tremors that progress in severity throughout the life of the animal. Furthermore, *Cln2*$^{-/-}$ mice present with locomotor difficulties, including what appear to be epileptic seizures at end stage of the disease, and lifespan was considerably shorter than wildtype animals. In addition, fluorescent storage material filled the cytoplasm of cells of most brain regions in mutant mice of 100 days or older. In the moderately atrophic brain of *Cln2*$^{-/-}$ mutant mice, disruption of myelin was observed and neurons contained curvilinear storage bodies, a hallmark of LINCL in humans. Autofluorescent storage material was also observed outside of the brain. Interestingly, the *CLN2*$^{-/-}$ mouse has been used to test the therapeutic efficacy of injection of adeno-associated virus (AAV) vectors carrying *Cln2*, as a cure for this disease in mice (Passini *et al.*, 2006). With this gene transfer a significant decrease in storage material was achieved, but the effects on neurodegeneration and behavior are unclear.

4.3.5 Finnish variant late infantile NCL, CLN5

The function of the CLN5 protein is still unknown. In cultured human cells the CLN5 protein was found to be glycosylated and localizes to lysosomes, although a cytoplasmic soluble form of this protein was found as well. The CLN5 protein with the most common mutation identified in Finnish variant late infantile NCL patients did not localize correctly to lysosomes (Isosomppi *et al.*, 2002). Using co-immunoprecipitation studies, the CLN5 protein was found to interact with the CLN2 and CLN3 proteins, while disease causing mutations in CLN5 disrupted the interaction with CLN2 but not with CLN3 (Vesa *et al.*, 2002). These interactions were the first indications that CLN proteins interconnect at the molecular level, suggestive of a common pathogenic pathway underlying these diseases. Strengthening this hypothesis is the observation that in fibroblasts from human patients with mutations in *CLN5*,

and *TPP1*, the *CLN3* mRNA levels were decreased to 65 % and 73 % of wildtype mRNA levels, respectively (Bessa *et al.*, 2006). A *Cln5* mouse model was generated with a targeted deletion of exon 3 (Kopra *et al.*, 2004). The progressive pathology of these mice resembles the pathology observed in human patients, with severe loss of vision occurring on average at week 21, prominent accumulation of autofluorescent material in the brain of six months old mutant mice. The accumulated material contained curvilinear and fingerprint profiles. Moreover, microarray expression analysis of cerebra of $Cln5^{-/-}$ mice indicated differential expression of genes involved in inflammatory processes, neuronal degeneration, and encoding myelin components, which is in agreement with the hypomyelination and the other neuronal problems observed in this model. The expression profile of *Cln5* mutant cerebra appears to display parallels to expression profiles of aging brain in mice, which suggests that premature aging may play a role in the pathogenesis of Finnish variant late infantile NCL.

4.3.6 Late infantile variant NCL, CLN6

The CLN6 protein was predicted to have seven transmembrane domains and localized to the endoplasmic reticulum (Wheeler *et al.*, 2002, Gao *et al.*, 2002, Mole *et al.*, 2004). The same localization was observed with proteins harboring vLINCL disease causing mutations. Investigation of gene expression profiles of CLN6-deficient cultured fibroblasts has lead to the observation that cholesterol homeostasis is disrupted in patient cell lines. Additional problems with extracellular matrix remodelling, signalling cascades and vesicular traffic are likely to underlie vLINCL disease pathogenesis (Teixeira *et al.*, 2006). Furthermore, overexpression of genes involved in apoptosis and inflammatory response was also observed, presumably reflecting cellular protection against stress and degeneration, and secondary inflammatory responses in cellular degeneration, respectively. Naturally occuring NCL disease models that are caused by mutations in genes homologous to *CLN6* are present in mice and sheep (Tyynela *et al.*, 2000, Wheeler *et al.*, 2002, Gao *et al.*, 2002). The *nclf* mice that were shown to have mutations in the murine homologue of *CLN6*, developed rear limb paresis after 8 months, which progressed into paralysis over several months and subsequent death (Bronson *et al.*, 1998, Wheeler *et al.*, 2002, Gao *et al.*, 2002). These mice also suffered from retinal degeneration present in four months old *nclf* mice and neuronal degeneration in six months old animals. In *nclf* mice as young as 11 days accumulated material could already be observed in many different kinds of cells. The naturally occurring ovine NCL, is caused by mutations in a gene that was mapped to a region on sheep chromosome 7 that is syntenic to the human 15q21-23 region that contains *CLN6* (Broom and Zhou, 2001, Tammen *et al.*, 2001, Oswald *et al.*, 2005). In these sheep brain mass started to decrease at 4 months of age compared to healthy age matched controls and by 12 months atrophy of cortical brain regions was macroscopically visible. Autofluorescent storage materials were present as early as 12 days in the cortical regions of the brain, and immunoreactivity of the Subunit c of the mitochondrial ATP synthase antibody was increased in the parieto-occipital cortex of brains of affected

sheep (Oswald *et al.*, 2005). Both the murine and ovine animal models closely resemble the vLINCL in humans and are being used to investigate the molecular mechanisms underlying the disorder.

4.3.7 Turkish variant late infantile NCL and Northern Epilepsy, CLN8

The function of the CLN8 protein is still unknown.The CLN8 protein was predicted to be a transmembrane protein of 286 amino acids. This protein localized to ER membrane and ER Golgi intermediate compartment (ERGIC) when *CLN8* cDNA was overexpressed in cultured cells and to ER in neurons, and this localization was not aborted when a disease causing mutations was introduced in the coding region (Lonka *et al.*, 2004, Lonka *et al.*, 2000). The mouse model for motor neuron degeneration (*mnd*) was the first described naturally occurring NCL disease model and it was caused by a mutation in the *Cln8* gene (Bronson *et al.*, 1993, Ranta *et al.*, 1999). The murine *Cln8* gene was shown to be ubiquitously expressed and its transcript could be identified throughout development of the mouse. The expression of the *Cln8* gene was shown to be increased in mice that were electrically stimulated to induce epileptic seizures (Lonka *et al.*, 2005). How a defect in the CLN8 protein may lead to this disease still has to be elucidated.

4.3.8 Congenital NCL, CTSD

The Cathepsin D protein is a lysosomal aspartic protease that belongs to the family of pepsin proteases and is involved in congenital NCL. The protein plays a role in several processes including: proliferation of cancer cells, apoptosis, inflammatory responses and regenerative processes. This peptidase is highly active and prominently present in the lysosomal compartment. The functions of the cathepsin D protein are conserved between species as diverse as humans, sheep, dogs, mice and fruitflies, since disruption of the cathepsin D gene leads to neurodegeneration and storage of autofluorescent materials in all of these organisms (Steinfeld *et al.*, 2006, Myllykangas *et al.*, 2005). Investigation of the Cathepsin D protein in these models may provide further insight into the etiology of Congenital NCL.

5 JNCL Disease Models

5.1 Mouse models for JNCL

For many lysosomal storage diseases that are caused by enzyme defects, a therapeutic strategy may be provided by gene transfer or enzyme replacement therapy. JNCL, however, is caused by mutations in a gene encoding a transmembrane protein of unknown function. Disease models in small vertebrates are imperative in the research of the molecular mechanisms underlying JNCL to minutely monitor the successive stages of disease progression and to develop and test therapeutic strategies (reviewed in Cooper *et al.*, 2006). Furthermore, the molecular basis of the affected processes can be studied on a cellular level in cultured cells derived from these animals.
To investigate JNCL etiology in mice, three murine models were generated. Two *Cln3* knock-out mouse models, exon 1-6 deletion mice and exon 7-8 deletion mice, were made by inserting a resistance cassette in the murine *Cln3* gene, replacing exons 1 to 6 and 7 to 8, respectively (Mitchison *et al.*, 1999, Katz *et al.*, 1999). The third model was a knock-in model generated by deleting exons 7 and 8 using the Cre-loxP technology. This deletion mimics the most common mutation, which is the 1.02 kb deletion, found in 85% of the human JNCL patients (Cotman *et al.*, 2002). These three models all display storage of autofluorescent material and neurodegeneration, thereby recapitulating important JNCL characteristics. Which mouse mutants eventually will be the most reliable model for JNCL is not yet clear. The models were generated in different genetic backgrounds, making the models difficult to compare. Each model needs to be backcrossed into the same genetic background before the mutants can be compared (Cooper *et al.*, 2006). However, clinical symptoms in these mutant mice appear milder than the effects of human *CLN3* mutations, e.g. the exon 1-6 deletion mice did not develop obvious neurological defects at 12 months of age (Mitchison *et al.*, 1999). The pathologic process may require a longer time interval to produce detectable symptoms or it may affect neurons of which the functionality is not readily and reliably testable in mice. JNCL mouse models have been used to investigate differential gene expression and cell lines derived from these mutants can be cultured and studied to examine effects of *Cln3* mutations at the cellular level.
Gene expression profiling of cerebella of exon 1-6 deletion mice showed altered expression levels of genes involved in neurotransmission, neuronal cell structure, development, immune response, lipid metabolism, and inflammation (Brooks *et al.*, 2003). From this study, in which 10 week old *Cln3* knock-out mice were compared with age-matched wild-types, it becomes clear that cerebellar expression levels are already changed before evidence of neurodegeneration can be observed. In another study, gene expression in whole brains of the same mouse model was compared with gene expression of whole brains of *Cln1* knockout mice and wild-type controls

(Elshatory *et al.*, 2003). The 10 week old *Cln3* exon 1-6 deletion mice used in this study showed differential expression of genes involved in neurotransmitter metabolism compared to wild type gene expression levels. When the expression levels of the *Cln3* mutants are compared with the *Cln1* mutants, the absence of overlap in differential expression is striking. The most downregulated gene in *Cln1* knock-out mice is the most upregulated gene in *Cln3* knock-out mice. This suggests that the effects of the *Cln3* and *Cln1* mutations are fundamentally different, and while caused by distinct molecular mechanisms the mutations lead to similar pathologies. Since loss of vision is the first symptom in human JNCL patients, gene expression levels present in cells of the eye of *Cln3* exon 1-6 deletion mice were determined and compared to wild type mice and with the cerebellar data set (Chattopadhyay *et al.*, 2004). In the eye, 18 genes were shown to be differentially regulated compared to cerebellar expression levels. Three of the downregulated genes, Cytochrome oxidase I, Cytochrome B, ATP synthase subunit B, are involved in energy production in mitochondria. This is an interesting observation, since Subunit c of the mitochondrial ATP synthase is the major component of the storage material and mitochondrial dysfunction has been suggested to underlie cell death in the eye. Moreover, decreased activity of mitochondrial ATP synthase was reported previously (Palmer *et al.*, 1992, Jolly *et al.*, 2002, Das and Kohlschutter, 1996). In addition to the expression profiling of cerebellum, brain and retina, cultured neuronal precursor cells obtained from *Cln3* knock-in mice were investigated. These cells resemble JNCL patient neurons in that Subunit c of the mitochondrial ATP synthase is accumulated (Fossale *et al.*, 2004). Lysosomal enzyme processing was also affected and lysosomes appeared smaller and labeled less intensely with Lysotracker Red. Additional phenotypes of these *Cln3* mutant cells in comparison to wild type cells encompassed decreased uptake of fluid phase markers, abnormally elongated mitochondria, and decreased ATP levels. Interestingly, autophagy and lysosomal trafficking were shown to be affected, possibly due to defective mitochondrial turnover, indicating that altered organellar maintenance may play a role in JNCL pathology (Cao *et al.*, 2006). Expression analysis of these *Cln3* mutant cells indicated differential expression of genes involved in three pathways or structural elements: glucose metabolism, cytoskeleton, and synaptosomes (Luiro *et al.*, 2006). Mitochondrial function was slightly affected in these cells, consistent with their changed ultrastructural morphology. Synaptosomes were suggested to be abnormal as demonstrated by a delay in neuronal depolarization. These mitochondrial and synaptosomal defects may underly primary cellular events that together with defective cytoskeletal components could lead to JNCL. Although the investigations of these mouse models has provided additional insight in disease progression and affected molecular mechanisms, much is still unresolved and may require other experimental models to elucidate the full functional spectrum of the Cln3 protein.

5.2 Lower eukaryotic model organisms

Since studying molecular processes underlying JNCL pathology in complicated vertebrate disease models is a difficult task and the results may be difficult to interpret detailed molecular analysis of the affected protein function may be more straightforward in less complex model organisms. Although JNCL is a human neurodegenerative disorder, CLN3 protein sequence comparison has lead to the identification of CLN3 homologues with high amino acid sequence similarity in

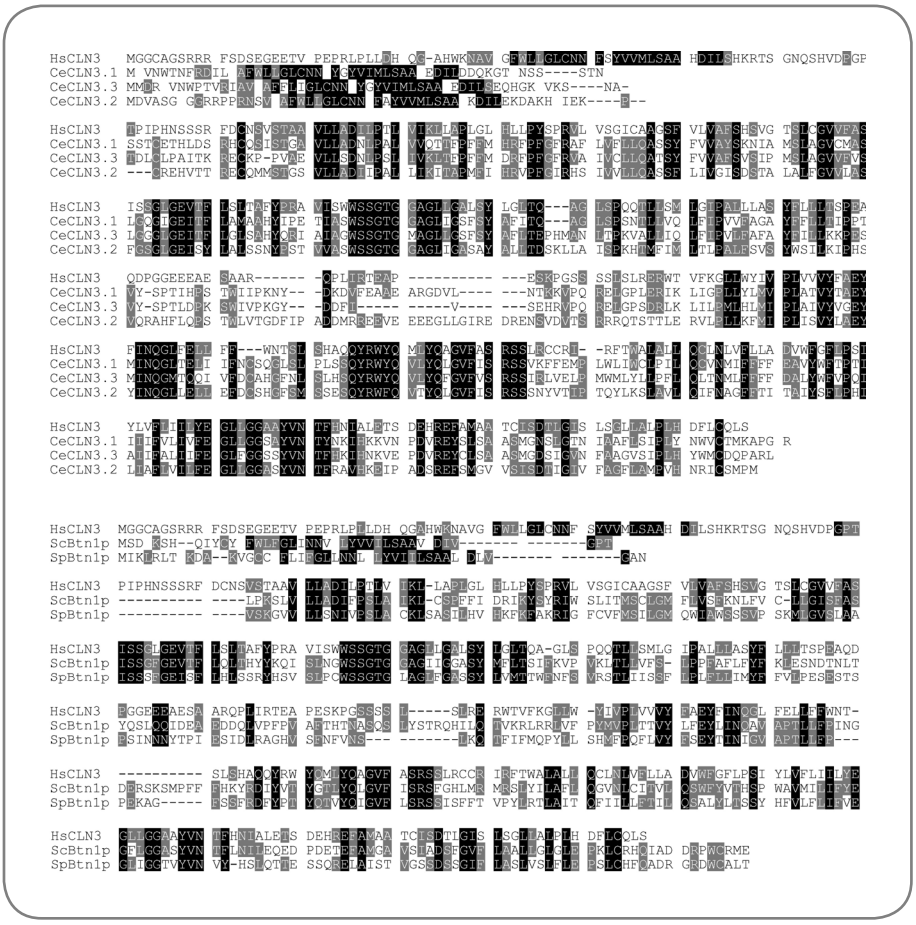

Figure 3 Human CLN3 protein sequence aligned with corresponding model organism homologous

Sequences were aligned using the multalin program. In the top sequence alignment the human sequence is compared with the three *C. elegans* (Ce) homologues sequences and in the bottom alignment with the *Saccharomyces cerevisiae* (Sc) and *Schizosaccharomyces pombe* (Sp) homologous sequences. Conserved amino acid residues are shown in black boxes, neutral substitutions in grey boxes.

Saccharomyces cerevisiae, *Schizosaccharomyces pombe*, and *Caenorhabditis elegans*. This conservation suggests that CLN3 protein function is partially conserved (Figure 3) (Taschner *et al.*, 1997, Corpet, 1988). Thus functional analysis might be performed in small model organisms with their powerful genetic and biochemical toolset. Even model organisms without a nervous system, e.g. yeast, have proven to be invaluable to characterize many human disorders. The data obtained with the smaller model organisms may then be extrapolated to vertebrate disease models to unravel details about possible additional functional aspects in a more complex environment.
Part of the following section, of which de Voer and Taschner were co-authors, was derived from: Phillips SN, Muzaffar N, Codlin S, Korey CA, Taschner PEM, de Voer G, Mole SE, Pearce DA. 2006. Characterizing pathogenic processes in Batten disease: Use of small eukaryotic model systems. Biochim Biophys Acta. 1762:906-19.

5.2.1 The yeast *Saccharomyces cerevisiae* JNCL model

S. cerevisiae is used to study the juvenile form of NCL in which *CLN3,* encoding a yet uncharacterized protein, is mutated (IBDC, 1995). The homolog to CLN3 is called Btn1p in the budding yeast S. cerevisiae. Btn1p, also designated Yhc3p, is 39% identical and 59% similar in amino acid sequence to human CLN3 (Figure 3) (Mitchison *et al.*, 1997). Similar to CLN3, Btn1p is a 46 kD integral membrane protein with several predicted phosphorylation, myristoylation, glycosylation, and farnesylation sites (Taschner *et al.*, 1997, Golabek *et al.*, 1999, Jarvela *et al.*, 1998, Ezaki *et al.*, 2003, Michalewski *et al.*, 1999, Pullarkat and Morris, 1997, Kaczmarski *et al.*, 1999). Importantly, the residues that are mutated in Batten disease patients are conserved in Btn1p, suggesting that the primary activity of the protein is conserved. Furthermore, Btn1p and CLN3 are functional homologs, because plasmid-derived CLN3 can complement for the absence of Btn1p in the *BTN1* deletion strain, *btn1*-Δ, confirming that the primordial function of CLN3 is conserved in yeast (Kim *et al.*, 2003, Pearce and Sherman, 1998). This property of the yeast model potentially offers a powerful tool to test the functionality of CLN3 and Btn1p constructs. For example, it is unclear if GFP fusions of CLN3 are functional (Haskell *et al.*, 1999), and a simple complementation assay in the yeast model could test this. Moreover, the yeast model has been used to test the ability of *CLN3* point mutants to complement *BTN1*, leading to the conclusion that disease severity correlated with the degree of complementation (Pearce and Sherman, 1998, Haskell *et al.*, 2000). Human CLN3 has been localized to the lysosome in various studies and cell types (Golabek *et al.*, 1999, Kyttala *et al.*, 2004, and reviewed in Phillips *et al.*, 2005, Pearce 2000). Similarly, Btn1p has been localized to the vacuole, the structure analogous to the higher eukaryotic lysosome, further emphasizing the relevance of the yeast model (Croopnick *et al.*, 1998, Pearce *et al.*, 1999b). To date, Btn1p has been implicated in three main cellular processes, two of which have been validated in mammalian models. Although these processes partially overlap, Btn1p has been linked to regulation of cellular pH, basic amino acid homeostasis, and nitric oxide production (Pearce *et al.*, 1999b, Chattopadhyay *et al.*, 2003, Pearce *et al.*, 1999c, Pearce *et al.*, 1999a).

5.2.2 Btn1p and the regulation of cellular pH

Using pH sensitive dyes, Pearce and colleagues first reported that the vacuolar pH in *btn1*-Δ cells was decreased compared to *BTN1*+ vacuoles at early growth and continued to increase throughout log and stationary phases (Pearce *et al.*, 1999b). More recently, it has been shown that as *btn1*-Δ cells grow, vacuolar pH will rise above normal (Padilla-Lopez and Pearce, 2006). Moreover, vacuolar pH in both normal and *btn1*-Δ strains was shown to be altered by extracellular pH. In *btn1*-Δ cells, the activity of the plasma membrane H+- ATPase is increased, likely acting to buffer altered vacuolar pH. This led to the discovery of a plate phenotype for the *btn1*-Δ strain, which due to the increased plasma membrane H+-ATPase activity has an elevated rate of media acidification. This elevated media acidification allows *btn1*-Δ cells to grow in the presence of D-(-)-threo-2-amino-1-[*p*-nitrophenyl]-1,3- propanediol (ANP), since the increased acidity of the medium renders ANP non-toxic to *btn1*-Δ cells, whereas ANP is toxic to *BTN1*+ cells (Pearce and Sherman, 1998, Pearce *et al.*, 1999a). In addition, when the vacuolar pH of *btn1*-Δ cells was artificially increased using chloroquine, the activity of the plasma membrane ATPase decreased strengthening the link between external and vacuolar pH (Pearce *et al.*, 1999b, Pearce *et al.*, 1999c). The pH and ANP results are in contrast to the *Schizosaccharomyces pombe* model, where an increased vacuolar pH and sensitivity to ANP are observed in the deletion (Gachet *et al.*, 2005)(see below). Subsequent follow up studies on the pH of lysosomes from human fibroblasts indicated that pH was slightly elevated in JNCL, suggesting that defects in human CLN3 also result in a disruption in the regulation of this organelle's pH (Pearce and Sherman, 1998, Golabek *et al.*, 2000). However, limitations in what can be explored in cell culture means that it is not feasible to explore the possibility of a correlation between the dynamic change from lower to higher pH of the lysosome and the disease. Nevertheless, it is clear that the processes that govern vacuolar/lysosomal pH are disrupted in the absence of a functional Btn1p/CLN3 ultimately leading to an elevated pH of this organelle.

5.2.3 A possible role of Btn1p and CLN3 in amino acid homeostasis

Besides altered vacuolar pH, alterations in arginine levels in *btn1*-Δ cells have been observed (Kim *et al.*, 2003). Both cytoplasmic and vacuolar levels of arginine and lysine and ATP-dependent vacuolar arginine uptake are significantly decreased in *btn1*-Δ (Kim *et al.*, 2003). This is interesting, since the vacuole acts as a storage organelle for sequestration of basic amino acids (Kitamoto *et al.*, 1988, Wiemken and Durr, 1974). Like the pH defects, vacuolar arginine transport returns to normal when human CLN3 is expressed in *btn1*-Δ. Moreover, lysosomes isolated from JNCL patient human lymphoblast cell lines demonstrate decreased arginine transport (Kim *et al.*, 2003, Ramirez-Montealegre and Pearce, 2005). The role of Btn1p in both regulating vacuolar pH and arginine transport has recently been clarified: the coupling of proton pumping and the activity of the vATPase was found to depend on extracellular pH (Padilla-Lopez and Pearce, 2006). Importantly, the *btn1*-Δ mutation results in an alteration in the coupling of proton pumping and the activity of the vATPase. Thus, defective arginine transport in *btn1*-Δ could result from an alteration

in the regulation of the electrochemical gradient driving this transport (Padilla-Lopez and Pearce, 2006). Interestingly, subsequent studies aimed at dissecting out whether alterations in intracellular arginine impact cells lacking Btn1p (*btn1*-Δ) have revealed that overexpression of Can1p, the plasma membrane basic amino acid transporter, is lethal (Regenberg *et al.*, 1999, Phillips *et al.*, 2006). It is tempting to speculate that the decrease in intracellular arginine and lysine levels may result from a buffering mechanism against arginine and lysine being toxic to cells lacking Btn1p (Regenberg *et al.*, 1999, Phillips *et al.*, 2006). Alternatively, it should be noted that *BTN1*$^{+}$ cells with either endogenous or overexpressed levels of Can1p have similar rates of plasma membrane arginine uptake, suggesting that *btn1*-Δ cells may lack the ability to regulate the amount or activity of Can1p at the plasma membrane, resulting in arginine and lysine toxicity (Phillips *et al.*, 2006). It is pertinent to point out that as amino acid levels, and possibly metabolism, are clearly affected by *btn1*-Δ, the studies described have avoided the typical use of auxotrophic markers for gene deletion and genetic studies (Adams *et al.*, 1997). In other words, *btn1*-Δ strains have identical amino acid growth requirements to that of wild type to avoid studying artifacts of altered amino acid metabolism.

5.2.4 Btn1p involved in nitric oxide synthesis

A recent study has highlighted a third pathway affected by the absence of Btn1p, namely nitric oxide (NO) synthesis (Osorio *et al.*, 2006). As arginine serves as the substrate for NO synthesis, this is also likely linked to the aforementioned alterations in arginine levels. Specifically, Osorio and colleagues demonstrated that *btn1*-Δ cells are more resistant to menadione due to defective synthesis of NO and consequent decreased levels of reactive oxygen and nitrogen species. If *btn1*-Δ cells are preincubated with arginine before menadione exposure, the phenotype is lost, suggesting that the decrease in nitric oxide results from the decrease in cellular arginine (Osorio *et al.*, 2006). Although this phenotype may be the consequence of the primary defect associated to lack of Btn1p, it could also underlie the pathophysiological aspects of the disease. It will be important to recapitulate these observations in human cell lines.

5.2.5 Btn1p has a genetic interaction with Btn2p

Microarray analysis of *btn1*-Δ strains revealed that BTN2 mRNA levels were increased in a *btn1*-Δ background (Pearce *et al.*, 1999b). Btn2p interacts with Yif1p, Rhb1p, and Ist2p, with deletion of BTN2 resulting in an altered localization of these proteins (Chattopadhyay *et al.*, 2003, Kim *et al.*, 2005, Chattopadhyay and Pearce, 2002). Yif1p is involved in ER to Golgi transport, Rhb1p is a small GTPase that has been implicated in plasma membrane arginine transport regulation, and Ist2p is a putative ion channel at the plasma membrane (Matern *et al.*, 2000, Urano *et al.*, 2000, Entian *et al.*, 1999, Mannhaupt *et al.*, 1994). Taken together, these observations would suggest that Btn2p is involved in trafficking. Btn2p does not have a true mammalian homolog, but as a cytosolic coiled-coil protein it shows very specific domain similarity to the higher eukaryotic protein Hook1. Hook1 is a microtubule binding protein involved in trafficking to the late endosome, multivesicular body formation, and endosomal

fusion (Kramer and Phistry, 1996, Kramer and Phistry, 1999, Richardson *et al.*, 2004, Sunio *et al.*, 1999, Walenta *et al.*, 2001). Upregulation of Btn2p may be explained by the pH alterations, since decreases in vATPase activity can have an effect on protein trafficking and degradation (Mellman, 1992, Mellman *et al.*, 1986, Trombetta *et al.*, 2003, Nishi and Forgac, 2002, Hurtado-Lorenzo *et al.*, 2006, Sun-Wada *et al.*, 2003, Sun-Wada *et al.*, 2004). Therefore, upregulation of Btn2p may result in a compensatory response to minimize disruptions in protein trafficking in *btn1*-Δ cells due to altered intracellular pH.
In summary, it appears that the primary defect in *btn1*-Δ involves a disrupted regulation of vacuolar pH, suggesting that Btn1p functions in a pH regulatory pathway. However, at this point a direct role for Btn1p in arginine homeostasis, nitric oxide production or protein trafficking cannot be ruled out. It is important to note that studies thus far have focused on determining the role for Btn1p through the use of *btn1*-Δ cells that lack Btn1p and are therefore based on a loss-of-function model, in which cells might be altering these pathways to compensate for the loss of Btn1p. It is possible that pH alterations are a secondary consequence of the loss of Btn1p, and the primary defect is yet to be elucidated. Future studies are focused on looking on the direct function of Btn1p, especially its role in coupling transport mechanisms with vATPase activity. S. cerevisiae has played and will continue to play a strong part in the efforts to understand JNCL.

5.2.6 JNCL in *Schizosaccharomyces pombe*, changes in pH and vacuole size

The fission yeast *Schizosaccharomyces pombe* homolog of human CLN3, termed Btn1p, is a predicted transmembrane protein of 396 amino acids that is 30% identical and 48% similar to its human counterpart (Figure 3). The *S. pombe* Δ*btn1* strain, deleted for the btn1 gene is viable, but shows subtle and reproducible defects in cell cycle progression, which could be rescued by human CLN3 (Gachet *et al.*, 2005). Average cell size is increased and the number of mitotic and dividing cells as well. In addition, Δ*btn1* mutant cell vacuoles are larger than wild type cell vacuoles (mean size of 1.3 μm and 0.9 μm, respectively), Δ*btn1* mutants have a broader vacuole size distribution, and Δ*btn1* cells have an elevation in vacuole pH of 1 pH unit (pH 5.1 compared to pH 4.1 for wild type cells). A correlation is known to exist between increased vacuole size and increased pH in fission yeast (Iwaki *et al.*, 2004), suggesting that Δ*btn1* mutant pH regulation is affected, which in turn influences vacuole size (Gachet *et al.*, 2005). The vacuolar size defect was restored to wild type levels when the Δ*btn1* strain was grown in acidic media (pH 4) confirming that vacuole size is a reflection of the increased pH of the vacuole in Δ*btn1* cells. In contrast to S. cerevisiae Δ*btn1* mutants, *S. pombe* btn1Δ cells were found to be sensitive for growth in media containing 1 mM ANP. Although the mechanism for this sensitivity in fission yeast remains to be determined, growth of *S. pombe* Δ*btn1* on plates containing 1 mM ANP was restored when this media was at pH 4, suggesting a relation between pH and ANP sensitivity (S. Codlin, unpublished). The basis for the difference in ANP sensitivity between *S. cerevisiae* and *S. pombe* may be in vacuolar pH (pH 6.2 and pH 4 respectively) (Gachet *et al.*, 2005).

5.2.7 *S. pombe btn1+* has a genetic interaction with vacuolar ATPase subunit *vma1+*

The vacuolar pH of S. pombe is similar to that of mammalian cells which are also acidic (Holopainen *et al.*, 2001). Expression of Btn1 and human CLN3 in fission yeast deleted for $btn1^+$ causes a decrease in pH of the vacuoles (Gachet *et al.*, 2005). These results are in contrast to overexpression studies of CLN3 in HEK293 cells (Golabek *et al.*, 2000), where lysosomal pH is increased but in agreement with studies on JNCL fibroblasts that had a slightly elevated lysosomal pH (Holopainen *et al.*, 2001). Cells deleted for $btn1^+$ and vATPase subunit $vma1^+$, which is involved in vacuolar acidification, exhibited slow growth and synthetic lethality at 30 °C, indicating a genetic interaction between *Btn1* and the vATPase subunit (Gachet *et al.*, 2005). While the molecular basis of this interaction has not been determined, previously described studies in S. cerevisiae implicating Btn1p in the coupling of proton pumping and the activity of the vATPase may provide a clue (Padilla-Lopez and Pearce, 2006).

5.2.8 Possible pre-vacuolar function of Btn1p

Overexpression of GFP-Btn1p and GFP-CLN3 constructs, which both have the GFP tags at the N-terminus, in Δ*btn1* cells complemented the vacuolar size and pH defects as well as the subtle cell growth defects, proving that Btn1p and CLN3 are functional homologs. In fission yeast, both Btn1p and CLN3 traffic to the vacuolar membrane via FM4-64 stained pre-vacuolar compartments, suggesting an endocytic trafficking route for Btn1p. Localization of Btn1p using a functional GFP-tagged Btn1p to the vacuole membrane was Ras GTPase Ypt7p dependent, with Btn1p being excluded from the vacuole and held in prevacuolar compartments in Δ*ypt7* cells (Gachet *et al.*, 2005). Cells deleted for both $Ypt7^+$ and $Btn1^+$ show synthetic lethality at 36 °C and vacuoles in these cells were larger than those of cells deleted for $Ypt7^+$ alone and again showed reduced pH. Btn1p must therefore have a functional role prior to reaching the vacuole, and this function impacts on vacuolar function.

5.2.9 Btn1p involved in osmoregulation in *S. pombe*

In addition to the subtle growth defects in cell cycle progression at 25 °C, Δ*btn1* cells are also temperature sensitive for growth at 37 °C (S. Codlin, unpublished). At this temperature, *btn1*Δ cells passed through no more than three cell cycles and subsequently lost their normal rod-shaped morphology, resulting in swollen and rounded cells. Cell lysis was found to be the subsequent cause of cell death. Electron microscopy reveals grossly thickened cell walls and septum regions, suggesting defects in the development of the main cell wall components, the α- and β-glucans. Indeed, Δ*btn1* cells were found to be highly sensitive to zymolase, a β-glucanase, but not to novozyme, an α-glucanase. Also, the swelling phenotype and cell lysis were completely rescued by the addition of 1 M sorbitol, an osmolyte, to the media, suggesting that the swelling and lysis may be caused by aberrant osmoregulation in Δ*btn1* cells (Gachet *et al.*, 2005).
This interesting link between JNCL and pH alteration phenotypes in *S. pombe* supports the use of fission yeast to study NCLs.

6 *Caenorhabditis elegans*

6.1 Introduction to *C. elegans* biology

In 1972 Sidney Brenner and colleagues started to study the genetics of development and behavior in the relatively simple non-parasitic soil-borne nematode *Caenorhabditis elegans* (Brenner, 1974). The first report described methods to generate and study mutants in this small easily manageable model organism, and the first library of mutants that was generated. *Caenorhabditis elegans* has a body length of approximately 1 mm, and can be cultured in the lab on Petri dishes that contain an agar lawn spread with bacteria, on which this nematode feeds. The nematode exists as a hermaphrodite that can self-fertilize, which is a major advantage, e.g. after mutagenesis or when performing crosses, as homozygotes can be obtained without a subsequent cross. *C. elegans* males can spontaneously arise through non-disjunction of the X chromosome, which occurs at an approximate rate of 1/1000 during gametogenesis (Hodgkin and Doniach, 1997). The hermaphrodite itself can produce 300 progenitors by self-fertilization and many more progeny will result from a cross with a male nematode. The *C. elegans* life cycle starts when the hermaphrodite lays eggs, containing embryos of which the development had started in the hermaphrodite uterus. In the eggs the nematodes develop and hatch to become L1 larvae and proceed their life cycle through four larval stages until adult life begins. During development at the L2 larval stage, *C. elegans* can develop into an alternative third larval stage, called the dauer stage, an inactive form in which the nematode can survive adverse environmental conditions. When the environment becomes favourable again, this organism can leave dauer stage and develop into an L4 larva after which normal nematode life can proceed. The normal life cycle from egg to egg-laying adult without dauer stage lasts three days at 20°C, and *C. elegans* has a life span of approximately three weeks.

6.2 *C. elegans* anatomy and development

The extensive anatomical studies have shown that the hermaphrodite nematode body consists of 959 somatic cells of which 302 are neurons. The rest of the cells constitute musculature, intestinal tract, reproductive system, and hypodermal cells (Figure 4). Studies of the developing embryo and larva have lead to a complete understanding of the cell lineage that was found to be identical from one nematode to the next, a remarkable trait and of importance when investigating the development of an organism (Sulston *et al.*, 1988). The cells of the nervous system were mapped and were also shown to be invariably wired and connected, enabling analysis of how neuronal connectivity influences *C. elegans* behavior (White *et al.*, 1988). The study of this

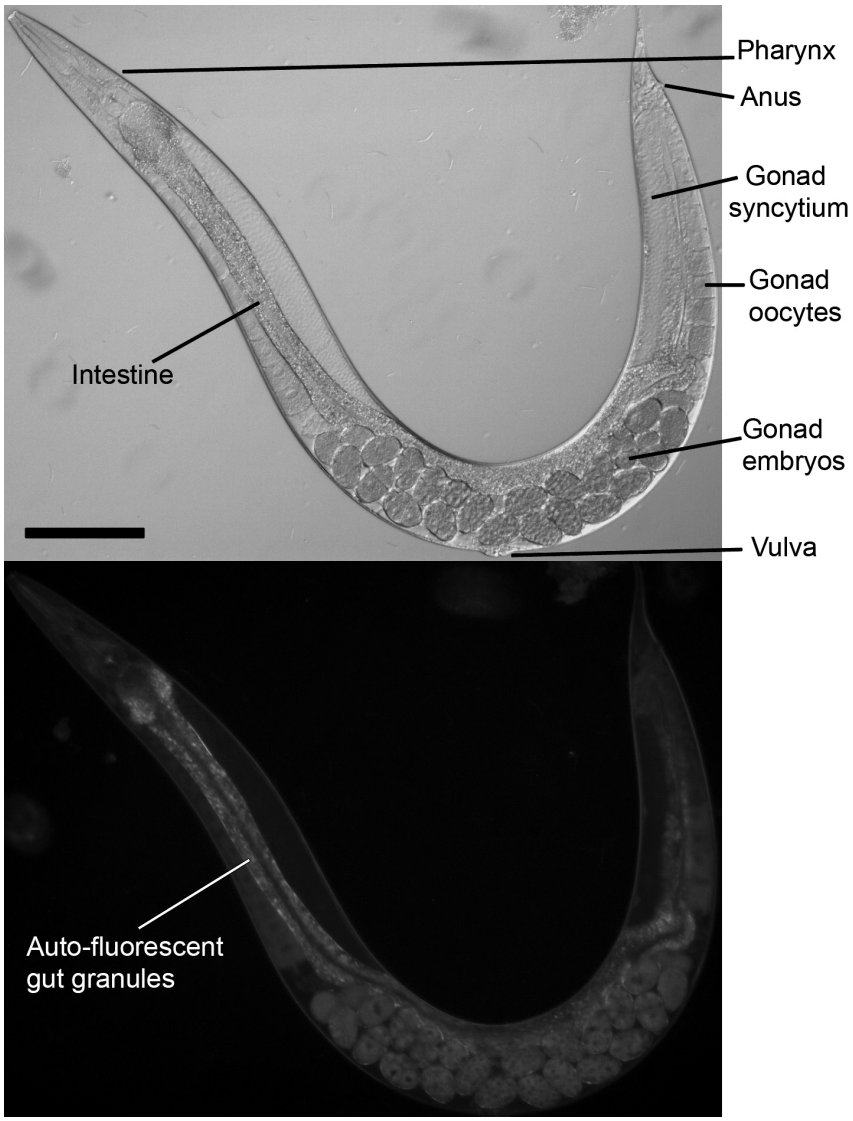

Figure 4 An adult hermaphrodite *Caenorhabditis elegans* nematode

In the top light micrograph Nomarksi image the worm body and its major constituents are depicted. In the bottom epifluorescence micrograph the autofluorescence of the same nematode can be seen visualized with a standard FITC filter set. The autofluorescent gut granules are particularly bright. (Bar=0,1 mm)

animal's development was partly facilitated by its transparency, and virtually every cell can be observed using differential interference contrast microscopy. Due to this and the efforts made on ultrastructural level, the nematode body now is a well known entity, in which every cell has its place and function, generating the possibility to investigate the effects of changes to these cells.

6.3 *C. elegans* genetics and manipulability

The diploid genome of *C. elegans* is completely sequenced and comprises 100 million base pairs divided over six chromosomes, five autosomes and one sex chromosome (*C. elegans* sequencing consortium, 1998). The genetic map is freely available to all researchers and it is obtainable from the *C. elegans* Genetics Center (CGC). Furthermore, the CGC collects, maintains and distributes mutants that were generated and studied over the years. The *C. elegans* bibliography is also maintained at the CGC and they coordinate genetic nomenclature, as well as provide and update the *C. elegans* web server (*C. elegans* web server: http://elegans.swmed.edu). Nematode mutants can be obtained through forward and reverse genetics approaches. If not present at the CGC, additional mutants can be ordered from the *C. elegans* gene knock out consortium (http://celeganskoconsortium.omrf.org) or a mutant library can be made by the researcher (Zwaal *et al.*, 1993, Jansen *et al.*, 1997). Alternatively, knock-down of gene expression is easily performed by RNA interference (RNAi) in a number of ways. Firstly, dsRNAi targeted against the gene of interest can be injected in the animal after which it will spread through the animal and by the action of the dicer complex the mRNA of the gene of interest will be degraded. Secondly, the nematodes can be soaked in a solution containing the dsRNA that will be taken up in the intestine and spread through the worm body. Thirdly, the nematodes can be grown on bacteria that express a transgene producing dsRNA: the worms will digest the bacteria and internalize the dsRNA to exert its interfering effect (Ahringer, 2006). Fourthly, transgenic nematodes can be generated that harbor an extrachromosomal array consisting of plasmid DNA on which an inducible promoter regulates the expression of an inverted repeat derived from the gene that is targeted by the RNAi. Upon induction of this promoter the inverted repeat will be expressed, generating a double stranded RNA molecule that will knock-down the endogenous transcript. With the completion of the genome sequence, whole genome approaches became feasible and RNAi for all predicted coding sequences was started (Ahringer, 2006). An additional feature of the extensive *C. elegans* genetic toolset is transformation by microinjection of the hermaphrodite germline that allows generation of transgenic animals in less than a week (Mello *et al.*, 1991). A large set of expression vectors is available for promoter analysis, ectopic expression analysis, inducible expression, tagging of any sequence with different fluorescent proteins or LacZ, and for use in RNAi experiments (Mello and Fire, 1995). In addition, a comprehensive collection of methods to manipulate and investigate *C. elegans* ia available (Epstein and Shakes, 1995, WormMethods: http://www.wormbook.org/toc_wormmethods.html).

6.4 *C. elegans* as a model organism

After comparing the genomes of man and nematode, it became clear that many protein sequences are conserved. Thus many human genes, in which mutations have been found causing genetic diseases, have homologues in the nematode, of which the function could be studied (Culetto and Sattelle, 2000). Although extrapolating the results obtained with the relatively simple nematode to a complex mammalian system may be a complicated task, the nematode could shed light on protein function and the molecular mechanisms they play a role in and how changes in these proteins affect their normal function. With its great number of homologues to human genes and its excellent genetic, biochemical, and cell biological experimental possibilities, *C. elegans* appears to be an ideal model organism to investigate the processes underlying human genetic disorders.

7 Aim and outline of this thesis

Juvenile Neuronal Ceroid Lipofuscinosis is a devastating lysosomal storage disorder disease of childhood for which there is no cure. While it is known to be caused by mutations in the *CLN3* gene, this gene encodes a protein of unknown function. Although several mouse models and yeast models exist to study the processes underlying this disease, the molecular mechanisms leading to JNCL are unknown. The aim of the work described in this thesis has been to elucidate CLN3 function by the establishment and study of a nematode *Caenorhabditis elegans* model for JNCL. The information that would be acquired with the *C. elegans* model for JNCL was expected to be extrapolatable to other model organisms, e.g. the murine model, to provide better understanding of the pathology underlying JNCL, which might then lead to the development of new treatments.

In chapter 2, we explored the potential of *C. elegans* to be used as a model organism for lysosomal storage diseases and for studying different aspects of lysosomal function. Therefore, we identified *in silico* putative homologues of proteins involved in lysosomal storage diseases and other lysosomal proteins, by comparing the human protein sequences to all predicted protein sequences of *C. elegans*. In addition, we surveyed the available phenotypic information of nematodes with mutations in any of the homologues, in order to get an overview of possible lysosomal phenotypes in the nematode. The feasibility of using these phenotypes in genetic screens for modifier alleles was discussed.
To generate a nematode model for JNCL the *C. elegans* genes homologous to *CLN3* were identified. This nematode tuned out to have three homologues and characterization of the three worm *cln-3* genes and their protein sequences was performed. The first *cln-3* deletion mutant was reported and the initial analysis the *cln-3.1* mutant *C. elegans* strain was done (chapter 3).
The function of the three *cln-3* proteins may have diverged during evolution, but they also may have similar functions in different cells. Therefore, spatial and temporal expression patterns of the nematode *cln-3* genes were determined. *C. elegans cln-3* deletion mutants were generated and characterized with particular emphasis on the cell types in which the genes are expressed (chapter 4). Furthermore, the extensive genetic toolset that has been developed for investigations in the nematode has been exploited to examine worm *cln-3* gene function.
We could not detect storage material in *C. elegans cln-3* mutants, possibly due to the short life span of the nematode. Three weeks may not be sufficient for accumulation to occur. Therefore, we set out to induce accumulation of the main component of the storage material Subunit c of the mitochondrial ATP synthase. *C. elegans* that inducibly

overexpressed Subunit c were generated and studied. The results of this work are described in chapter 5.
The work described in this thesis is concluded by a general discussion in chapter 6, in which also future directions are provided.

References

Adams A, Gottschling DE, Kaiser CA, Stearns T. 1997. Methods in Yeast Genetics: A Cold Spring Harbor Laboratory Course Manual 9-17.

Aderem A, Underhill DM. 1999. Mechanisms of phagocytosis in macrophages. Annu Rev Immunol.17:593-623.

Ahringer J, ed. Reverse genetics. 2006. WormBook, ed. The C. elegans Research Community, WormBook, doi/10.1895/wormbook.1.47.1, http://www.wormbook.org.

Ahtiainen L, Van Diggelen OP, Jalanko A, Kopra O. 2003 Palmitoyl protein thioesterase 1 is targeted to the axons in neurons. J Comp Neurol. 455:368-77.

Amalfitano A, Bengur AR, Morse RP, Majure JM, Case LE, Veerling DL, Mackey J, Kishnani P, Smith W, McVie-Wylie A, Sullivan JA, Hoganson GE, Phillips JA III, Schaefer GB, Charrow J, Ware RE, Bossen EH, Chen YT. 2001. Recombinant human acid alpha-glucosidase enzyme therapy for infantile glycogen storage disease type II: results of a phase I/II clinical trial. Genet. Med. 3: 132-138.

Andrews NW. Regulated secretion of conventional lysosomes. 2000 Trends Cell Biol. 10:316-21.

Anikster Y, Shotelersuk V, Gahl WA. 1999. CTNS mutations in patients with cystinosis. Hum Mutat. 14:454-8.

d'Azzo A, Andria G, Strisciuglio P, Galjaard H. 2001. Galactosialidosis, In: The Metabolic and Molecular Basis of Inherited Disease. Scriver CR, Valle D, Beaudet AL, Sly WS (editors). McGraw-Hill Professional Book Group: New York, USA

Bainton DF. The discovery of lysosomes. J Cell Biol. 1981 Dec;91(3 Pt 2):66s-76s.

Bargal R, Avidan N, Ben-Asher E, Olender Z, Zeigler M, Frumkin A, Raas-Rothschild A, Glusman G, Lancet D, Bach G. 2000. Identification of the gene causing mucolipidosis type IV. Nature Genet. 26:118-121.

Barton NW, Furbish FS, Murray GJ, Garfield M, Brady RO. 1990. Therapeutic response to intravenous infusions of glucocerebrosidase in a patient with Gaucher disease. Proc Natl Acad Sci U S A. 87:1913-6.

Beck M. 2007. New therapeutic options for lysosomal storage disorders: enzyme replacement, small molecules and gene therapy. Hum Genet. 121:1-22

Bernardini F, Warburton MJ. 2001. The substrate range of tripeptidyl-peptidase I. Eur J Paediatr Neurol. 5 Suppl A:69-72.

Bessa C, Teixeira CA, Mangas M, Dias A, Sa Miranda MC, Guimaraes A, Ferreira JC, Canas N, Cabral P, Ribeiro MG. 2006. Two novel CLN5 mutations in a Portuguese patient with vLINCL: Insights into molecular mechanisms of CLN5 deficiency. Mol Genet Metab. In press.

Beutler E, Grabowski GA. 2001. Gaucher disease, In: The Metabolic and Molecular Basis of Inherited Disease. Scriver CR, Valle D, Beaudet AL, Sly WS (editors). McGraw-Hill Professional Book Group: New York, USA

Blott EJ, Griffiths GM. 2002 Secretory lysosomes. Nat Rev Mol Cell Biol 3:122-31

Brenner S. 1974. The genetics of Caenorhabditis elegans. Genetics 77:71-94.

Bright NA, Gratian MJ, Luzio JP. 2005. Endocytic delivery to lysosomes mediated by concurrent fusion and kissing events in living cells. Curr Biol. 15:360-5.

Bronson RT, Lake BD, Cook S, Taylor S, Davisson MT. 1993. Motor neuron degeneration of mice is a model of neuronal ceroid lipofuscinosis (Batten's disease). Ann Neurol. 33:381-5.

Bronson RT, Donahue LR, Johnson KR, Tanner A, Lane PW, Faust JR. 1998. Neuronal ceroid lipofuscinosis (nclf), a new disorder of the mouse linked to chromosome 9. Am J Med Genet. 77:289-97.

Brooks AI, Chattopadhyay S, Mitchison HM, Nussbaum RL, Pearce DA. 2003. Functional categorization of gene expression changes in the cerebellum of a Cln3-knockout mouse model for Batten disease. Mol Genet Metab. 78:17-30.

Broom MF, Zhou C. 2001. Fine mapping of ovine ceroid lipofuscinosis confirms orthology with CLN6. Eur J Paediatr Neurol. 5 Suppl A:33-5.

Brown WJ, Goodhouse J, Farquhar MG. Mannose-6-phosphate receptors for lysosomal enzymes cycle between the Golgi complex and endosomes. J Cell Biol. 1986 Oct;103(4):1235-47.

Camp LA, Verkruyse LA, Afendis SJ, Slaughter CA, Hofmann SL. 1994. Molecular cloning and expression of palmitoyl-protein thioesterase. J. Biol. Chem. 269:23212-23219.

Cao Y, Espinola JA, Fossale E, Massey AC, Cuervo AM, MacDonald ME, Cotman SL. 2006. Autophagy is disrupted in a knock-in mouse model of juvenile neuronal ceroid lipofuscinosis. J Biol Chem. 281:20483-93.

Charron P, Villard E, Sebillon P, Laforet P, Maisonobe T, Duboscq-Bidot L, Romero N, Drouin-Garraud V, Frebourg T, Richard P, Eymard B, Komajda M. 2004. Danon's disease as a cause of hypertrophic cardiomyopathy: a systematic survey. Heart 90:842-846.

Chattopadhyay S, Pearce DA. 2002. Interaction with Btn2p is required for localization of Rsglp: Btn2p-mediated changes in arginine uptake in Saccharomyces cerevisiae. Eukaryot Cell. 1:606-12.

Chattopadhyay S, Roberts PM, Pearce DA. 2003. The yeast model for Batten disease: a role for Btn2p in the trafficking of the Golgi-associated vesicular targeting protein, Yif1p. Biochem Biophys Res Commun. 302:534-8.

Chattopadhyay S, Kingsley E, Serour A, Curran TM, Brooks AI, Pearce DA. 2004. Altered gene expression in the eye of a mouse model for batten disease. Invest Ophthalmol Vis Sci. 45:2893-905.

Chen CS, Bach G, Pagano RE. 1998. Abnormal transport along the lysosomal pathway in mucolipidosis, type IV disease. Proc Nat Acad Sci. 95:6373-6378.

Cho S, Dawson G. 2000 Palmitoyl protein thioesterase 1 protects against apoptosis mediated by Ras-Akt-caspase pathway in neuroblastoma cells. J Neurochem. 74:1478-88.

Conner SD, Schmid SL. Regulated portals of entry into the cell. Nature. 2003 Mar 6;422(6927):37-44.

Cooper JD, Russell C, Mitchison HM. 2006. Progress towards understanding disease mechanisms in small vertebrate models of neuronal ceroid lipofuscinosis. Biochim Biophys Acta. 1762:873-89

Cosma MP, Pepe S, Annunziata I, Newbold RF, Grompe M, Parenti G, Ballabio A. 2003. The multiple sulfatase deficiency gene encodes an essential and limiting factor for the activity of sulfatases. Cell. 113: 445-456.

Corpet F. 1988. Multiple sequence alignment with hierarchical clustering. Nucleic Acids Res. 16:10881-90.

Cotman SL, Vrbanac V, Lebel LA, Lee RL, Johnson KA, Donahue LR, Teed AM, Antonellis K, Bronson RT, Lerner TJ, MacDonald ME. 2002. Cln3(Deltaex7/8) knock-in mice with the common JNCL mutation exhibit progressive neurologic disease that begins before birth. Hum Mol Genet. 11:2709-21.

Croopnick JB, Choi HC, Mueller DM. 1998. The subcellular location of the yeast Saccharomyces cerevisiae homologue of the protein defective in the juvenile form of Batten disease. Biochem Biophys Res Commun. 250:335-41.

Culetto E, Sattelle DB. 2000. A role for Caenorhabditis elegans in understanding the function and interactions of human disease genes. Hum Mol Genet. 9:869-77.

Das AM, Kohlschutter A. 1996. Decreased activity of the mitochondrial ATP-synthase in fibroblasts from children with late-infantile and juvenile neuronal ceroid lipofuscinosis. J Inherit Metab Dis. 19:130-2.

DE DUVE C. The lysosome. Sci Am. 1963 May;208:64-72.

Dell'Angelica EC, Shotelersuk V, Aguilar RC, Gahl WA, Bonifacino JS. 1999. Altered trafficking of lysosomal proteins in Hermansky-Pudlak syndrome due to mutations in the beta-3A subunit of the AP-3 adaptor. Molec Cell. 3:11-21.

Dell'Angelica EC. 2004. The building BLOC(k)s of lysosomes and related organelles.
Curr Opin Cell Biol. 16:458-64.

Dierks T, Schmidt B, Borissenko LV, Peng J, Preusser A, Mariappan M, von Figura K. 2003 Multiple sulfatase deficiency is caused by mutations in the gene encoding the human C(alpha)-formylglycine generating enzyme. Cell. 113:435-44.

van Diggelen OP, Keulemans JL, Winchester B, Hofman IL, Vanhanen SL, Santavuori P, Voznyi YV. 1999 A rapid fluorogenic palmitoyl-protein thioesterase assay: pre- and postnatal diagnosis of INCL. Mol Genet Metab. 66:240-4.

van Diggelen OP, Thobois S, Tilikete C, Zabot MT, Keulemans JL, van Bunderen PA, Taschner PE, Losekoot M, Voznyi YV. 2001. Adult neuronal ceroid lipofuscinosis with palmitoyl-protein thioesterase deficiency: first adult-onset patients of a childhood disease. Ann Neurol. 50:269-72.

Di Pietro SM, Falcon-Perez JM, Dell'Angelica EC. 2004. Characterization of BLOC-2, a complex containing the Hermansky-Pudlak syndrome proteins HPS3, HPS5 and HPS6. Traffic. 5:276-83.

Elshatory Y, Brooks AI, Chattopadhyay S, Curran TM, Gupta P, Ramalingam V, Hofmann SL, Pearce DA. 2003. Early changes in gene expression in two models of Batten disease. FEBS Lett. 538:207-12.

Entian KD, Schuster T, Hegemann JH, Becher D, Feldmann H, Guldener U, Gotz R, Hansen M, Hollenberg CP, Jansen G, Kramer W, Klein S, Kotter P, Kricke J, Launhardt H, Mannhaupt G, Maierl A, Meyer P, Mewes W, Munder T, Niedenthal RK, Ramezani Rad M, Rohmer A, Romer A, Hinnen A. 1999. Functional analysis of 150 deletion mutants in Saccharomyces cerevisiae by a systematic approach Mol Gen Genet. 262:683-702.

Epstein HF, Shakes DC. 1995. Methods in Cell Biology: *C. elegans* modern biological analysis of an organism. Volume 48, Academic Press, San Diego.

Eskelinen EL, Tanaka Y, Saftig P. 2003. At the acidic edge: emerging functions for lysosomal membrane proteins. Trends Cell Biol. 13:137-45.

Ezaki J, Takeda-Ezaki M, Koike M, Ohsawa Y, Taka H, Mineki R, Murayama K, Uchiyama Y, Ueno T, Kominami E. 2003. Characterization of Cln3p, the gene product responsible for juvenile neuronal ceroid lipofuscinosis, as a lysosomal integral membrane glycoprotein. J Neurochem. 87:1296-308.

Von Figura K Gieselmann V, Jaeken J. 2001. Metachromatic Leukodystrophy, In: The Metabolic and Molecular Basis of Inherited Disease. Scriver CR, Valle D, Beaudet AL, Sly WS (editors). McGraw-Hill Professional Book Group: New York, USA

Fossale E, Wolf P, Espinola JA, Lubicz-Nawrocka T, Teed AM, Gao H, Rigamonti D, Cattaneo E, MacDonald ME, Cotman SL. 2004. Membrane trafficking and mitochondrial abnormalities precede Subunit c deposition in a cerebellar cell model of juvenile neuronal ceroid lipofuscinosis. BMC Neurosci. 5:57.

Futerman AH, van Meer G. The cell biology of lysosomal storage disorders. Nat Rev Mol Cell Biol. 2004 Jul;5(7):554-65.

Gachet Y, Codlin S, Hyams JS, Mole SE. 2005. btn1, the Schizosaccharomyces pombe homologue of the human Batten disease gene CLN3, regulates vacuole homeostasis. J Cell Sci. 118:5525-36.

Gahl WA. 2003. Early oral cysteamine therapy for nephropathic cystinosis. Eur J Pediatr. 162 Suppl 1:S38-41.

Gao H, Boustany RM, Espinola JA, Cotman SL, Srinidhi L, Antonellis KA, Gillis T, Qin X, Liu S, Donahue LR, Bronson RT, Faust JR, Stout D, Haines JL, Lerner TJ, MacDonald ME. 2002 Mutations in a novel CLN6-encoded transmembrane protein cause variant neuronal ceroid lipofuscinosis in man and mouse. Am J Hum Genet 70:324-35.

Glaser RL, Hickey AJ, Chotkowski HL, Chu-LaGraff Q. 2003 Characterization of Drosophila palmitoyl-protein thioesterase 1. Gene 312:271-9.

Goebel HH, Mole SE, Lake BD, editors. 1999. The neuronal ceroid lipofuscinosis (Batten disease). Amsterdam: IOS Press.

Golabek AA, Kaczmarski W, Kida E, Kaczmarski A, Michalewski MP, Wisniewski KE. 1999. Expression studies of CLN3 protein (battenin) in fusion with the green fluorescent protein in mammalian cells *in vitro*. Mol Genet Metab. 66:277-82.

Golabek AA, Kida E, Walus M, Kaczmarski W, Michalewski M, Wisniewski KE. 2000. CLN3 protein regulates lysosomal pH and alters intracellular processing of Alzheimer's amyloid-beta protein precursor and cathepsin D in human cells. Mol Genet Metab. 70:203-13.

Grabowski GA. 2005. Recent clinical progress in Gaucher disease. Curr Opin Pediatr. 17:519-24.

Gravel RA, Kaback MM, Proia RL, Sandhoff K, Suzuki K, Suzuki K. 2001. The GM2 gangliosidoses, In: The Metabolic and Molecular Basis of Inherited Disease. Scriver CR, Valle D, Beaudet AL, Sly WS (editors). McGraw-Hill Professional Book Group: New York, USA

Gupta P, Soyombo AA, Atashband A, Wisniewski KE, Shelton JM, Richardson JA, Hammer RE, Hofmann SL. 2001 Disruption of PPT1 or PPT2 causes neuronal ceroid lipofuscinosis in knockout mice. Proc. Nat. Acad. Sci. 98:13566-13571.

Haskell RE, Derksen TA, Davidson BL. 1999. Intracellular trafficking of the JNCL protein CLN3. Mol Genet Metab. 66:253-60.

Haskell RE, Carr CJ, Pearce DA, Bennett MJ, Davidson BL. 2000. Batten disease: evaluation of CLN3 mutations on protein localization and function. Hum Mol Genet. 9:735-44.

HERS HG. 1963. alpha-Glucosidase deficiency in generalized glycogenstorage disease (Pompe's disease). Biochem J. 86:11-6

Hirschhorn R, Reuser AJJ. 2001. Glycogen storage disease Type II: Acid α-glucosidase (Acid maltase) deficiency, In: The Metabolic and Molecular Basis of Inherited Disease. Scriver CR, Valle D, Beaudet AL, Sly WS (editors). McGraw-Hill Professional Book Group: New York, USA

Hodgkin J, Doniach T. 1997. Natural variation and copulatory plug formation in Caenorhabditis elegans. Genetics. 146:149–164.

Holopainen JM, Saarikoski J, Kinnunen PK, Jarvela I. 2001. Elevated lysosomal pH in neuronal ceroid lipofuscinoses (NCLs). Eur J Biochem. 268:5851-6.

Van den Hout JM, Kamphoven JH, Winkel LP, Arts WF, De Klerk JB, Loonen MC, Vulto AG, Cromme-Dijkhuis A, Weisglas-Kuperus N, Hop W, Van Hirtum H, Van Diggelen OP, Boer M, Kroos MA, Van Doorn PA, Van der Voort E, Sibbles B, Van Corven EJ, Brakenhoff JP, Van Hove J, Smeitink JA, de Jong G, Reuser AJ, Van der Ploeg AT. 2004. Long-term intravenous treatment of Pompe disease with recombinant human alpha-glucosidase from milk. Pediatrics. 113:e448-57.

Huizing M, Anikster Y, Gahl WA. 2001. Hermansky-Pudlak syndrome and Chediak-Higashi syndrome: disorders of vesicle formation and trafficking. Thromb Haemost. 86:233-45.

Hurtado-Lorenzo A, Skinner M, El Annan J, Futai M, Sun-Wada GH, Bourgoin S, Casanova J, Wildeman A, Bechoua S, Ausiello DA, Brown D, Marshansky V. 2006. V-ATPase interacts with ARNO and Arf6 in early endosomes and regulates the protein degradative pathway. Nat Cell Biol. 8:124-36.

IBDC (The International Batten Disease Consortium). 1995. Isolation of a novel gene underlying Batten disease, CLN3. Cell 82:949-57.

Introne W, Boissy RE, Gahl WA. 1999. Clinical, molecular, and cell biological aspects of Chediak-Higashi syndrome. Mol Genet Metab. 68:283-303.

Isosomppi J, Heinonen O, Hiltunen JO, Greene ND, Vesa J, Uusitalo A, Mitchison HM, Saarma M, Jalanko A, Peltonen L. 1999. Developmental expression of palmitoyl protein thioesterase in normal mice. Brain Res Dev Brain Res. 118:1-11.

Isosomppi J, Vesa J, Jalanko A, Peltonen L. 2002. Lysosomal localization of the neuronal ceroid lipofuscinosis CLN5 protein. Hum Mol Genet. 11:885-91.

Iwaki T, Goa T, Tanaka N, Takegawa K. 2004. Characterization of Schizosaccharomyces pombe mutants defective in vacuolar acidification and protein sorting. Mol Genet Genomics. 271:197-207.

Jalanko A, Vesa J, Manninen T, von Schantz C, Minye H, Fabritius AL, Salonen T, Rapola J, Gentile M, Kopra O, Peltonen L. 2005. Mice with Ppt1Deltaex4 mutation replicate the INCL phenotype and show an inflammation-associated loss of interneurons. Neurobiol Dis. 18:226-41.

Jansen G, Hazendonk E, Thijssen KL, Plasterk RH.1997. Reverse genetics by chemical mutagenesis in Caenorhabditis elegans. Nat Genet. 17:119-21.

Jarvela I, Sainio M, Rantamaki T, Olkkonen VM, Carpen O, Peltonen L, Jalanko A. 1998. Biosynthesis and intracellular targeting of the CLN3 protein defective in Batten disease. Hum Mol Genet. 7:85-90.

Jolly RD, Brown S, Das AM, Walkley SU. 2002. Mitochondrial dysfunction in the neuronal ceroid-lipofuscinoses (Batten disease). Neurochem Int. 40:565-71.

Kaczmarski W, Wisniewski KE, Golabek A, Kaczmarski A, Kida E, Michalewski M. 1999. Studies of membrane association of CLN3 protein. Mol Genet Metab. 66:261-4.

Karim MA, Nagle DL, Kandil HH, Burger J, Moore KJ, Spritz RA. 1997. Mutations in the Chediak-Higashi syndrome gene (CHS1) indicate requirement for the complete 3801 amino acid CHS protein. Hum Molec Genet. 6:1087-1089.

Katz ML, Shibuya H, Liu PC, Kaur S, Gao CL, Johnson GS. 1999. A mouse gene knockout model for juvenile ceroid-lipofuscinosis (Batten disease). J Neurosci Res. 57:551-6.

Ketting RF, Haverkamp TH, van Luenen HG, Plasterk RH. 1999. Mut-7 of C. elegans, required for transposon silencing and RNA interference, is a homolog of Werner syndrome helicase and RNaseD. Cell. 99:133-41.

Kim Y, Ramirez-Montealegre D, Pearce DA. 2003. A role in vacuolar arginine transport for yeast Btn1p and for human CLN3, the protein defective in Batten disease. Proc Natl Acad Sci U S A. 100:15458-62.

Kim Y, Chattopadhyay S, Locke S, Pearce DA. 2005. Interaction among Btn1p, Btn2p, and Ist2p reveals potential interplay among the vacuole, amino acid levels, and ion homeostasis in the yeast Saccharomyces cerevisiae. Eukaryot Cell. 4:281-8.

Kim SJ, Zhang Z, Hitomi E, Lee YC, Mukherjee AB. 2006. Endoplasmic reticulum stress-induced caspase-4 activation mediates apoptosis and neurodegeneration in INCL. Hum Mol Genet. 15:1826-34.

Kitamoto K, Yoshizawa K, Ohsumi Y, Anraku Y. 1988. Dynamic aspects of vacuolar and cytosolic amino acid pools of Saccharomyces cerevisiae. J Bacteriol. 170:2683-6.

Kopra O, Vesa J, von Schantz C, Manninen T, Minye H, Fabritius AL, Rapola J, van Diggelen OP, Saarela J, Jalanko A, Peltonen L. 2004. A mouse model for Finnish variant late infantile neuronal ceroid lipofuscinosis, CLN5, reveals neuropathology associated with early aging. Hum Mol Genet. 13:2893-906.

Korey CA, MacDonald ME. 2003 An over-expression system for characterizing Ppt1 function in Drosophila. BMC Neurosci. 4:30.

Kornfeld S, Sly WS. 2001. I-Cell disease and Pseudo-Hurler Polydystrophy: Disorders of Lysosomal Enzyme Phosphorylation and Localization. In: The Metabolic and Molecular Basis of Inherited Disease. Scriver CR, Valle D, Beaudet AL, Sly WS (editors). McGraw-Hill Professional Book Group: New York, USA

Kramer H, Phistry M. 1996. Mutations in the Drosophila hook gene inhibit endocytosis of the boss transmembrane ligand into multivesicular bodies. J Cell Biol. 133:1205-15.

Kramer H, Phistry M. 1999. Genetic analysis of hook, a gene required for endocytic trafficking in drosophila. Genetics. 151:675-84.

Kyttala A, Ihrke G, Vesa J, Schell MJ, Luzio JP. 2004. Two motifs target Batten disease protein CLN3 to lysosomes in transfected nonneuronal and neuronal cells. Mol Biol Cell. 15:1313-23.

Landrieu P, Blanche S, Vanier MT, Metral S, Husson B, Sandhoff K, Fischer A. 1998. Bone marrow transplantation in metachromatic leukodystrophy caused by saposin-B deficiency: a case report with a 3-year follow-up period. J Pediatr. 133:129-32.

Li W, Rusiniak ME, Chintala S, Gautam R, Novak EK, Swank RT. 2004. Murine Hermansky-Pudlak syndrome genes: regulators of lysosome-related organelles. Bioessays. 26:616-28.

Lin L, Sohar I, Lackland H, Lobel P. 2001. The human CLN2 protein/tripeptidyl-peptidase I is a serine protease that autoactivates at acidic pH. J Biol Chem. 276: 2249-2255.

Liscum L. Niemann-Pick type C mutations cause lipid traffic jam. Traffic. 2000 Mar;1(3):218-25.

Lonka L, Kyttala A, Ranta S, Jalanko A, Lehesjoki AE. 2000. The neuronal ceroid lipofuscinosis CLN8 membrane protein is a resident of the endoplasmic reticulum. Hum Mol Genet. 9:1691-7.

Lonka L, Salonen T, Siintola E, Kopra O, Lehesjoki AE, Jalanko A. 2004. Localization of wild-type and mutant neuronal ceroid lipofuscinosis CLN8 proteins in non-neuronal and neuronal cells. J Neurosci Res. 76:862-71.

Lonka L, Aalto A, Kopra O, Kuronen M, Kokaia Z, Saarma M, Lehesjoki AE. 2005. The neuronal ceroid lipofuscinosis Cln8 gene expression is developmentally regulated in mouse brain and up-regulated in the hippocampal kindling model of epilepsy. BMC Neurosci. 6:27.

Lu JY, Hofmann SL. 2006. Thematic review series: lipid posttranslational modifications. Lysosomal metabolism of lipid-modified proteins. J Lipid Res. 47:1352-7.

Luiro K, Kopra O, Blom T, Gentile M, Mitchison HM, Hovatta I, Tornquist K, Jalanko A. 2006. Batten disease (JNCL) is linked to disturbances in mitochondrial, cytoskeletal, and synaptic compartments. J Neurosci Res. 84:1124-38.

Luzio JP, Poupon V, Lindsay MR, Mullock BM, Piper RC, Pryor PR. Membrane dynamics and the biogenesis of lysosomes. Mol Membr Biol. 2003 Apr-Jun;20(2):141-54.

Mannhaupt G, Stucka R, Ehnle S, Vetter I, Feldmann H. 1994. Analysis of a 70 kb region on the right arm of yeast chromosome II. Yeast. 10:1363-81.

Matern H, Yang X, Andrulis E, Sternglanz R, Trepte HH, Gallwitz D. 2000. A novel Golgi membrane protein is part of a GTPase-binding protein complex involved in vesicle targeting. Embo J 19: 4485-92.

Mellman I, Fuchs R, Helenius A. 1986. Acidification of the endocytic and exocytic pathways. Annu Rev Biochem. 55:663-700.

Mellman I. 1992. The importance of being acid: the role of acidification in intracellular membrane traffic. J Exp Biol. 172:39-45.

Mellman I, Warren G. 2000. The road taken: past and future foundations of membrane traffic. Cell. 100:99-112.

Mello CC, Kramer JM, Stinchcomb D, Ambros V. 1991. Efficient gene transfer in C.elegans: extrachromosomal maintenance and integration of transforming sequences. EMBO J. 10:3959-70.

Mello C, Fire A. 1995. DNA transformation. Methods Cell Biol. 48:451-82.

Michalewski MP, Kaczmarski W, Golabek AA, Kida E, Kaczmarski A, Wisniewski KE. 1999. Posttranslational modification of CLN3 protein and its possible functional implication. Mol Genet Metab. 66:272-6.

Mitchison HM, Taschner PE, Kremmidiotis G, Callen DF, Doggett NA, Lerner TJ, Janes RB, Wallace BA, Munroe PB, O'Rawe AM, Gardiner RM, Mole SE. 1997. Structure of the CLN3 gene and predicted structure, location and function of CLN3 protein. Neuropediatrics. 28:12-4.

Mitchison HM, Bernard DJ, Greene ND, Cooper JD, Junaid MA, Pullarkat RK, de Vos N, Breuning MH, Owens JW, Mobley WC, Gardiner RM, Lake BD, Taschner PE, Nussbaum RL. 1999. Targeted disruption of the Cln3 gene provides a mouse model for Batten disease. The Batten Mouse Model Consortium. Neurobiol Dis. 6:321-34.

Mole SE, Mitchison HM, Munroe PB. Molecular basis of the neuronal ceroid lipofuscinoses: mutations in CLN1, CLN2, CLN3, and CLN5. Hum Mutat. 1999;14(3):199-215.

Mole SE, Zhong NA, Sarpong A, Logan WP, Hofmann S, Yi W, Franken PF, van Diggelen OP, Breuning MH, Moroziewicz D, Ju W, Salonen T, Holmberg V, Jarvela I, Taschner PE. 2001. New mutations in the neuronal ceroid lipofuscinosis genes. Eur J Paediatr Neurol.;5 Suppl A:7-10.

Mole SE, Michaux G, Codlin S, Wheeler RB, Sharp JD, Cutler DF. 2004. CLN6, which is associated with a lysosomal storage disease, is an endoplasmic reticulum protein. Exp Cell Res. 298:399-406.

Murphy RF. Maturation models for endosome and lysosome biogenesis. Trends Cell Biol. 1991 Oct;1(4):77-82.

Myllykangas L, Tyynela J, Page-McCaw A, Rubin GM, Haltia MJ, Feany MB. 2005. Cathepsin D-deficient Drosophila recapitulate the key features of neuronal ceroid lipofuscinoses. Neurobiol Dis. 19:194-9.

Nazarian R, Falcon-Perez JM, Dell'Angelica EC. 2003. Biogenesis of lysosome-related organelles complex 3 (BLOC-3): a complex containing the Hermansky-Pudlak syndrome (HPS) proteins HPS1 and HPS4. Proc Natl Acad Sci U S A. 100:8770-5.

Neufeld EF. 1989 Natural history and inherited disorders of a lysosomal enzyme, beta-hexosaminidase. J Biol Chem. 264:10927-30.

Nishi T, Forgac M. 2002. The vacuolar (H+)-ATPases--nature's most versatile proton pumps. Nat Rev Mol Cell Biol. 3:94-103.

Osorio N, Carvalho A, Almeida A, Padilla-Lopez S, Ludovico P, Leao C, Pearce DA, Rodrigues F. 2006. Nitric oxide signaling pathway is disrupted in the yeast model for Batten disease. Embo J. (Manuscript submitted).

Oswald MJ, Palmer DN, Kay GW, Shemilt SJ, Rezaie P, Cooper JD. 2005. Glial activation spreads from specific cerebral foci and precedes neurodegeneration in presymptomatic ovine neuronal ceroid lipofuscinosis (CLN6). Neurobiol Dis. 20:49-63.

Padilla-Lopez S, Pearce DA. 2006. Saccharomyces cerevisiae lacking Btn1p modulate vacuolar ATPase activity to regulate pH imbalance in the vacuole. J Biol Chem. 281:10273-80.

Palmer DN, Fearnley IM, Walker JE, Hall NA, Lake BD, Wolfe LS, Haltia M, Martinus RD, Jolly RD. 1992. Mitochondrial ATP synthase Subunit c storage in the ceroid-lipofuscinoses (Batten disease). Am J Med Genet 42:561-7.

Passini MA, Dodge JC, Bu J, Yang W, Zhao Q, Sondhi D, Hackett NR, Kaminsky SM, Mao Q, Shihabuddin LS, Cheng SH, Sleat DE, Stewart GR, Davidson BL, Lobel P, Crystal RG. 2006, Intracranial delivery of CLN2 reduces brain pathology in a mouse model of classical late infantile neuronal ceroid lipofuscinosis. J Neurosci. 26:1334-42.

Pearce DA, Sherman F. 1998. A yeast model for the study of Batten disease. Proc Natl Acad Sci U S A. 95:6915-8.

Pearce DA, Nosel SA, Sherman F. 1999a. Studies of pH regulation by Btn1p, the yeast homolog of human Cln3p. Mol Genet Metab. 66:320-3.

Pearce DA, Ferea T, Nosel SA, Das B, Sherman F. 1999b. Action of BTN1, the yeast orthologue of the gene mutated in Batten disease. Nat Genet. 22:55-8.

Pearce DA, Carr CJ, Das B, Sherman F. 1999c. Phenotypic reversal of the btn1 defects in yeast by chloroquine: a yeast model for Batten disease. Proc Natl Acad Sci U S A. 96:11341-5.

Pearce DA. 2000. Localization and processing of CLN3, the protein associated to Batten disease: where is it and what does it do? J Neurosci Res. 59:19-23.

Phillips SN, Benedict JW, Weimer JM, Pearce DA. 2005. CLN3, the protein associated with batten disease: structure, function and localization. J Neurosci Res. 79:573-83.

Phillips SN, Muzaffar N, Codlin S, Korey CA, Taschner PEM, de Voer G, Mole SE, Pearce DA. 2006. Characterizing pathogenic processes in Batten disease: Use of small eukaryotic model systems. Biochim Biophys Acta. 1762:906-19.

Phillips SN, Wolfe DW, Seehafer SS, Pearce DA. 2006. A BTN1 deletion strain requires tight control of arginine levels. Hum Mol Genet. (Manuscript in preparation).

Pineda-Trujillo N, Cornejo W, Carrizosa J, Wheeler RB, Munera S, Valencia A, Agudelo-Arango J, Cogollo A, Anderson G, Bedoya G, Mole SE, Ruiz-Linares A. 2005. A CLN5 mutation causing an atypical neuronal ceroid lipofuscinosis of juvenile onset. Neurology. 64:740-2.

LaPlante JM, Ye CP, Quinn SJ, Goldin E, Brown EM, Slaugenhaupt SA, Vassilev PM. 2004. Functional links between mucolipin-1 and Ca(2+)-dependent membrane trafficking in mucolipidosis IV. Biochem. Biophys. Res. Commun. 322:1384-1391.

Pompe JC. 1932. Over idiopathische hypertrophie van het hart. Ned Tijdschr Geneeskd. 76:304-312.

Porter MY, Turmaine M, Mole SE. 2005 Identification and characterization of Caenorhabditis elegans palmitoyl protein thioesterase1. J Neurosci Res. 79:836-48.

Pullarkat RK, Morris GN. 1997. Farnesylation of Batten disease CLN3 protein. Neuropediatrics. 28:42-4.

Ramirez-Montealegre D, Pearce DA. 2005. Defective lysosomal arginine transport in juvenile Batten disease. Hum Mol Genet. 14:3759-73.

Rafi MA, Zhang XL, DeGala G, Wenger DA. 1990. Detection of a point mutation in sphingolipid activator protein-1 mRNA in patients with a variant form of metachromatic leukodystrophy. Biochem Biophys Res Commun. 166:1017-23.

Rafi MA, Amini S, Zhang XL, Wenger DA. 1992. Correction of sulfatide metabolism after transfer of prosaposin cDNA to cultured cells from a patient with SAP-1 deficiency. Am J Hum Genet. 50:1252-8.

Ranta S, Zhang Y, Ross B, Lonka L, Takkunen E, Messer A, Sharp J, Wheeler R, Kusumi K, Mole S, Liu W, Soares MB, Bonaldo MF, Hirvasniemi A, de la Chapelle A, Gilliam TC, Lehesjoki AE. 1999. The neuronal ceroid lipofuscinoses in human EPMR and mnd mutant mice are associated with mutations in CLN8. Nat Genet. 23:233-6.

Ranta S, Topcu M, Tegelberg S, Tan H, Ustubutun A, Saatci I, Dufke A, Enders H, Pohl K, Alembik Y, Mitchell WA, Mole SE, Lehesjoki AE. 2004. Variant late infantile neuronal ceroid lipofuscinosis in a subset of Turkish patients is allelic to Northern epilepsy. Hum Mutat 23:300-5.

Rapola. 1993. Neuronal Ceroid Lipofuscinsoses in Childhood. Perspect Pediatr Pathol 17:7-44.

Regenberg B, During-Olsen L, Kielland-Brandt MC, Holmberg S. 1999. Substrate specificity and gene expression of the amino-acid permeases in Saccharomyces cerevisiae. Curr Genet. 36:317-28.

Richardson SC, Winistorfer SC, Poupon V, Luzio JP, Piper RC. 2004. Mammalian late vacuole protein sorting orthologues participate in early endosomal fusion and interact with the cytoskeleton. Mol Biol Cell. 15:1197-210.

Riddle DL, Blumenthal T, Meyer BJ, Priess JR (editors). 1997. *C. elegans* II. Cold Spring Harbor Laboratory Press, Cold Spring Harbor, NY.

Santavuori P, Rapola J, Nuutila A, Raininko R, Lappi M, Launes J, Herva R, Sainio K. 1991. The spectrum of Jansky-Bielschowsky disease. Neuropediatrics. 2:92-6.

Savukoski M, Klockars T, Holmberg V, Santavuori P, Lander ES, Peltonen L. 1998. CLN5, a novel gene encoding a putative transmembrane protein mutated in Finnish variant late infantile neuronal ceroid lipofuscinosis. Nat Genet. 19:286-8.

Schuchman EH, Desnick RJ. 2001. Niemann-Pick Disease Types A and B: Acid Sphingomyelinase Deficiencies. In: The Metabolic and Molecular Basis of Inherited Disease. Scriver CR, Valle D, Beaudet AL, Sly WS (editors). McGraw-Hill Professional Book Group: New York, USA

Schulz A, Dhar S, Rylova S, Dbaibo G, Alroy J, Hagel C, Artacho I, Kohlschutter A, Lin S, Boustany RM. 2004. Impaired cell adhesion and apoptosis in a novel CLN9 Batten disease variant. Ann Neurol. 56:342-50.

Schulz A, Mousallem T, Venkataramani M, Persaud-Sawin DA, Zucker A, Luberto C, Bielawska A, Bielawski J, Holthuis JC, Jazwinski SM, Kozhaya L, Dbaibo GS, Boustany RM. 2006. The CLN9 protein, a regulator of dihydroceramide synthase. J Biol Chem. 281:2784-94.

Scriver CR, Valle D, Beaudet AL, Sly WS (editors). 2001. The Metabolic and Molecular Basis of Inherited Disease. McGraw-Hill Professional Book Group: New York, USA

Siintola E, Partanen S, Stromme P, Haapanen A, Haltia M, Maehlen J, Lehesjoki AE, Tyynela J. 2006. Cathepsin D deficiency underlies congenital human neuronal ceroid-lipofuscinosis. Brain. 129:1438-45.

Sleat DE, Donnelly RJ, Lackland H, Liu CG, Sohar I, Pullarkat RK, Lobel P. 1997. Association of mutations in a lysosomal protein with classical late-infantile neuronal ceroid lipofuscinosis. *Science* 277:1802-1805.

Sleat DE, Wiseman JA, El-Banna M, Kim KH, Mao Q, Price S, Macauley SL, Sidman RL, Shen MM, Zhao Q, Passini MA, Davidson BL, Stewart GR, Lobel P. 2004. A mouse model of classical late-infantile neuronal ceroid lipofuscinosis based on targeted disruption of the CLN2 gene results in a loss of tripeptidyl-peptidase I activity and progressive neurodegeneration. J Neurosci. 24:9117-26.

Spritz RA. 1999A. Multi-organellar disorders of pigmentation: tied up in traffic. Clin Genet. 55:309-17.

Spritz RA. 1999B. Multi-organellar disorders of pigmentation: intracellular traffic jams in mammals, flies and yeast. Trends Genet. 15:337-40.

Starzyk K, Richards S, Yee J, Smith SE, Kingma W. 2007. The long-term international safety experience of imiglucerase therapy for Gaucher disease. Mol Genet Metab. 90:157-63.

Steinfeld R, Reinhardt K, Schreiber K, Hillebrand M, Kraetzner R, Bruck W, Saftig P, Gartner J. 2006. Cathepsin D deficiency is associated with a human neurodegenerative disorder. Am J Hum Genet. 78:988-98.

Storrie B, Desjardins M. The biogenesis of lysosomes: is it a kiss and run, continuous fusion and fission process? Bioessays. 1996 Nov;18(11):895-903.

Sugie K, Yamamoto A, Murayama K, Oh SJ, Takahashi M, Mora M, Riggs JE, Colomer J, Iturriaga C, Meloni A, Lamperti C, Saitoh S, Byrne E, DiMauro S, Nonaka I, Hirano M, Nishino I. 2002. Clinicopathological features of genetically confirmed Danon disease. Neurology. 58:1773-8.

Sulston J, Horvitz HR, Kimble J. 1988. Cell lineage. In: The nematode Caenorhabditis elegans (ed. W.B. Wood and the Community of C. elegans Researchers), pp. 457-489. Cold Spring Harbor Laboratory, Cold Spring Harbor, New York

Sunio A, Metcalf AB, Kramer H. 1999. Genetic dissection of endocytic trafficking in Drosophila using a horseradish peroxidase-bride of sevenless chimera: hook is required for normal maturation of multivesicular endosomes. Mol Biol Cell. 10:847-59.

Sun-Wada GH, Wada Y, Futai M. 2003. Lysosome and lysosome-related organelles responsible for specialized functions in higher organisms, with special emphasis on vacuolar-type proton ATPase. Cell Struct Funct. 28:455-63.

Sun-Wada GH, Wada Y, Futai M. 2004. Diverse and essential roles of mammalian vacuolar-type proton pump ATPase: toward the physiological understanding of inside acidic compartments. Biochim Biophys Acta. 1658:106-14.

Suter A, Everts V, Boyde A, Jones SJ, Lullmann-Rauch R, Hartmann D, Hayman AR, Cox TM, Evans MJ, Meister T, von Figura K, Saftig P. Overlapping functions of lysosomal acid phosphatase (LAP) and tartrate-resistant acid phosphatase (Acp5) revealed by doubly deficient mice. Development. 2001 Dec;128(23):4899-910.

Tabara H, Sarkissian M, Kelly WG, Fleenor J, Grishok A, Timmons L, Fire A, Mello CC. 1999. The rde-1 gene, RNA interference, and transposon silencing in C. elegans. Cell. 99:123-32.

Tammen I, Cook RW, Nicholas FW, Raadsma HW. 2001. Neuronal ceroid lipofuscinosis in Australian Merino sheep: a new animal model. Eur J Paediatr Neurol. 5 Suppl A:37-41.

Taschner PE, de Vos N, Breuning MH. 1997. Cross-species homology of the CLN3 gene. Neuropediatrics. 28:18-20.

Teixeira CA, Lin S, Mangas M, Quinta R, Bessa CJ, Ferreira C, Sa Miranda MC, Boustany RM, Ribeiro MG. 2006. Gene expression profiling in vLINCL CLN6-deficient fibroblasts: Insights into pathobiology. Biochim Biophys Acta. 1762:637-46.

The *C. elegans* sequencing consortium. 1998. Genome sequence of the nematode C. elegans: a platform for investigating biology. Science. 282:2012-8

Trombetta ES, Ebersold M, Garrett W, Pypaert M, Mellman I. 2003. Activation of lysosomal function during dendritic cell maturation. Science. 299:1400-3.

Tsuji S, Martin BM, Barranger JA, Stubblefield BK, LaMarca ME, Ginns EI. 1988. Genetic heterogeneity in type I Gaucher disease: multiple genotypes in Ashkenazic and non-Ashkenazic individuals. Proc. Nat. Acad. Sci. 85: 2349-2352.

Tyynela J, Sohar I, Sleat DE, Gin RM, Donnelly RJ, Baumann M, Haltia M, Lobel P. 2000. A mutation in the ovine cathepsin D gene causes a congenital lysosomal storage disease with profound neurodegeneration. EMBO J. 19:2786-92.

Urano J, Tabancay AP, Yang W, Tamanoi F. 2000. The Saccharomyces cerevisiae Rheb G-protein is involved in regulating canavanine resistance and arginine uptake. J Biol Chem. 275:11198-206.

Vellodi A. Lysosomal storage disorders. Br J Haematol. 2005 Feb;128(4):413-31.

Verheijen FW, Verbeek E, Aula N, Beerens CE, Havelaar AC, Joosse M, Peltonen L, Aula P, Galjaard H, van der Spek PJ, Mancini GM. 1999. A new gene, encoding an anion transporter, is mutated in sialic acid storage diseases. Nature Genet. 23:462-465.

Verkruyse LA, Hofmann SL. 1996. Lysosomal targeting of palmitoyl-protein thioesterase. J Biol Chem. 271:15831-6.

Vesa J, Chin MH, Oelgeschlager K, Isosomppi J, DellAngelica EC, Jalanko A, Peltonen L. 2002. Neuronal ceroid lipofuscinoses are connected at molecular level: interaction of CLN5 protein with CLN2 and CLN3. Mol Biol Cell. 13:2410-20.

De Voer G, Jansen G, van Ommen GJ, Peters DJ, Taschner PE. 2001. Caenorhabditis elegans homologues of the CLN3 gene, mutated in juvenile neuronal ceroid lipofuscinosis. Eur J Paediatr Neurol. 5 Suppl A:115-20.

Voznyi YV, Keulemans JL, Mancini GM, Catsman-Berrevoets CE, Young E, Winchester B, Kleijer WJ, van Diggelen OP. 1999. A new simple enzyme assay for pre- and postnatal diagnosis of infantile neuronal ceroid lipofuscinosis (INCL) and its variants. J Med Genet. 36:471-4.

Walenta JH, Didier AJ, Liu X, Kramer H. 2001. The Golgi-associated hook3 protein is a member of a novel family of microtubule-binding proteins. J Cell Biol. 152:923-34.

Wheeler RB, Sharp JD, Schultz RA, Joslin JM, Williams RE, Mole SE. 2002. The gene mutated in variant late-infantile neuronal ceroid lipofuscinosis (CLN6) and in nclf mutant mice encodes a novel predicted transmembrane protein. Am J Hum Genet. 70:537-42.

White J, Southgate E, Durbin R. 1988. Neuroanatomy. In The nematode Caenorhabditis elegans (ed. W.B. Wood and the Community of C. elegans Researchers), pp. 433-455. Cold Spring Harbor Laboratory, Cold Spring Harbor, New York

Wiemken A, Durr M. 1974. Characterization of amino acid pools in the vacuolar compartment of Saccharomyces cerevisiae. Arch Microbiol. 101:45-57.

Williams RE, Lake BD, Elleder M, Sharp JD. 1999. CLN6 Variant Late Infantile/Early Juvenile NCL, In: The neuronal ceroid lipofuscinosis (Batten disease). Goebel HH, Mole SE, Lake BD, (editors). IOS Press: Amsterdam, The Netherlands.

Winkel LP, Kamphoven JH, van den Hout HJ, Severijnen LA, van Doorn PA, Reuser AJ, van der Ploeg AT. 2003. Morphological changes in muscle tissue of patients with infantile Pompe's disease receiving enzyme replacement therapy. Muscle Nerve. 27:743-51.

Winkel LP, Van den Hout JM, Kamphoven JH, Disseldorp JA, Remmerswaal M, Arts WF, Loonen MC, Vulto AG, Van Doorn PA, De Jong G, Hop W, Smit GP, Shapira SK, Boer MA, van Diggelen OP, Reuser AJ, Van der Ploeg AT. 2004. Enzyme replacement therapy in late-onset Pompe's disease: a three-year follow-up. Ann Neurol. 55:495-502.

Wisniewski KE, Rapin I, Heaney-Kieras J. 1988. Clinico-pathological variability in the childhood neuronal ceroid-lipofuscinoses and new observations on glycoprotein abnormalities. Am J Med Genet Suppl. 5:27-46.

Wisniewski KE, Kida E, Walus M, Wujek P, Kaczmarski W, Golabek AA. 2001. Tripeptidyl-peptidase I in neuronal ceroid lipofuscinoses and other lysosomal storage disorders. Eur J Paediatr Neurol. 5 Suppl A:73-9.

Wisniewski KE, Zhong N, editors. 2001b. Advances in Genetics. Batten disease: Diagnosis, Treatment and Research. San Diego: Academic Press.

Wreden CC, Wlizla M, Reimer RJ. 2005. Varied mechanisms underlie the free sialic acid storage disorders. J Biol Chem 280:1408-16.

Wrobe D, Henseler M, Huettler S, Pascual Pascual SI, Chabas A, Sandhoff K. 2000. A non-glycosylated and functionally deficient mutant (N215H) of the sphingolipid activator protein B (SAP-B) in a novel case of metachromatic leukodystrophy (MLD). J Inherit Metab Dis. 23:63-76.

Zarzour W, Kleta R, Frangoul H, Suwannarat P, Jeong A, Kim SY, Wayne AS, Gunay-Aygun M, White J, Filipovich AH, Gahl WA. 2005. Two novel CHS1 (LYST) mutations: clinical correlations in an infant with Chediak-Higashi syndrome. Mol Genet Metab. 85:125-32.

Zhou XY, van der Spoel A. Rottier R, Hale G, Willemsen R, Berry GT, Strisciuglio P, Andria G, d'Azzo A. 1996. Molecular and biochemical analysis of protective protein/cathepsin A mutations: correlation with clinical severity in galactosialidosis. Hum Molec Genet 5:1977-1987.

Zwaal RR, Broeks A, van Meurs J, Groenen JT, Plasterk RH. 1993. Target-selected gene inactivation in Caenorhabditis elegans by using a frozen transposon insertion mutant bank. Proc Natl Acad Sci U S A. 90:7431-5.

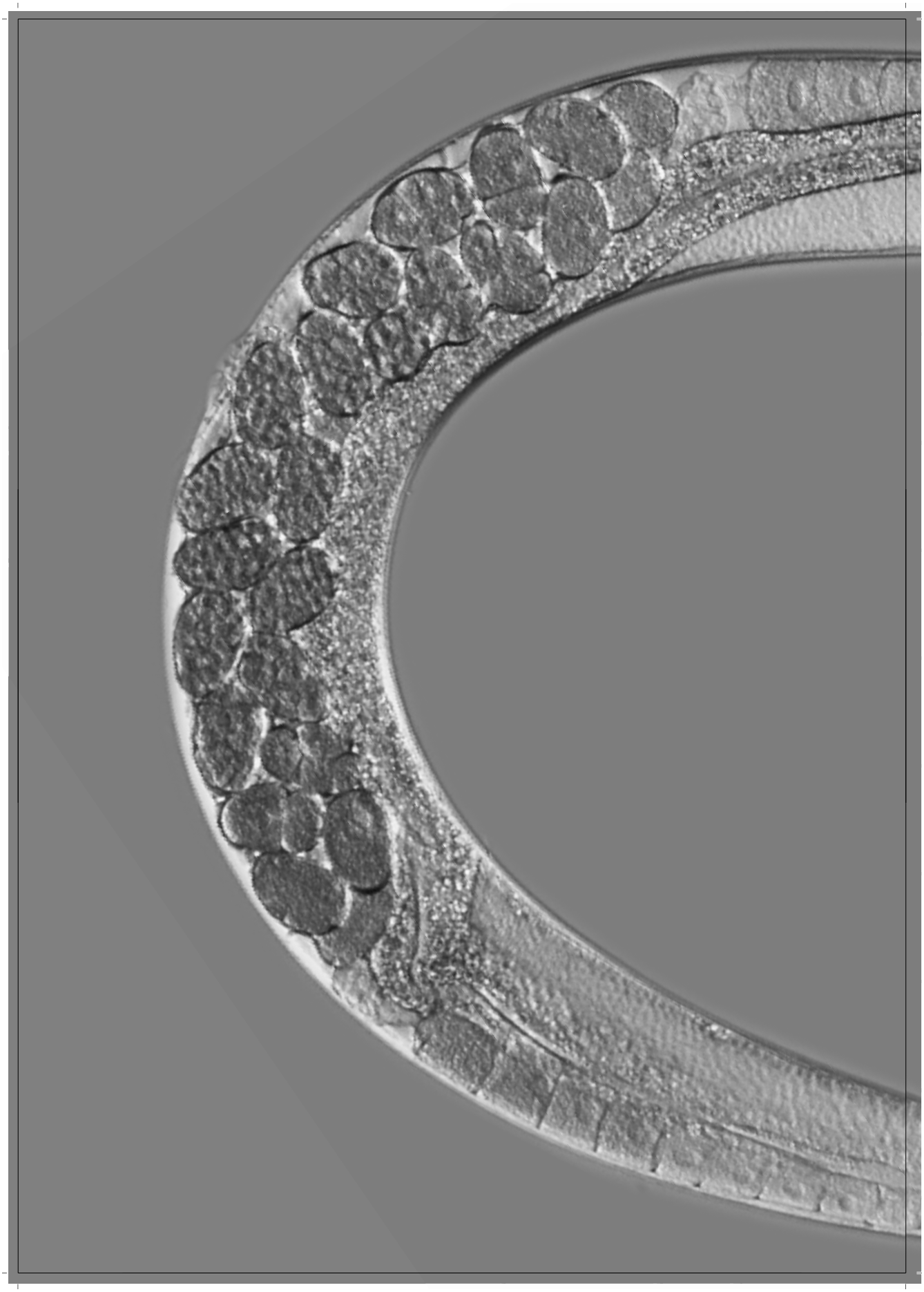

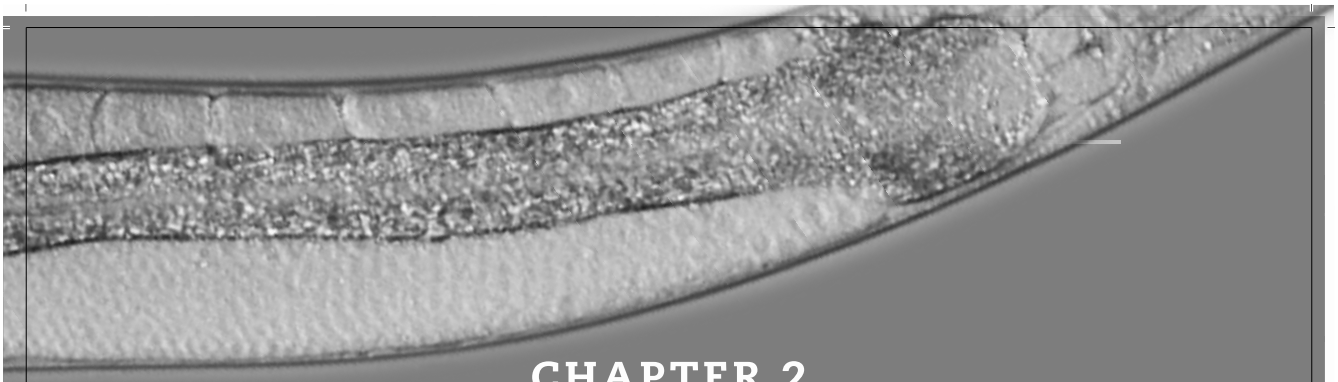

CHAPTER 2

Caenorhabditis elegans as a model for Lysosomal Storage Disorders

Gert de Voer[1], Dorien J.M. Peters, Peter E.M. Taschner #

Department of Human and Clinical Genetics, Leiden University Medical Center, Leiden, The Netherlands
[1]Present address: The Cell Microscopy Center, Department of Cell Biology and Institute of Biomembranes, University Medical Center Utrecht, Utrecht, The Netherlands
Author responsible for correspondence: Peter E. Taschner
Department of Human Genetics
Center for Human and Clinical Genetics
Postzone S-04-P
P.O. Box 9600
2300 RC Leiden
The Netherlands
Telephone +31 (0)71-5269424
Fax +31 (0)71-5268285
e-mail: P.Taschner@lumc.nl
Subject index: *Caenorhabditis elegans*, lysosomal storage disease, lysosome

Running head title: *Caenorhabditis elegans* and lysosomal storage disorders

Abstract

The nematode *C. elegans* is the simplest animal model available to study human disease. In this review, the homologues of human genes involved in lysosomal storage disorders and normal lysosomal function have been listed. In addition, the phenotypes of mutants, in which these genes have been disrupted or knocked down, have been summarized and discussed. From the overview we can conclude that the phenotypic spectrum of worm models of lysosomal storage disorders varies from lethality to none obvious with a large variety of intermediate phenotypes. It is also clear that the genetic power of *C. elegans* provides a means to identify genes involved in lysosomal biogenesis and function, although genetic screens for loss or gain of easily distinguishable intermediate phenotypes are most successful.

Introduction

The lysosome

Christian De Duve discovered, in 1949, the cellular bodies in which digestion occurs and called them lysosomes, since they contained mixtures of lytic enzymes, reviewed in [1]. These organelles were identified due to the application of different homogenization procedures. Gentle homogenization allows the lysosomes to stay intact and therefore to contain the enzymatic activity inside, whereas drastic homogenization causes disruption of the lysosomal membranes permitting measurements of lysosomal enzyme activity. De Duve [1] drew a parallel between the digestive tract of a multicellular organism and the "digestive tract" of a cell, both having a resistant envelope with multiple functions, e.g., to protect the rest of the organism or cell from digestion, uptake and secretion of compounds, and to maintain the degradative environment. Moreover, he reasoned that defective functioning of lysosomes could possibly lead to incomplete breakdown and subsequent accumulation of the indigestible substance, eventually causing the cell that harbors the defective lysosomes to become inoperative or even go into apoptosis. Since De Duve's original discovery, significant progress has been made in elucidating the processes taking place in the lysosomes, although much is still unknown.

Lysosomes and degradation and transport

Most eukaryotic cells contain lysosomes, which exist in a variety of shapes and sizes. These acidic degradative organelles are surrounded by a single lysosomal membrane and have a pH of about 5, which is lower than the cytoplasmic pH of approximately 7.2. They contain 50-60 hydrolytic enzymes, collectively called the acid hydrolases that usually reside in the lysosomal lumen. In contrast, the lysosomal membrane proteins are functional in a variety of processes such as lysosome biogenesis, maintenance of endosomal transport, lysosomal enzyme targeting and autophagy [2]. Most of the hydrolytic enzymes are transported to the lysosomes via the 'direct' mannose 6-phosphate pathway, while lysosomal membrane proteins use both the 'direct' pathway and the 'indirect' pathway via the plasma membrane, to travel to the lysosome [3], [4].
Lysosomes obtain their constituents and material to be degraded through vesicular trafficking. For example, transport vesicles containing hydrolytic enzymes can combine with lysosomes or vesicles filled with endocytosed compounds called endosomes. After the endocytosed materials have been degraded, lysosomal proteins can be recycled, catabolized materials can be reused as building blocks for the anabolic processes

in the cell, and waste products may be excreted from the cell. Furthermore, similar processes of vesicular fission or fusion, and intralysosomal degradation may occur with autophagosomes in order to recycle old or obsolete organelles or other parts of the cell.

Lysosomal storage diseases

When any process discussed above is not working properly, this may lead to partly or completely dysfunctional lysosomes that are unable to degrade specific compounds causing their accumulation (See [5] for a detailed description of lysosomal storage diseases). The mass of stored materials can cause the lysosomes to become inflexible or enlarged cellular compartments that are disrupting other processes taking place in the cell, thus leading to a lysosomal storage disorder. Most of the lysosomal storage diseases are caused by defects in hydrolytic enzymes, such as the acid α-glucosidase deficiency in the first described lysosomal storage disorder, Pompe disease (MIM232300)[6]. Acid α-glucosidase deficiency causes storage of glycogen in lysosomes of numerous tissues. In the most severe form of this disease, patients suffer from prominent cardiomegaly, hypotonia, hepatomegaly and they finally die due to cardiorespiratory failure, usually before the age of two [7].
In addition to enzyme deficiencies, disturbed protein sorting or vesicular trafficking may also lead to lysosomal storage disorders, e.g., in mucolipidosis type II or I-cell disease (MIM252500). Cells of mesenchymal origin have reduced phosphotransferase activity in the Golgi apparatus and fail to add a phosphate group to the mannose residues already present on the lysosomal enzyme precursors. Lack of the proper modification leads to secretion of the lysosomal enzymes instead of normal transport to the lysosomes [8]. Affected cells contain dense inclusions of storage material, hence the name inclusion cell or I-cell disease. I-cell disease patients generally suffer from severe progressive psychomotor retardation and premature death in the first decade of life.
The severe pathologies of other lysosomal storage disorders has prompted research into the etiology of the more than 40 known lysosomal storage diseases [9], [10].
For most diseases causative mutations have been described and possible treatments are being developed. For instance, enzyme replacement therapy can be used to treat Gaucher disease, in which the gene encoding the enzyme acid β-glucosidase is mutated [11]. For most lysosomal storage diseases only symptomatic treatment of the patients is possible at the moment. Although much is known concerning lysosomal processes and the mechanisms required for a lysosome to be functional, some questions remain unanswered: whether and how undigested accumulated materials cause the symptoms observed in patients suffering from lysosomal storage diseases or whether the accumulation is a primary or merely a side effect [12]. With the innovative developments in technology for genome and protein analysis, e.g., completion of sequencing projects, microarray analysis techniques, the detailed examination and description of model organisms in which the processes involved in these diseases can be studied, and the development of other whole genome approaches, we may expect to get more insight in these processes in the future.

Human lysosomal diseases and *C. elegans*

To investigate the mechanisms underlying lysosomal storage disorders and their relation with the disease phenotype, appropriate model organisms are required. These organisms preferably should be eukaryotic, multicellular organisms, but straightforward to use and genetically easily modifiable. Furthermore, to identify genes homologous to the genes involved in these heritable disorders, the genome of the model organism should be fully sequenced and the developmental life-course should be well characterized to study mutant phenotypes. Moreover, since neurological symptoms are common in lysosomal storage diseases, the presence of a well described nervous system would certainly be an advantage. Therefore, we have investigated the potential of the nematode *Caenorhabditis elegans* as a model organism for lysosomal storage disorders. This nematode is a convenient and nowadays widely used model organism, initially described by Sydney Brenner [13]. *C. elegans* has an entirely known cell lineage, a very well characterized and invariably wired nervous system, and this organism is amenable to large genetic screens. These worms exist in two sexes: hermaphrodites that self-fertilize to obtain homozygous mutants and males that can be used to perform crosses. Moreover, a comprehensive toolset for worm research on a genetic, cellular, and behavioral level is available and gene specific loss-of-function mutations can easily be phenocopied using RNAi by microinjection, soaking or feeding methods. Whole genome approaches have delivered a vast amount of data, even on previously unannotated sequences, providing clues to the function of the putative proteins [14]. We have compared all human protein sequences known to be involved in lysosomal storage disorders with *C. elegans* protein sequences to identify the putative worm homologues of these lysosomal disease proteins. Subsequently, we collected all phenotypes of nematodes with mutations in the putative homologous genes in order to get an overview of all possible lysosomal phenotypes present in the worm. Similar comparisons were performed with human proteins that were involved in lysosomal processes but that were still unassociated with disease. The homologues and their phenotypes were listed, as were those of the already known *C. elegans* loci involved in lysosomal function, encompassing all possible lysosomal phenotypes that are known in *C. elegans* at the moment. The feasibility of using these lysosomal phenotypes in genetic screens for modifying mutations was studied to discuss the possibilities of investigating the molecular genetic mechanisms the *C. elegans* homologue is involved in.

Results

C. elegans homologues to human lysosomal storage disease genes

We identified *C. elegans* homologues for almost all 58 human genes associated with lysosomal storage diseases (Table 1). Most of the human disease genes have only a single homologue, except *NPC1* (two homologues), *CLN3* and *SMPD1* (both three homologues). Conversely, a single worm homologue has been identified for each of three human gene pairs, *HEXA-HEXB*, *GLA-NAGA* and *GALNS-ARSA*. For all 42 *C. elegans* homologues, information on gene function can be found in literature and in the Wormbase database [15]. Ten of these *C. elegans* genes, which have been studied individually in the nematode, are homologous to genes involved in mucolipidosis type IV (MIM252650), Niemann-Pick type C (MIM257220), Danon disease (MIM300257), Hermansky Pudlak Syndrome-2 (MIM608233) and congenital, infantile, and juvenile forms of neuronal ceroid lipofuscinosis (NCL) (MIM610127, MIM256730, and MIM204200, respectively). Data on the other 32 genes were derived from sequence similarities or came from whole genome approaches, such as microarray analyses [16], and whole genome RNAi experiments [17]. After RNAi knockdown of 35 genes, worm phenotypes ranged from none (26 times) to (embryonic) lethality (twice) with seven subtle intermediate phenotypes (Table 1). Although mutants have been isolated for 19 of the genes, 7 out of the 11 mutants characterized had a mainly subtle phenotype. The available information about nematode homologues to human lysosomal storage disease genes is summarized below in order to get an overview of all possible phenotypes of worm models for lysosomal storage disorders.

Table 1 Human Lysosomal Storage Disorder Genes and their C. elegans Homologues

Lysosomal storage disorder	Human Gene	MIM number a)	C. elegans Homologue	% f)	Function of human protein	C. elegans Mutant c)	RNAi and phenotypes e)
Neuronal ceroid lipofuscinoses (NCL)							
Infantile NCL	PPT1 (CLN1)	600722	F44C4.5	54	Palmitoyl-protein thioesterase 1 precursor (EC 3.1.2.22)	ppt-1	M: delayed egg-laying, abnormal mitochondria; R: None observed
(Congenital ovine NCL)	CTSD	116840	R12H7.2b)	61	Cathepsin D precursor (EC 3.4.23.5)	asp-4 d)	R: Ced
Late infantile NCL	TPP1 (CLN2)	204500	None		Tripeptidyl-peptidase 1 precursor (EC 3.4.14.9)		
Juvenile NCL	CLN3	204200	F07B10.1	53	Unknown	cln-3.1	M: slightly reduced life span; R: None observed
			C01G8.2	49		cln-3.2	M: slightly reduced brood size; R: None observed
			ZC190.1	62		cln-3.3	R: None observed

Late infantile NCL, Finnish variant	CLN5	256731	None		Unknown		
Late infantile NCL, Indian variant	CLN6	601780	None		Unknown		
Northern epilepsy	CLN8	600143	None		Unknown		
Oligosaccharidoses							
Alpha-mannosidosis	MAN2B1	248500	F55D10.1	52	Lysosomal alpha-mannosidase precursor (EC 3.2.1.24)		R: None observed
Beta-mannosidosis	MANBA	248510	C33G3.4	53	Beta-mannosidase precursor (EC 3.2.1.25)		R: None observed
Fucosidosis	FUCA1	230000	W03G11.3	50	Tissue alpha-L-fucosidase precursor (EC 3.2.1.51)		R: None observed
Farber's disease	ASAH1	228000	K11D2.2	62	Acid ceramidase precursor (EC 3.5.1.23)	asah-1 d)	R: Age, Reduced lifespan
Aspartylglucosaminuria	AGA	208400	R04B3.2	56	N(4)-(beta-N-acetylglucosaminyl)-L-asparaginase precursor (EC 3.5.1.26)		R: None observed
Galactosialidosis	PPGB	256540	F41C3.5	59	Lysosomal protective protein precursor (EC 3.4.16.5)		R: None observed
Sphingolipidoses							
Tay-Sachs disease, GM2 gangliosidosis I	HEXA	272800	T14F9.3	56	Beta-hexosaminidase alpha chain precursor (EC 3.2.1.52)	?	M: ND; R: None observed
Sandhoff disease, GM2 gangliosidosis II	HEXB	268800	T14F9.3	55	Beta-hexosaminidase beta chain precursor (EC 3.2.1.52)		
GM2-gangliosidosis type ab	GM2A	272750	None		Ganglioside GM2 activator precursor		
Krabbe disease	GALC	245200	C29E4.10	31	Galactocerebrosidase precursor (EC 3.2.1.46)		R: None observed
Gaucher disease	GBA	606463	F11E6.1	42	Glucosylceramidase precursor (EC 3.2.1.45)		R: None observed
Variant metachromatic leukodystrophy	PSAP	176801	C28C12.7	21	Proactivator polypeptide precursor, prosaposin	spp-10	M, R: None observed
Variant Gaucher disease	PSAP	176801	C28C12.7	21	Proactivator polypeptide precursor, prosaposin	spp-10	
Variant Tay-Sachs disease (gm2-gangliosidosis)	PSAP	176801	C28C12.7	21	Proactivator polypeptide precursor, prosaposin	spp-10	
Niemann-Pick disease A&B	SMPD1	257200	ZK455.4	55	Sphingomyelin phosphodiesterase precursor (EC 3.1.4.12)	asm-2 d)	R: None observed
			W03G1.7	53		asm-3	M: ND; R: None observed
			B0252.2	52		asm-1 d)	R: None observed
Niemann-Pick disease C1	NPC1	257220	F09G8.4	47	Niemann-Pick C1 protein precursor	ncr-2 (npc-2)	M: hypersensitive to cholesterol deprivation, hyperactive egg-layer, slow development, inappropriate dauer forming; R: Emb
			F02E8.6	46		ncr-1 (npc-1)	M: hypersensitive to cholesterol deprivation, hyperactive egg layer, slow development, inappropriate dauer forming; R: None observed

Fabry's disease, sphingolipidosis	GLA	301500	R07B7.11	54	Alpha-galactosidase A precursor (EC 3.2.1.22)	gana-1 d)	R: Reduced enzyme activity
Schindler disease	NAGA	104170	R07B7.11	53	Alpha-N-acetylgalactosaminidase precursor (EC 3.2.1.49)	gana-1 d)	R: Reduced enzyme activity
Mucopolysaccharidoses							
Mucopolysaccharidosis type I, Hurler/Scheie syndrome	IDUA	252800	None		Alpha-L-iduronidase precursor (EC 3.2.1.76)		
Mucopolysaccharidosis type II, Hunter syndrome	IDS	309900	None		Iduronate 2-sulfatase precursor (EC 3.1.6.13)		
Mucopolysaccharidosis type IIIA, Sanfilippo disease IIIA	SGSH	252900	F26H9.1	35	N-sulphoglucosamine sulphohydrolase precursor (EC 3.10.1.1)	chis-1	M: ND, R: None observed
Mucopolysaccharidosis type IIIB, Sanfilippo disease IIIB	NAGLU	252920	K09E4.4	42	Alpha-N-acetylglucosaminidase precursor (EC 3.2.1.50)		R: None observed
Mucopolysaccharidosis type IIIB, Sanfilippo disease IIIC	HGSNAT	252930	None		Heparan-alpha-glucosaminide N-acetyltransferase (E.C. 2.3.1.78)		
Mucopolysaccharidosis type IIID, Sanfilippo disease IIID	GNS	252940	K09C4.8	40	N-acetylglucosamine-6-sulfatase precursor (EC 3.1.6.14)	sul-1	M, R: None observed
Mucopolysaccharidosis type IVB, Morquio syndrome B	GLB1	230500	T19B10.3	41	Beta-galactosidase precursor (EC 3.2.1.23)		R: None observed
Mucopolysaccharidosis type IVA, Morquio syndrome A	GALNS	253000	D1014.1	41	N-acetylgalactosamine-6-sulfatase precursor (EC 3.1.6.4)	sul-2	M, R: None observed
Metachromatic leucodystrophy	ARSA	250100	D1014.1	40	Arylsulfatase A precursor (EC 3.1.6.8)	sul-2	
Mucopolysaccharidosis type VI, Maroteaux-Lamy	ARSB	253200	C54D2.4	33	Arylsulfatase B precursor (EC 3.1.6.12)	sul-3 d)	R: None observed
Mucopolysaccharidosis type VII, Sly syndrome	GUSB	253220	Y105E8B.9	39	Beta-glucuronidase precursor (EC 3.2.1.31)		R: None observed
Hyaluronidase deficiency (Mucopolysaccharidosis type IX)	HYAL1	601492	T22C8.2	31	Hyaluronidase-1 precursor (EC 3.2.1.35)		R: None observed
Lysosomal transporter defects							
Nephropathic cystinosis	CTNS	606272	C41C4.7	48	Cystinosin	ctns-1	M: ND, R: None observed
Infantile sialic acid storage disorder(ISSD) and Salla disease	SLC17A5	604322	C38C10.2	60	Sodium/sialic acid cotransporter, sialin		R: None observed
Lysosomal trafficking defects							
Mucolipidosis, type IV	MCOLN1	605248	R13A5.1	55	Mucolipin-1	cup-5	M: maternal-effect embryonic lethal; R: None observed
Hermansky-Pudlak syndrome	HPS1	604982	None		Biogenesis of lysosome-related organelles complex 3 component		
	AP3B1 (HPS2)	603401	R11A5.1	56	AP-3 complex subunit beta-1	apb-3 (apt-6)	M: ND; R: Emb, Let, Lva, Dpy, fat content reduced
	HPS3	606118	None		Biogenesis of lysosome-related organelles complex 2 component		

	HPS4	606682	None		Biogenesis of lysosome-related organelles complex 3 component		
	HPS5	607521	W09G3.6	27	Biogenesis of lysosome-related organelles complex 2 component		R: fat content reduced
	HPS6	607522	None		Biogenesis of lysosome-related organelles complex 2 component		
	DTNBP1 (HPS7)	607145	None		Dystrobrevin-binding protein 1 (Dysbindin), BLOC1 subunit		
	BLOC1S3 (HPS8)	609762	None		Biogenesis of lysosome-related organelles complex-1 subunit 3		
	VPS33A	610034	B0303.9	25	Vacuolar protein sorting 33A	slp-1	M: ND, R: None observed
Mucolipidosis, types II and IIIA	GNPTAB	607840	None		N-acetylglucosamine-1-phosphotransferase subunits alpha/beta precursor (EC 2.7.8.17)		
Mucolipidosis, type IIIC	GNPTG	607838	ZK1307.8	38	N-acetylglucosamine-1-phosphotransferase subunit gamma precursor (EC 2.7.8.17)	?	M: ND, R: None observed
Others							
Glycogen storage disease type II, Pompe disease	GAA	232300	D2096.3	37	Lysosomal alpha-glucosidase precursor (EC 3.2.1.20)	?	M, R: ND
Chediak-Higashi syndrome	LYST (CHS1)	214500	VT23B5.2	32	Lysosomal-trafficking regulator	?	M: ND, R: None observed
			F10F2.1	34			R: response to contact abnormal
Wolman disease / cholesteryl ester storage disease	LIPA	278000	R11G11.14	59	Lysosomal acid lipase/ cholesteryl ester hydrolase precursor (EC 3.1.1.13)		R: Him, fat content reduced
Glycogen storage disease type Iib, Danon disease	LAMP2	300257	C03B1.12	25	Lysosome-associated membrane glycoprotein 2 precursor	lmp-1	M: gut lighter, one type of intestinal granule missing; R:Clr
Sialidosis	NEU1	256550	None		Sialidase-1 precursor (EC 3.2.1.18)		
Multiple sulfatase deficiency	SUMF1	272200	None		Sulfatase-modifying factor 1 precursor		
Lipoid proteinosis of Urbach and Wiethe	ECM1	602201	None		Extracellular matrix protein 1 precursor		
Dyggve-Melchior-Clausen dysplasia/Smith-McCort dysplasia	DYM	607461	C47D12.2	96	Dymeclin		R: Emb, Let, Muv
Cathepsin E deficiency	CTSE	116890	R12H7.2b)	59	Cathepsin E precursor (EC 3.4.23.34)	asp-4 d)	R: Ced

a) Online Mendelian Inheritance in Man (http://www.ncbi.nlm.nih.gov/Omim/searchomim.html)

b) Due to high similarity between cathepsin homologues, the highest unidirectional man-worm hit is shown

c) ? Deletion mutant, gene name unknown. Old gene designations are shown between parentheses

d) Gene name assigned, but no mutant available

e) M: Mutant, R: RNAi, ND: not determined

f) % Similarity to human gene

C. elegans cup-5, homologous to the Mucolipidosis type IV gene *MCOLN1*, and lysosome biogenesis

Mucolipidosis type IV, caused by mutations in the *MCOLN1* gene, is a neurodegenerative lysosomal storage disorder of which the main symptoms are psychomotor retardation and ophthalmologic abnormalities [18], [19], [20]. Ultrastructural analysis of patient tissues usually reveals many enlarged vacuoles, presumably lysosomes in which lipids are stored as well as water-soluble granulated substances. The *MCOLN1* gene encodes the lysosomal membrane protein h-mucolipin-1, which has six predicted transmembrane domains and functions as a non-selective cation channel of which the activity is modulated by pH [21]. The *C. elegans MCOLN1* homologue *cup-5* is a functional orthologue of the human *MCOLN1* gene, since the phenotype of *cup-5* mutants, heterogeneous enlarged vacuoles and embryonic lethality, can be rescued by expressing the human gene in these mutants [22]. Mutations in the *cup-5* gene were identified by screening for mutants with disrupted endocytosis [23], and in mutants with affected programmed cell death [22]. The *cup-5* gene is expressed in most tissues in adult worms, and subcellularly localized to nascent and mature lysosomes [24]. Similar to patient cells, cells from *cup-5* mutants have enlarged vacuoles and lysosomes, apparently due to defective lysosomal degradation processes. The CUP-5 protein was suggested to play a role in lysosome biogenesis or maturation [25], because h-mucolipin-1 was shown to be a Ca^{2+}-permeable channel [26], and Ca^{2+} transport is essential for fusion of late endosomes and lysosomes and for reformation of lysosomes [27]. Interestingly, through a screen for modifier alleles, a mutation in the *mrp-4* gene, encoding an endosomal-lysosomal ABC transporter, was shown to suppress *cup-5* lethality and rescue the lysosomal degradation and developmental defects of the *cup-5* mutants [28]. In the *cup-5* mutants, degradation of the ABC transporter was suggested to be delayed, causing an imbalance in the endosomal-lysosomal import of compounds, which probably interferes with normal degradation processes. The affected degradation is thought to lead to starvation of the cells and independently to developmental defects. Absence of the ABC transporter results in rescue of lysosomal function, thereby permitting the cells to survive. Whether similar events contribute to the cellular and neuronal degeneration in Mucolipidosis type IV patients is still unknown, but if this is the case reducing the activity of ABC transporters might provide for a therapy for the treatment of mucolipidosis type IV.

Nematode Niemann-Pick type C homologues involved in cholesterol trafficking

Multiple forms of Niemann-Pick disease exist, either caused by deficient acid sphingomyelinase activity leading to accumulation of sphingomyelin in Niemann-Pick type A and B [29], [30], or by defective cholesterol trafficking resulting in lysosomal storage of unesterified cholesterol in Niemann-Pick type C [31]. Symptoms caused by acid sphingomyelinase deficiency vary from hepatosplenomegaly and progressive neurodegenerative disease to pulmonary infiltration. Patients suffering from defective cholesterol trafficking also display progressive neurological disease and possibly

prominent hepatic damage. Three acid sphingomyelinase (ASM) homologues were identified in *C. elegans*, while in other organisms only one *ASM* could be identified [32]. Unfortunately, according to the Wormbase database, mutants for only one of the *C. elegans* ASM homologues are available, but their phenotypes were not described. No *ASM* RNAi phenotypes emerged from whole genome approaches [15], but RNAi targeted against multiple *ASM* genes perhaps could result in an interesting knock-down phenotype and provide a model for Niemann-Pick type A and B.

Niemann-Pick type C can be caused by mutations in two genes, *NPC1* and *NPC2*, encoding proteins with NPC and sterol sensing domains that are implicated in retrograde transport from sterols and other cargo from lysosomes [31], [33], [34]. Each has one worm homologue, *ncr-1* and *ncr-2*, respectively [35]. Worms without *ncr-1* are hypersensitive to lack of cholesterol, an essential substance for the nematode, and to exposure to progesterone, which can inhibit intracellular cholesterol trafficking in mammalian cells [35], [36]. In contrast, *ncr-2* single mutants appear superficially wild type. Whereas *ncr-2; ncr-1* double mutants display constitutive inappropriate dauer formation, which could be rescued by microinjection of NCR-2 or NCR-1wildtype genes, suggesting both proteins play redundant roles to prevent dauer formation under favorable conditions. The dauer is a relatively stress-resistant alternative larval life stage that the animal can form when it develops under stressful conditions. Furthermore, *ncr-2; ncr-1* double mutants have abnormal morphology of certain neurons during transient dauer stage. Other *ncr-2; ncr-1* double mutant phenotypes encompass developmental pleiotropic phenotypes similar to *daf-9* and *daf-12* mutants including reproductive defects, concordant reduced brood size and life span, vulval abnormalities and disruption of the alae cuticle. Epistasis analysis placed NCR-1 and NCR-2 upstream of DAF-9 in the dauer formation pathway [35], [36]. Therefore, the NCR-1 and NCR-2 proteins that were suggested to play a role in intracellular cholesterol trafficking may provide the substrate for DAF-9, the ER localized cytochrome P450 enzyme, which catalyzes a reaction to form a lipophilic hormone for the DAF-12 nuclear receptor [37], [38]. Under cholesterol-deprived conditions, *ncr-2*; *ncr-1* double mutant worms could be unable to efficiently traffic this hormone progenitor to the site of DAF-9 action and hence stimulate dauer formation due to absence of the signal to bypass the dauer stage. Further examination of how the mutations in *NCR-1* and *NCR-2* lead to the other phenotypes, and, most interestingly, the abnormal neuronal morphology, may elucidate other functional aspects of these proteins..

C. elegans LMP-1 protein, homologous to the Danon disease protein LAMP2, involved in lysosome biogenesis

Mutations in the lysosome-associated membrane protein-2 gene (*LAMP2*) cause glycogen storage disease type IIb or Danon disease, characterized by cardiomyopathy, myopathy and variable mental retardation [39]. Originally, Danon disease was described as a variant glycogen storage disease type II, since acid-maltase or alpha-glucosidase activity was normal [40]. LAMP2 and structurally similar LAMP1 are heavily glycosylated lysosomal membrane proteins with one transmembrane domain

and a major intralysosomal part, and are thought to be functional in lysosome stability and integrity [2]. LAMP-1 and LAMP-2 knock-out mice have been generated to investigate LAMP protein function [41], [42]. LAMP-2 knock-out mice suffered from cardiomyopathy and accumulation of autophagic vacuoles, similar to human Danon disease patients. LAMP-1 knock-out mice displayed no overt phenotype but overexpressed LAMP-2, suggesting functional redundancy. Additional functional and morphological studies of the heart of LAMP-2 knock-out mice showed that these mice suffered from contractile dysfunction that was suggested to be due to morphological changes [43]. However, how mutations in *LAMP-2* cause these morphological changes and why the autophagic vacuoles accumulate is still unknown. Kostich and coworkers [44] have searched the *C. elegans* genome for LAMP like sequences and identified a LAMP homologue *lmp-1*, which has a lysosomal targeting sequence (GYXXΦ, in which Φ is a large hydrophobic amino acid residue and X any amino acid) at its COOH terminus. A BLAST search with the human LAMP2 protein sequence against the *C. elegans* protein database Wormpep [15] results in two hits, LMP-1 and LMP-2, the latter of which has no GYXXΦ motif. Nematode *lmp-1* deletion mutants are viable and fertile, show alternative intestinal granule populations, and apparent loss of one type of granule, hence *LMP-1* is likely to be functional in lysosome biogenesis or maintenance [44]. How loss of the *lmp-1* gene causes this change in granule composition and whether autophagy is affected in these mutants remains to be elucidated. This could be done by investigating the genetic interactions of the nematode *lmp-1* gene by screening for mutations that modify the Lmp-1 phenotype. Additional players that are involved in LMP-1 function could be identified by isolation of other mutants with the Lmp-1 phenotype. The feasibility of these screens depends on the ease with which the *lmp-1* gut granule loss can be scored under a standard Differential Interference Contrast (DIC) microscope [45].

Hermansky Pudlak syndrome type 2 (HPS-2) and the AP 3a homologue in the worm implicated in development

The heterogenous group of diseases termed the Hermansky-Pudlak syndrome (HPS) are pathologically characterized by prolonged bleeding, albinism and lysosomal storage of ceroid, and presumably result from defects in multiple cytoplasmic organelles, such as melanosomes, platelet-dense granules, and lysosomes [46]. Mutations in eight genes, *HPS1 - HPS8*, have been shown to cause this disorder and the proteins encoded by these genes are thought to be involved in the biogenesis or transport of lysosomes or lysosome related organelles [47], [48]. The HPS-1 and HPS-4 proteins appear to form a complex that might play a role in the biogenesis of lysosomes [49], [50]. These proteins were suggested to function independently from the AP-3 complex which is involved in formation of carrier vesicles and cargo recruitment, for protein transport. We could not identify *C. elegans* sequences homologous to HPS-1, HPS-3, HPS-4, and HPS-6 by mere protein sequence comparison, suggesting that these proteins are simply not present in the nematode or their sequences have diverged beyond recognition. HPS-5, HPS-7 and HPS-8 have putative homologous proteins in the nematode, but these have not yet been investigated individually and the high throughput approaches did not elucidate

any functional aspects of these proteins [15]. HPS-2 is caused by mutations in the gene encoding the β3a subunit of the adaptor protein 3 (AP-3) complex [51]. Although AP-3 is involved in the sorting of transmembrane proteins from endosomes and the *trans*-Golgi network to lysosomes and endosome-lysosome related organelles, it is unknown how altered AP-3 function leads to HPS-2 [52], [53]. The *C. elegans* homologue for this protein, Apb-3, appears to be required for development as RNAi knock-down of the *apb-3* transcript causes embryonic and larval lethality [54]. Interestingly, worm knock-outs for two other AP-3 complex subunits, *apt-6* and *apt-7*, encoding β3 and μ3 subunits respectively, have an embryonic gut granule loss (Glo) phenotype and larvae and adult mutant worms have less autofluorescent gut granules [55]. The autofluoresent gut granules are presumed to be secondary lysosomes that may contain yolk or other nutrients [56], [44]. This raises the possibility that loss of gut granules due to affected Apb-3 function leads to nutrient deprivation and subsequent lethality in *apb-3* RNAi worms. Additional investigations, such as genetic screens for alleles modifying the larval arrest or the Glo phenotypes, could provide further insight into AP-3 dependent processes and the precise role of AP-3 in protein trafficking.

Neuronal ceroid lipofuscinoses (NCL) and the worm *ppt-1*, *asp-4* and *cln-3* homologues

The congenital, infantile and juvenile forms of NCL are caused by mutations in the *CTSD*, *PPT1* and *CLN3* genes respectively, which all lead to severe neurodegenerative disorders with similar disease progression but with different age of onset [57], [58], [59]. Initial symptoms include visual deterioration followed by epileptic seizures, progressing to a state of dementia and ending in premature death [10]. In addition to the differences between the age of onset and the genes affected, the NCLs can also be distinguished by the typical patterns of the lipopigment accumulations found in lysosomes of neurons and other cell types [60]. No direct links have been established between the causative mutations, the observed pathology and the accumulated material. The most severe form of the NCLs, congenital neuronal ceroid lipofuscinosis, is very rare and thus far only 10 patients have been described [57]. Patients suffering from this disease are microcephalic, may have seizures and die soon after birth. This disease was found to be caused by mutations in the *CTSD* gene encoding cathepsin D and strongly resembles the congenital ovine neuronal ceroid lipofuscinosis previously identified in sheep [61]. The nematode homologue of the *CTSD* gene *asp-4* is also the closest homologue of the human *CTSE* gene, which is mutated in CTSE deficiency, a disease distinct from NCL [62]. Asp-4 was shown to be involved in necrotic cell death as *asp-4* RNAi knockdown leads to decreased cell death, signifying its role as an executioner protease [63]. Thus, altered cell death may underlie the etiology of congenital neuronal ceroid lipofuscinosis.

PPT1 encodes the lysosomal enzyme palmitoyl protein thioesterase-1, which cleaves thioester linkages in S-acylated (palmitoylated) proteins and facilitates the removal of the palmitate residues [64]. In neurons however, PPT1 is also found in non-lysosomal compartments, synaptic vesicles and synaptosomes [65]. The *C. elegans* *CLN1* homologue is designated *ppt-1* and worms mutated in their *ppt-1* gene display

mitochondrial abnormalities at an ultrastructural level, and an egg laying defect or egl phenotype, where eggs hatch inside the parent [66]. This reproductive 'bagging' phenotype could be used in genetic screens to identify modifier genes, although this may be a rather laborious task. Alternatively, enhancement of the *ppt-1* mutant phenotype may result in a more robust phenotype that is more useful for genetic screens.

The juvenile NCL gene *CLN3* encodes a transmembrane protein, which is thought to be primarily localized to lysosomes and may be implicated in pH regulation or amino acid transport [60]. The nematode has three homologous genes, *cln-3.1*, *cln-3.2*, and *cln-3.3*, which when mutated and combined into one triple mutant strain causes a mild decrease in life span and brood size [67]. This phenotype is not suitable for genetic screens and requires an enhancement of the phenotype or an additional investigation of the *cln-3* mutants to establish a clear-cut difference between mutants and wild type as a basis for genetic screening to search for modifier genes.

C. elegans homologues to human genes associated with lysosomal function involved in other disorders

Apart from tissue-specific expression, several proteins with a clear lysosomal localization in certain cell types may exert their function at a different location in others. Depending on the importance of these proteins for the normal function of a specific cell type, mutations in genes encoding these proteins may impair the non-lysosomal function more than the lysosomal function. As a result, lysosomal storage is not observed in diseases caused by mutations in these genes. We have compiled a list of thirteen disease genes encoding proteins without lysosomal localization in the most affected cell types or organs and their worm homologues (Table 2). Three of these genes, *CTSC*, *MPO* and *TCIRG1* belong to gene families with multiple homologues in the worm. Remarkably, most of these genes seem to be associated with defects in polarized cells, such as renal tubular cells in renal acidosis or osteoclasts in osteopetrosis. About half of their proteins are localized in the plasma membrane. Most are subunits of the conserved vacuolar ATPase pumping protons through the plasma, lysosomal and other organellar membranes, but CLCN7 is a channel for chloride ions compensating the positive charges of the protons. Several proteins are involved in non-lysosomal degradation processes for which lysosomes provide hydrolytic enzymes, such as CTSC and CTSK. One of these processes is bone resorption, which is performed by specialized cells called osteoclasts [68]. On contact with bone, part of their membrane can form a ruffled border and create a resorptive pit, which is acidified and filled with hydrolytic enzymes by lysosomes to degrade bone. Defects in the acidification or the hydrolytic enzymes can prevent bone resorption leading to osteopetrosis. Bone defects similar to those in osteopetrosis have been observed in mucopolysaccharidosis type VII and have also been attributed to malfunctioning osteoclasts [69]. Thus, with the environment of the resorptive pit resembling that of a lysosome, one might look at osteopetrosis as a kind of extracellular lysosomal disorder. The remaining four genes,

Table 2 *C. elegans* Homologues to Human Genes associated with Lysosomal Function involved in other Disorders

Human disorders without lysosomal storage caused by lysosomal protein defects	Human Gene	MIM Number a)	C. elegans Homologue	% f)	Function/Name	C. elegans Mutant b)	RNAi and mutant phenotypes c)
Renal tubular acidosis with deafness	ATP6V1B2	606939	F20B6.2	92	ATPase, H+ transporting, lysosomal 56/58kDa V1 subunit B1	vha-12	M: ND; R: Ste Emb Let Adl Lvl Lva Prl Locomotion abnormal
			Y110A7A.12	87		spe-5?	M: Defective spermatogenesis; R: Emb Let Lvl Lva Adl Prl Locomotion abnormal Maternal sterile
Renal tubular acidosis with deafness	ATP6V1B1	192132	F20B6.2	92	ATPase, H+ transporting, lysosomal 56/58kDa V1 subunit B2	vha-12	
			Y110A7A.12	87		spe-5?	
Renal tubular acidosis, type I	ATP6V0A4	605239	F35H10.4	61	Vacuolar H+-ATPase V0 sector, subunit a	vha-5	M: homozygous lethal; R: Emb Let Lvl Lva Gro Prl Pvl Clr Bmd Sck Locomotion abnormal
Pyknodysostosis	CTSK	601105	T03E6.7	60	Cysteine proteinase Cathepsin K	cpl-1	M: ND; R: Gro Emb Let Locomotion abnormal
Haim-Munk syndrome	CTSC	602365	T10H4.12 d)	52	Cysteine proteinase Cathepsin C	cpr-3	M: ND; R: Emb
Papillon-Lefevre syndrome	CTSC	602365					
Juvenile periodontitis	CTSC	602365					
Myeloperoxidase deficiency	MPO	606989	ZK994.3 d)	55	Peroxidase catalyzing hypochlorous acid production	pxn-1	M:ND; R: None observed
Infantile malignant autosomal recessive osteopetrosis	TCIRG1	604592	ZK637.8 d)	57	ATPase, H+ transporting, lysosomal, V0 subunit A3	unc-32	M: severe coiler; R: Emb Let Gro Sck
	(OC116, TIRC7)						Locomotion abnormal Maternal sterile Pvl
Infantile malignant autosomal recessive osteopetrosis	CLCN7	602727	R07B7.1	91	Chloride channel 7	clh-6	M:ND; R: None observed
Autosomal dominant osteopetrosis	CLCN7	602727	R07B7.1	91		clh-6	
Infantile malignant autosomal recessive osteopetrosis	OSTM1	607649	F42A8.3	76	Osteopetrosis-associated transmembrane protein 1	?	M:ND; R: None observed
Lowe Syndrome	OCRL	309000	C16C2.3	86	phosphatidylinositol 4,5-bisphosphate-5-phosphatase	ocrl-1 e)	R: None observed
Corneal fleck dystrophy	PIP5K3	609414	VF11C1L.1	66	phosphatidylinositol 4-phosphate 5-kinase	ppk-3	M: Ste, Emb, enlarged lysosomes; R: None observed
Chorea acanthocytosis	VPS13A	605978	T08G11.1	95	Vacuolar protein sorting 13A		R: None observed
Arthrogryposis, renal dysfunction and cholestasis	VPS33B	608552	C56C10.1	46	Vacuolar protein sorting 33B		R: None observed

a) Online Mendelian Inheritance in Man (http://www.ncbi.nlm.nih.gov/Omim/searchomim.html)
b) ? Deletion mutant, gene name unknown
c) M: Mutant, R: RNAi, ND: not determined
d) Multiple hits with human protein. No reciprocal best hit due to higher similarity of worm protein to a different human protein. One-directional hit with highest similarity shown
e) Gene name assigned, but no mutant available
f) % Similarity to human gene

OCRL1, *PIP5K3*, *VPS13A*, and *VPS33B* play a role in lysosomal protein trafficking and lysosomal maturation. Mutant and/or RNAi knockdown phenotypes have been determined for all 13 genes, but no obvious lysosomal phenotype was observed apart from the enlarged lysosomes in the *ppk-3* mutants with their lysosomal maturation defect [70].

C. elegans homologues to human genes involved in lysosomal functioning

To complement the collection of potential lysosomal phenotypes of the worm, we have generated a list of 92 human lysosomal genes not yet implicated in disease and searched for their worm homologues (Table 3).
At least one worm homologue was found for 84 human lysosomal genes. In some cases, for example vacuolar ATPase subunit genes, the same worm homologue was found for several human genes or vice versa, indicating that these genes have been duplicated or lost in one organism compared to the other. In five other cases, the human gene is part of a gene family with many members, which is also represented in the worm, for instance, the cathepsin and lectin families.
For each of the 94 worm homologues listed, we have collected the available information about their mutant and RNAi knockdown phenotypes. Mutants for 40 homologues have been identified, but only half of them have been characterized phenotypically. Six of these have no obvious phenotype and seven genes lack a gene symbol. Most of the homologues have been included in genome-wide RNAi knockdown experiments, but for 57 of them no phenotype was observed. The most common phenotype observed in RNAi knockdown experiments for these genes was embryonic lethality (Emb: 28 times) followed by lethality (Let: 22 times) and larval arrest (Lva: 15 times). A selection of these homologues with interesting phenotypes is discussed below.

The *C. elegans* LRP-2/glycoprotein 330 homologue is essential for nematode life

LRP2/glycoprotein 330 is a very interesting member of the LDL receptor protein (LRP) family. This protein is involved in endocytosis, and its role in development appears to gain interest, due to investigation of its mouse, zebrafish and worm homologues [71]. The *C. elegans* homologue of this protein, *lrp-1* was shown to be essential for growth and development of the nematode, as *lrp-1* mutants arrest their development as larvae [72]. The most prominent morphological effect of mutations in *lrp-1* arose due to problems with shedding of the cuticle, which normally is renewed at each larval stage. Moreover, homozygote *lrp-1* mutants also are moderately dumpy and small, providing another indication for aberrant cuticle renewal, but cuticle synthesis appeared to be normal in these mutants. The dumpy phenotype has been observed previously in worms that had problems with cuticle synthesis [73]. Interestingly, wildtype worms that were starved for cholesterol phenocopied *lrp-1* mutants, supporting

a role for LRP-1 in sterol endocytosis. Recently, a genetic interaction was identified between LRP-1 and *hgrs-1*, which is involved in sorting of endocytosed proteins [74]. In *hgrs-1* mutants, the LRP-1 protein was mislocalized, indicating that *hgrs-1* is required for correct endocytic trafficking of the LRP-1 protein. The phenotype of *hgrs-1* mutants resembled that of *lrp-1* mutants and wildtype worms starved for cholesterol. Similarly, other genetic or biochemical interactions may be identified, through screening for *lrp-1*-like mutant phenotypes or modifiers of the RNAi phenotype.

The multifunctional role of cathepsin Z in nematode development

The cathepsin Z protein is a cystein protease that acts as a carboxymonopeptidase and is incorporated in the phagosome [75]. The protein was detected in cells of the immune system and in tumor cells and was suggested to also play a role in cell adhesion dependent on β2-integrin [76]. The nematode homologue of this protein, CPZ-1, was shown to be essential for development as RNAi knockdown and mutation of *cpz-1* both lead to embryonic or larval lethality in part of the worm population [77]. Whether this developmental arrest is caused by defective phagosome function or cell adhesion or has another cause, remains to be elucidated. The exact function of CPZ-1 could be further investigated in *cpz-1* mutants or worms depleted for CPZ-1 by RNAi knockdown.

A *C. elegans* chloride channel involved in endocytosis

The chloride channel protein CLC-3 may play a role in the stabilization of membrane potential also of intracellular organelles, transepithelial transport, cell volume regulation, and endocytosis [78]. Interestingly, deletion of the homologous mouse gene, *Clc3*, causes hippocampal neurodegeneration and retinal degeneration [79]. This was suggested to be the result of glutamate toxicity in synaptic vesicles or defective acidification in the endosomal or recycling pathway. Their ubiquitously expressed *C. elegans* homologue *CLH-5* was shown to be involved in receptor mediated endocytosis, because depletion of the protein by RNAi caused an endocytosis defect similar to the *cup-5* mutant [80]. The phenotype of *CLH-5* RNAi was somewhat milder than the *CUP-5* RNAi phenotype, which could be explained by redundancy of multiple other chloride channels.

Human genes involved in lysosomal functioning without *C. elegans* homologues

Eight of the human genes listed in Table 3 have no worm counterpart based on protein sequence similarity. Four of them encode subunits of a complex involved in the biogenesis of lysosome-related organelles, BLOC1, of which eight subunits have been identified [81]. The worm has only homologues of one BLOC1 subunit involved in Hermansky-Pudlak syndrome, DTNBP1, and the BLOC1S1, BLOC1S2, and SNAPAP subunits, which are not associated with human disease. It is unclear whether these proteins are part of a conserved BLOC1 core complex which on its own can play a role in organelle biosynthesis, or whether they interact with unidentified partners, or have acquired a different function.

The other genes without homologues are involved in immunity or encode enzymes. One of these, the PCYOX1 gene encodes an enzyme involved in the degradation of prenylcysteines [82]. Although knockout mice accumulate prenylcysteines in brain cells, this does not seem to lead to lysosomal storage, brain pathology or histological features normally associated with lysosomal storage diseases. It is tempting to speculate that the accumulating prenylcysteines can be localized in (lysosomal) membranes without problems until their concentration starts to destabilize these membranes or the altered membrane composition interferes with the function of membrane proteins.

Table 3 Human genes encoding lysosomal proteins or proteins involved in lysosomal function unassociated with disease

Human Gene	Protein	MIM Number	C. elegans Homologue	% g)	Mutant / CGC Name a)	RNAi and mutant phenotypes b)	KO or spontaneous mouse mutants
ABCA2	ATP binding cassette transporter 2	600047	Y39D8C.1	53	abt-4	M, R: None observed	
ABCA3	ATP binding cassette transporter 3	601615	Y39D8C.1	54	abt-4	M, R: None observed	
ABCA5	ATP binding cassette transporter 5		Y39D8C.1	45	abt-4	M, R: None observed	
ABCB9	ATP binding cassette transporter B9	605453	W04C9.1	41	haf-4	M: Glo; R: Emb Gro Let	
			F43E2.4	40	haf-2	M, R: None observed	
ACP2	Lysosomal acid phosphatase 2	171650	T13B5.3	33		R: None observed	nax, acp2 null
			B0361.7	32		R: None observed	
			F52E1.8	32		R: None observed	
ACP5	Acid phosphatase 5	171640	F02E9.7	36		R: None observed	
ACPT	Acid phosphatase, testicular	606362	B0361.7	34		R: None observed	
			F52E1.8	32		R: None observed	
			T21B6.2	32		R: None observed	
ACPP	Acid phospatase, prostate	171790	T13B5.3	32		R: None observed	
			R13H4.3	50		R: None observed	
AP3B2	AP-3 adaptor complex, subunit Beta 2	602166	R11A5.1	69	apb-3	M: ND; R: Emb, Let, Lva, Dpy, fat content reduced	
AP3D1	AP-3 adaptor complex, subunit Delta 1	607246	W09G10.4B	65	apd-3 (apt-5) f)	R: Emb Let Lva Dpy	mocha
AP3M1	AP-3 adaptor complex, subunit Mu1	610366	F53H8.1	80	apm-3 (apt-7) f)	M: Glo; R: Emb Let Lva Dpy fat content reduced	
AP3M2	AP-3 adaptor complex, subunit Mu2		F53H8.1	79	apm-3 (apt-7) f)		
AP3S1	AP-3 adaptor complex, subunit Sigma 1	601507	Y48G8AL.14	86	aps-3 (apt-8) f)	R: Emb Let Lva Dpy maternal sterile	
AP3S2	AP-3 adaptor complex, subunit Sigma 2	602416	Y48G8AL.14	88	aps-3 (apt-8) f)		
ARL8B	ADP-ribosylation factor-like 8B		Y57G11C.13	95	arl-8	R: Emb Let	
ARSD	arylsulfatase D	300002	Arylsulfatase family c)	57			
ASAHL	N-acylsphingosine amidohydrolase (acid ceramidase)- like	607469	Y55D5A.3	29		R: None observed	
ATP6AP1	ATPase, H+ transporting, lysosomal accessory protein 1	300197	Y55H10A.1	30	vha-19	M: Let or Ste; R: Ste Sck	
ATP6AP2	ATPase, H+ transporting, lysosomal accessory protein 2	300556	R03E1.2	23		R: Lva Emb Let Unc Lvl	

ATP6V0A1	ATPase, H+ transporting, lysosomal V0 subunit a isoform 1	192130	ZK637.8f	57	unc-32	M: Unc; R: Ste Pvl Sck Emb Let Unc Gro	
ATP6V0A2	ATPase, H+ transporting, lysosomal V0 subunit a isoform 2		ZK637.8	47	unc-32	M: Unc; R: Ste Pvl Sck Emb Let Unc Gro	
ATP6V0B	ATPase, H+ transporting, lysosomal 21kDa, V0 subunit b	603717	T01H3.1	64	vha-4	R: Stp Emb Unc Lvl Clr	
ATP6V0C	ATPase, H+ transporting, lysosomal 16kDa, V0 Subunit c	108745	R10E11.2	67	vha-2	M: ND; R: Ste Emb Let,	
ATP6V0D1	ATPase, H+ transporting, lysosomal 38kDa, V0 subunit d1	607028	C30F8.2	75	vha-16 f)	R: Let Lvl Lva Emb Maternal sterile	
ATP6V0D2	ATPase, H+ transporting, lysosomal 38kDa, V0 subunit d2		C30F8.2	81			
ATP6V0E1	ATPase, H+ transporting, lysosomal 9kDa, V0 subunit e1	603931	F49C12.13	71	vha-17	M: ND; R: Ste Sck Emb Lvl Lva	
ATP6V0E2	ATPase, H+ transporting, V0 subunit e2		F49C12.13	75			
ATP6V1A	ATPase, H+ transporting, lysosomal 70kDa, V1 subunit A	607027	Y49A3A.2	82	vha-13 f)	R: Emb Let Gro Lva Prl maternal sterile	
ATP6V1C1	ATPase, H+ transporting, lysosomal 42kDa, V1 Subunit c1	603097	Y38F2AL.3A	56	vha-11 f)	R: Ste Emb Let Gro small Sck Lvl Lva Stp maternal sterile decreased broodsize	
ATP6V1C2	ATPase, H+ transporting, lysosomal 42kDa, V1 Subunit c2		Y38F2AL.3A	50	vha-11 f)	R: Ste Emb Let Gro small Sck Lvl Lva Stp maternal sterile decreased broodsize	
ATP6V1D	ATPase, H+ transporting, lysosomal 34kDa, V1 subunit D		F55H2.2	68	vha-14 f)	R: Emb Let Lva	
ATP6V1E1	ATPase, H+ transporting, lysosomal 31kDa, V1 subunit E1	108746	C17H12.14	58	vha-8 (pes-6)	M: ND; R: Ste Emb Let Gro Lva decreased broodsize	
ATP6V1E2	ATPase, H+ transporting, lysosomal 31kDa, V1 subunit E2		C17H12.14	57	vha-8 (pes-6)	M: ND; R: Ste Emb Let Gro Lva decreased broodsize	
ATP6V1F	ATPase, H+ transporting, lysosomal 14kDa, V1 subunit F	607160	ZK970.4	70	vha-9 f)	R: Emb Let Lvl Unc Lva maternal sterile	
ATP6V1G1	ATPase, H+ transporting, lysosomal 13kDa, V1 subunit G1	607296	F46F11.5	53	vha-10 f)	R: Emb Lvl Ste Etv	
ATP6V1G2	ATPase, H+ transporting, lysosomal 13kDa, V1 subunit G2	606853	F46F11.5	35	vha-10 f)	R: Emb Lvl Ste Etv	
ATP6V1G3	ATPase, H+ transporting, lysosomal 13kDa, V1 subunit G3		F46F11.5	42	vha-10 f)	R: Emb Lvl Ste Etv	
ATP6V1H	ATPase, H+ transporting, lysosomal 50/57 kDa, V1 subunit H	608861	T14F9.1	45	vha-15 f)	R: Emb Let Lva Prl Lvl Bli	
BLOC1S1	Biogenesis of lysosome-related organelles complex 1 (BLOC1) subunit 1	601444	T20G5.10	67		R: None observed	
BLOC1S2	Biogenesis of lysosome-related organelles complex 1 (BLOC1) subunit 2	609768	Y73B6BL.30	62		R: None observed	
BLOC1S3	Biogenesis of lysosome-related organelles complex 1 (BLOC1) subunit 3	609672	None d)				
CD222	IGF2R	147280	F23D12.2	34		R: None observed	
CD63	Lysosomal membrane glycoprotein CD63/GP53	155740	T23D8.2	34	tsp-7	R: None observed	
			T14G10.6	27	tsp-12	M, R: None observed	
CD68	CD68	153634	Lectin family c)				
CLCN3	Chloride channel	600580	C07H4.2	45	clh-5	M: Let, Ste; R: mild endocytosis defect (compared to cup-5)	clcn3
CLCN6	Chloride channel	602726	R07B7.1	60	clh-6	M: ND; R: None observed	clcn6
CNO	cappuccino, homolog of mouse, BLOC1 subunit	605695	None				cappuccino

CPVL	carboxypeptidase, vitellogenic-like	609780	Serine carboxypeptidase family c)	54			
CTBS	Chitobiase	600873	T01C4.1	25		R: None observed	
CTSB	Cathepsin B	116810	F57F5.1 e)	52	?	M: ND; R: Emb Unc Lva	ctsb
			W07B8.5	48	cpr-5 f)	R: None observed	
			C52E4.1	51	cpr-1 (gcp-1)	M: ND; R: None observed	
			F44C4.3	36	cpr-4	M: ND; R: None observed	
			C25B8.3	49	cpr-6	M, R: None observed	
			W07B8.4	49		R: None observed	
			W07B8.1	43		R: None observed	
			F36D3.9	45	cpr-2 f)	R: None observed	
			T10H4.12	45	cpr-3	M: ND: R: Emb Let	
			F32H5.1	40		R: Gro	
			Y65B4A.2	42		R: None observed	
CTSF	Cathepsin F	603539	F41E6.6	49	tag-196	M: mild Unc Egl; R: None observed	ctsf
			R09F10.1	35		R: None observed	
			R07E3.1	35	?	M: ND; R: None observed	
CTSH	Cathepsin H	116820	K02E7.10	37		R: None observed	
			C50F4.3	30	tag-329	M: Gro Lvl decreased broodsize; R: None observed	
			Y113G7B.15	33		R: None observed	
CTSL	Cathepsin L	116880	T03E6.7	49	cpl-1	M: ND; R: Emb Let Gro Unc	ctsl
			Y51A2D.8	32		R: None observed	
CTSL2	Cathepsin L2	603308	Y71H2AR.2	38		R: None observed	
CTSS	Cathepsin S	116845	Y40H7A.10	33	?	M: ND; R: None observed	
			F15D4.4	30		R: None observed	
CTSZ	Cathepsin Z	603169	F32B5.8	55	cpz-1	M: ND; R: Emb Let Lva Bmd Mlt maternal sterile	
			M04G12.2	50	cpz-2	M: ND, R: None observed	
DNASE2	Deoxyribonuclease II, lysosomal	126350	F09G8.2	34	tag-198	M, R: None observed	
ENTPD4	ectonucleoside triphosphate diphosphorylase 4	607577	C33H5.14 c)	32	ntp-1 f)	R: None observed	
GGH	gamma-glutamyl hydrolase	601509	None				
HLA-DMA	major histocompatibility complex, class II, DM alpha	142855	None				
HLA-DMB	major histocompatibility complex, class II, DM beta	142856	None				
HYAL2	Hyaluronidase 2	603551	T22C8.2	31		R: None observed	
IFI30	Interferon-inducible protein 30	604664	F37H8.5	51		R: None observed	
			C02D5.2	50		R: None observed	
LAMP1	Lysosomal-associated membrane protein 1	153330	C05D9.2	36	lmp-2 f)	R: None observed	
LAMP3	Lysosomal-associated membrane protein 3	605883	Lectin family c)				
LAPTM4A	lysosomal associated protein transmembrane 4A		C05E11.3	46		R: None observed	
			F23D12.1	50		R: None observed	
LAPTM4B	lysosomal associated protein transmembrane 4B		C05E11.3	45		R: None observed	
LAPTM5	Lys.-assoc. multispanning membrane protein-5	601476	C05E11.3	28		R: None observed	
LGMN/ PRSC1	legumain; hydrolysis of asparaginyl bonds	602620	T28H10.3	42		R: Emb Let	

LRP2	Glycoprotein 330	600073	F29D11.1	30	lrp-1	M: Lvl Mlt; R: Gro Prl Mlt Unc Lvl Bmd Dpy Lva Rup Mig	
LYPLA3	lysophospholipase 3 (lysosomal phospholipase A2)	609362	M05B5.4	46		R: fat content reduced	
MUTED	muted, homolog of mouse, BLOC1 subunit	607289	None				muted
NAGPA	N-acetylglucosamine-1-phosphodiester alpha-N-acetylglucosaminidase	607985	EGF-like domain family c)				
OSBP	Oxysterol binding protein	167040	Y47D3A.17	64	obr-1 f)	R: Emb Let	
PAQR8	progestin and adipoQ receptor family member VIII	607780	K11C4.2	26		R: None observed	
PCYOX1	prenylcysteine oxidase 1		None				
PLDN	pallidin, BLOC-1 subunit	604310	None				
PPT2	Palmitoyl-protein thioesterase 2 precursor	603298	F44C4.5	51	ppt-1	M: delayed egg-laying , abnormal mitochondria; R: None observed	
PRCP	prolylcarboxypeptidase	176785	ZK112.1	41	pcp-1 f)	R: None observed	
PRDX6	peroxiredoxin 6; Involved in redox regulation of the cell	602316	Y38C1AA.11	50	prdx-6 f)	R: ND	
PRSS16	protease, serine 16 (thymus)	607169	K12H4.7A	48		R: None observed	
			C26B9.5	44		R: None observed	
			F19C7.2	45		R: None observed	
			F19C7.4	43		R: None observed	
			F23B2.11	46	pcp-3 f)	R: None observed	
			F23B2.12	45	pcp-2	M: ND, R: None observed	
RAB7A	Ras oncogene family member RAB7A	602298	W03C9.3	86	rab-7	M: ND; R: Emb Let Bmd Dpy Prl Ced fat content reduced	
SCARB2	Lysosomal integral membrane protein II (CD36L2/LGP85/ LIMP II)	602257	Y49E10.20	28	?	M: ND; R: Pvl maternal sterile	scarb2
			Y76A2B.6	28	?	M: ND; R: None observed	
SLC30A2	solute carrier family 30 member 2, Zinc transporter	609617	T18D3.3	69	?	M: ND, R: None observed	
SLC36A1	solute carrier family 36 member 1	606561	T27A1.5	34		R: RIC	
SNAPAP	snapin, SNARE and BLOC-1 component	607007	C02B10.2	51	?	M: ND; R: Emb	
SNX1	sorting nexin 1	601272	C05D9.1	59	snx-1	M: Egl, slightly bloated, HSN migration defects; R: None observed	
STX7	syntaxin 7	603217	F36F2.4	58	syn-13	M: None observed; R: Emb Let	
STX12	syntaxin 12	606892	F36F2.4	58			
SYBL1/ VAMP7	synaptobrevin-like 1	300053	Y69A2AR.6	53		R: None observed	
SYT7	synaptotagmin 7	604146	C08G5.4	62	snt-6	R: None observed	
TMEM9	transmembrane protein 9. Involved in intracellular transport endosomes and lysosomes		R12C12.6	55		R: None observed	

a) ? Deletion mutant, gene name unknown
b) Phenotype abbrevations: Bli: blistered; Bmd: organism morphology abnormal, Ced: cell death abnormal; Clr: clear; Dpy: dumpy; Egl: egg laying defect; Emb: embryonal lethal; Glo: gut fluorescence loss; Gro: slow growth; Lva: larval arrest; Lvl: larval lethal;
Mig: cell migration abnormal; Mlt: molting defect; Prl: paralyzed; Pvl: protruding vulva; Ric: aldicarb resistant; Rup: exploded through vulva; Sck: sick; Ste: sterile; Stp: sterile progeny; Unc: uncoordinated
c) BLAST hit > 1 e-5, but no reciprocal BLAST hits; when given: similarity with highest hit
d) None: Blast hit < 1 e-5
e) Due to similarity of cathepsin protein sequences, different homologous pairs are shown
f) Gene name assigned, but no mutant available
g) % Similarity to human gene

Comparison of phenotypes related to *C. elegans* loci affecting lysosomal function

Mutation or RNAi knockdown phenotypes for each of the worm loci presumed to be involved in lysosomal function and missing from the tables presented above were mainly collected using the following criteria: changes should occur in either the gut autofluorescence caused by secondary lysosomes, or size, number or electron density of the lysosomal vesicles (Table 4). In addition, specific phenotypes, such as the cup phenotype, which are associated with at least one known lysosomal protein, were included. Following the initial screens, genetic mapping has led to the identification of several genes involved in the Cup and Glo phenotypes. The loci *cup-2*, *cup-4*, *glo-4* and *glo-5* were found to encode homologues to *DERL1*, *CHRNB1*, *HERC4* and *ABCB1*, respectively [80], [55], [83]. In addition, three existing *rme* mutants displayed the Cup phenotype [80], whereas five known genes were involved in the Glo phenotype [55] (Table 4). These genes encode proteins with functions in other locations within the cell. Many of these proteins probably play an important role in the processes discussed in the introduction: lysosome biogenesis, maintenance of endosomal transport and lysosomal enzyme targeting. The associated phenotypes vary in severity, but are relatively subtle and more similar to those in Table 1 than compared to those in Tables 2 and 3.

Table 4 *C. elegans* phenotypes associated with changes in lysosomal function

Mutant or RNAi phenotype	Primary gene Associated with Lysosomal Phenotype	C. elegans Locus Name	Gene Name	Human Homologue	% a)	Function of (human) protein	MIM Number	References
coelomocyte uptake defect,	cup-5		R13A5.1	MCOLN1	55	Mucolipin-1	605248	Nature Genet 28: 64 (2001)
accumulation of refractile cell corpses		cup-1, cup-3,	?	?				Genetics159: 133 (2001)
		cup-6 - cup-11						PNAS 99: 4355 (2002)
		cup-2	F25D7.1	DERL1	65	Misfolded protein degradation in ER	608813	
		cup-4	C02C2.3	CHRNB1	43	acetylcholine receptor	100710	
		rme-1	W06H8.1	EHD1	81	intracellular sorting	605888	Genetics159: 133 (2001)
		rme-6	F49E7.1	GAPVD1	52	Rab5-activating protein 6, endocytosis		Genetics159: 133 (2001)
		rme-8	F18C12.2	DNAJC13	64	DnaJ (Hsp40) homolog		Genetics159: 133 (2001)
gut granule biosynthesis defect	glo-1							
		glo-1	R07B1.12	RAB32	66	Ras oncogen family member RAB32		
		glo-3	?	?				
		glo-4	F07C3.4	HERC4	43	hect domain and RLD 4, ubiquitin ligase		
		pgp-2 (glo-5)	C34G6.4	ABCB1	66	ATP binding cassette transporter B1	171050	Mol Biol Cell 18: 995 (2007)
		haf-4	W04C9.1	ABCB9	41	ATP binding cassette transporter B9	605453	

		apt-6	R11A5.1	AP3B1 (HPS2)	56	AP-3 complex subunit beta-1	603401	
		apt-7	F53H8.1	AP3M1	80	AP-3 complex, subunit Mu1	610366	
		vps-16	C05D11.2	VPS16	44	Vacuolar protein sorting-associated protein	608550	
						16 homolog		
		vps-41	F32A6.3	VPS41	51	Vacuolar protein sorting-associated protein	605485	
						41 homolog		
loss of one type of intestinal granule	lmp-1		C03B1.12	LAMP1	57	Lysosomal-associated membrane protein	153330	J Cell Sci 113: 2595 (2000)
vacuolated intestinal cells, egg retention,	cad-1		?	?				Genetics 119: 355 (1988)
reduced aspartic protease activity,								J Biol Chem 275: 26359 (2000)
enzyme processing defect?								
slow development, premature egg laying	ncr-1		F02E8.6	NPC1	46	Niemann-Pick C1 protein precursor	257220	Curr Biol 10: 527 (2000)
dauer-constitutive (Daf-c) phenotype	ncr-1; ncr-2		F09G8.4	NPC1	47	Niemann-Pick C1 protein precursor	257220	Curr Biol 10: 527 (2000)
DNA in intestinal lumen not degraded	nuc-1		C07B5.5	DNASE2B	54	deoxyribonuclease II beta		Genetics 129: 79 (1991)
major endodeoxyribonuclease reduced >95%								Science 220: 1277 (1983)
condensed chromatin persists after apoptosis								
acc of enlarged lysosomes, paralysis during 1st larval	idi-1		K06H7.9	IDI1	56	isopentenyldiphosphate isomerase	604055	Mol Gen Genomics 273: 158 (2005)
stage, larval arrest, persistent apoptotic corpses								
coiler; very sluggish, moves poorly; slightly Egl	unc-101	unc-101	K11D2.3	AP1M1	88	AP-1 complex, subunit Mu1	603535	Genes Dev. 8: 60 (1994)
slightly short; defecation defects,								
abnormal FITC staining; subviable.								
Abnormal adult males tails and spicules								

a) % Similarity to human gene

Summary and conclusion

Most of the human genes involved in lysosomal storage disorders have single *C. elegans* homologues (Table 1). A few human genes have more than one worm counterpart and vice versa. The reason for the existence of multiple worm homologues of *SMPD1* and *CLN3* is unclear, although temporal and spatial expression patterns differ for the *asm* and *cln-3* paralogues [32], [67]. The representation of three human enzyme-encoding gene pairs, *HEXA-HEXB*, *GLA-NAGA* and *GALNS-ARSA*, by single worm homologues might be considered as an indication of simpler biochemical pathways in the worm. The worm GANA-1 homologue combines the GLA and NAGA enzyme activities into one multifunctional enzyme [84]. Still, from several genes (e.g., 6 *HPS* and 4 *CLN* genes) involved in human lysosomal storage disorders no worm counterparts could be identified using BLAST searches with protein sequences. It is tempting to speculate that this is associated in part with the lack of cell types with specialized lysosome-related cell organelles, such as melanosomes, in the worm. This may also explain why the worm lacks four subunits of the BLOC1 complex involved in the biogenesis of lysosome-related organelles (Table 3). Furthermore, due the complexity of the human brain, man may require a larger repertoire of CLN proteins, some of which have additional roles in synaptic vesicles. In general, however, the proteins necessary for normal lysosomal function seem to be conserved between man and worm.

Mutation or RNAi knockdown phenotypes were available for 147 of the 149 worm genes listed in Tables 1-3. The phenotypes ranged from embryonic lethality via subtle intermediate phenotypes to none observed. If observed, mutant and RNAi knockdown phenotypes of lysosomal storage disease related worm homologues (Table 1) or lysosomal worm mutants (Table 4) seem to be more subtle than those of homologues, which are not yet associated with lysosomal storage disease (Table 3).

The worm models of human lysosomal storage disorders have diverse phenotypes ranging from seemingly apparent lysosomal nature, such as the endocytosis defect in *cup-5* mutants or *lmp-1* mutants that have lost one type of intestinal granule presumed to be pre-lysosomes, to phenotypes that appear less directly related to lysosomes, such as the disturbed cholesterol trafficking of the *ncr* mutants, developmental arrest or decreased life span or brood size. Whether the latter phenotypes are directly caused by defective lysosomal processes in the worm remains to be determined. Alternatively, the developmental defects and embryonic lethality could also be caused by preceding defects, e.g., in endosomal transmembrane protein sorting in *apb-3* mutants [54].

Severe phenotypes, such as (embryonic) lethality and larval arrest, are observed for genes encoding parts of the vacuolar proton pump. An explanation might be that the latter genes play an important role in multiple processes and organelles and that their inactivation leads to pleiotropic effects, having larger impact on the worm and thus creating a more severe phenotype. In man, disruption of these genes might also have

severe pleiotropic effects. The existence of multiple copies of vacuolar proton pump genes, however, might result in sufficient redundancy to prevent severe effects unless multiple genes are hit.

Many other nematode homologues are on the other end of the spectrum and lack mutant and RNAi knockdown phenotypes. One explanation is that other proteins with a redundant function complement the effect of the genetic lesion or knockdown. Alternatively, most of the mutants were tested under standard laboratory conditions, which are presumed to be ideal growth conditions evading the possible stress that may be required for the manifestation of a phenotype. Furthermore, the life span of worms may be too short to reveal a phenotype. In addition, even when a knock-out mutation would cause a phenotype, RNAi knock-down of gene function will not always result in a phenotype [85]. Last but not least, much of the data was generated in regular genome-wide RNAi screens, which yield a mass of data potentially providing a starting point for the investigation of any individual gene, but present the researcher with the risk to overlook certain subtle phenotypes. Although coelomocyte uptake (Cup) and loss of gut autofluorescence (Glo) phenotypes are relatively easy to score using fluorescence microscopy [80], [55], these were not scored in the genome-wide RNAi screens. Determining a difference in number, size or electron density of the lysosomal vesicles (Lmp-1, Idi phenotypes) however, requires time-consuming ultrastructural investigations. Detection of such intricate phenotypes is usually not included in regular genome-wide RNAi screens.

From the compilation presented here, we may conclude that the nematode *C. elegans* has largely the same number of genes involved in lysosomal processes as man and that the worm is a suitable model organism to investigate lysosomal storage diseases. It became clear that some of the specific phenotypes associated with changes in lysosomal proteins can also be caused by defects in proteins, which do not localize to lysosomes, but exert their function in lysosome biogenesis, maintenance of endosomal transport and lysosomal protein targeting. Their human homologues might be good candidates for disorders with lysosomal storage or lysosomal dysfunction without known cause. The identification of additional worm mutants by genetic screens would help to identify new players in the different processes necessary for normal lysosomal function and potential new candidates for human hereditary disorders. The advantage of the most observed worm phenotypes in Table 3, developmental arrest or lethality in any life stage, is the relative ease with which genetic screens can be done for modifiers of these robust phenotypes. The nature of the mutant, genetic or RNAi knockdown, also determines the screenability of modifier genes as well as the penetrance of the phenotype. The subtle phenotypes observed in many of the lysosomal mutants of the worm, however, suggest that it may not be trivial to perform screens for new mutants.

Acknowledgments

This work was financially supported by the Center for Biomedical Genetics.

References

[1] C. De Duve, The lysosome, *Sci Am*. **208** (1963), pp. 64-72.

[2] E.L. Eskelinen, Y. Tanaka, P. Saftig, At the acidic edge: emerging functions for lysosomal membrane proteins, *Trends Cell Biol*. **3** (2003), pp. 137-45.

[3] C. Mullins and J.S. Bonifacino, The molecular machinery for lysosome biogenesis. *Bioessays.* **4** (2001), pp. 333-43.

[4] J.P. Luzio, V. Poupon, M.R. Lindsay, B.M. Mullock, R.C. Piper, P.R. Pryor, Membrane dynamics and the biogenesis of lysosomes. *Mol Membr Biol.* **2** (2003), pp. 141-54.

[5] C.R. Scriver and W.S. Sly WS (Eds.), *The metabolic and molecular basis of inherited disease*, 8th edition, McGraw-hill, Inc., New York, (2000).

[6] J.C. Pompe, Over idiopathische hypertrophie van het hart. Ned Tijdschr Geneeskd. **76** (1932), pp. 304-312.

[7] R. Hirschhorn and A.J.J. Reuser, Glycogen storage disease type II: Acid α-Glucosidase (acid maltase) deficiency, in: C.R. Scriver, W.S. Sly (Eds.), *The metabolic and molecular bases of inherited disease*, 8th edition, McGraw-Hill Inc., New York (2001), pp. 3389-3420.

[8] S. Kornfeld and W.S. Sly, I-cell disease and pseudo-Hurler polydystrophy: Disorders of lysosomal enzyme phosphorylation and localization, in: C.R. Scriver, W.S. Sly (Eds.), *The metabolic and molecular bases of inherited disease*, 8th edition, McGraw-Hill Inc., New York, (2001), pp. 3421-3452.

[9] A. Vellodi, Lysosomal storage disorders. *Br J Haematol.* **128** (2005), pp. 413-31.

[10] J. Rapola, Neuronal ceroid-lipofuscinoses in childhood. *Perspect Pediatr Pathol.***17** (1993), pp. 7-44

[11] R. Schiffmann and R.O. Brady, New prospects for the treatment of lysosomal storage diseases. *Drugs.* **62** (2002), pp. 733-42.

[12] A.H. Futerman and G. van Meer, The cell biology of lysosomal storage disorders. *Nat Rev Mol Cell Biol.* **7** (2004), pp. 554-65.

[13] S. Brenner, The genetics of Caenorhabditis elegans. *Genetics.* **77** (1974), pp. 71-94.

[14] P.E. Kuwabara and N. O'Neil, The use of functional genomics in *C. elegans* for studying human development and disease. *J Inherit Metab Disease.* **24** (2001), pp. 127-138.

[15] WormBase web site, http://www.wormbase.org, release WS173, date March 23, 2007

[16] S.L. Kim, J. Lund, M. Kiraly, K. Duke, M. Jiang, J.M. Stuart, A. Eizinger, B.N. Wylie, G.S. Davidson, A gene expression map for Caenorhabditis elegans. *Science.* **293** (2001), pp. 2087-92.

[17] R.S. Kamath, A.G. Fraser, Y. Dong, G. Poulin, R. Durbin, M. Gotta, A. Kanapin, N. Le Bot, S. Moreno, M. Sohrmann, D.P. Welchman, P. Zipperlen, J. Ahringer, Systematic functional analysis of the Caenorhabditis elegans genome using RNAi. *Nature.* **421** (2003), pp. 231-7.

[18] R. Bargal, N. Avidan, E. Ben-Asher, Z. Olender, M. Zeigler, A. Frumkin, A. Raas-Rothschild, G. Glusman, D. Lancet, G. Bach, Identification of the gene causing mucolipidosis type IV. *Nat Genet.* **26** (2000), pp. 118-23.

[19] M.T. Bassi, M. Manzoni, E. Monti, M.T. Pizzo, A. Ballabio, G. Borsani, Cloning of the gene encoding a novel integral membrane protein, mucolipidin-and identification of the two major founder mutations causing mucolipidosis type IV. *Am J Hum Genet.* **67** (2000), pp. 1110-20.

[20] M. Sun, E. Goldin, S. Stahl, J.L. Falardeau, J.C. Kennedy, J.S. Acierno Jr, C. Bove, C.R. Kaneski, J. Nagle, M.C. Bromley, M. Colman, R. Schiffmann, S.A. Slaugenhaupt, Mucolipidosis type IV is caused by mutations in a gene encoding a novel transient receptor potential channel. *Hum Mol Genet.* **9** (2000), pp. 2471-8.

[21] M.K. Raychowdhury, S. Gonzalez-Perrett, N. Montalbetti, G.A. Timpanaro, B. Chasan, W.H. Goldmann, S. Stahl, A. Cooney, E. Goldin, H.F. Cantiello, Molecular pathophysiology of mucolipidosis type IV: pH dysregulation of the mucolipin-1 cation channel. *Hum Mol Genet.* **13** (2004), pp. 617-27.

[22] B.M. Hersh, E. Hartwieg, H.R. Horvitz, The Caenorhabditis elegans mucolipin-like gene cup-5 is essential for viability and regulates lysosomes in multiple cell types. *Proc Natl Acad Sci U S A.* **99** (2002), pp. 4355-60.

[23] H. Fares, I. Greenwald, Regulation of endocytosis by CUP-5, the Caenorhabditis elegans mucolipin-1 homolog. *Nat Genet.* **28** (2001), pp. 64-8.

[24] S. Treusch, S. Knuth, S.A. Slaugenhaupt, E. Goldin, B.D. Grant, H. Fares H, Caenorhabditis elegans functional orthologue of human protein h-mucolipin-1 is required for lysosome biogenesis. *Proc Natl Acad Sci U S A.* **101** (2004), pp. 4483-8.

[25] L. Schaheen, H. Dang, H. Fares,. Basis of lethality in C. elegans lacking CUP-5, the Mucolipidosis Type IV orthologue. *Dev Biol.* **293** (2006), pp. 382-91.

[26] J.M. LaPlante, J. Falardeau, M. Sun, M. Kanazirska, E.M. Brown, S.A. Slaugenhaupt, P.M. Vassilev, Identification and characterization of the single channel function of human mucolipin-1 implicated in mucolipidosis type IV, a disorder affecting the lysosomal pathway. *FEBS Lett.* **532** (2002), pp. 183-7.

[27] P.R. Pryor, B.M. Mullock, N.A. Bright, S.R. Gray, J.P. Luzio, The role of intraorganellar Ca(2+) in late endosome-lysosome heterotypic fusion and in the reformation of lysosomes from hybrid organelles. *J Cell Biol.* (2000), pp. 1053-62.

[28] L. Schaheen, G. Patton, H. Fares H, Suppression of the cup-5 mucolipidosis type IV-related lysosomal dysfunction by the inactivation of an ABC transporter in C. elegans. *Development.* **133** (2006), pp. 3939-48

[29] M.T. Vanier and K. Suzuki, Niemann–Pick disease, in: *Neurodystrophies and Neurolipidioses*, H.W. Moser (Eds.), vol. 66, Handbook of Clinical Neurology, Elsevier B.V., Amsterdam, 1996, pp. 133–162.

[30] E.H. Schuchman, R.J. Desnick Type A and B Niemann–Pick disease: deficiencies of acid sphingomyelinase activity, in: C.R. Scriver, W.S. Sly (Eds.), *The metabolic and molecular bases of inherited disease*, 8th edition, McGraw-Hill Inc., New York (2001), pp. 3589–3610.

[31] E.D. Carstea, J.A. Morris, K.G. Coleman, S.K. Loftus, D. Zhang, C. Cummings, J. Gu, M.A. Rosenfeld, W.J. Pavan, D.B. Krizman, J. Nagle, M.H. Polymeropoulos , S.L. Sturley, Y.A. Ioannou, M.E. Higgins, M. Comly, A. Cooney, A. Brown, C.R. Kaneski, E.J. Blanchette-Mackie, N.K. Dwyer, E.B. Neufeld, T.Y. Chang, L. Liscum, J.F. Strauss 3rd, K. Ohno, M. Zeigler, R. Carmi, J. Sokol, D. Markie, R.R. O'Neill, O.P. van Diggelen, M. Elleder, M.C. Patterson, R.O. Brady, M.T. Vanier, P.G. Pentchev, D.A. Tagle, Niemann-Pick C1 disease gene: homology to mediators of cholesterol homeostasis. *Science.* **277** (1997), pp. 228-231.

[32] X. Lin, M.O. Hengartner, R. Kolesnick, Caenorhabditis elegans contains two distinct acid sphingomyelinases. *J Biol Chem.* **273** (1998), pp. 14374-9.

[33] S. Naureckiene, D.E. Sleat, H. Lackland, A. Fensom, M.T. Vanier, R. Wattiaux, M. Jadot, P. Lobel, Identification of HE1 as the second gene of Niemann-Pick C disease. *Science.* **290** (2000), pp. 2298-2301.

[34] E.N. Neufeld, M. Wastney, S. Patel, S. Suresh, A.M. Cooney, N.K. Dwyer, C.F. Roff, K. Ohno, J.A. Morris, E.D. Carstea, J.P. Incardona, J.F. Strauss 3rd, M.T. Vanier, M.C. Patterson, R.O. Brady, P.G. Pentchev, E.J. Blanchette-Mackie, The Niemann-Pick C1 protein resides in a vesicular compartment linked to retrograde transport of multiple lysosomal cargo. *J Biol Chem.* **274** (1999), pp. 9627-35.

[35] M. Sym, M. Basson, C. Johnson, A model for Niemann-Pick type C disease in the nematode Caenorhabditis elegans. *Curr Biol.* **10** (2000), pp. 527-30.

[36] J. Li, G. Brown, M. Ailion, S. Lee, J.H. Thomas NCR-1 and NCR-2, the C. elegans homologs of the human Niemann-Pick type C1 disease protein, function upstream of DAF-9 in the dauer formation pathways. *Development.* **131** (2004), pp. 5741-52.

[37] B. Gerisch and A. Antebi, Hormonal signals produced by DAF-9/cytochrome P450 regulate C. elegans dauer diapause in response to environmental cues. *Development.* **131** (2004), pp. 1765-76.

[38] H.Y. Mak and G. Ruvkun Intercellular signaling of reproductive development by the C. elegans DAF-9 cytochrome P450. *Development.* **131** (2004), pp. 1777-86.

[39] I. Nishino, J. Fu, K. Tanji, T. Yamada, S. Shimojo, T. Koori, M. Mora, J.E. Riggs, S.J. Oh, Y. Koga, C.M. Sue, A. Yamamoto, N. Murakami, S. Shanske, E. Byrne, E. Bonilla, I. Nonaka, S. DiMauro, M. Hirano, Primary LAMP-2 deficiency causes X-linked vacuolar cardiomyopathy and myopathy (Danon disease). *Nature.* **406** (2000), pp. 906-10.

[40] M.J. Danon, S.J. Oh, S. DiMauro, J.R. Manaligod, A. Eastwood, S. Naidu, L.H. Schliselfeld, Lysosomal glycogen storage disease with normal acid maltase. *Neurology.* **31** (1981), pp. 51-7.

[41] N. Andrejewski, E.L. Punnonen, G. Guhde, Y. Tanaka, R. Lullmann-Rauch, D. Hartmann, K. von Figura, P. Saftig, Normal lysosomal morphology and function in LAMP-1-deficient mice. *J Biol Chem.* **274** (1999), pp. 12692-701.

[42] Y. Tanaka, G. Guhde, A. Suter, E.L. Eskelinen, D. Hartmann, R. Lullmann-Rauch, P.M. Janssen, J. Blanz, K. von Figura, P. Saftig, Accumulation of autophagic vacuoles and cardiomyopathy in LAMP-2-deficient mice. *Nature.* **406** (2000), pp. 902-6.

[43] J. Stypmann, P.M. Janssen, J. Prestle, M.A. Engelen, H. Kogler, R. Lullmann-Rauch, L. Eckardt, K. von Figura, J. Landgrebe, A. Mleczko, P. Saftig, LAMP-2 deficient mice show depressed cardiac contractile function without significant changes in calcium handling. *Basic Res Cardiol.* **101** (2006), pp. 281-91.

[44] M. Kostich, A. Fire, D.M. Fambrough, Identification and molecular-genetic characterization of a LAMP/CD68-like protein from Caenorhabditis elegans. *J Cell Sci.* **113** (2000), pp. 2595-606.

[45] E.M. Jorgensen, S.E. Mango, The art and design of genetic screens: Caenorhabditis elegans. *Nat Rev Genet.* **3** (2002), pp. 356-69.

[46] J. Oh, L. Ho, S. Ala-Mello, D. Amato, L. Armstrong, S. Bellucci, G. Carakushansky, J.P. Ellis, C.T. Fong, J.S. Green, E. Heon, E. Legius, A.V. Levin, H.K. Nieuwenhuis, A. Pinckers, N. Tamura, M.L. Whiteford, H. Yamasaki, R.A. Spritz, Mutation analysis of patients with Hermansky-Pudlak syndrome: a frameshift hot spot in the HPS gene and apparent locus heterogeneity. *Am J Hum Genet.* **62** (1998), pp. 593-8.

[47] N.V. Morgan, S. Pasha, C.A. Johnson, J.R. Ainsworth, R.A. Eady, B. Dawood, C. McKeown, R.C. Trembath, J. Wilde, S.P. Watson, E.R. Maher, A germline mutation in BLOC1S3/reduced pigmentation causes a novel variant of Hermansky-Pudlak syndrome (HPS8). *Am J Hum Genet.* **78** (2006), pp. 160-6.

[48] S.M. Di Pietro and E.C. Dell'Angelica, The cell biology of Hermansky-Pudlak syndrome: recent advances. *Traffic.* **6** (2005), pp. 525-33.

[49] R. Nazarian, J.M. Falcon-Perez, E.C. Dell'Angelica, Biogenesis of lysosome-related organelles complex 3 (BLOC-3): a complex containing the Hermansky-Pudlak syndrome (HPS) proteins HPS1 and HPS4. *Proc Natl Acad Sci U S A.* **100** (2003), pp. 8770-5.

[50] J.A. Martina, K. Moriyama, J.S. Bonifacino, BLOC-3, a protein complex containing the Hermansky-Pudlak syndrome gene products HPS1 and HPS4. *J Biol Chem.* **278** (2003), pp. 29376-84.

[51] E.C. Dell'Angelica, V. Shotelersuk, R.C. Aguilar, W.A. Gahl, J.S. Bonifacino, Altered trafficking of lysosomal proteins in Hermansky-Pudlak syndrome due to mutations in the beta-3A subunit of the AP-3 adaptor. *Molec. Cell.* **3** (1999), pp. 11-21.

[52] A.A. Peden, V. Oorschot, B.A. Hesser, C.D. Austin, R.H. Scheller RH, J. Klumperman, Localization of the AP-3 adaptor complex defines a novel endosomal exit site for lysosomal membrane proteins. *J Cell Biol.* **164** (2004), pp. 1065-76.

[53] S. Fontana, S. Parolini, W. Vermi, S. Booth, F. Gallo, M. Donini, M. Benassi, F. Gentili, D. Ferrari, L.D. Notarangelo, P. Cavadini, E. Marcenaro, S. Dusi, M. Cassatella, F. Facchetti, G.M. Griffiths, A. Moretta, L.D. Notarangelo, R. Badolato, Innate immunity defects in Hermansky-Pudlak type 2 syndrome. *Blood.* **107** (2006), pp. 4857-64

[54] J. Shim and J. Lee, The AP-3 clathrin-associated complex is essential for embryonic and larval development in Caenorhabditis elegans. *Mol Cells.* **19** (2005), pp. 452-7.

[55] G.J. Hermann, L.K. Schroeder, C.A. Hieb, A.M. Kershner, B.M. Rabbitts, P. Fonarev, B.D. Grant, J.R. Priess, Genetic analysis of lysosomal trafficking in Caenorhabditis elegans. *Mol Biol Cell.* **16** (2005), pp. 3273-88.

[56] G.V. Clokey and L.A. Jacobson, The autofluorescent "lipofuscin granules" in the intestinal cells of Caenorhabditis elegans are secondary lysosomes. *Mech Ageing Dev.* **35** (1986), pp. 79-94.

[57] E. Siintola, S. Partanen, P. Stromme, A. Haapanen, M. Haltia, J. Maehlen, A.E. Lehesjoki, J. Tyynela, Cathepsin D deficiency underlies congenital human neuronal ceroid-lipofuscinosis. *Brain.* **129** (2006), pp. 1438-1445.

[58] J. Vesa, E. Hellsten, L.A. Verkruyse, L.A. Camp, J. Rapola, P. Santavuori, S.L. Hofmann, L. Peltonen, Mutations in the palmitoyl protein thioesterase gene causing infantile neuronal ceroid lipofuscinosis. *Nature.* **376** (1995), pp. 584–587.

[59] IBDC, Isolation of a novel gene underlying Batten disease, CLN3. The International Batten Disease Consortium. *Cell.* **82** (1995), pp. 949-57.

[60] S.E. Mole, R.E. Williams, H.H. Goebel, Correlations between genotype, ultrastructural morphology and clinical phenotype in the neuronal ceroid lipofuscinoses. *Neurogenetics.* **6** (2005), pp. 107-26.

[61] J. Tyynela, I. Sohar, D.E. Sleat, R.M. Gin, R.J. Donnelly, M. Baumann, M. Haltia, P. Lobel, A mutation in the ovine cathepsin D gene causes a congenital lysosomal storage disease with profound neurodegeneration. *EMBO J.* **19** (2000), pp. 2786-92.

[62] M. Yanagawa, T. Tsukuba, T. Nishioku, Y. Okamoto, K. Okamoto, R. Takii, Y. Terada, K.I. Nakayama, T. Kadowaki, K. Yamamoto, Cathepsin E deficiency induces a novel form of lysosomal storage disorder showing the accumulation of lysosomal membrane sialoglycoproteins and the elevation of lysosomal pH in macrophages. *J Biol Chem.* **282** (2007), pp. 1851-62.

[63] P. Syntichaki, K. Xu, M. Driscoll, N. Tavernarakis, Specific aspartyl and calpain proteases are required for neurodegeneration in C. elegans. *Nature.* **419** (2002), pp. 939-44.

[64] S.J. Kim, Z. Zhang, E. Hitomi, Y.C. Lee, A.B. Mukherjee, Endoplasmic reticulum stress-induced caspase-4 activation mediates apoptosis and neurodegeneration in INCL. *Hum Mol Genet.* **15** (2006), pp. 1826-34.

[65] M. Lehtovirta, A. Kyttälä, E.L. Eskelinen, M. Hess, O. Heinonen, A. Jalanko, Palmitoyl protein thioesterase (PPT) localizes into synaptosomes and synaptic vesicles: implications for infantile neuronal ceroid lipofuscinosis (INCL). *Hum Mol Gen.* **10** (2001), pp. 69–75.

[66] M.Y. Porter, M. Turmaine, S.E. Mole, Identification and characterization of Caenorhabditis elegans palmitoyl protein thioesterase1. *J Neurosci Res.* **79** (2005), pp. 836-48.

[67] G. De Voer, P. van der Bent, A.J. Rodrigues, G.J. van Ommen, D.J. Peters, P.E. Taschner, Deletion of the Caenorhabditis elegans homologues of the CLN3 gene, involved in human juvenile neuronal ceroid lipofuscinosis, causes a mild progeric phenotype. *J Inherit Metab Dis.* **28** (2005) pp. 1065-80.

[68] S.L. Teitelbaum, Y. Abu-Amer, F.P. Ross Molecular mechanisms of bone resorption. *J Cell Biochem.* **59** (1995), pp. 1–10.

[69] M.A. Monroy, F.P. Ross, S.L. Teitelbaum, M.S. Sands, Abnormal osteoclast morphology and bone remodeling in a murine model of a lysosomal storage disease. *Bone.* **30** (2002), pp. 352-9.

[70] A.S. Nicot, H. Fares, B. Payrastre, A.D. Chisholm, M. Labouesse, J. Laporte, The Phosphoinositide Kinase PIKfyve/Fab1p Regulates Terminal Lysosome Maturation in Caenorhabditis elegans. *Mol Biol Cell.* **17** (2006), pp. 3062-3074.

[71] C.E. Fisherand S.E. Howie, The role of megalin (LRP-2/Gp330) during development. *Dev Biol.* **296** (2006), pp. 279-297.

[72] J. Yochem, S. Tuck, I. Greenwald, M. Han, A gp330/megalin-related protein is required in the major epidermis of Caenorhabditis elegans for completion of molting. *Development.* **126** (1999), pp. 597-606.

[73] J.M. Kramer, Extracellular matrix, in: C. elegans II, D.L. Riddle, T. Blumenthal, B.J. Meyer, J.R. Priess (Eds.) Cold Spring Harbor Laboratory Press, New York, (1997), pp. 471-500.

[74] N. Roudier, C. Lefebvre, R. Legouis. CeVPS-27 is an endosomal protein required for the molting and the endocytic trafficking of the low-density lipoprotein receptor-related protein 1 in Caenorhabditis elegans. *Traffic.* **6** (2005), pp. 695-705.

[75] A.M. Lennon-Dumenil, A.H. Bakker, R. Maehr, E. Fiebiger, H.S. Overkleeft, M. Rosemblatt, H.L. Ploegh , C. Lagaudriere-Gesbert, Analysis of protease activity in live antigen-presenting cells shows regulation of the phagosomal proteolytic contents during dendritic cell activation. *J Exp Med.* **196** (2002), pp. 529-40.

[76] N. Obermajer, A. Premzl, T. Zavasnik Bergant, B. Turk, J. Kos, Carboxypeptidase cathepsin X mediates beta2-integrin-dependent adhesion of differentiated U-937 cells. *Exp Cell Res.* **312** (2006), pp. :2515-27.

[77] S.Hashmi J. Zhang, Y. Oksov, S. Lustigman, The Caenorhabditis elegans cathepsin Z-like cysteine protease, Ce-CPZ-1, has a multifunctional role during the worms' development. *J Biol Chem.* **279** (2004), pp. 6035-45

[78] A.M. Schriever, T. Friedrich, M. Pusch, T.J. Jentsch, CLC chloride channels in Caenorhabditis elegans. *J Biol Chem.* **274** (1999), pp. 34238-44.

[79] S.M. Stobrawa, T. Breiderhoff, S. Takamori, D. Engel, M. Schweizer, A.A. Zdebik, M.R. Bosl, K. Ruether, H. Jahn, A. Draguhn, R. Jahn, T.J. Jentsch, Disruption of ClC-3, a chloride channel expressed on synaptic vesicles, leads to a loss of the hippocampus. *Neuron.* **29** (2001), pp. 185-96.

[80] H. Fares and I. Greenwald, Genetic analysis of endocytosis in Caenorhabditis elegans: coelomocyte uptake defective mutants. *Genetics.* **159** (2001), pp. 133-45.

[81] M. Starcevic and E.C. Dell'Angelica, Identification of snapin and three novel proteins (BLOS1, BLOS2, and BLOS3/reduced pigmentation) as subunits of biogenesis of lysosome-related organelles complex-1 (BLOC-1). *J Biol Chem.* **279** (2004), pp. 28393-401.

[82] A. Beigneux, S.K. Withycombe, J.A. Digits, W.R. Tschantz, C.A. Weinbaum, S.M. Griffey, M. Bergo, P.J. Casey, S.G. Young , Prenylcysteine lyase deficiency in mice results in the accumulation of farnesylcysteine and geranylgeranylcysteine in brain and liver. *J Biol Chem* **277** (2002) pp. 38358-63.

[83] L.D. Schroeder, S. Kremer, M.J. Kramer, E. Currie, E. Kwan, J.L. Watts, A.L. Lawrenson, G.J. Hermann, Function of the Caenorhabditis elegans ABC Transporter PGP-2 in the Biogenesis of a Lysosome-related Fat Storage Organelle. *Mol Biol Cell.* **18** (2007). pp. 995-1008.

[84] J. Hujova, J. Sikora, R. Dobrovolny, H. Poupetova, J. Ledvinova, M. Kostrouchova, M. Hrebicek, Characterization of gana-1, a Caenorhabditis elegans gene encoding a single ortholog of vertebrate alpha-galactosidase and alpha-N-acetylgalactosaminidase. *BMC Cell Biol.* **6** (2005), pp. 5.

[85] C.I. Bargmann High-throughput reverse genetics: RNAi screens in Caenorhabditis elegans. *Genome Biol.* **2** (2001), REVIEWS1005.

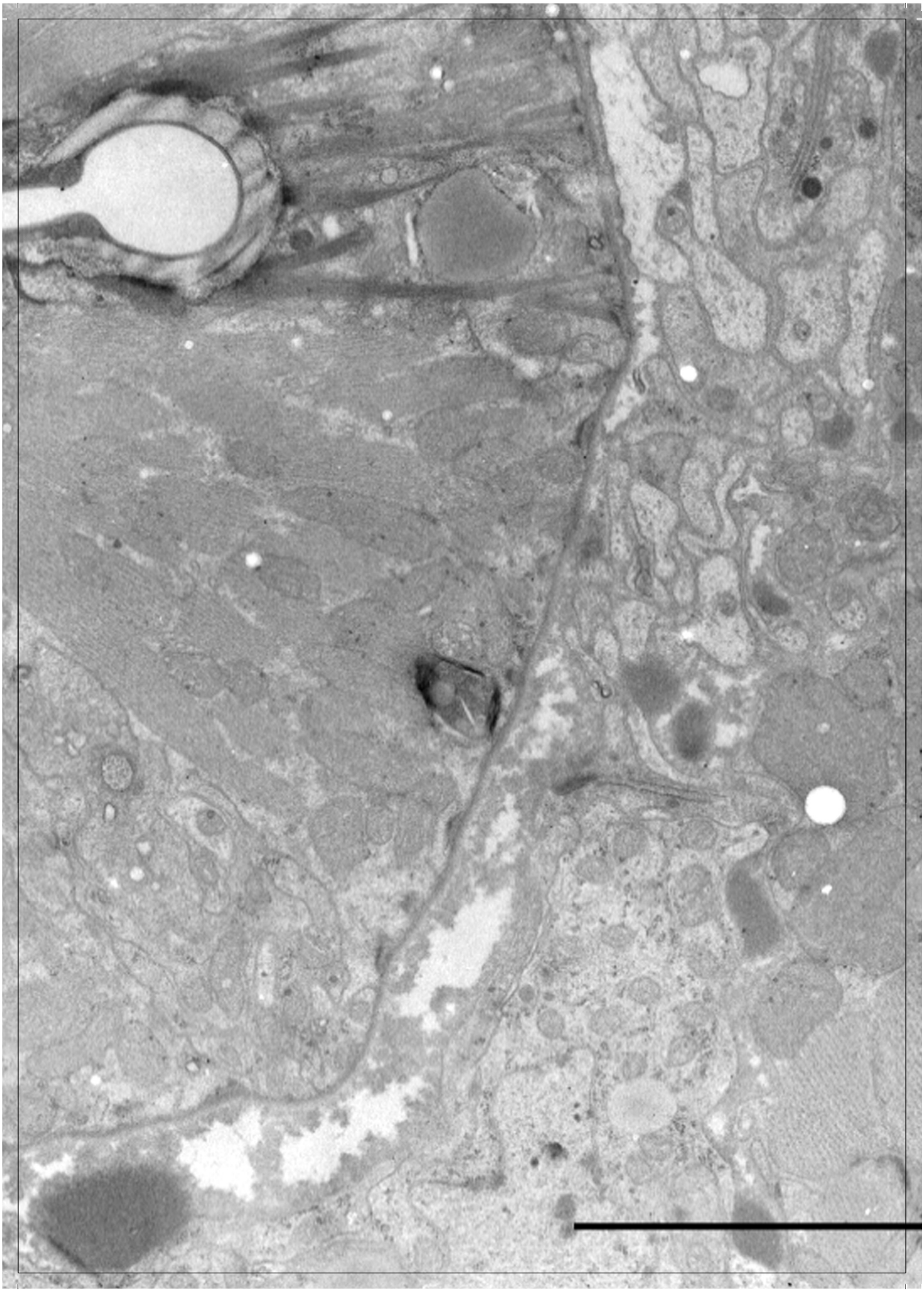

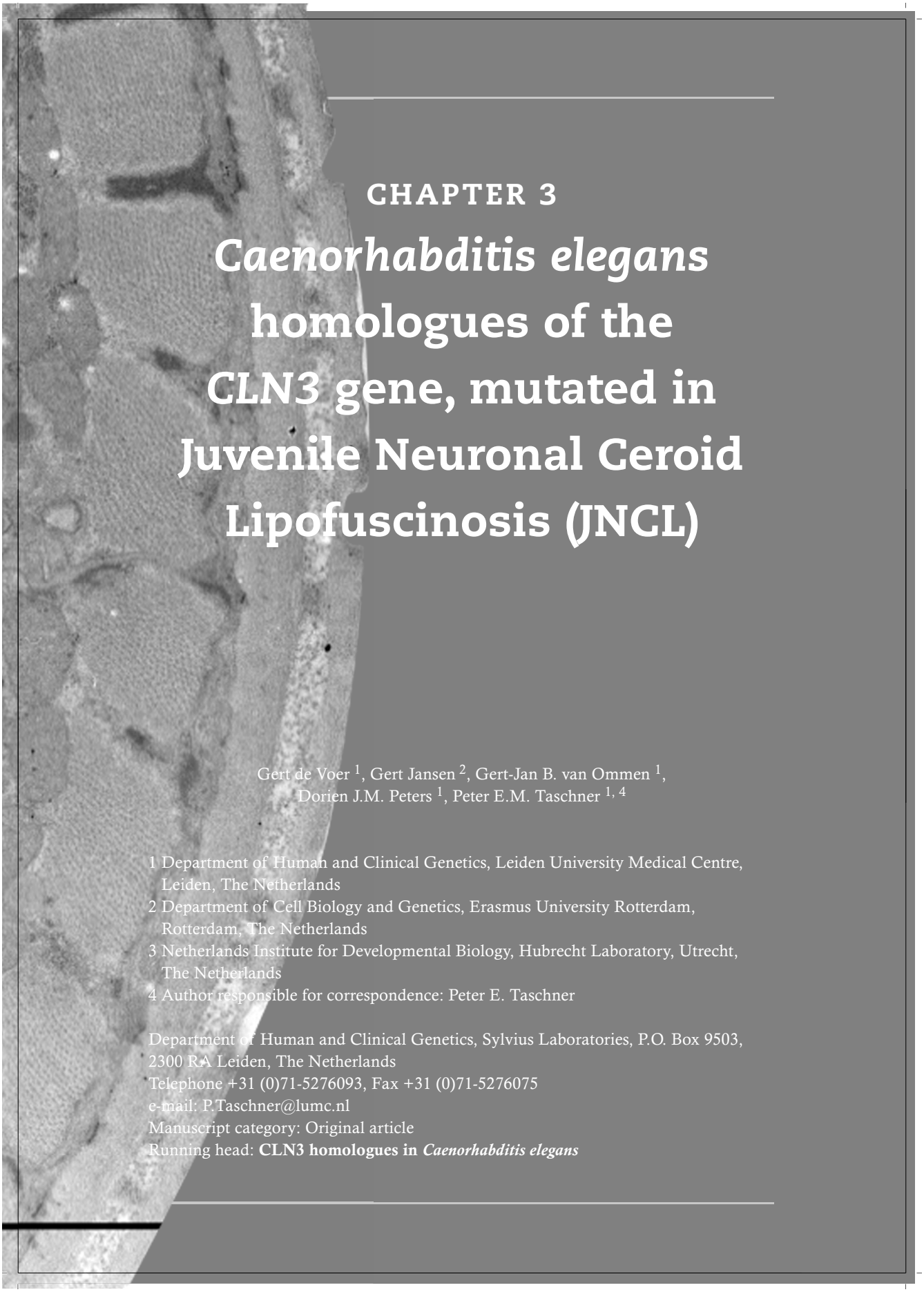

CHAPTER 3

Caenorhabditis elegans homologues of the *CLN3* gene, mutated in Juvenile Neuronal Ceroid Lipofuscinosis (JNCL)

Gert de Voer [1], Gert Jansen [2], Gert-Jan B. van Ommen [1],
Dorien J.M. Peters [1], Peter E.M. Taschner [1, 4]

1 Department of Human and Clinical Genetics, Leiden University Medical Centre, Leiden, The Netherlands
2 Department of Cell Biology and Genetics, Erasmus University Rotterdam, Rotterdam, The Netherlands
3 Netherlands Institute for Developmental Biology, Hubrecht Laboratory, Utrecht, The Netherlands
4 Author responsible for correspondence: Peter E. Taschner

Department of Human and Clinical Genetics, Sylvius Laboratories, P.O. Box 9503, 2300 RA Leiden, The Netherlands
Telephone +31 (0)71-5276093, Fax +31 (0)71-5276075
e-mail: P.Taschner@lumc.nl
Manuscript category: Original article
Running head: **CLN3 homologues in *Caenorhabditis elegans***

Abstract

Neuronal ceroid lipofuscinoses (NCL) are the most common hereditary neurodegenerative disorders of childhood. The first symptom of this heterogeneous group of devastating lysosomal storage diseases is progressive visual failure. The different forms of NCL can be specified by age of onset, clinical features and characteristics of the accumulated materials. The juvenile form, Batten-Spielmeyer-Vogt disease caused by mutations in the CLN3 gene, is the most frequent form of the disease in which loss of vision becomes apparent at the age 5 – 8 years. The gene was found to encode a novel integral membrane protein localising to the lysosomes, confirming that the primary defect in NCL is in lysosomal function. The CLN3 protein function is still unknown, and is examined in several model organisms. We are studying the nematode *Caenorhabditis elegans*, and identified three CLN3 homologues. In order to investigate the role of the CLN3 protein in *C. elegans*, CeCLN3 deletion mutants are being isolated from an ethyl methanesulphonate (EMS)-induced deletion mutant library. Examination of these mutants may provide us with information that will help dissecting the processes in which the CLN3 protein is involved. In this library two mutated *C. elegans* CLN3 loci have been identified, of which one mutant, NL748, was isolated. This mutant contains a deletion of the whole gene. The deletion mutant was characterised regarding the life span, and showed no prominent difference compared to wild-type.

Keywords: Neuronal ceroid lipofuscinosis – Batten disease – NCL – CLN3 – *Caenorhabditis elegans*

Introduction

The neuronal ceroid lipofuscinoses form a group of lysosomal storage diseases with a devastating nature [1]. This group of congenital children's disorders has an incidence of 1:12 500 births in Northern Europe and the USA, and 1:100 000 elsewhere [2, 3]. Clinical features of this diverse neurodegenerative disease are on-going ocular deterioration, epileptic fits, and gradual dementia. Ultimately the patients die in a vegetative state [1]. On account of the differences among the disease-types, particularly starting age, one can discriminate between infantile, late infantile, juvenile, and adult NCL. A common feature of all forms of NCL is the accumulation of autofluorescent lipopigments in neurons and to a lesser extent in other cell types [1]. The major accumulated component in most types of NCL, with the exception of the infantile form, was found to be Subunit *c* of the mitochondrial ATP synthase [4, 5].

The most abundant form of NCL is the juvenile form, JNCL or Batten-Spielmeyer-Vogt disease[1]. It has been linked to the CLN3 gene in which mutations, most often a 1.02 kb deletion, are causing the disease[6]. The function of the CLN3 protein is still unknown, but it is situated in the lysosomes[7], and the Golgi apparatus[8], which supports the observation of failing lysosomal operation. So far, no direct link between the gene product and the accumulated Subunit *c* has been established.

To characterise the CLN3 protein, research was done in model organisms. Sequence comparison indicated the existence of CLN3 homologues in several organisms, including *Mus musculus, Saccharomyces cerevisiae*, and *C. elegans* [9]. Natural mutants displaying NCL symptoms occur in a wide range of animal species [10]. However none of these models are caused by mutations in the CLN3 gene, which should be the case for an ideal JNCL model. In order to study the function of normal and mutated CLN3 proteins two CLN3 knockout mouse models [11, 12], and one knockout yeast model [13] have been developed. The murine models are expected to be of great use in the process of developing and testing new treatments, but may be too complex for functional studies. The knockout yeast model [13] appears to be useful for investigations at the cellular level. On the other hand a yeast model can not provide any knowledge about the role of the CLN3 protein in a multicellular environment, e.g. in the nervous system, where the major defect in NCL patients is observed.

A relatively simple multicellular eukaryote is needed to fill the gap between these two model organisms, and to investigate the processes the CLN3 protein is involved in. The nematode *C. elegans* might fill this gap since this is a small, easy manageable organism with a distinct number of cells of known lineage and a completely described anatomy. Furthermore *C. elegans* has a nervous system, consisting of 302 neurons with 7600 mapped synaptic junctions [14]. Probably the nematode will allow us to investigate the function of the CLN3 genes in different cell types, including the most affected cells in humans, the neurons. The availability of the CLN3 homologues, the nervous system, and the other advantages mentioned above make *C. elegans* a suitable model organism to research the neuronal ceroid lipofuscinoses.

Materials and Methods

Strains and growth conditions

We used *Caenorhabditis elegans* strains: wild-type Bristol N2, mutant *mev-1* (kn1) [15, 16], kindly provided by Dr. N. Ishii, is a positive control on account of its increased accumulation of lipofuscin. CLN3 deletion mutant NL748 (*pk479*) which was derived from an N2 background.
All nematodes were cultured at 20 °C as previously described [17].

Sequence comparison and alignment

The three *C. elegans* CLN3 homologues were identified by means of a Blastp search http://www.ncbi.nlm.nih.gov/BLAST/ using the human CLN3 protein sequence. The nematode's CLN3 homologues were aligned to the human, Genbank Accession number U32680, canine L76281, murine U68064, rabbit U92812, Drosophila AE003522, and yeast Z49334 CLN3 protein sequences, using ClustalW v. 1.8 on the Baylor College of Medicine server http://gc.bcm.tmc.edu:8088/. Boxshade 3.21 was used to indicate conservation between species in the alignment http://www.ch.embnet.org/software/BOX_form.html. *C. elegans* CLN3 proteins were compared to eachother concerning sequence identity and similarity.

Isolation of deletion mutants

A *C. elegans* ethyl methanesulphonate (EMS)-induced deletion mutant library was constructed by Jansen *et al* [18]. The CLN3 deletion mutants were isolated by screening with nested PCR primers, and by using the protocol as previously described [18]. Primers that are approximately 3 kb apart were designed from the genomic sequences of the CLN3 homologues.
To isolate CeCLN3-1 deletion mutants, library pools were screened using a nested PCR. The first PCR was performed with primer pair: CeCLN3-1 F1 (5' CGC GTT TCC AGT ATT CTC AG 3') and CeCLN3-1 R1 (5' CTG GAA CTA CGA ATT GAG GG 3'), this was nested with primer pair: CeCLN3-1 F2 (5' TTC CAG AAG GAC AGT CTA GG 3') and CeCLN3-1 R2 (5' TAG ACA TGT CAA CGA GCT CC 3'). When after the PCR screening an aberrant band was detected, this band was cut out gel and sequenced using primer pair F2, and R2 and standard sequencing procedures. After isolation of a mutant subline, the mutation was transferred into a clean background by backcrossing six times with wild-type N2 to minimise the occurrence of mutations in other genes.

CeCLN3-2 deletion mutants were isolated by screening the library pools using primer pair: CeCLN3-2 F1 (5' TTCTGCGAAAAATTGAATCCC 3') and CeCLN3-2 R1 (5' TTC GGG TTC GGT CAG TTA TC 3'), this was nested with primer pair: CeCLN3-2 F2 (5'AAT TCC AGA ATG GAT GTG GC 3') and CeCLN3-2 R2 (5' CAA CGG AGA TAT GGT TTC AAA G 3').

Characterisation of longevity of *C. elegans* mutants

Hundred worms from pools of synchronously growing L1 wild-type N2, mutant NL748, and mutant *mev-1* strains were plated individually on 5 cm petri-dishes, and were cultured under standard conditions at 20 °C as described above. The nematodes were counted, and checked for movement almost daily, and placed onto a fresh dish in case any progeny appeared. If the worms were not moving, a tap on the head was used to examine their reflexes. When no movement was observed after a tap on the head, the worm was scored as being dead.

Results

Sequence comparison

The human CLN3 protein sequence was compared to *C. elegans* protein sequences using a Blastp search. Three matches were found, situated on cosmids F07B10 (Genbank Accession number Z77656), C01G8 (U80439), and ZC190 (AF078788). The genes have been named CeCLN3-1, CeCLN3-2, and CeCLN3-3 respectively, encoding putative proteins of 424, 435, and 375 amino acids respectively. Additional details about the nematodes CLN3 homologues can be seen in table 1. The protein sequences of CLN3-1 and CLN3-2 share 43% identity and 63% similarity, CLN3-1 and CLN3-3 49% identity and 62% similarity, and CLN3-2 and CLN3-3 show 37% identity and 52% similarity. Sequence analyses predict 9, 7, and 9 exons respectively for CeCLN3-1, CeCLN3-2, and CeCLN3-3 (Figure 1). To examine the sequences for conserved stretches an alignment was done with the amino acid sequences of human, canine, murine, rabbit, Drosophila, and yeast CLN3 proteins (Figure 2). Comparison of the CLN3 protein sequences indicates that the predicted proteins contain several conserved regions that may be important for CLN3 protein function.

Table 1 The three *C. elegans* CLN3 homologues, and some of their characteristics

Gene	**cosmid**	**genomic** size (bp)	**amino** acids	**% identity** to human CLN3	**% similarity** to human CLN3	**chromosomal** localisation	**Genbank** accession numbers
CeCLN3-1	F07B10	2017	424	36	53	V	Z77656
CeCLN3-2	C01G8	3928	435	36	49	I	U80439
CeCLN3-3	ZC190	2660	375	39	62	V	AF078788

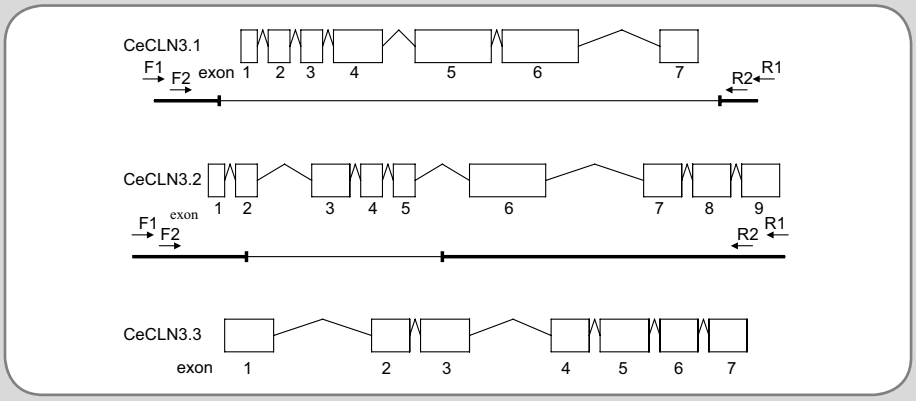

Figure 1 The genomic structure of the *C. elegans* CLN3 homologues CeCLN3-1, CeCLN3-2, and CeCLN3-3

The deletions are indicated by the thin line directly under the genes CeCLN3-1 and CeCLN3-2; the primers (F1, R1, F2, and R2) used to detect the deletion indicated by arrows. The exons are indicated by boxes and the introns are indicated by upside down V's.

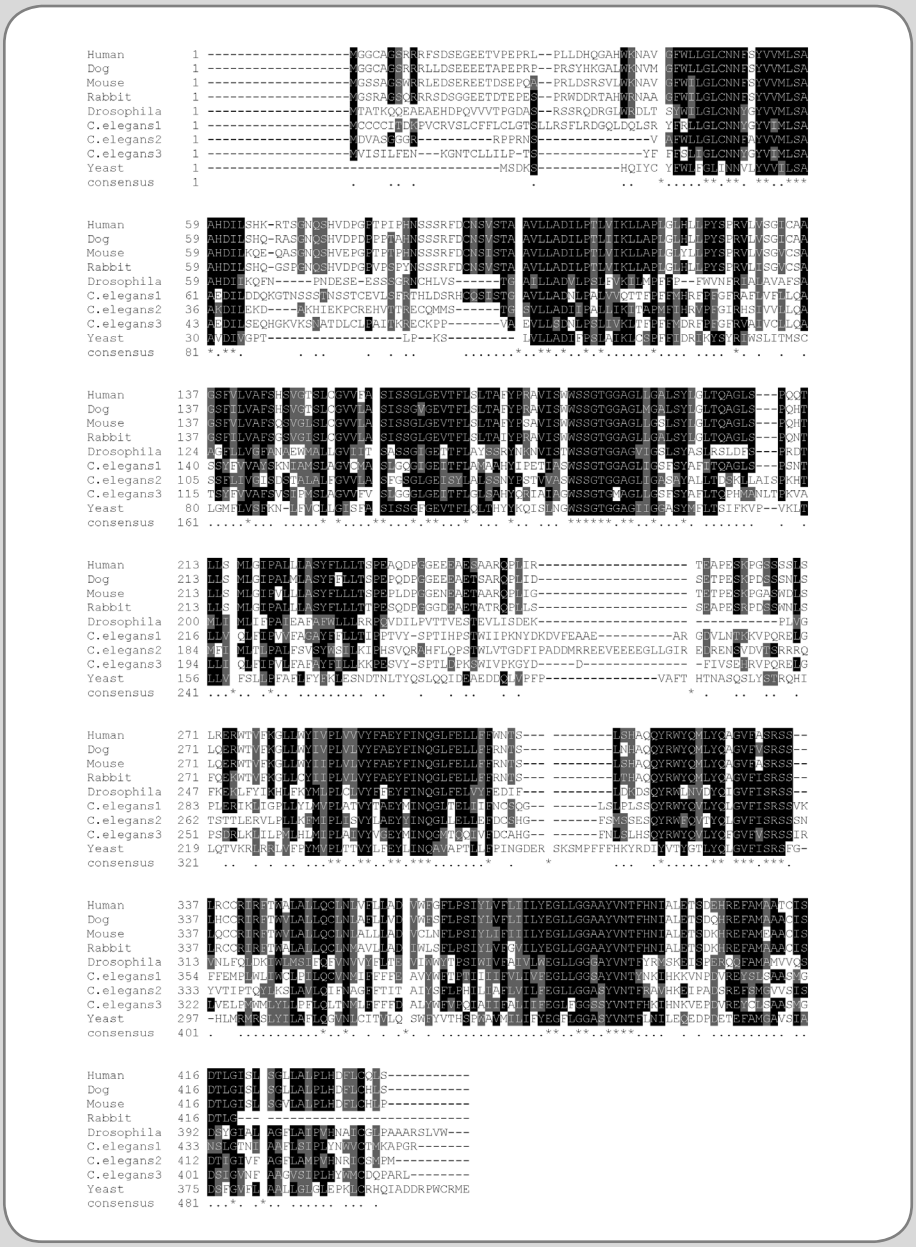

Figure 2 Alignment of the sequences from human, canine, murine, rabbit, Drosophila, *C. elegans*, and yeast CLN3 proteins

To obtain maximum homology the Genefinder sequences of the genes, *C.elegans* and *Drosophila melanogaster* sequences have been adjusted with regard to reading frames. Conserved amino acid residues are shown in black boxes, neutral substitutions in grey boxes. The consensus sequence is indicated by asterisks when fully conserved, and by dots when more than 50 % conserved between species.

Isolation of deletion mutants

In order to get more insight in gene functions CLN3 deletion mutants were isolated from an ethyl methanesulphonate (EMS)-induced deletion mutant library[18]. The primary screening of this mutant library indicated that the library pools contain mutants with deletions in two out of three *C. elegans* CLN3 genes, CeCLN3-1, and CeCLN3-2. A mutant with a deletion in CeCLN3-1 was isolated from the mutant pools. This mutant was found to carry a 2.5 kb deletion (Figure 1), and has been designated NL748. Sequence analysis indicated that the region from 100 bp upstream of the start codon to 330 bp downstream of the stop codon is deleted. Therefore, the mutant NL748 carries a null allele (*pk 479*) of the CLN3 homologue CeCLN3-1.

Phenotypic characterisation of NL748

The NL748 mutants exhibit no obvious phenotypic alterations. Examination in closer detail at the behavioural and the cellular level is required to detect an aberrant phenotype. In a life-span experiment longevity of the N2 wild-type, the *mev-1* mutant, and the NL748 mutant nematodes was determined. The *mev-1* mutant strain is a positive control because it has been shown to age faster than the wild-type (N2) strain[16]. Figure 3 was created by dividing the number of living worms at the moment of counting by the total number of worms at the beginning of the experiment.
No dramatic difference in longevity has been observed between the N2 wild-type and the NL748 deletion mutant, whereas the *mev-1* mutant clearly exhibits a shorter life span.

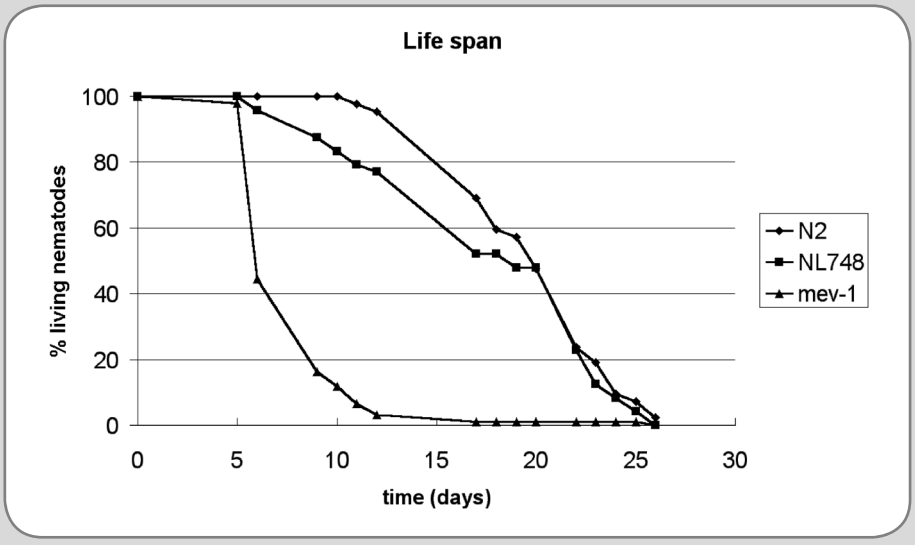

Figure 3 Life-span of N2 wild-type, NL748 deletion mutant, and *mev-1* mutant
The NL748 mutant strain shows no different longevity compared to the wild-type.

Discussion

Although Batten disease has been studied extensively, and the CLN3 gene was identified in 1995 no protein function has been established yet. The CLN3 protein is under survey in different eukaryotic species. In the mouse, targeted disruption of the CLN3 gene was used to create a model for JNCL[11]. When these mice are homozygous for their CLN3 null alleles, they display a neuronal storage disorder with the same characteristics seen in Batten disease patients. For instance, the *Cln3-/-* mice exhibit progressive accumulation of autofluorescent material in the neurons. In addition, inclusions were found that contained Subunit c of mitochondrial ATP-synthase. Although the mice show characteristic features of JNCL, they did not develop obvious clinical symptoms by 12 months of age. Furthermore, the naturally occurring mouse models for NCL[19, 20] display more severe cellular changes than the *Cln3-/-* knock-out. Whereas additional research in the mouse model is necessary, another model organism, yeast, provides an abundance of information at the cellular level. In yeast a CLN3 orthologue, BTN1[13], was knocked out resulting in a viable mutant that is able to degrade mitochondrial ATP-synthase. The BTN1 protein localises to the vacuole, which functions as a lysosome, and regulates osmosis in the yeast cell. BTN1 knock-out yeast are resistant to ANP (D-(-)-threo-2-amino-1-[*p*-nitrophenyl]-1,3-propanediol) since they have improved their ability to acidify the growth medium. In fact the pH of the mutant vacuole is lowered early in the growth phase, and this effect can be rescued by introducing the human CLN3 gene, indicating a connection between CLN3 and cellular pH regulation. Although yeast proves to be a suitable model for investigation at the cellular level, it unfortunately is a unicellular organism which makes it arduous to extrapolate the results provided by the experiments with this organism to the clinical picture of the disease. The nematode *C. elegans* is a multicellular very elaborately described organism, and has the advantages that its genome and anatomy of the nervous system have been well characterised. Which make it a more attractive model organism to study the functions of homologues of genes involved in human neurodegenerative disorders.

In *C. elegans* we identified three CLN3 homologous genes CeCLN3-1, CeCLN3-2, and CeCLN3-3, allowing functional studies at the protein level, and of the processes the protein is involved in. The CLN3 protein sequence alignment reveals several conserved areas present in all examined species, suggesting that they are essential for protein function. The different number of exons and the different predicted exon-intron boundaries of the CLN3 genes of *C. elegans*, point to ancient duplications in the nematode.

The next logical step is analysis of mutants. To do so, we analysed a *C. elegans* mutant library and identified deletion mutants for two of the genes. For CeCLN3-1 a mutant, NL748, was isolated. For CeCLN3-2 a mutant was localised in a mutant pool, and

will be isolated in the near future. Mutant NL748 did not show an obvious phenotype although the whole gene was deleted. This could be due to redundancy, because three CLN3 homologues are available. Another possibility may be that CeCLN3-1 is not a functional *C. elegans* CLN3 gene but only a rudiment, and one of the other genes is functional. Also, CLN3 might prove to be a gene involved in stress situations, therefore the phenotype will be examined under different stress conditions. We will continue the phenotypic characterisation studies of the NL748 deletion mutants, focussing on sensory behaviour because we expect to find neurological defects since NCL mainly manifests itself in the neurons. Similar experiments will be performed for the other mutants as well as for double and triple mutants.
To study the disability of the mutants in closer detail it is necessary to know in which cells, and in what life stage the CeCLN3 genes are being transcribed. That is why CeCLN3 expression studies are being performed. These experiments should make cellular differences between wild-type and NL748 mutant easier to detect.
We expect that analysis of *C. elegans* CLN3 mutants will provide us with information about the processes in which the CLN3 proteins play a role, and will give further insight into the functions of the CLN3 protein and in the mechanism of neurodegeneration in NCL.

Acknowledgements

This study was supported by the Centre for Biomedical Genetics. We thank Dr. N. Ishii for kindly providing the *mev-1* mutant, and Dr. S. White for critically reading the manuscript.

References

1. Rapola J. Neuronal ceroid lipofuscinoses in childhood. Perspect Pediatr Pathol 1993; 17: 7-44.

2. Rider JA, Rider DL. Batten's disease. Past, present, and future. Am J Med Genet 1988; 5 (Suppl): 21-26.

3. Uvebrant P, Hagberg B. Neuronal ceroid lipofuscinoses in Scandinavia: epidemiology and clinical pictures. Neuropediatrics 1997; 28: 6-8.

4. Palmer DN, Fearnley IM, Walker JE, *et al.* Mitochondrial ATP synthase Subunit *c* storage in the ceroid-lipofuscinoses (Batten disease). Am J Med Genet 1992; 42: 561-567.

5. Hall NA, Lake BD, Dewji NN, Patrick AD. Lysosomal storage of Subunit *c* of mitochondrial ATP synthase in Batten's disease (ceroid lipofuscinosis). Biochem J 1991; 275: 269-272.

6. International Batten Disease Consortium. Cell 1995; 82: 949-957.

7. Järvelä I, Sainio M, Rantamaki T, *et al.* Biosynthesis and intracellular targeting of the CLN3 protein defective in Batten disease. Hum Mol Genet 1998; 7: 85-90.

8. Kremmidiotis G, Lensink IL, Bilton RL, *et al.* The Batten disease gene product (CLN3p) is a Golgi integral membrane protein. Hum Mol Genet 1999; 8: 523-531.

9. Taschner PEM, de Vos N, Breuning MH. Cross-species homology of the CLN3 gene. Neuropediatrics 1997; 28: 18-20.

10. Jolly RD. Comparative biology of the neuronal ceroid lipofuscinoses (NCL): An overview. Am J Med Genet 1995; 57: 307-311.

11. Mitchison HM, Bernard DJ, Greene ND, *et al.* Targeted disruption of the CLN3 gene provides a mouse model for Batten disease. Neurobiol Dis 1999; 6: 321-334.

12. Katz ML, Shibuya H, Liu PC, *et al.* A mouse gene knockout model for juvenile ceroid-lipofuscinosis (Batten disease). J Neurosci Res 1999; 57: 551-556.

13. Pearce DA, Sherman F. A yeast model for the study of Batten disease. Proc Natl Acad Sci USA 1998; 95: 6915-6918.

14.White JG, Southgate E, Thomson JN, Brenner S. The structure of the nervous system of Caenorhabditis elegans. Philos Trans R Soc Lond (Biol) 1986; 314: 1-340.

15. Hosokawa H, Ishii N, Ishida H, *et al.* Rapid accumulation of fluorescent material with aging in an oxygen-sensitive mutant mev-1 of Caenorhabditis elegans. Mech Ageing Dev 1994; 74: 161-170.

16. Ishii N, Fujii M, Hartman PS, *et al.* A mutation in succinate dehydrogenase cytochrome *b* causes oxidative stress and ageing in nematodes. Nature 1998; 394: 694-697.

17. Sulston J, Hodgkin J. Methods. In: Wood WB (ed) The nematode *Caenorhabditis elegans*. Cold Spring Harbor, NY. Cold Spring Harbor Laboratory, 1988: 587-606.

18. Jansen G, Hazendonk E, Thijssen KL, and Plasterk RH. Reverse genetics by chemical mutagenesis in Caenorhabditis elegans. Nature Genet 1997; 17: 119-121.

19. Bronson RT, Donahue LR, Johnson KR, *et al.* Neuronal ceroid lipofuscinosis (*ncl*), a new disorder of the mouse linked to chromosome 9. Am J Med Genet 1998; 77: 289-297.

20. Messer A, Plummer J, Maskin P, Coffin JM, Frankel WN. Mapping of the motor neuron degeneration (*Mnd*) gene, a mouse model of amyotrophic lateral sclerosis (ALS). Genomics 1992;13: 797-802.

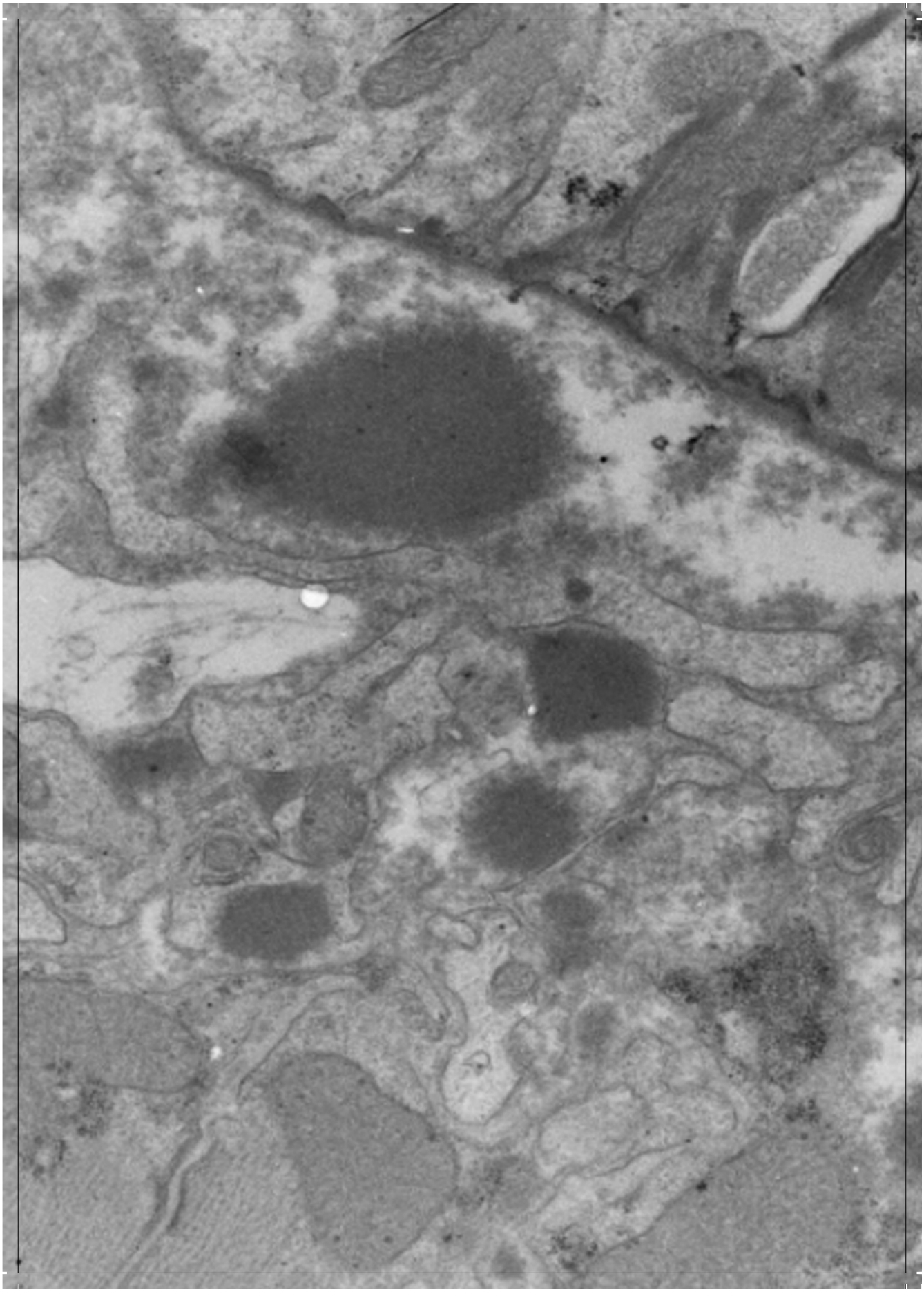

CHAPTER 4

Deletion of the *Caenorhabditis elegans* homologues of the *CLN3* gene, involved in human Juvenile Neuronal Ceroid Lipofuscinosis (JNCL), causes a mild progeric phenotype

Gert de Voer, Paola van der Bent, Ana João G. Rodrigues *,
Gert-Jan B. van Ommen, Dorien J.M. Peters, Peter E.M. Taschner #

Department of Human Genetics, Center for Human and Clinical Genetics, Leiden University Medical Center, Leiden, The Netherlands
* ICVS, School of Health Sciences, Minho University, Gualtar Campus, Braga, Portugal
# Correspondence: Department of Human Genetics, Center for Human and Clinical Genetics, Sylvius Laboratories, Leiden University Medical Center, P.O. Box 9503, 2300 RA Leiden, The Netherlands, Telephone +31 (0)71-5276093, Fax +31 (0)71-5276075
e-mail: P.Taschner@lumc.nl
Running head title: *Caenorhabditis elegans cln-3* mutants
Subject index: *CLN3*, *Caenorhabditis elegans*, Batten

Summary

The *CLN3* gene is involved in Juvenile Neuronal Ceroid Lipofuscinosis (JNCL) or Batten-Spielmeyer-Vogt disease, a severe hereditary neurodegenerative lysosomal storage disorder characterized by progressive disease pathology, with loss of vision as the first symptom. Another characteristic of JNCL is the lysosomal accumulation of autofluorescent lipopigments, forming fingerprint storage patterns visible by electron microscopy. The function of the CLN3 protein is still unknown, although the evolutionary conserved CLN3 protein is being functionally analyzed using different experimental models. We have explored the potential of the nematode *C. elegans* as a model for Batten disease in order to bridge the gap between the unicellular yeast and very complex mouse JNCL models. *C. elegans* has three genes homologous to *CLN3*, for each of which deletion mutants were isolated. *Cln-3.1* deletion mutants have a decreased life span, and *cln-3.2* deletion mutants a decreased brood size. However, the neuronal or movement defects, aberrant lipopigment distribution or accumulation observed in JNCL were not found in worms. To detect possible redundancy, single deletion mutants were crossed to obtain double and triple mutants, which were viable, but showed no JNCL-specific defects. The *cln-3* triple mutants show a more prominent decrease in life span and brood size, the latter most conspicuously at the end of the egg-laying period, suggesting premature aging. To focus our functional analysis we examined the *C. elegans cln-3* expression patterns, using promoter-Green Fluorescent Protein gene fusions. Fluorescence patterns suggest *cln-3.1* expression in the intestine, *cln-3.2* expression in the hypoderm, and *cln-3.3* expression in intestinal muscle, male specific posterior muscle, and hypoderm. Further life stage and tissue-specific analysis of the processes causing the phenotype of the *cln-3* triple mutants may provide more information about the function of the CLN3 protein and contribute to a better understanding of the basic processes affected in Batten disease patients.

Introduction

Mutations in the *CLN3* gene cause the juvenile and most frequent form of the neuronal ceroid lipofuscinoses (NCLs) or Batten disease (The International Batten Disease Consortium 1995). The NCLs are devastating lysosomal storage diseases collectively comprising the most common inherited neurodegenerative disorders of childhood with an incidence of 1 in 12,500. Patients suffering from NCL display a gradual neurological decline starting with loss of vision, generally between 4 – 10 years of age for JNCL (McKusick 204200) patients, followed by epileptic seizures and a state of dementia ending in premature death (Rapola 1993). In addition, the NCLs are characterized by lysosomal lipopigment accumulations, which form typical storage patterns the so-called fingerprints in JNCL patients.

Truncating and missense mutations can disrupt the *CLN3* gene and cause similar pathology (Mole et al 2001). The *CLN3* gene encodes a protein that is predicted to be very hydrophobic and contains 5 – 7 transmembrane domains (Mao et al 2003). The CLN3 protein has been localized in lysosomes and synaptosomes (Jarvela et al 1998, Golabek et al 1999, Kida et al 1999, Ezaki et al 2003, Luiro et al 2001), but other localizations in or near nuclei and plasma membranes, Golgi apparatus, and mitochondria have also been reported (Margraf et al 1999, Kremmidiotis et al 1999, Katz et al 1997). Furthermore, Btn1p, the yeast *Saccharomyces cerevisiae* CLN3 homologue localizes to the vacuole, which functions as the yeast lysosome, and may be involved in vacuolar pH homeostasis (Pearce et al 1999 B). Moreover, yeast *Btn1* mutants display upregulation of the gene encoding Btn2p, which interacts with and is necessary for the correct localization of Rsg1p, a down regulator of an arginine/lysine transporter. Mislocalization of Rsg1p in *Btn2* mutants causes an elevated rate of uptake of arginine (Chattopadhyay et al 2000, Chattopadhyay and Pearce 2002). Increased levels of arginine and lysine were found in the vacuoles of yeast *Btn1* mutants compared to wild type (Kim et al 2003). Sera of *Cln3* knockout mice contain elevated levels of lysine and several other amino acids compared to wild type, further suggesting a role for the Cln3 protein in (lysosomal) amino acid transport (Pearce et al 2003). Interestingly, Btn2p contains homology to HOOK1 in humans and *Drosophila*, and HOOK1 regulates endocytosis in the latter (Kramer and Phistry 1996). Luiro et al (2004) found a weak biochemical interaction of CLN3 with HOOK1, and showed that JNCL fibroblasts were impaired in receptor-mediated endocytosis. Taken together, the CLN3 protein might combine amino acid and proton transport, resulting in changes of amino acid levels as well as endosomal/lysosomal pH, and thereby affecting receptor-mediated endocytosis.

The precise mechanism of JNCL pathogenesis remains unknown, although investigations in the unicellular *Btn1* yeast mutants and in neurologically very complex *Cln3* knockout mouse models have proven valuable in elucidating details about the

disease process. We have investigated the potential of the nematode *Caenorhabditis elegans* as a model for JNCL, since a disease model with a simple nervous system might fill the gap between the yeast and mouse model systems. The nematode is a relatively simple organism consisting of 959 cells, of which 302 are neurons. It has an entirely mapped and invariant cell-lineage and nervous system, and an extensive genetic toolset is available. Due to the presence of homologues to human disease genes, Culetto and Sattelle (2000) suggested that *C. elegans* may be an ideal model organism for studying these genes. Moreover, the nematode is a convenient model to explore human neurodegenerative diseases, as demonstrated by the development of disease models for Niemann-Pick type C (McKusick 257220), mucolipidosis type IV (McKusick 252650), and neurodegeneration caused by expanded poly-glutamine repeats (Sym et al 2000, Fares and Greenwald 2001, Faber et al 2002). Since the *C. elegans* genome contains three *CLN3* homologues (de Voer et al 2001), we report here the expression patterns of the three *cln-3* genes and the phenotypes of *C. elegans cln-3* mutants.

Materials and Methods

Strains and growth conditions

C. elegans strains used in this study were wild type Bristol N2, the *cln-3* deletion mutants NL796 [*cln-3.1(pk479)*V] (kindly provided by the Plasterk lab), VC113 [*cln-3.2(gk41)* I], VC146 [*cln-3.3(gk118)*V] (both kindly provided by the *C. elegans* gene knock out consortium), and the neuronal GFP reporter strain OH441 *otIs45 V[unc-119::GFP]* (kindly provided by the Caenorhabditis Genetics Center). The *cln-3* deletion mutants were backcrossed six times to the wild type N2 background and re-designated XT1, XT2, and XT3, respectively, before starting phenotypic analysis (Figure 1). The *cln-3* single deletion mutants were crossed to obtain *cln-3* double mutants XT4[*cln-3.1(pk479)cln-3.3(gk118)*V], XT5[*cln-3.2(gk41)*I; *cln-3.1(pk479)*V], XT6[*cln-3.2(gk41)*I; *cln-3.3(gk118)*V], and triple mutants XT7[*cln-3.2(gk41)*I; *cln-3.1(pk479)cln-3.3(gk118)*V]. General methods for culturing, manipulation and genetics of *C. elegans* were described previously (Epstein and Shakes 1995). Unless indicated otherwise all worm strains were grown at 20 °C.

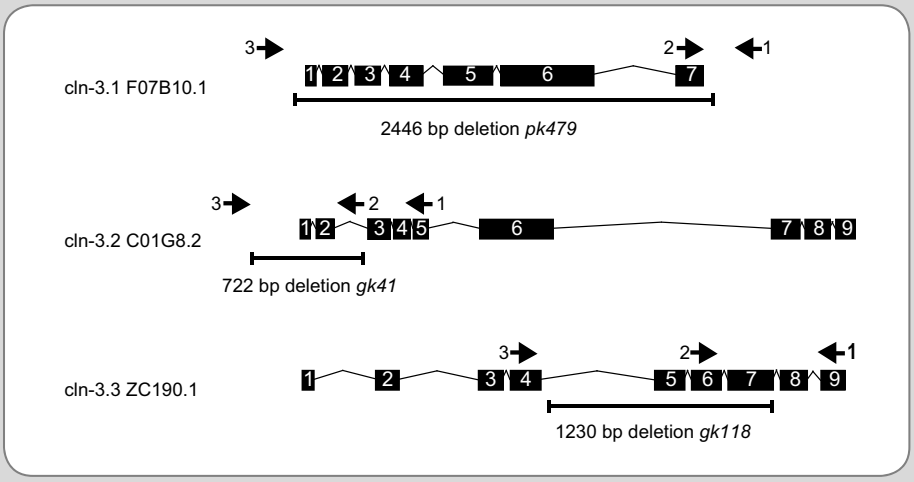

Figure 1 Schematic exon-intron structure of the *cln-3* genes

Exons that are indicated by filled numbered boxes separated by introns (^). Deletions are depicted by the black lines below the gene structures. Numbered arrows indicate the primers used to screen for the presence of the deletions (see table 1).

Bacterial strains used for cloning, DH10B (GIBCO DRL Life Technologies), and DY380 (kindly provided by Donald Court), were grown on Luria-Bertani medium supplemented with appropriate antibiotics if necessary (25 µg/ml kanamycin, 50 µg/ml ampicillin, 12.5 µg/ml tetracyclin). Plasmids used for cloning were pPD95-77 (kindly provided by Andrew Fire, Carnegie Institute of Washington, Baltimore, MD), pBluescript KS+ (Stratagene, La Jolla, CA), and pUC4K (Acc. no. X06404). Cosmids used for generating the *cln-3* reporter constructs were F07B10 (*cln-3.1*, Acc. no. Z77656), C01G8 containing a four-gene operon including *cln-3.2* (*cln-3.2*, Acc. no. U80439) (Blumenthal et al 2002), and ZC190 (*cln-3.3*, Acc. no. AF078788) (kindly provided by John Sulston).

Phenotypic analysis

To assess movement, morphology and anatomy worms were observed throughout all stages of life using a dissection microscope (Leica MZ-FLIII). Worms were mounted on freshly prepared 2% agarose pads on microscope slides, were anaesthetized with 20 mM sodium azide in M9 buffer and covered with a cover slip for observation at a higher magnification and for fluorescence analysis using an inverted microscope (Zeiss Axiovert S100), a fluorescence microscope (Leica DM-RA2), or a confocal laser scanning microscope (Leica TCS SP2-RS). Neuronal integrity was assessed by testing mechanosensation using nose-touch and body touch assays (Kaplan and Horvitz 1993), thermotaxis using the isothermal tracking assay (Hedgecock and Russell 1975), normal body movement as above, and potential changes in the wiring of the nervous system after introduction of the *unc-119::GFP* reporter construct, which expresses GFP in virtually all neurons, by crossing with strain OH441. Lysosomes and acidic organelles were stained by transferring animals to M9 buffer containing 13.2 µg/ml LysoTracker Red (Molecular Probes), or 50 µg/ml Acridine Orange (Sigma), and incubating for 3h followed by destaining for 2h on plates with bacteria. Alterations in lipid content and distribution were analyzed by comparing wild type and mutant worms stained with the lipophilic fluorescent dye Nile Red (Sigma) that was added to the nematode laboratory diet to a final concentration of 0.05 µg/ml (Ashrafi et al 2003). Electron microscopy of 3-day, 7-day, and 17-day old worms was performed as described by Hall (1995) to visualize changes in ultrastructural morphology of lysosomes, mitochondria, and neurons, as well as alterations in gut granule population observed in other mutants by EM (Kostich et al 2000, Hersh et al 2002). Therefore, the populations of vesicles in intestinal, hypodermal and neuronal cells were closely examined in transverse sections of *cln-3* triple mutant and wild type nematodes. In short, worms were anaesthetized with 8% ethanol in M9 buffer, dissected in fixative (1.5% glutaraldehyde in 0.1 M cacodylate buffer) and fixed for 2h, followed by post-fixation in 1% Osmium tetroxide, standard propylene oxide-epon treatment and embedding.

GFP reporter constructs

The *cln-3.1*::GFP reporter construct pLU01 was generated by inserting a 2266 bp *Pst*I-*Nsi*I fragment of cosmid F07B10, containing the putative *cln-3.1* promoter into the *Pst*I site of GFP reporter plasmid pPD95-77, using standard cloning procedures (Sambrook et al 1989).
Cosmid C01G8 containing the *erm-1 - dnj-4 - dhs-1 - cln-3.2* operon was used to generate a *cln-3.2*::GFP reporter construct using recombineering, cloning by homologous recombination, in DY380 cells (Lee et al 2001)(Supplementary material, figure S1). In two steps we subcloned a 16297 bp *Xba*I-*Kpn*I fragment, containing the putative operonic promoter and the entire operon until part of exon three of the *cln-3.2* gene, from cosmid C01G8 into *Xba*I-*Kpn*I digested pBluescript KS+ to generate pLU13. In addition, we generated pLU15, a partial *cln-3.2*::GFP construct, by cloning a 3142 bp *Bam*HI-*Kpn*I fragment from cosmid C01G8 into *Bam*HI-*Kpn*I digested pPD95-77, which also contained a 1.3 kb *Eco*RI kanamycin resistance cassette from pUC4K into the *Eco*RI site of pPD95-77. Finally, recombineering was used to integrate the *cln-3.2*::GFP fusion into the complete operon by electroporation of a 4807 bp *Sca*I-*Bbs*I fragment from pLU15 into DY380/pLU13 cells followed by selection for homologous recombination between the two identical regions of pLU13 and pLU15, e.g. the *cln-3.2* upstream region and its first exons and the ampicillin gene, leading to pLU02.
To generate the *cln-3.3*::GFP reporter plasmid, we first made a deletion clone of cosmid ZC190, pLU17, by consecutive digestions with *Stu*I and *Afl*II and subsequent self-ligations, deleting 12526 and 10090 bp fragments, respectively. Next, the GFP reporter and kanamycin resistance cassette of pLU14 was PCR-amplified using forward primer 5' **GGCAGAAGTACTACTCTCGGACAATCTACCAAGTCTCATT** AACATTTTCAGGAGGACCC 3', and reverse primer 5' **CATCCAGTAATGAAGTGGGATTGATACTCCTGCTGCGAAG** TTTGAACTTTTGCTTTGCC 3', which contain homology (shown in bold) to part of exon 3 and part of exon 9 of the *cln-3.3* gene respectively. Recombineering was used for the final step of the construction of the *cln-3.3*::GFP reporter plasmid, pLU03. After electroporation of the pLU14 PCR product into DY380/pLU17 cells, we selected for the replacement of part of the *cln-3.3* gene by recombination between the 40-bp ends of the PCR product and the homologous sequences in pLU17 resulting in an in frame fusion between the first part of the c*ln-3.3* protein and GFP in pLU03. All constructs obtained with recombineering were verified by sequencing on an ABI3700 automated sequencer.

Nematode transformation

Transgenic *C. elegans* strains were obtained by microinjection of promoter GFP reporter plasmid DNA at a concentration of 100 ng/µl together with marker plasmid pRF4, *rol-6* (*su1006*), into the distal arm of the wild type hermaphrodite gonad as described previously (Mello and Fire 1995).

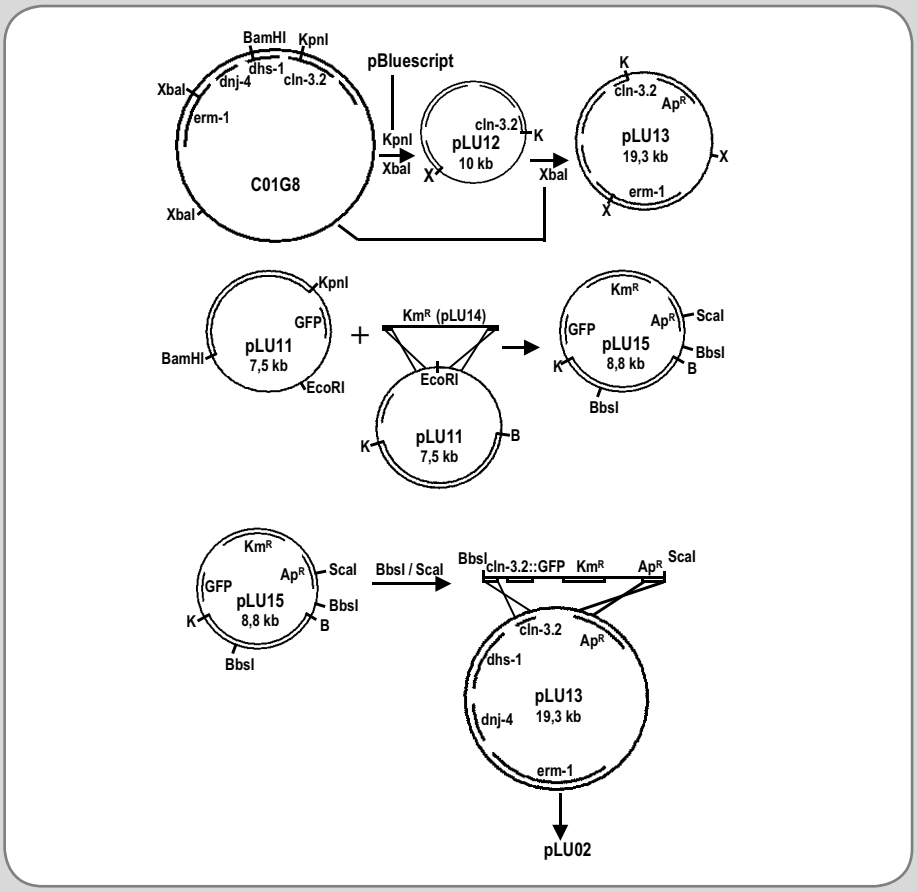

Supplementary figure S1

To generate a cln-3.2::GFP reporter construct we subcloned a 7000 bp XbaI-KpnI fragment as depicted above, containing part of the cln-3.2 gene from cosmid C01G8 into XbaI-KpnI digested pBluescript KS+ to generate pLU12. The 9297 bp XbaI fragment containing the putative operonic promoter and part of erm-1 from cosmid C01G8 was introduced into the XbaI site of pLU12 to generate pLU13, containing the complete operon with exception of part of exon three to exon 9 of cln-3.2. In addition, we cloned a 3142 bp BamHI-KpnI fragment containing the upstream region until the first part of exon three of the cln-3.2 gene from cosmid C01G8 into BamHI-KpnI digested pPD95-77, to generate the partial cln-3.2::GFP construct pLU11. Insertion of a 1.3 kb EcoRI kanamycin resistance cassette from pUC4K into the EcoRI site of pPD95-77 resulted in pLU14. The last two steps of the cloning procedure were achieved by recombineering (cloning by homologous recombination)(Lee et al 2001). In the first recombineering step, after electroporation of the 1470 bp BstBI-DraI kanamycin resistance cassette from pLU14 into DY380/pLU11 cells, we selected for the replacement of the pLU11 EcoRI site by the kanamycin resistance cassette by recombination between their homologous flanking sequences, resulting in pLU15, which contains part of cln-3.2 exon 3 fused in frame to GFP. In the last recombineering step, the cln-3.2::GFP fusion was integrated into the complete operon by electroporation of a 4807 bp ScaI-BbsI fragment from pLU15 into DY380/pLU13 cells followed by selection for homologous recombination between the two identical regions of pLU13 and pLU15, e.g. the cln-3.2 upstream region and its first exons and the ampicillin gene, leading to pLU02.

Detection of mutant alleles

After each cross with *cln-3* mutants the segregation of *cln-3* alleles in the progeny was analyzed by single worm PCR (Williams 1995), using three primers to distinguish mutant and wild type alleles (Table 1).

Table 1 Primers to detect *cln-3* mutant and wild type (WT) alleles

Gene	Allele	Forward primer (5' – 3')	Reverse primer (5' – 3')	Product size (bp)
cln-3.1	WT	cln-3.1.1 TTACGGTTGAACGATTGCAG	cln-3.1.2 GAAACTCGCTGGGAACAAAT	246
cln-3.1	WT	cln-3.1.2 GAAACTCGCTGGGAACAAAT	cln-3.1.3 TCTCAAAAACCAAAAACGACA	2947
cln-3.1	mutant	cln-3.1.2 GAAACTCGCTGGGAACAAAT	cln-3.1.3 TCTCAAAAACCAAAAACGACA	500
cln-3.2	WT	cln-3.2.1 TCCGAGACCACTACCGAAAC	cln-3.2.3 GGGCAATTCTTCGACACCT	1237
cln-3.2	WT	cln-3.2.2 GCAGGCATGAAAACCCATAA	cln-3.2.3 GGGCAATTCTTCGACACCT	377
cln-3.2	mutant	cln-3.2.1 TCCGAGACCACTACCGAAAC	cln-3.2.3 GGGCAATTCTTCGACACCT	497
cln-3.3	WT	cln-3.3.1 CATTGAAGCAGCGGAAAGAC	cln-3.3.2 CGAACACAGAGTCCCACAGA	659
cln-3.3	WT	cln-3.3.1 CATTGAAGCAGCGGAAAGAC	cln-3.3.3 TAGTTTGGGTGGAGGATTGG	1660
cln-3.3	mutant	cln-3.3.1 CATTGAAGCAGCGGAAAGAC	cln-3.3.3 TAGTTTGGGTGGAGGATTGG	447

Life span assay

On day 0 the animals were synchronized by bleaching (Epstein and Shakes 1995). From day 1 worms were transferred to fresh plates, and this was repeated daily while the animals were producing progeny (Larsen et al 1995). Once reproduction had ceased the animals were transferred to fresh plates periodically. Animals were scored as dead if they failed to show movement, or pharyngeal pumping, and failed to respond to a gentle tap on the head with a platinum wire. Animals that crawled off the plates were not included in the analysis. This experiment was performed three times.

Brood size assay

Synchronized animals were grown on plates individually. While the worms produced progeny they were transferred to fresh plates regularly so that the amount of progeny could be counted reliably. Progeny were counted 2-3 days after eggs were laid. This experiment was done three times.

Statistical analysis

Data were analyzed using Microsoft Excel and SPSS.
The Logrank-test was used to analyze life span assay results.
An unpaired t-test was applied to determine the statistical significance of the brood size assay.

Results

Cln-3 mutants are viable and show no apparent neuronal and lysosomal defects

All three *cln-3* single deletion mutants were checked for obvious morphological, neuronal or movement defects, or lethality, but none were found. In order to detect possible redundancy of the *cln-3* genes, we crossed the *cln-3* single mutants to obtain *cln-3* double and triple mutants. The *cln-3* double mutant nematodes were also viable, displayed no obvious morphological, neuronal or movement defects, or increased embryonic or larval lethality, as were *cln-3* triple mutants. Therefore, the further characterization of the effect of *cln-3* mutations was performed in *cln-3* triple mutants, which displayed no defects in mechanosensation and thermotaxis. We crossed *cln-3* triple mutants and strain OH441 that expresses GFP from the unc-119 promoter in all neurons to visualize potential changes in the nervous system, and found no differences between mutants and wild types (data not shown). Ultrastructural analysis of *cln-3* triple mutants and wild type controls using electron microscopy did not reveal changes in neurons and lipid containing vesicles or accumulation of lysosomal storage material (Supplementary figure S2, and data not shown). Furthermore, the lysosomes of *cln-3* triple mutants were analyzed using Lysotracker Red and Acridine Orange staining and appeared similar to wild type (Supplementary figure S3). In addition, the lipid distribution in *cln-3* triple mutants as observed by fluorescence analysis of worms grown on standard *C. elegans* diet containing Nile Red appeared comparable to wild type.

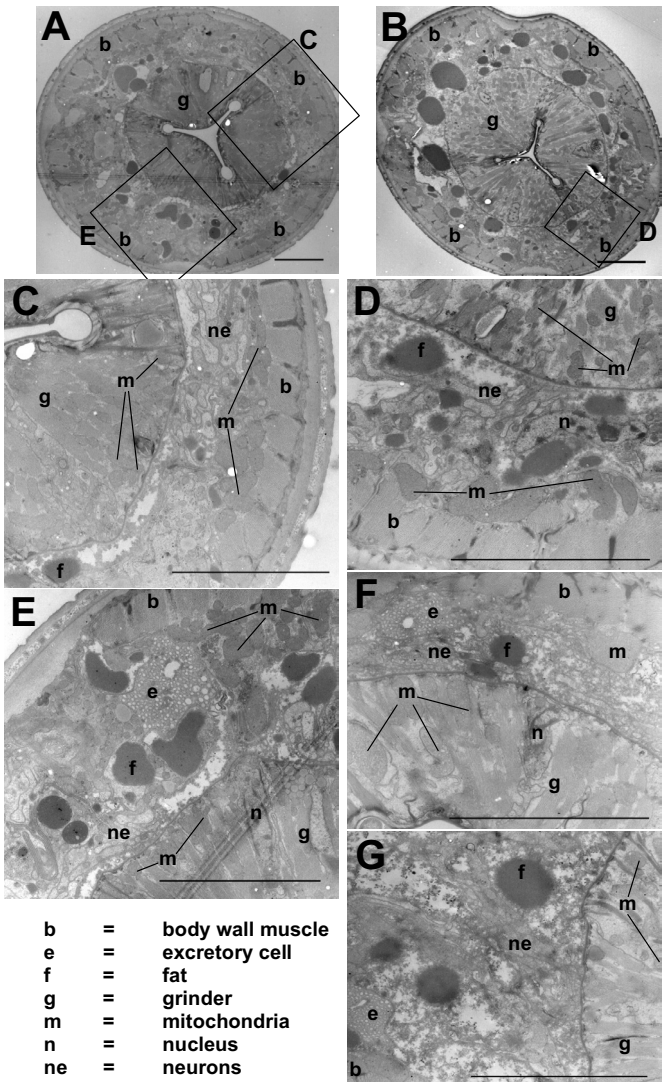

Supplementary figure S2 Electron microscopical analysis of adult cln-3 triple mutant and wild type worms

No changes in the ultrastructural morphology of lysosomes, mitochondria, and neurons, or alterations in gut granule populations are observed in electronmicrographs of cln-3 triple mutant (A, C, E) and wild type (B, D, F, G) adult worms. Scale bar represents 5 μm.

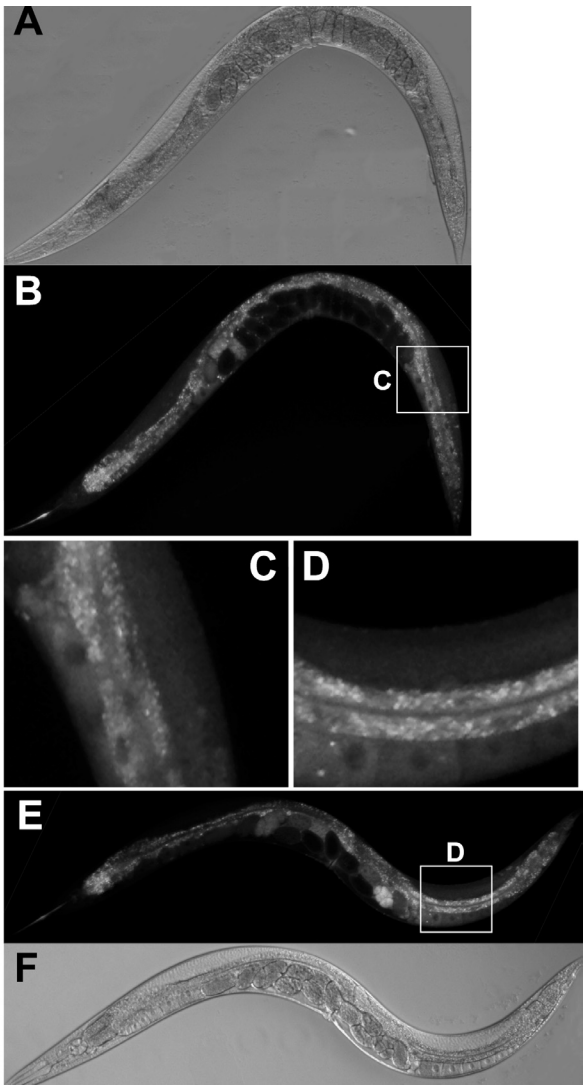

Supplementary figure S3 No difference in staining of lysosomes by Lysotracker Red between cln-3 triple mutants and wild type N2

Fluorescence (B-E) and Nomarski (A, F) pictures of cln-3 triple mutants (A-C) and wild type N2 (D-F) display comparable distribution and intensities of fluorescence in lysosomes and other acidic vesicles or compartments. Cells of the intestine show an abundance of stained vesicles flanking the lumen of the negative intestine (C, D). Mildly positive Lysotracker Red staining of parts of the gonad is regularly observed in both strains. Identical exposure times were used for the fluorescence pictures.

Cln-3 mutants show decreased life span and brood size

The life span and brood size of *cln-3* mutant nematodes were analyzed as part of their phenotypical characterization. *Cln-3.1* single and *cln-3* triple mutants showed a decreased life span, average 18.5 and 16.8 days respectively, compared to 20.0 days for N2, (p=0.0319 and p=0.0042, respectively) (Figure 2), whereas *cln-3.2* and *cln-3.3* single mutants showed no significant difference from wild type (data not shown).
The brood sizes of *cln-3.2* single mutants and *cln-3* triple mutants were significantly decreased, average 287 progeny for both, compared to 306 progeny for the wild type, (Figure 3a, p=0.0466, and p=0.0359, respectively). In the daily progeny count, *cln-3* triple mutants had significant lower numbers of progeny on the third day of egg laying compared to N2 (p=0.0211)(Figure 3b), although the variances of the brood sizes of both strains were not significantly different (p=0.0850).

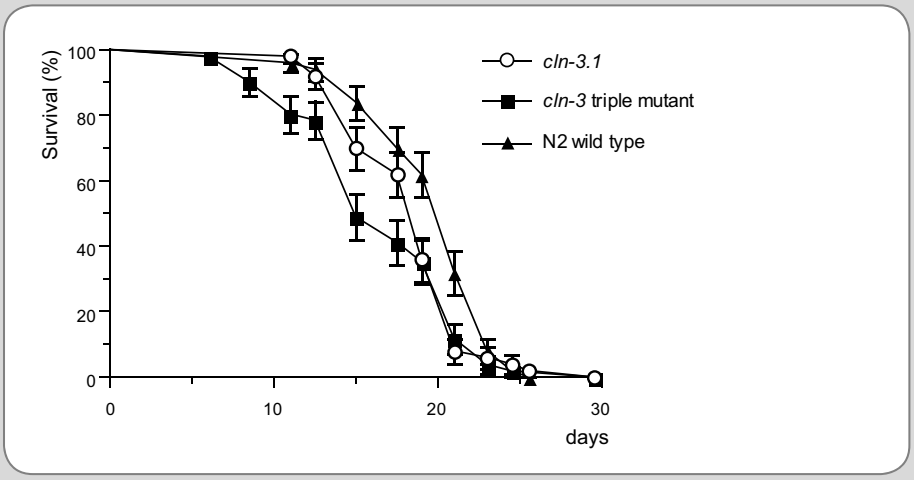

Figure 2 Life spans of *cln-3.1* single and *cln-3* triple mutant hermaphrodites

The relative survival of *cln-3.1* single (○, n=50) and *cln-3* triple mutants (■, n=51) is decreased compared to N2 wild type (▲, n=50), all grown at 20 °C. Survival has been plotted against time; error bars depict S.E.M. The figure represents one of three experiments giving similar results.

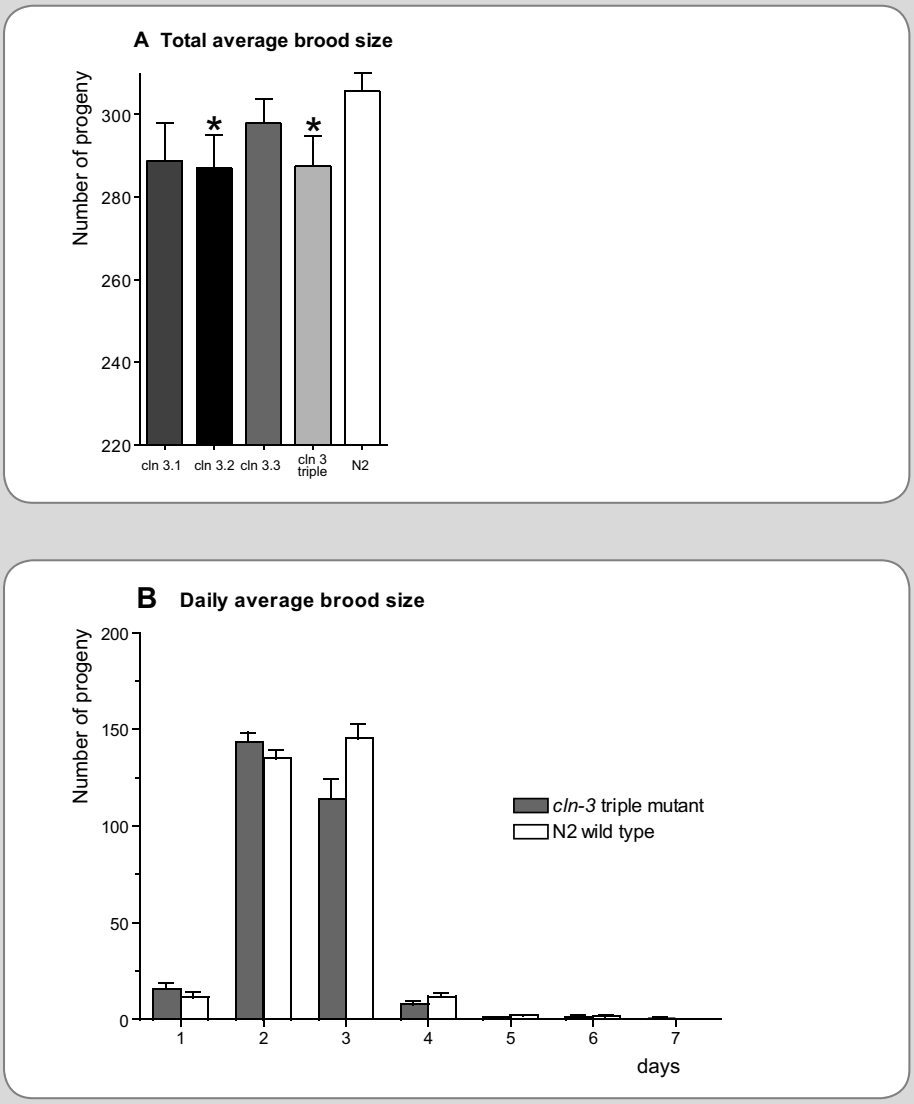

Figure 3 Brood sizes of *cln-3* single and *cln-3* triple mutants hermaphrodites

(A) Average total brood sizes of *cln-3* triple mutants (n=24) and *cln-3.2* single mutants (n=25) prove to differ significantly (*) from wild type (n=25).

(B) *Cln-3* triple mutants have less offspring than N2 wild type, most prominently on day three of the egg-laying period when observed on a daily basis (p=0.0211). Depicted are the average brood sizes; error bars represent S.E.M. The figure represents two experiments.

Cln-3.1::GFP intestinal fluorescence

Cln-3 spatial and temporal expression patterns were analyzed in order to focus the phenotypic analysis of the *cln-3* mutants on the specific stages of the life cycle and the cell types, in which the *cln-3* genes are expressed and presumably functional (Summarized in table 2). The *cln-3.1*::GFP transgenic hermaphrodite and male

Table 2 Temporal and spatial *cln-3*::GFP expression patterns.

Gene	Life stage	Location
cln-3.1	embryo, larva, adult	intestinal cells, most likely int2 to int8
cln-3.2	adult	hypodermal cells
cln-3.3	adult	intestinal muscle, male specific posterior muscle and hypodermal cells

nematodes displayed fluorescence in the intestine, most likely in cells designated int2 to int8, whereas the most anterior and posterior segments of the intestine remained negative from the embryonic comma-stage on throughout adult life (Figure 4, and data not shown). Intestinal cells of *cln-3.1*::GFP transgenic embryos and larvae exhibited bright speckled fluorescence (Figure 4A, C, E), in contrast to a diffuse cytoplasmic fluorescence in transgenic adults (Figure 4D). Furthermore, transgenic L2 and L3 larvae displayed intestinal fluorescence visible as threads near the apical cytoplasmic membrane (Figure 4E).

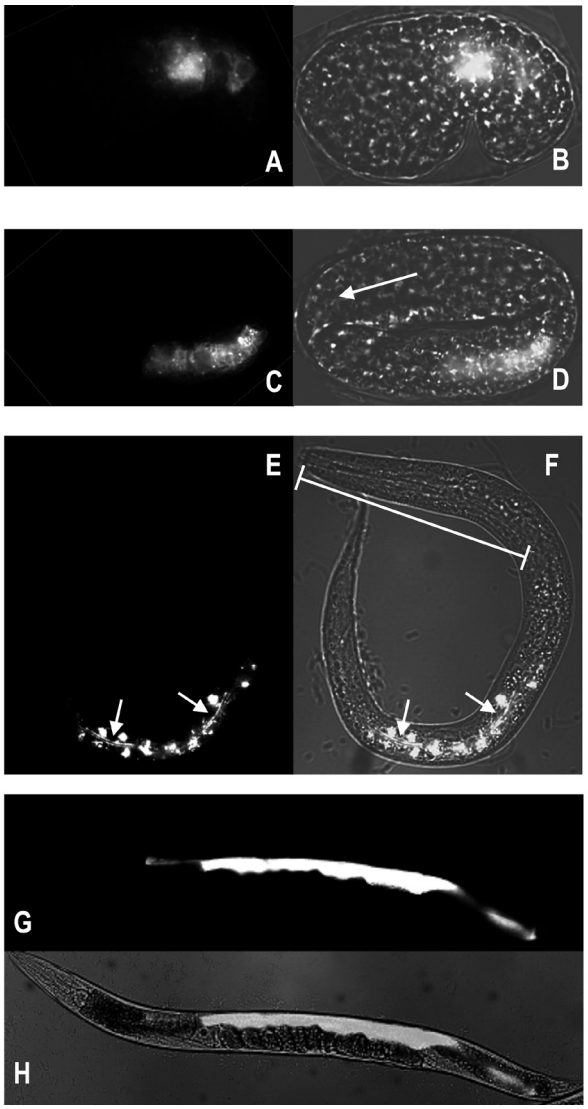

Figure 4 ***Cln-3.1*::GFP fluorescence in the intestine**

Fluorescence (A, C, E, G) and bright field-fluorescence overlay (B, D, F, H) pictures of cln-3.1::GFP expressing *C. elegans*, displaying fluorescence in the intestine. Anterior is to the left and dorsal is up, unless indicated otherwise. Comma stage (A, B) and three-fold stage (C, D) embryos show fluorescence in cells of the E-lineage that will develop into the intestine. The white arrow (D) indicates the most anterior part of the pharynx. L2 larva (E, F) showing intestinal fluorescence clearly localized to vesicles and closely located to or localized in the apical membrane as indicated by the white arrows (E); the white bar designates the pharynx. Adult hermaphrodite nematode (G, H) showing diffuse fluorescence in the intestine, most anterior and posterior cells do not fluoresce.

Cln-3.2::GFP fluorescence in the hypoderm

No fluorescent signal could be discerned in embryos present in *cln-3.2*::GFP transgenic adults, in newly laid eggs from transgenic adults or in transgenic larvae. Adult *cln-3.2*::GFP transgenic hermaphrodite and male nematodes displayed fluorescence in the hypoderm visible as multiple thread-like patterns with regular interruptions and mild belt-like patterns running alongside of the body of the animal, both clearly distinguishable from autofluorescence (Figure 5, and data not shown). Furthermore, punctate fluorescence in the pharynx and faint fluorescence in cells lining the cuticle of the head could be observed (data not shown).

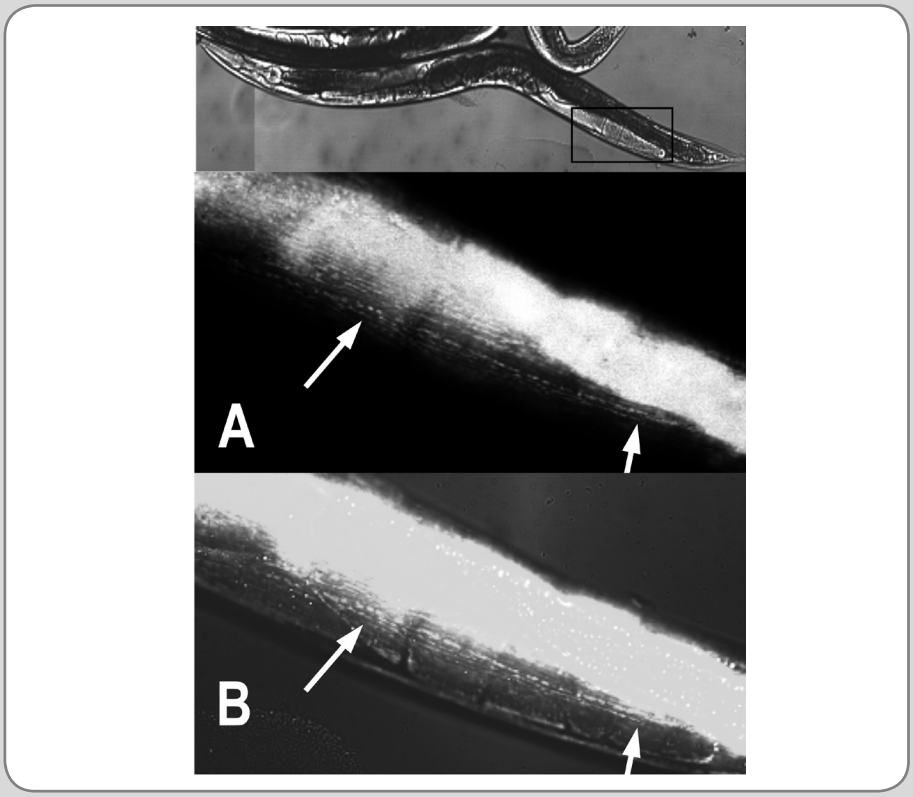

Figure 5 ***Cln-3.2*::GFP fluorescence in the hypoderm**

Fluorescence (A), bright field- fluorescence overlay (B), and bright field overview pictures of *cln-3.2*::GFP expressing adult hermaphrodite nematode, displaying hypodermal fluorescence. (A) Arrows indicate fluorescent discontinuous lines that run parallel to the body, belonging to the hypoderm just below the cuticle.

Cln-3.3::GFP fluorescence in intestinal and male-specific posterior diagonal muscle cells and hypoderm

Embryos present in *cln-3.3*::GFP transgenic adults, newly laid eggs and transgenic larvae displayed no fluorescent signal, whereas adult transgenic nematodes showed mild fluorescence in the intestinal muscle and in the hypoderm just beneath the cuticle (Figure 6A, C). In addition, male transgenic nematodes displayed fluorescence in male-specific posterior diagonal muscle cells (Figure 6E).

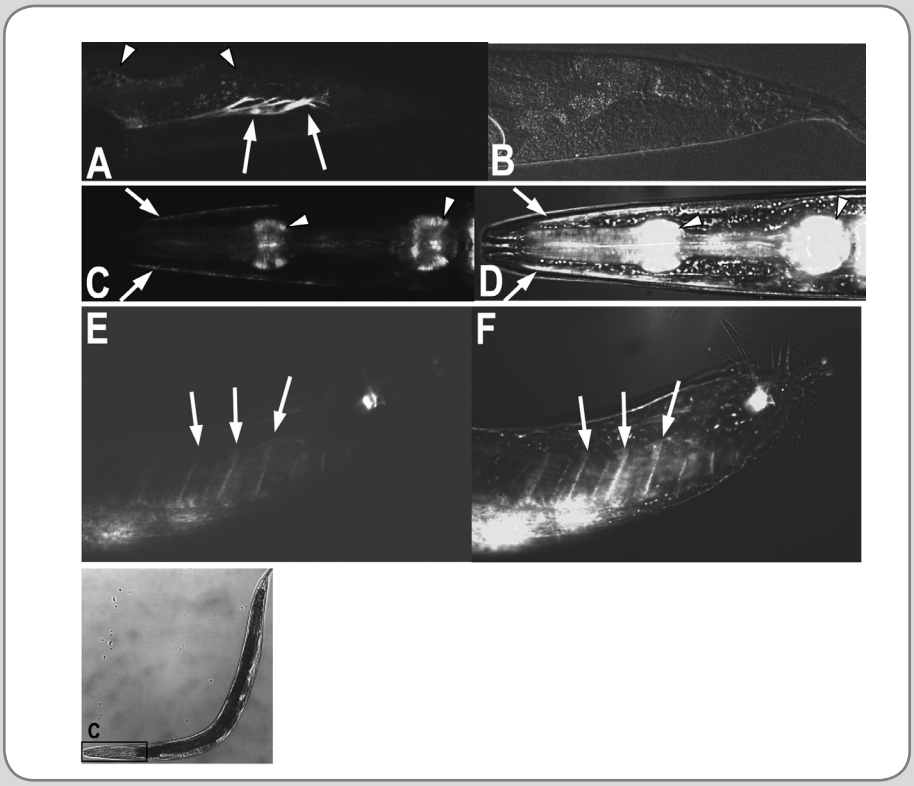

Figure 6 ***Cln-3.3*::GFP fluorescence in hypoderm and intestinal and male-specific posterior diagonal muscles**

Fluorescence (A, C, E), Nomarski (B), bright field overlay (D, F), and bright field overview pictures of cln-3.3::GFP expressing worms showing intestinal muscle, hypoderm and male-specific posterior diagonal muscle fluorescence. Confocal laser scanning microscope and Nomarski pictures of *C. elegans* adult hermaphrodite tail (A, B) with intestinal muscle fluorescence indicated by arrows (A) and autofluorescent gut granules are indicated by the arrowheads. Fluorescence microscopy shows hypodermal fluorescence in the pharynx indicated by arrows and autofluorescence present in the muscles of the pharyngeal bulbs as indicated by the arrowheads (C, D). Arrows indicate fluorescence in male-specific tail diagonal muscles (E).

Discussion

In order to investigate whether *C. elegans cln-3* mutants may contribute to a better understanding of the processes disturbed in JNCL we have determined the phenotypes of *C. elegans cln-3* mutants and the *cln-3* gene expression patterns. Here we show that *cln-3* triple mutants exhibited no neuronal defects, no abnormal movement, or aberrant behavior. We could not detect changes in lipid accumulations, autofluorescence or altered lysosome morphology, quantity, and ultrastructure between *cln-3* triple mutant and wild type worms. Thus, *cln-3* triple mutants display neither the main characteristics of Batten disease in humans, such as neurological decline and accumulation of lipopigments nor the abnormal mitochondrial morphology of the *C. elegans ppt-1* model for Infantile Neuronal Ceroid Lipofuscinosis (Porter et al 2005). Therefore, we were unable to exploit the benefits of the well-characterized nervous system of *C. elegans* in a more detailed investigation of the neuronal degeneration, which occurs in JNCL. We found that deletion of the *C. elegans cln-3.1* gene causes a mild decrease in life span, which is more prominent in *cln-3* triple mutants, indicating functional redundancy. In addition, *cln-3.2* single and *cln-3* triple mutants display a mild decrease in brood size, predominantly on day three of the egg-laying period. RNAi for *cln-3.2* also resulted in limited embryonic lethality (Piano et al 2002), suggesting a role for *cln-3.2* during embryonic development.

We analyzed the spatial and temporal expression patterns of the *cln-3* genes using transgenic worms carrying promoter-GFP fusions, to examine what kind of cells or tissues express the *cln-3* genes at which moment, and might be affected most by the mutations. Each promoter-GFP fusion also contains the first two and part of the third exon of the *cln-3* gene. This may result in the particular subcellular localization of the fluorescence observed in the *cln-3.1*::GFP and the *cln-3.2*::GFP transgenic worms, but which should not be regarded as indicative for the localization of the *cln-3* proteins. The *cln-3.1*::GFP fluorescence pattern suggests a role for *cln-3.1* in the intestine. The gut cells form the digestive tract, secreting enzymes into the lumen and absorbing and storing processed nutrients in numerous storage granules (White 1988). Furthermore, in the intestine yolk protein synthesis takes place (Kimble and Sharrock 1983). *C. elegans cln-3.1* might be involved in pH regulation of intestinal lysosomes or the intestinal lumen similar to the role of the yeast CLN3 homologue in vacuolar pH regulation (Pearce et al 1999A). However, altered lysosomal pH regulation of *cln-3* mutants could not be demonstrated by Lysotracker Red and Acridine Orange staining, possibly because the pH difference may be too subtle to observe using these methods or lysosomal pH changes do not occur in *cln-3* mutants (Suppl. Figure S3, and data not shown).

Fluorescence patterns in *cln-3.2*::GFP transgenic worms suggest *cln-3.2* expression in the hypoderm, as the locations of the fluorescent signals resemble those of the hypodermal signals observed in *nhr-66*::GFP and *che-14*::GFP transgenics, and those obtained with the hypodermal marker antibody MH4 (Mounsey 2000, Michaux et al 2000, Waterston 1988). The hypoderm, the external epithelium, is involved in cuticle formation and shedding, phagocytosis of apoptotic cells, and formation of storage granules (Sulston et al 1983, White 1988). Several hypodermal cells act as blast cells during postembryonic development, but no somatic cell divisions take place in adults (Sulston 1988).
Since *C. elegans* cuticle formation mutants predominantly have striking morphologic phenotypes and *cln-3.2* expression is limited to adults with their fully formed cuticle, a direct involvement of *cln-3.2* in cuticle formation seems unlikely (Friedman et al 2000, Hashmi et al 2004). Defects in additional hypodermal functions, storage granule formation and phagocytosis were not observed in *cln-3* mutants by electron microscopy or by staining of lysosomes and fat (Melendez et al 2003, Hersh et al 2002). But *C. elegans ced-3* and *ced-4* mutants, in which nearly all apoptosis is eliminated, are also superficially wild type (Hengartner 1997).
Adult *cln-3.3*::GFP transgenic nematodes display fluorescence in the intestinal muscle, the male-specific posterior diagonal tail muscles and in the hypodermis. The intestinal muscle and male specific tail muscles are functional in defecation and mating respectively (Waterston 1988). *Cln-3* triple mutants displayed no aberrant defecation cycles lengths or patterns compared to wild type. Furthermore, *cln-3* triple mutant males were able to mate, fertile, and generated normal numbers of males (data not shown).
We have observed *C. elegans cln-3* expression only in part of the nematode body, while in humans the *CLN3* gene transcript is present in all cell types, although hardly detectable in the most affected organ in Batten disease patients, the brain (The International Batten Disease Consortium 1995). We cannot exclude that the *C. elegans cln-3* genes are expressed and functional in every cell type of the nematode at levels below the GFP fluorescence detection threshold. Expression in the nematode germline might be absent by transgene silencing (Kelly 1997).

We have focused the phenotypic analysis of *cln-3* triple mutants on the specific tissues and life stages in which the *cln-3* genes are expressed, but did not detect a clear and useful phenotype for genetic screens to identify modifier genes and elucidate the mechanisms and genetic pathways involved in this terrible disease. The *cln-3* triple mutants show decreased life span and brood size, but may not be an optimal model for Batten disease, because comparable JNCL disease symptoms, e.g. neurological and movement defects and accumulated materials, are not observed in *cln-3* mutant nematodes. Nonetheless, we expect the *C. elegans cln-3* genes to be functionally equivalent on the molecular level to their counterparts in other species based on their protein sequence homology. Therefore, the *cln-3* mutants described here still have the potential to lead to a better understanding of the molecular mechanisms involved in Batten disease by allowing comparison of data obtained with the yeast model with those from a simple but well-characterized multicellular organism.

Acknowledgements

Part of this work was funded by the Center for Biomedical Genetics (CBG), the Batten Disease Support and Research Association (BDSRA), and the European Union, EU project NCL models (LSHM-CT-2003-503051). We thank Ronald Plasterk and Marieke van der Horst for help with isolation of the *cln-3.1* deletion mutant, Hans van der Meulen for performing electron microscopy, Andrew Fire for providing GFP vectors, Don Court for providing the DY380 bacterial strain, the International C. elegans Gene Knockout Consortium (http://celeganskoconsortium.omrf.org), specifically the *C. elegans* Reverse Genetics Core Facility at the University of British Columbia, which is funded by the Canadian Institute for Health Research, Genome Canada, Genome BC, the Michael Smith Foundation, and the National Institutes of Health, for the *cln-3.2* and *cln-3.3* deletion mutants. Some nematode strains used in this work were provided by the *Caenorhabditis* Genetics Center, which is funded by the NIH National Center for Research Resources (NCRR). We thank Gert Jansen and Rik Korswagen for helpful discussions.

References

Ashrafi K, Chang FY, Watts JL et al (2003) Genome-wide RNAi analysis of Caenorhabditis elegans fat regulatory genes. *Nature* **421**: 268-272.

Blumenthal T, Evans D, Link CD et al (2002) A global analysis of Caenorhabditis elegans operons. *Nature* **417**: 851-854.

Chattopadhyay S, Muzaffar NE, Sherman F, Pearce DA (2000) The yeast model for batten disease: mutations in BTN1, BTN2, and HSP30 alter pH homeostasis. *J Bacteriol* **182**: 6418-6423.

Chattopadhyay S, Pearce DA (2002) Interaction with Btn2p is required for localization of Rsglp: Btn2p-mediated changes in arginine uptake in Saccharomyces cerevisiae. *Eukaryot Cell* **1**: 606-612.

Culetto E, Sattelle DB (2000) A role for Caenorhabditis elegans in understanding the function and interactions of human disease genes. *Hum Mol Genet* **9**: 869-877.

Epstein HF, Shakes DC (1995) *Caenorhabditis elegans:* Modern Biological Analysis of an Organism. In Epstein HF, Shakes DC, eds. *Methods in Cell Biology*. San Diego: Academic Press.

Ezaki J, Takeda-Ezaki M, Koike M et al (2003) Characterization of Cln3p, the gene product responsible for juvenile neuronal ceroid lipofuscinosis, as a lysosomal integral membrane glycoprotein. *J Neurochem* **87**: 1296-1308.

Faber PW, Voisine C, King DC, Bates EA, Hart AC (2002) Glutamine/proline-rich PQE-1 proteins protect Caenorhabditis elegans neurons from huntingtin polyglutamine neurotoxicity. *Proc Natl Acad Sci U S A* **99**: 17131-17136.

Fares H, Greenwald I (2001) Regulation of endocytosis by CUP-5, the Caenorhabditis elegans mucolipin-1 homolog. *Nat Genet* **28**: 64-68.

Friedman L, Higgin JJ, Moulder G, Barstead R, Raines RT, Kimble J (2000) Prolyl 4-hydroxylase is required for viability and morphogenesis in Caenorhabditis elegans. *Proc Natl Acad Sci U S A* **97**: 4736-4741.

Golabek AA, Kaczmarski W, Kida E, Kaczmarski A, Michalewski MP, Wisniewski KE (1999) Expression studies of CLN3 protein (battenin) in fusion with the green fluorescent protein in mammalian cells in vitro. *Mol Genet Metab* **66**: 277-282.

Hall DH (1995) Electron microscopy and three dimensional image reconstruction. In Epstein HF, Shakes DC, eds. *Methods in Cell Biology*. San Diego: Academic Press, 395-436.

Hashmi S, Zhang J, Oksov Y, Lustigman S (2004) The Caenorhabditis elegans cathepsin Z-like cysteine protease, Ce-CPZ-1, has a multifunctional role during the worms' development. *J Biol Chem* **279**: 6035-6045.

Hedgecock EM, Russell RL (1975) Normal and mutant thermotaxis in the nematode Caenorhabditis elegans. *Proc Natl Acad Sci U S A* **72**: 4061-4065.

Hengartner MO (1997) Cell Death. In Riddle DL, Blumenthal T, Meyer BJ, Priess JR, eds. *C. elegans II.* New York: Cold Spring Harbor Laboratory Press, 383 – 415.

Hersh BM, Hartwieg E, Horvitz HR (2002) The Caenorhabditis elegans mucolipin-like gene cup-5 is essential for viability and regulates lysosomes in multiple cell types. *Proc Natl Acad Sci U S A* **99**: 4355-4360

The International Batten Disease Consortium (1995) Isolation of a novel gene underlying Batten disease (CLN3). *Cell* **82**: 949-957.

Jarvela I, Sainio M, Rantamaki T et al (1998) Biosynthesis and intracellular targeting of the CLN3 protein defective in Batten disease. *Hum Mol Genet* **7**: 85-90.

Kaplan JM, and Horvitz HR (1993) A dual mechanosensory and chemosensory neuron in *Caenorhabditis elegans*. *Proc Natl Acad Sci USA* **90**: 2227-2231.

Katz ML, Gao CL, Prabhakaram M, Shibuya H, Liu PC, Johnson GS (1997) Immunochemical localization of the Batten disease (CLN3) protein in retina. *Invest Ophthalmol Vis Sci* **38**:2375-2386.

Kelly WG, Xu S, Montgomery MK, Fire A (1997) Distinct requirements for somatic and germline expression of a generally expressed Caernorhabditis elegans gene. *Genetics* **146**:227-238.

Kida E, Kaczmarski W, Golabek AA, Kaczmarski A, Michalewski M, Wisniewski KE (1999) Analysis of intracellular distribution and trafficking of the CLN3 protein in fusion with the green fluorescent protein in vitro. *Mol Genet Metab* **66**:265-271.

Kim Y, Ramirez-Montealegre D, Pearce DA (2003) A role in vacuolar arginine transport for yeast Btn1p and for human CLN3, the protein defective in Batten disease. *Proc Natl Acad Sci U S A* **100**:15458-15462.

Kimble J, Sharrock WJ (1983) Tissue-specific synthesis of yolk proteins in Caenorhabditis elegans. *Dev Biol* **96**:189-196.

Kostich M, Fire A, Fambrough DM (2000) Identification and molecular-genetic characterization of a LAMP/CD68-like protein from Caenorhabditis elegans. *J Cell Sci* **113**:2595-606.

Kramer H, Phistry M (1996) Mutations in the Drosophila hook gene inhibit endocytosis of the boss transmembrane ligand into multivesicular bodies. *J Cell Biol* **133**:1205-1215.

Kremmidiotis G, Lensink IL, Bilton RL et al (1999) The Batten disease gene product (CLN3p) is a Golgi integral membrane protein. *Hum Mol Genet* **8**:523-531.

Larsen PL, Albert PS, Riddle DL (1995) Genes that regulate both development and longevity in Caenorhabditis elegans. *Genetics* **139**:1567-83.

Lee EC, Yu D, Martinez de Velasco J et al (2001) A highly efficient *Escherichia coli*-based chromosome engineering system adapted for recombinogenic targeting and subcloning of BAC DNA. *Genomics* **73**:56–65.

Luiro K, Kopra O, Lehtovirta M, Jalanko A (2001) CLN3 protein is targeted to neuronal synapses but excluded from synaptic vesicles: new clues to Batten disease. *Hum Mol Genet* **10**:2123-31.

Luiro K, Yliannala K, Ahtiainen L et al (2004) Interconnections of CLN3, Hook1 and Rab proteins link Batten disease to defects in the endocytic pathway. *Hum Mol Genet* **13**:3017-3027.

Margraf LR, Boriack RL, Routheut AA et al (1999) Tissue expression and subcellular localization of CLN3, the Batten disease protein. *Mol Genet Metab* **66**:283-289.

Mao Q, Foster BJ, Xia H, Davidson BL (2003) Membrane topology of CLN3, the protein underlying Batten disease. *FEBS Lett* **541**:40-46.

Melendez A, Talloczy Z, Seaman M, Eskelinen EL, Hall DH, Levine B (2003) Autophagy genes are essential for dauer development and life-span extension in C. elegans. *Science* **301**:1387-91.

Mello C, Fire A (1995) DNA transformation. In Epstein HF, Shakes DC, eds. *Methods in Cell Biology*. San Diego: Academic Press, 451-82.

Michaux G, Gansmuller A, Hindelang C, Labouesse M (2000) CHE-14, a protein with a sterol-sensing domain, is required for apical sorting in C. elegans ectodermal epithelial cells. *Curr Biol* **10**: 1098-107.

Mitchell WA, Porter M, Kuwabara P, Mole SE (2001) Genomic structure of three CLN3-like genes in Caenorhabditis elegans. *Eur J Paediatr Neurol* **5**:Suppl A:121-5.

Mole SE, Zhong NA, Sarpong A et al (2001) New mutations in the neuronal ceroid lipofuscinosis genes. *Eur J Paediatr Neurol* **5**:Suppl A:7-10.

Mounsey A (2000) Hypodermal expression pattern of nhr-66. Retrieved from http://www.wormbase.org/db/gene/expression?name=Expr438;class=Expr_pattern 25/01/2005.

Pearce DA, Ferea T, Nosel SA, Das B, Sherman F (1999A) Action of BTN1, the yeast orthologue of the gene mutated in Batten disease. *Nat Genet* **22**:55-58.

Pearce DA, Nosel SA, Sherman F (1999B) Studies of pH regulation by Btn1p, the yeast homolog of human Cln3p. *Mol Genet Metab* **66**:320-323.

Pearce DA, McCall K, Mooney RA, Chattopadhyay S, Curran TM (2003) Altered amino acid levels in sera of a mouse model for juvenile neuronal ceroid lipofuscinoses. *Clin Chim Acta* **332**:145-148.

Piano F, Schetter AJ, Morton DG et al (2002) Gene clustering based on RNAi phenotypes of ovary-enriched genes in C. elegans. *Curr Biol* **12**:1959-1964.

Porter MY, Turmaine M, Mole SE (2005) Identification and characterization of Caenorhabditis elegans palmitoyl protein thioesterase1. *J Neurosci Res* **79**:836-48.

Rapola J (1993) Neuronal ceroid-lipofuscinoses in childhood. *Perspect Pediatr Pathol* **17**:7-44.

Sambrook J, Fritsch EF, Maniatis T, eds. (1989) *Molecular Cloning a Laboratory Manual*. New York: Cold Spring Harbor Laboratory Press.

Sulston JE, Schierenberg E, White JG, Thomson JN (1983) The embryonic cell lineage of the nematode Caenorhabditis elegans. *Dev Biol* **100**:64-119.

Sulston JE (1988) Cell lineage. In Wood WB and the Community of *C. elegans* Researchers eds. *The nematode* Caenorhabditis elegans. New York: Cold Spring Harbor Laboratory Press, 123 – 155.

Sym M, Basson M, Johnson C (2000) A model for Niemann-Pick type C disease in the nematode Caenorhabditis elegans. *Curr Biol* **10**:527-530.

The International Batten Disease Consortium (1995) Isolation of a novel gene underlying Batten disease, *CLN3*. *Cell* **82**: 949-957.

De Voer G, Jansen G, van Ommen GJ, Peters DJ, Taschner PE (2001) Caenorhabditis elegans homologues of the CLN3 gene, mutated in juvenile neuronal ceroid lipofuscinosis. *Eur J Paediatr Neurol* **5**:Suppl A:115-20.

Waterston RH (1988) Muscle. In Wood WB and the Community of *C. elegans* Researchers eds. *The nematode* Caenorhabditis elegans. New York: Cold Spring Harbor Laboratory Press, 281-335.

White J (1988) The anatomy. In Wood WB and the Community of *C. elegans* Researchers eds. *The nematode* Caenorhabditis elegans. New York: Cold Spring Harbor Laboratory Press, 81–122.

Williams BD (1995) Genetic mapping with polymorphic sequence-tagged sites. In Epstein HF, Shakes DC, eds. *Methods in Cell Biology*. San Diego: Academic Press, 81-96.

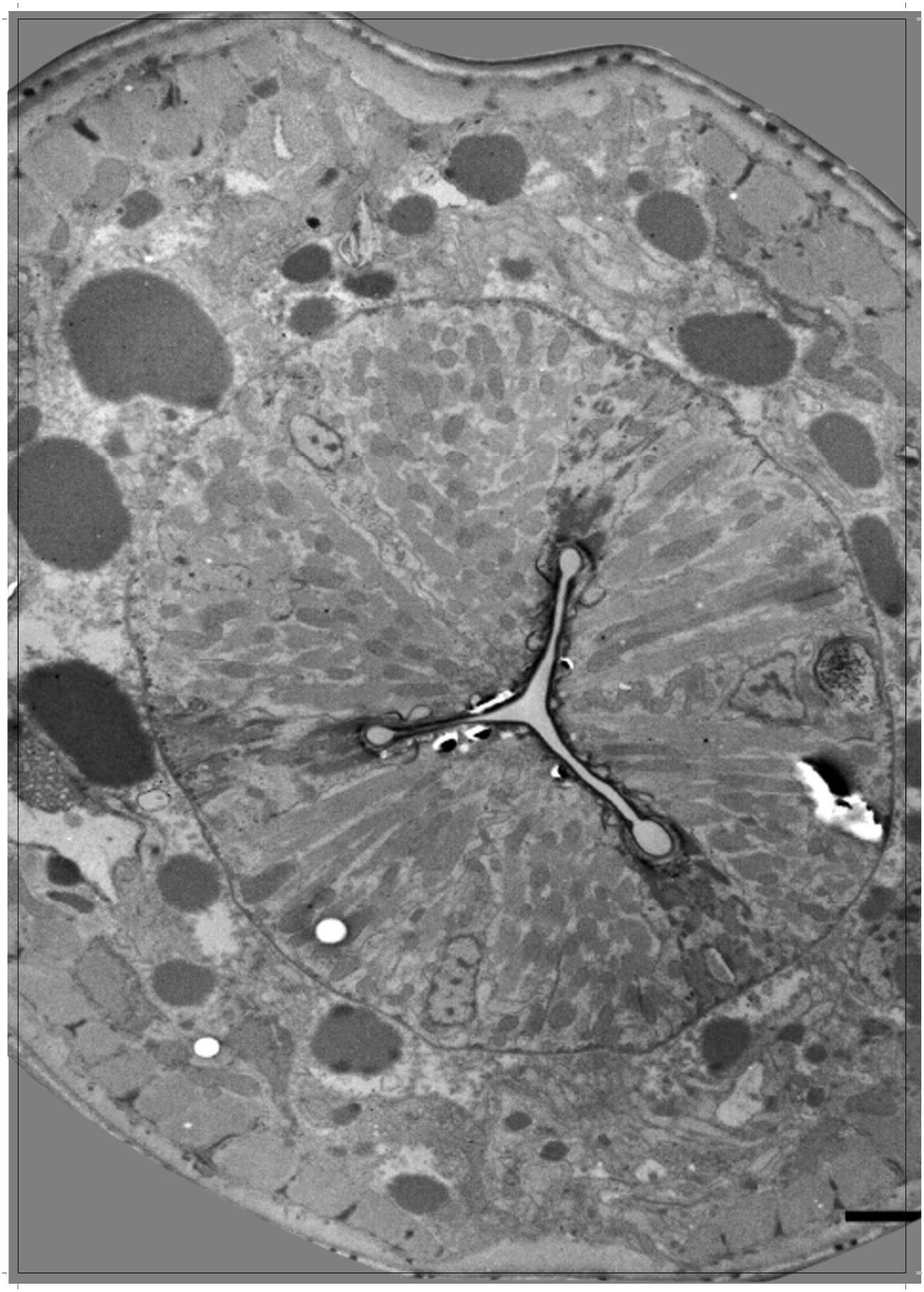

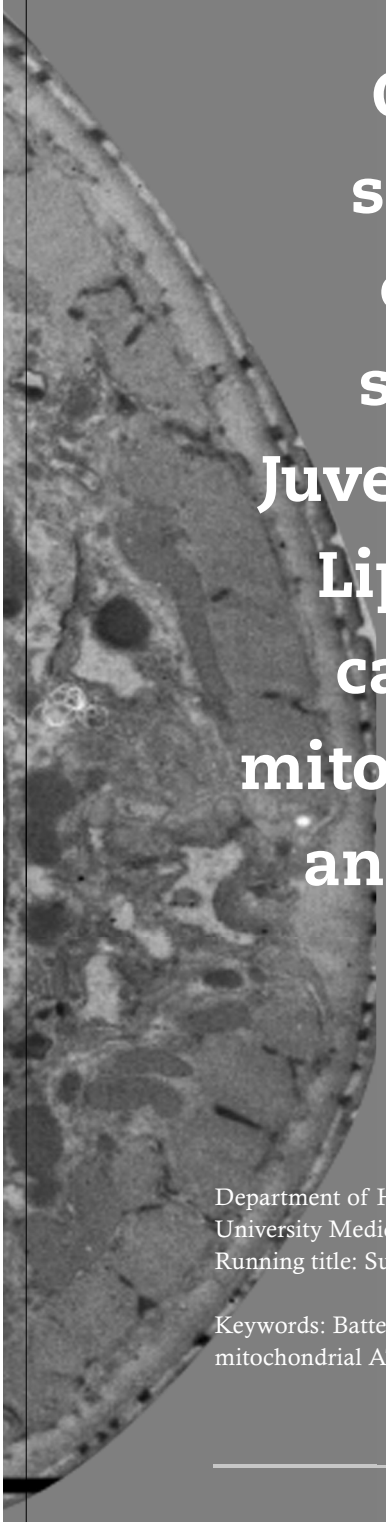

CHAPTER 5

Overexpression of subunit c, the main component of the storage material in Juvenile Neuronal Ceroid Lipofuscinosis (JNCL), causes disruption of mitochondria in *C. elegans* and subsequent death

Gert de Voer, Ronald O.B. de Keizer,
Paola van der Bent, Gert-Jan B. van Ommen,
Dorien J.M. Peters, Peter E.M. Taschner

Department of Human Genetics, Center for Human and Clinical Genetics, Leiden University Medical Center, Leiden, The Netherlands
Running title: Subunit c overexpression in *C. elegans*

Keywords: Batten disease, *Caenorhabditis elegans*, Subunit *c*, mitochondria, mitochondrial ATP synthase, *atp-9*

Summary

Subunit c of the mitochondrial ATP synthase is normally localized in the F_0 part of the ATP synthase complex, but it also forms the main component of the storage material in most of the severe hereditary neurodegenerative lysosomal storage disorders known as Neuronal Ceroid Lipofuscinoses (NCL, Batten disease). The juvenile form of NCL (JNCL) can be caused by mutations in the *CLN3* gene, of which the nematode *Caenorhabditis elegans* has three copies. Deletions in all three *cln-3* genes of the worm only caused a decreased life span and brood size without any lysosomal Subunit c storage. Since the normal life span of the worm might be too short for Subunit c accumulation, we hypothesized that Subunit c overexpression might induce lipopigment accumulation and neuronal phenotypes in *cln-3* triple mutants. Therefore, we have constructed and characterized Subunit c overexpressing nematodes, which demonstrated for the first time that overexpression of the hydrophobic Subunit c protein in a metazoan animal has deleterious effects. Subunit c overexpression causes nematodes to disintegrate, possibly by spontaneous pore-forming in mitochondria and perhaps other organelles. Milder overexpression causes egg laying defects and tail bulges in wildtype and *cln-3* triple mutant backgrounds.

Introduction

Subunit c of the mitochondrial ATP synthase (hereafter designated Subunit c) is the main component of the lysosomal storage material found in nearly all forms of the most common inherited neurodegenerative disorders of childhood, the neuronal ceroid lipofuscinoses (NCL) [1]. The juvenile NCL (JNCL or Batten disease), which is characterized by loss of vision between 4 and 8 years of age, epileptic seizures, dementia, and premature death, is the most prevalent form [2]. In tissues of Batten disease patients, the autofluorescent storage material containing Subunit c can be detected by electron microscopy as typical fingerprint patterns. JNCL is caused by mutations in the *CLN3* gene, encoding a protein of unknown function [3], and the relationship between the *CLN3* gene and Subunit c accumulation still remains unclear. Normally Subunit c is located in the mitochondrial ATP synthase complex, where 10 - 14 molecules form part of the F_0 inner mitochondrial membrane channel, [4]. This leads to the question why and how Subunit c ends up in the lysosomes of a Batten patient. In patients, the expression levels of two of the genes encoding subunit c, *ATP5G1* and *ATP5G2*, appear to be normal, excluding overproduction of these two genes as a cause of Subunit c accumulation [5]. A third gene, *ATP5G3*, encoding Subunit c with a different leader peptide but identical mature protein was identified later [6]. Only the mature form has been found in storage material, suggesting that defects in the transport and processing of the Subunit c protein can be excluded and that the stored Subunit c originates from mitochondria, which are autophagocytosed at the end of their lifetime. The highly hydrophobic Subunit c also accumulates in the lysosomes of cells from late infantile NCL patients, which are deficient for the lysosomal proteolytic enzyme tripeptidyl peptidase I, *TPPI*, suggesting that the lysosomal Subunit c degradation is compromised in JNCL. To elucidate the function of the *CLN3* gene, cultured cells, murine, worm, and yeast JNCL disease models are being used [7, 8, 9, 10, 11, 12]. The simple model organisms are probably more suitable for the elucidation of the genetic pathways and molecular mechanisms involved in JNCL. The yeast model for JNCL has been used successfully for investigations at biochemical and cellular level, but extrapolating the data obtained with this model to a multicellular environment or to structurally differentiated cells, such as neurons, will be difficult. Therefore, we have initiated work on the nematode *Caenorhabditis elegans*, a relatively simple multicellular organism, which may provide a model for investigating the *CLN3* gene at a functional level [12]. An extensive genetic toolset is available to investigate genes and gene products in this worm and it is amenable to large genetic screens for the elucidation of genetic pathways [13, 14]. In addition, the well-characterized nervous system of the nematode, which is completely mapped and invariantly wired, is an asset when investigating mechanisms underlying a neuronal disorder [15]. Since *C. elegans* has three genes homologous to *CLN3* with potentially overlapping function, *cln-3* triple

mutants, which were expected to have no functional Cln3 protein, were generated. The *cln-3* triple mutants showed a mild progeric phenotype, displaying a decreased life span and brood size. We were unable, however, to detect any neurological, morphological, or movement differences between *cln-3* mutants and wild type worms [16]. No increased autofluorescent lipopigment accumulation was observed on an ultrastructural level. Similar observations in the yeast JNCL model suggest that this is probably due to the short life span of both organisms. Therefore, we hypothesized that overexpression of Subunit c protein might induce lipopigment accumulation and a phenotype useful for genetic screens in the JNCL worm model. Proteins accumulating in several other neurodegenerative diseases have been overproduced successfully in *C. elegans*. Worms overexpressing human α-synuclein were generated to elucidate the pathophysiology of synucleopathies, including Parkinson's disease, implicating torsins in α-synuclein induced neurodegeneration [17, 18]. Additional *C. elegans* models were engineered to overexpress polyglutamine repeat containing proteins or β-amyloid, which are found in aggregates in human patients suffering from Huntington's or Alzheimer's disease, respectively [19, 20]. These Huntington models were used to reveal genetic pathways involved in polyglutamine neurotoxicity, and to detect pharmacological rescue of polyglutamine cytotoxicity [21, 22]. To overexpress Subunit c in the worm after heat shock induction, we first identified the *C. elegans* Subunit c gene *atp-9* by sequence homology and subsequently generated nematodes carrying an *atp-9* transgene under control of the *hsp-16.2* heat shock promoter. This promoter was selected, because it can drive expression in neuronal cells, which are most affected in human patients, and in intestinal cells, where the *C. elegans cln-3.1* gene is expressed [23, 16]. Here, we demonstrate that Subunit c overexpression has a deleterious effect on nematodes, which does not seem to be enhanced by the presence of *cln-3* mutations that are expected to interfere with lysosomal Subunit c degradation.

Materials and Methods

Strains and growth conditions

General methods used for *C. elegans* culturing, manipulation and genetics were as described [24]. Nematodes were cultured on NGM plates, plated with *Escherichia coli* strain OP50 as their food source [25]. Unless indicated otherwise, all strains were grown at 20 °C. Existing strains used in this study were wild type Bristol N2, *cln-3* triple mutants XT7 (*cln-3.2(gk41)*I; *cln-3.1(pk479)cln-3.3(gk118)*V) [16], and CL2070 (*dvIs70[hsp-16.2::GFP; rol-6(su1006)]*) robustly expressing GFP after heat shock [26]. For this study two independent Subunit c overexpressing strains XT23 (*hgEx5[hsp-16.2::atp-9; rol-6(su1006)]*) and XT24 (*hgEx6[hsp-16.2::atp-9; rol-6(su1006)]*) that contain the construct as an extrachromosomal array were generated. XT59 (*hgEx12[rol-6(su1006)]*) which only contains the *rol-6* transgene was generated as a control. In XT33 (*hgIs3[hsp-16.2::atp-9; rol-6(su1006)]VIx*), the construct is integrated in the nematode genome. XT31 (*hgEx10[hsp-16.2::GFP::atp-9; rol-6(su1006)]*) and XT32 (*hgEx11[hsp-16.2::GFP::atp-9; rol-6(su1006)]*) contain the GFP-Subunit c fusion overexpressing construct. XT33 and XT7 were crossed to generate XT57 (*cln-3.2(gk41)*I; *cln-3.1(pk479) cln-3.3(gk118)*V; *hgIs3[hsp-16.2::atp-9; rol-6(su1006)]VIx*) *cln-3* triple mutants capable of Subunit c overexpression after heat shock. Detection of the *cln-3* alleles was performed as described by De Voer *et al.*[16]. Nematode populations were synchronized as described previously [24]. For cloning purposes, bacterial strains DH10B (GIBCO BRL Life Technologies, Gaithersburg, USA), and DY380 (kindly provided by Donald Court) [27], were grown on Luria-Bertani medium supplemented with appropriate antibiotics if necessary (25 μg/ml kanamycin, 50 μg/ml ampicillin, 12.5 μg/ml tetracyclin). Plasmids used for cloning were pPD95-77 and pPD48-78 (kindly provided by Andrew Fire, Carnegie Institute of Washington, Baltimore, USA) [28].

Generation of overexpression constructs

Standard cloning procedures were performed as described [29]. The nematode homologue of the human genes encoding Subunit c of the mitochondrial ATP synthase was identified by BLASTp (http://www.ncbi.nlm.nih.gov/BLAST/) searches using the sequences of the largest protein variants of the three isoforms of the human genes (isoform 1 (*ATP5G1*) Genbank Acc.no. NM_005175, isoform 2 (*ATP5G2*) Genbank Acc.no. NM_001002031, isoform 3 (*ATP5G3*) Genbank Acc.no. NM_001002256). Y82E9BR.3, the *C. elegans* homologue with the lowest E-value, was localized on chromosome III, on cosmid Y82E9BR (Genbank Acc.no. AC090999), and has obtained the approved gene name *atp-9*. The protein sequences of the three

human isoforms, bovine isoform 1 (ATP5G1 Gen bank Acc.no. NM_176649), murine isoform 1 (Atp5g1 Genbank Acc.no. NP_031532), yeast Oli1p (Genbank Acc. no. NP_009319), and nematode ATP-9 were aligned using ClustalW v.1.8 on the Baylor College of Medicine server (http://searchlauncher.bcm.tmc.edu/multi-align/multi-align.html). The ClustalW output was processed using Boxshade 3.21 (http://www.ch.embnet.org/software/BOX_form.html) to indicate conservation between species. The putative mitochondrial localization and signal peptide cleavage site of the nematode protein was predicted by the computer program Mitoprot [30]. The *atp-9* gene was PCR amplified using N2 wild type genomic DNA as a template, and primers F scMAS 5' CAAGGATCCGAACTTTCATCCAGCCAT 3' and R scMAS 5' AAAGGTACCAAACAAAAATCGGCTATAAAAC 3'. The *Bam*HI and *Kpn*I sites underlined in the primer sequences were used , for insertion into *Bam*HI and *Kpn*I digested ectopic expression vector pPD49-78 togenerate Subunit c overexpression construct, pLU06 (*hsp-16.2::atp-9*). The *hsp-16.2::GFP::atp-9* fusion construct, pLU07, was generated by inserting the Green Fluorescent Protein (GFP) gene between the Subunit c gene sequences encoding the putative signal peptide and the mature protein in pLU06 by recombineering, cloning by homologous recombination, in DY380 cells [27]. In short, DY380 was electrotransformed with the Subunit c overexpression plasmid pLU06. DY380/pLU06 cells were incubated for 15 minutes at 42 °C while shaking vigorously, to induce the phage λ genes Exo, Beta, and Gam that are integrated in the bacterial chromosome, and are regulated by a temperature sensitive repressor. Induced DY380/pLU06 cells were made electrocompetent and transformed with a linear GFP reporter construct, created by PCR, using pPD95-77 as template DNA, and primers Forward GFP N-term 5' **CGTCGCTGCCCGCATGATCAGCACCACCGTCGCCCGCAAG** ACATTTTCAGGAGGACCC 3' and Reverse GFP N-term 5' **TCCAACGGTGGCGGCTCCAGCTCCGATGTACTTGGCAGCAGAGTCGATGTC** TAGTTCATCCATGCCATGTGTA 3'. These primers contain tails homologous to part of exon two of the *C. elegans atp-9* gene (shown in bold), to allow integration of the GFP gene in the *atp-9* open reading frame by homologous recombination between the ends of the PCR product and the homologous *atp-9* sequences in pLU06. Approximately 10,000 colonies were screened for the presence of the GFP construct, by colony blots probed with radioactively labeled GFP PCR product. Correct integration of the GFP gene in the Subunit c open reading frame of a positive clone was initially confirmed by restriction digestion and PCR. All constructs were checked by sequencing on an ABI 3700 DNA Analyzer at the Leiden Genome Technology Center.

Nematode transformation and integration

Transformation of *C. elegans* was performed by microinjection of the overexpression construct plasmid pLU06 or pLU07 at a concentration of 100 μg/ml together with a marker plasmid pRF4, *rol-6* (*su1006*) at a concentration of 50 μg/ml into the distal arm of the wild type hermaphrodite gonad as described previously [28]. Microinjection of pLU06

and pRF4 resulted in heat shock-inducible Subunit c overexpressing strains XT23 and XT24, in which the overexpression constructs, were transmitted as extrachromosomal arrays. Integrated line XT33 was generated by X-ray irradiation of XT23 followed by outcrossing six times as described previously [28]. The heat shock inducible GFP Subunit c fusion overexpressing strains XT31 and XT32 were obtained after injecting the GFP Subunit c fusion construct pLU07 and roller marker plasmid pRF4.

Overexpression induction of Subunit c

Overexpression of Subunit c was driven by the *hsp-16.2* heat shock promoter from pPD49-78, which can be induced by incubating *C. elegans* at 33 °C [23]. Heat shock inductions were performed by incubating parafilm sealed NGM agar plates containing synchronized worms and OP50 bacteria in a 33 °C waterbath, for various time intervals indicated. Prolonged cultivation in a 25 °C incubator was used to obtain less intense induction.

Determination of viability, life span and brood size

Synchronized Subunit c overexpressing and N2 wild type worms were subjected to heat shocks of 0, 15, 30, 45, 60, 90, 120, and 150 minutes at 33 °C. 17 hours later, movement of the grinder, the muscular part of the pharynx, which is used for uptake, grinding up of bacteria, and transport of bacterial debris to the intestine, and is easily visible with a standard dissection microscope, was scored to measure the viability of the worms. Life span and brood size determinations at 25 °C and the statistical analysis of their data were performed as described previously [16]. Worms that were forming bags or had crawled off the plate were removed from the experiment.

LysoTracker Red and MitoTracker Red staining

The lysosomes and mitochondria were stained by incubating worms in M9 buffer containing LysoTracker Red (33 μM end concentration, 2 h) or MitoTracker Red CMXRos (10 μM end concentration, 1 h) (Molecular Probes, Breda, the Netherlands). After staining the worms were transferred to NGM agar plates containing OP50 bacteria for approximately two hours to decrease intestinal background staining.

Electron Microscopy

To study the effects of Subunit c overexpression on ultrastructural level electron microscopy was performed on synchronized L3/L4 larvae from Subunit c overexpressing and wild type worms after a two-hour heat shock at 33 °C and a two-

hour recovery at 20 °C. Worms incubated for four hours at 20 °C were used as non-induced controls. Worms were rapidly picked from plates, transferred to anesthetizing solution (8 % ethanol in M9 buffer), dissected in fixative (1.5 % glutaraldehyde in 0.1 M cacodylate buffer) and fixed for 2h, followed by post-fixation in 1 % Osmium tetroxide, standard propylene oxide-epon treatment and embedding.

Detection of overexpression levels by RT-PCR

The expression levels of the endogenous *atp-9* gene, the *atp-9* overexpression construct, and the *ama-1* control gene were determined using real time RT-PCR as follows. Samples containing 15 worms taken at 30 min intervals before, during, and after 2 hr heat shock at 33 °C were lysed in a 45 µl volume as described before [31]. First strand cDNA synthesis was performed in a Tetrad PTC-225 Gradient Cycler (Bio-Rad Laboratories, Inc., Waltham, MA, USA) with the Superscript First strand Synthesis System for RT-PCR (Invitrogen, Carlsbad, CA, USA) according to the manufacturer's recommendations. The cDNA was analyzed with primer sets F-*atp-9*: 5'- GTACTGCCAGCGCCTTG –3', R-*atp-9*: 5'- CAGCAGAGTCGATGTCCTTG –3', and F-*ama-1*: 5'- GTACAATGCGGATTTCGATG –3', R-*ama-1*: 5'- CTGGACGATACCCATGACTG –3', using SYBR Green PCR Master Mix (Applied Biosystems, Foster City, CA, USA) for real time RT-PCR in a TaqMan HT7900 (Applied Biosystems). Real time RT-PCR data were processed with the SDS 2.2.2 software (Applied Biosystems), and the CT-values were imported into the Qgene Excel macro [32] to calculate the ratio between the mean normalized expression levels of the *atp-9* gene and the *ama-1* control gene.

Isolation of mitochondrial protein fractions and protein detection by Western Blotting

The expression of Subunit c and GFP-Subunit c in mitochondrial fractions and total worm lysates of induced and non-induced Subunit c overexpressing and wild type worms was analyzed using western blot experiments. Mitochondrial fractions were isolated from nematodes after 2 h heat shock at 33 °C and 1 h recovery at 20 °C, and from uninduced controls, as follows. Worms were washed twice in M9 buffer, resuspended in 5 ml buffer A (0.25M sucrose, 10mM HEPES pH 7.4, and complete Protease Inhibitor Cocktail (Roche Diagnostics, Almere, The Netherlands)) and frozen at -20 °C. Nematodes were homogenized with intermediate cooling on ice in a glass S-Potter tissue homogenizer with glass pestle (Braun, Melsungen, Germany). After centrifugation for 5 minutes at 4000 rpm, pellets were resuspended in 1 ml buffer B (0.25M sucrose, 20mM Tris pH 7.4, 2mM EDTA, and complete Protease Inhibitor Cocktail), followed by centrifugation for 5 minutes at 4000 rpm. The supernatant was centrifuged for 45 minutes at 13000 rpm and the pellets were dissolved in 100 µl buffer B. Protein concentrations were determined using the BCA assay (Pierce, Etten-Leur,

The Netherlands). Mitochondrial protein fractions were separated on 20% Tricine-SDS/PAGE gels and blotted onto PVDF membrane. Ponceau staining of the blots was used to verify that equal amounts of protein had been loaded on gel. Whole lysates of induced and non-induced nematodes were prepared by boiling worms, washed with M9 buffer, in standard SDS-PAGE sample buffer for ten minutes. Approximately equal amounts of whole protein lysates were separated on 12% polyacrylamide gels and blotted to PVDF membrane. For detection of Subunit c in mitochondrial fractions we used a polyclonal antiserum raised against synthetic peptides corresponding to the amino-terminal residues 1-11 of the mature, fully processed human Subunit c protein, which contains two neutral substitutions compared to the predicted *C. elegans* N-terminal Subunit c sequence (Figure 1) [5], as the primary antibody at a 1:67.5 dilution (kindly provided by E. Kominami) [33]. For detection of GFP polyclonal antiserum (kindly provided by W. Hendriks) [34] was used at a 1:7500 dilution as the primary antibody. Primary antibodies were detected using goat anti-rabbit-horseradish peroxidase conjugate diluted 1:10,000 (Jackson ImmunoResearch Laboratories, Soham, UK) with the Supersignal® WestPico chemiluminescent substrate (Perbio Science, Etten-Leur, The Netherlands).

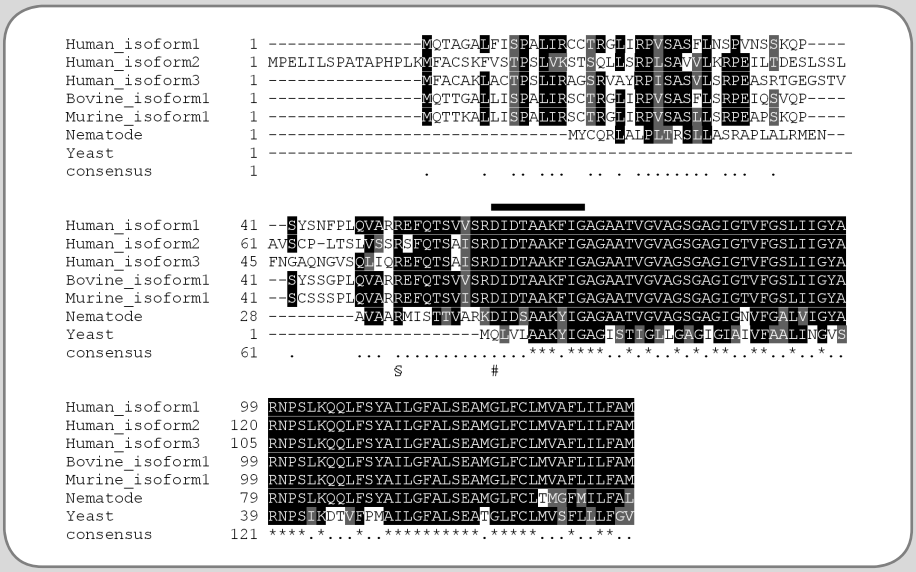

Figure 1 Alignment of the human, bovine, murine, *C. elegans*, and yeast Subunit c protein sequences

The sequence alignment of unprocessed predicted Subunit c protein of the mitochondrial ATP synthase shows strong conservation in the carboxy-terminal half of the protein. Conserved amino acids are depicted in black boxes, neutral substitutions in grey boxes. The consensus sequence is indicated by asterisks when completely conserved and by dots when more than 50% conserved between species. The cleavage site predicted to be used during the processing of the *C. elegans* preprotein (§), the first eleven amino acid peptide of the mature Subunit c protein used by Kominami [33] to raise antibodies (bar), and the amino acid before which the GFP sequence was inserted to create the GFP-Subunit c fusion protein (#) are indicated.

Results

C. elegans has one homologue of Subunit c of the mitochondrial ATP synthase, *atp-9*

To investigate the possibility to induce an easily detectable phenotype in *cln*-3 triple mutants using Subunit c overexpression constructs, we set out to identify the *C. elegans* Subunit c gene. The human Subunit c isoforms 1, 2, and 3 were used in a BLASTp search of the WormPep database [35] with default parameter settings to identify homologous sequences in the *C. elegans* genome, resulting in the following three hits: Y82E9BR.3 (E-value of 2.5 e-34), R10E11.2 and Y38F2AL.4 (E-value of 0.0024 for both). The Y82E9BR.3 protein sequence showed 65% identity and 76% similarity to human Subunit c isoform 1, and was predicted to be the worm Subunit c homologue (approved gene name *atp-9*). Computer program Mitoprot predicted mitochondrial localization of the ATP-9 protein with a putative signal peptide cleavage site between amino acids 41 and 42. The ATP-9 protein sequence was aligned to human, bovine, murine and yeast Subunit c sequences, showing high conservation of the mature protein sequences, but more variation between the amino acids of the mitochondrial signal peptide (Figure 1). PCR amplified genomic DNA of *atp-9* was used to generate the Subunit c overexpressing transgenic worm strains XT23 and XT24 carrying extrachromosomal arrays and XT 33 carrying an integrated array.

Induction of overexpression of Subunit c is deleterious to nematodes

All transgenic strains carrying arrays of the *atp-9* gene under control of the *hsp-16.2* heat shock promoter were severely damaged by a two-hour heat shock at 33°C. XT33 nematodes carrying integrated arrays of the *atp-9* gene were selected for detailed investigations. Twenty hours after heat shock, Subunit c overexpressing worms showed slow or no movement, even after gentle prodding with a platinum wire, suggesting Subunit c overexpression causes lethality, while wild type worms moved constantly at any time after heat shock with exception of the naturally occurring period of lethargus between two larval stages. To determine how fast Subunit c overexpression affects viability, we assessed grinder movement 17 hours after heat shocks of different duration (Figure 2A). Grinder movement was absent in more than half of the counted population after a 45-min heat shock at 33°C and in almost all worms after a two-hour heat shock, while virtually none of the wild type worms lost grinder movement after heat shock. Heat shocked XT33 worms showed overall structural impairment, increased transparency due to loss of pigment present in gut granules and a crumpled appearance, as early as five hours after the end of the heat shock (Results not shown).

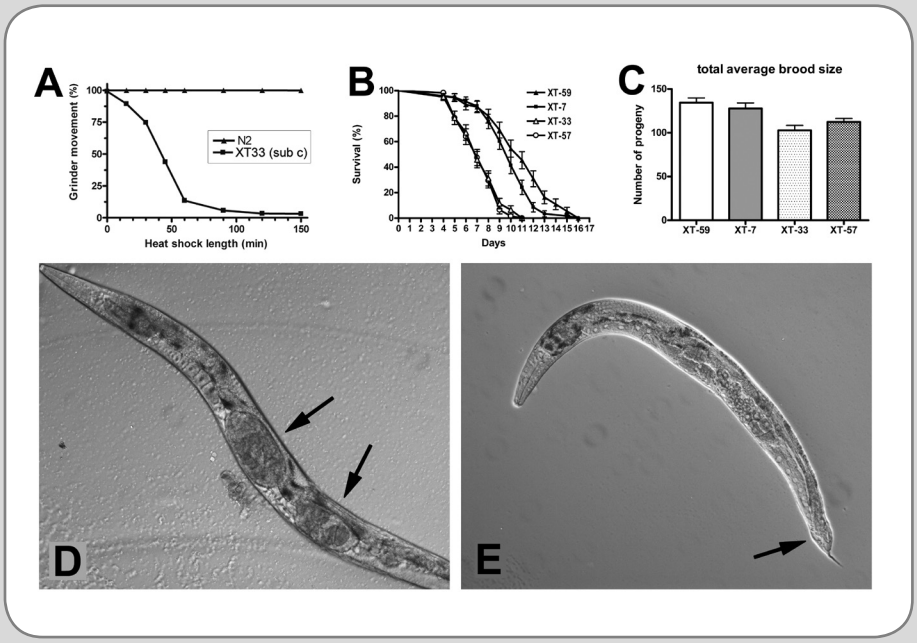

Figure 2 Subunit c overexpression alters survival (A, B), brood size (C) and morphology (D, E)

Subunit c overexpressing nematodes XT33 (for each time point n>230) display severe loss of viability determined as reduced grinder movement compared to wild type N2 (for each time point n>800) twenty hours after heat shock at 33ºC (A). On the X-axis heat shock exposure time is depicted, and the Y-axis displays the percentage of worms showing grinder movement. This experiment was performed twice and resulted in similar numbers, shown here is the result of one experiment. The relative survival of transgenic worms carrying the integrated Subunit c overexpression array on wild type (▲, n=61) and *cln-3* triple mutant backgrounds (○, n=61) is decreased compared to transgenic *rol-6* controls (Δ, n=55) and *cln-3* triple mutants (■, n=58), all grown at 25 ºC (B). Survival is plotted against time; error bars represent SEM. The figure represents one of two experiments giving similar results. Average total brood sizes of transgenic worms XT33 and XT57 carrying the integrated Subunit c overexpression array on wild type (n=61) and *cln-3* triple mutant backgrounds (n=61), respectively, differ significantly (□, P<0.0001) from XT59 transgenic *rol-6* controls (n=55) and XT7 *cln-3* triple mutants (n=58) at 25 ºC (C). Average brood sizes are depicted; error bars represent SEM. The figure represents two experiments. In XT33 grown for five days at 25 ºC, mild Subunit c overexpression causes gonadal phenotypes, e.g. enlarged oval shaped ´bags´ (arrows in D), and morphological abnormalities, e.g. tail swelling (arrow in E).

In contrast, pigmented gut granules, normal internal structures, and straight body contour were still present in non-induced transgenic worms, and wild type worms.
We also tested whether growth at a lower temperature would reduce the activity of the heat shock promoter and would allow the XT33 worms to survive. Grown at 25 °C, XT33 worms have a reduced lifespan and display a decreased brood size (Figure 2B, C). To test whether the survival would be affected by lysosomal Subunit c degradation defects, which are observed in the presence of CLN3 mutations in man, we transferred the integrated array into the *cln-3* triple mutant strain XT7 by crossing with strain XT33, resulting in strain XT57. Mutations in all three *cln-3* genes did not alter the survival or brood size of strain XT57 compared to XT33 (Figure 2B, C). After five days at 25 °C, XT33 and XT57 worms displayed enlarged oval structures, resembling huge embryos, in the gonads, and deformations at the tail of the animal (Figure 2D, E). Both phenotypes were absent from N2 wild type worms grown under identical conditions. The phenotypes of XT33 and of transgenic strains XT23 and XT24 carrying extrachromosomal *atp-9* arrays were similar, suggesting that the integration event did not affect the phenotype.

Overexpression of Subunit c alters lysosomal and mitochondrial staining

To determine whether Subunit c overexpression affected lysosomes and mitochondria, we stained these organelles using the fluorophores Lysotracker Red and Mitotracker Red, respectively. A two-hour heat shock at 33 ºC caused diffuse Lysotracker Red fluorescence throughout the whole body of the XT33 animals with more intense staining of the gonad and some intestinal cells, (Figure 3, left half of the panel). Before induction, the staining of lysosomes and other acidic compartments appeared punctate and localized to granules in the intestine, which are presumably the abundant secondary lysosomes reported previously [37]. The loss of punctate staining coincides with the increased transparency observed after heat shock (Figure 3 M, O). Similar lysosomal staining patterns were observed on a *cln-3* triple mutant background in XT57 mutants (data not shown).Wild type nematodes displayed staining of the intestinal granules before and after heat shock (Figure 3 E, F). Comparable results were obtained with the acidophilic dye Acridine Orange (data not shown).
Subunit c overexpression caused an almost complete disappearance of Mitotracker Red staining in transgenic XT33 animals, leaving only the tip of the pharynx fluorescent and the first cells and lumen of the intestine faintly visible (Figure 3, right half of the panel). Without induction transgenic and wild type animals were stained intensely, in particular the pharyngeal muscles, neurons, intestine, and gonads were visible (Figure 3 G, H). Similar mitochondrial staining patterns were observed on a *cln-3* triple mutant background in XT57 mutants (data not shown).Wild type worms displayed intense staining overall before and after heat shock (Figure 3 H, L).

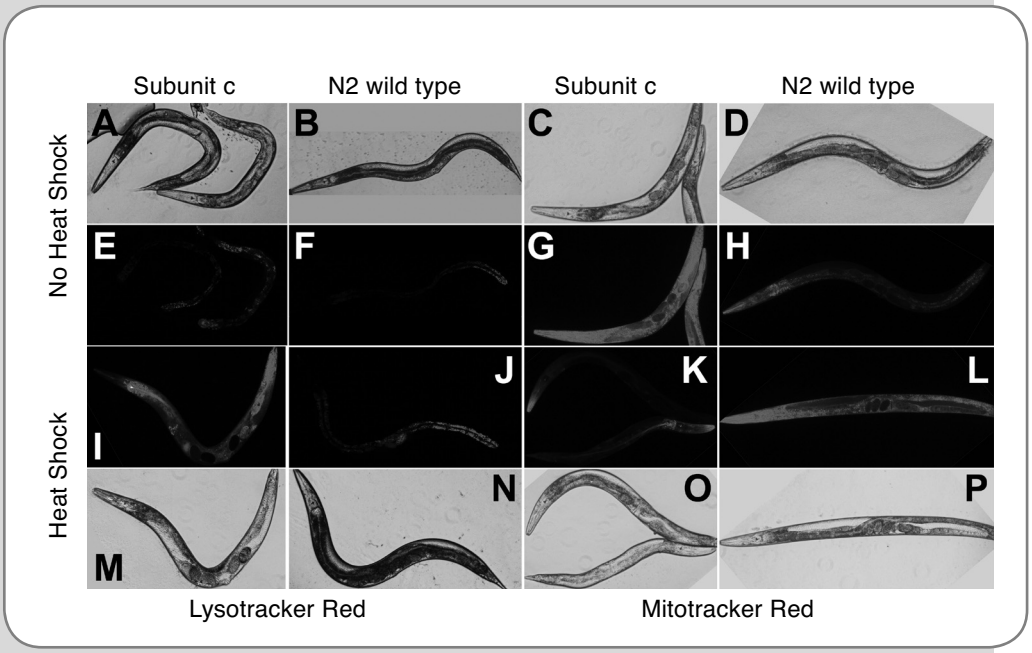

Figure 3 Subunit c overexpression causes diffuse Lysotracker Red and severely decreased Mitotracker Red fluorescence

Nomarski (A-D, M-P) and fluorescence (E- H, I- L) micrographs show XT33 Subunit c overexpression (A, C, E, G, I, K, M, O), and N2 wild type (B, D, F, H, J, L, N, P) nematodes. Worms were either stained immediately after a 2-hr heat shock induction at 33ºC (bottom panel) or stained without heat shock (top panel). Subunit c overexpression caused diffuse Lysotracker Red staining of the body and loss of punctate staining in the intestine (I) and increased transparency (M, O), whereas heat shocked wild type worms (J) show fluorescence patterns similar to the uninduced wild type and Subunit c transgenic worms (E, F). Induced Subunit c overexpression nematodes show strongly decreased Mitotracker Red staining (K) compared to induced wild type (L), and uninduced wild type (H) and Subunit c transgenic nematodes (G). Without induction the whole body is fluorescent, most intensely in pharyngeal and intestinal cells (G, H).

Overexpression of Subunit c affects mitochondria

The altered Lysotracker and Mitotracker staining after induction of Subunit c overexpression prompted us to assess the ultrastructural integrity of the transgenic worms. Electron micrographs of Subunit c overexpressing nematodes consistently showed abnormal mitochondrial ultrastructure, specifically with disorganized cristae, or disrupted or completely vanished inner and outer membranes (Figure 4 A, B, C). In

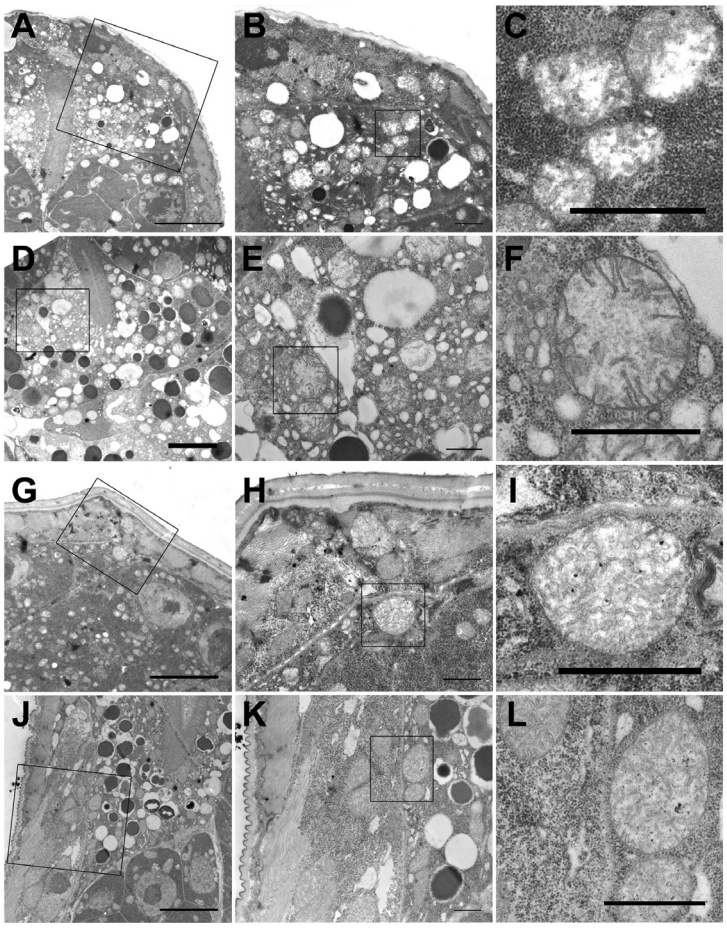

Figure 4 Subunit c overexpression causes disruption of mitochondrial ultrastructure

Electronmicrographs of XT33 Subunit c overexpression (A-F) and N2 wild type (G-L) worms show that heat shock induction, for two hours at 33ºC followed by a two-hour recovery at 20ºC, causes mitochondria to become disrupted in Subunit c transgenic worms (A-C). Induced wild type worms (G-I) show intact mitochondria, comparable to uninduced wild type (J-L). Mitochondria of uninduced Subunit c transgenic worms seem to have less cristae compared to wildtype (F). (Scale bars = 5µm in A, D, G, J and 1µm in B, C, E, F, H, I, K, L).

contrast, mitochondria of non-induced transgenic worms appeared intact (Figure 4 D, E, F), with only few mitochondria displaying disorganized cristae and most inner and outer membranes remaining unimpaired. Before and after heat shock, mitochondria of wild type worms were normal and contained many intact cristae and entire inner and outer membranes (Fig 4 G-L). We could not detect lipopigment storage patterns on the electron micrographs after induction of Subunit c overexpression or other changes in the appearance of vesicles, which might be stained with Lysotracker (Figure 4, and data not shown).

Overexpression of GFP-Subunit c fusion constructs

For easy detection of Subunit c overexpression in living worms, we also generated a GFP-Subunit c fusion construct, containing the 41 amino acid mitochondrial targeting signal of the ATP-9 protein followed by GFP and the mature Subunit c protein (Figure 1). The localization and cleavage site of the GFP-Subunit c fusion protein predicted by Mitoprot was similar to that of the Subunit c protein without the GFP insertion. After a two-hour heat shock at 33 °C, transgenic nematode strains XT31 and XT32 displayed phenotypes similar to the Subunit c overexpression strain XT33, such as loss of internal structures, increased transparency and lethality. Furthermore, in GFP-Subunit c transgenic worms GFP fluorescence could be observed from L1 larval to adult stages after induction. In larval stages intense fluorescence was observed in the intestine and muscles of the pharynx with less intense signal in muscles, hypoderm, and neurons, whereas most adult worms showed fluorescence only in intestine and pharyngeal muscles (Figure 5, and data not shown). GFP fluorescence became visible

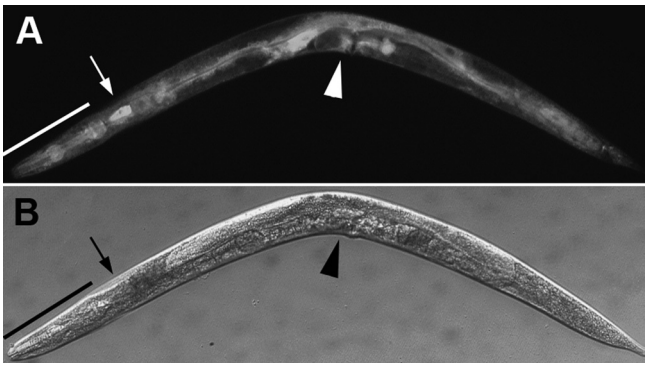

Figure 5 GFP::Subunit c fusion fluorescence in various nematode tissues

Fluorescence (A) and Nomarski (B) pictures of a XT31 GFP::Subunit c overexpression worm, showing GFP fluorescence in the muscles of the pharynx (bar) five hours after a two-hour heat shock at 33°C. All intestinal cells are fluorescent; some with high intensity (arrow). Fluorescence can also be observed in muscles of the vulva (arrowhead) and in the hypoderm just below the cuticle, which confines the nematode body.

near the end of the two-hour heat shock induction period and lasted for more than two days. Without heat shock induction, about 1 % of the transgenic worms displayed GFP fluorescence limited to a single cell with variable position in the intestine (data not shown).

Subunit c overexpression on protein level

To demonstrate overexpression and correct processing of the Subunit c protein we used antibodies against the human Subunit c protein and GFP on Western blots containing mitochondrial protein fractions and whole worm lysates from induced and non-induced Subunit c transgenic and wild type nematodes. An antibody raised against a synthetic N-terminal human Subunit c peptide was used, because an antibody against *C. elegans* Subunit c was not available. The human Subunit c antibody detected proteins of approximately 7 kDa in the mitochondrial fractions, but not in other fractions, of XT33 Subunit c transgenic and wild type worms, regardless of induction, suggesting cross-reactivity to the endogenous Subunit c protein worm (Figure 6A, and data

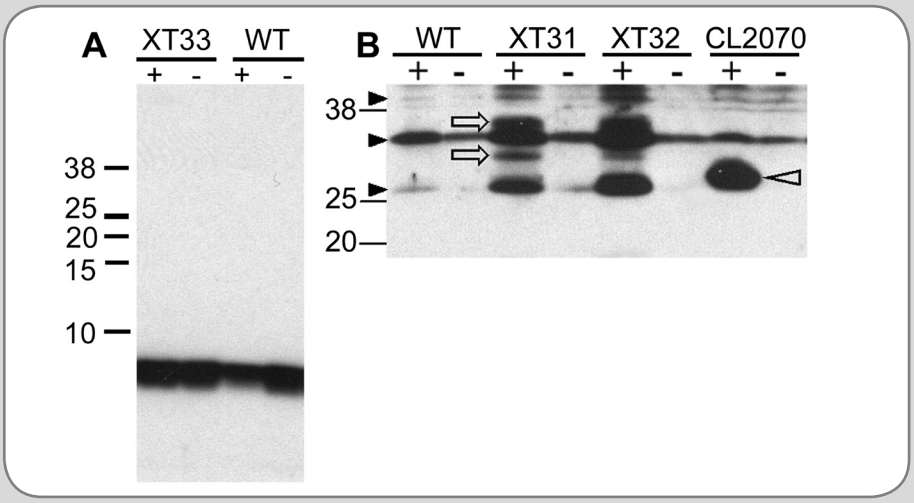

Figure 6 Subunit c and GFP::Subunit c overexpression on protein level

(A) Antibodies raised against a peptide from the human mature Subunit c protein detect one similarly intense band in mitochondrial protein fractions of induced (+) and uninduced (-) XT33 Subunit c transgenic worms . Induced (+) and uninduced (-) N2 wild type (WT) mitochondrial fractions contained the same band of approximately 7 kDa. Induced wild type fractions appeared to contain slightly less Subunit c protein. XT31 and XT32 worms overexpress GFP::Subunit c after a two hour heat shock at 33ºC (B). In lysates of induced GFP::Subunit c transgenic worms (XT31 and XT32, + lanes), the polyclonal anti-GFP antibody recognizes an extra band of 34 kDa, the expected size of the GFP::Subunit c fusion protein, and another of 30 kDa (open arrows). The lane of the inducible GFP expressing CL2070 worms contains a relatively intense band with the expected size of GFP, approximately 27 kDa (open arrowhead). Almost all lanes exhibit the same background pattern (black arrowheads).

not shown). After the 33 °C heat shock, wild type fractions appeared to contain less Subunit c protein, while similar amounts were detected in uninduced and induced Subunit c transgenic worms and in untreated wild type worms.
Poly-clonal anti-GFP antibodies detected two protein bands of approximately 34 kDa and 30 kDa in total lysates of GFP-Subunit c transgenic strains XT31 and XT32 after heat shock (Figure 6B). The 34kDa protein has the expected size of a fusion protein consisting of 7kDa Subunit c and 27kDa GFP [38]. The 30kDa band clearly differs from the 27 kDa GFP protein expressed by GFP transgenic strain CL2070 and from the background bands observed in all worm lysates and may represent a breakdown product of the fusion protein. The 34 kDa and 30 kDa bands were not present on blots of mitochondrial fractions of XT31 and XT32 worms (results not shown).

Overexpression of Subunit c transcript on RNA level

The Subunit c protein produced by the transgenes after heat shock induction can not be distinguished from the endogenous protein by Western blot analysis (Figure 6A). Since the amount of protein did not increase, we decided to determine whether the construct was properly induced after heat shock. Real time RT-PCR analysis of the *atp-9* gene and the *ama-1* control gene in XT33 and N2 controls indicates an increase of Subunit c transcription in XT33 during heat shock (Figure 7). Transcript levels increased from approximately 3-fold after 30 min to approximately 17-fold after 2 hrs, reaching 22-fold increased levels at 30 min after the shift back to 20 °C. These data indicate normal induction of the Subunit c transgene, whereas the endogenous *atp-9* gene is not induced in N2. Measurements extending past the last sample time were not reproducible probably due to the deleterious effects of the heat shock exposure.

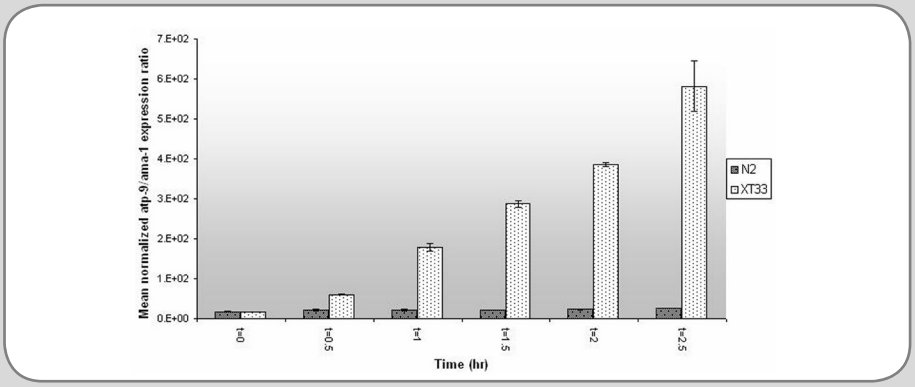

Figure 7 Overexpression of *atp-9* in XT33 after heat shock induction

The expression levels of the *atp-9* gene and the *ama-1* control gene were measured in triplicate by real time RT-PCR on RNA samples of 15 XT33 and N2 worms, respectively, taken at different time points before (t=0), during and after (t=2.5) heat shock. The mean expression level of the *atp-9* gene was normalized against the mean *ama-1* expression level using the Qgene Excel macro [32]. Error bars indicate the standard error of the mean normalized expression.

Discussion

We have generated transgenic worms, which overexpress *atp-9*, the *C. elegans* homologue of the gene encoding Subunit c of the mitochondrial ATP synthase under control of the hsp16.2 promoter. To our knowledge, we have demonstrated for the first time that overexpression of the hydrophobic Subunit c construct in a metazoan animal has deleterious effects. Induction of the Subunit c transgene at high temperature caused progressive deterioration with worms displaying a crumpled appearance, overall shrinking of their body, loss of movement, increased transparency due to loss of pigmented gut granules, and rapid loss of viability. The same phenotypes were observed in strains carrying GFP-Subunit c fusion transgenes. As expected, the pattern of GFP fluorescence in these strains overlaps with the strongly affected cells and corresponds to the expression pattern previously described for the *hsp-16.2* gene (Figure 5)[23]. Mild overexpression allowed the transgenic worms to survive, although with reduced lifespan and brood size and altered morphology demonstrating a correlation between the strength of the induction and the severity of the phenotype. Our initial hypothesis was that Subunit c overexpression might result in more Subunit c protein in mitochondria, which might become destabilized, turned over, and engulfed by autophagosomes at higher rates. Since subunits of mitochondrial respiratory chain complexes have never been overexpressed before in nematodes, it is difficult to predict which course of events could lead to the observed phenotype after Subunit c transgene induction. Three hours after the end of the 33°C heat shock, most mitochondrial label had disappeared, suggesting loss of mitochondrial membrane potential [39]. The disrupted mitochondrial ultrastructure corroborated this observation. Furthermore, the loss of energy due to disruption of the mitochondrial electrochemical gradient probably reduced the amount of energy available for movement and organelle acidification, causing more diffuse lysosomal staining throughout the animal.
No evidence for lysosomal storage or other vesicle abnormalities was observed in electronmicrographs.
Since the fluorescence of the GFP-Subunit c fusion protein was not very strong in relation to the expected abundance of Subunit c in mitochondria, the Subunit c expression level might be less than expected. Western blots of mitochondrial protein fractions suggest that Subunit c protein levels are not increased substantially after induction, although we observe 22-fold excess of Subunit c mRNA in the transgenic worms after heat shock. Furthermore, the GFP-Subunit c fusion protein was only detectable in total lysates and not in mitochondrial protein fractions, suggesting that the GFP tag interfered with the normal localization of Subunit c or resulted in rapid degradation. Nevertheless, the phenotypes of the transgenic strains are similar in the presence or absence of the GFP tag. Taken together, this might either indicate that a small excess of Subunit c or GFP-Subunit c fusion protein in mitochondria is sufficient

to disrupt mitochondrial function. An excess of Subunit c protein might exert its deleterious effect through spontaneous assembly into ring-like structures forming pores in the inner mitochondrial membrane, similar to the pores formed spontaneously in artificial membranes [40-43]. Alternatively, a deviation from the correct stoichiometry of a functional multisubunit ATP-synthase complex might saturate mitochondrial chaperones and interfere with the normal processing or oligomerization of other essential mitochondrial proteins.

In case the excess Subunit c or GFP-Subunit c fusion proteins in mitochondria are degraded rapidly, the induction of the Subunit c transgenes might interfere with mitochondrial function in a more indirect manner. The Subunit c construct in the transgenic worms was designed to contain the *atp*-9 mitochondrial targeting sequence for correct mitochondrial localization of the protein, but has the *myo-3* 3' UTR in stead of its original 3' UTR. If one assumes that the presence of the preprotein sequence is sufficient for mRNA localization, the transgenic mRNA could be correctly localized to mitochondria and translated on mitochondrial polysomes. Although little is known about the transcription, transport, localization, and translation of transcripts from nuclear genes encoding mitochondrial protein in the worm, the efficient localization of these mRNAs in other species appears to rely on *cis*-acting elements in the presequence containing a mitochondrial targeting sequence (MTS) and in the 3' untranslated region (UTR) [44 - 47]. The presequence coding region seems to be sufficient for the localization adjacent to the outer mitochondrial membrane of several human and yeast mRNAs, but the presence of both the presequence and the 3'UTR increases the formation of mitochondrial polysomes [48] and the amount of protein fully translocated into the mitochondria, suggesting that the 3'UTR plays a role in mRNA sorting on the mitochondrial surface [49] or in mitochondrial import of the protein [50]. During translation nascent precursor proteins become associated with chaperones to prevent loss of mitochondrial import competence, aggregation, or degradation by cellular proteases [51, 52]. The absence of the atp-9 *cis*-acting 3' UTR element from the transgenic *atp*-9 transcripts might reduce their transport to mitochondria and result in cytoplasmic Subunit c production. An excess of cytoplasmic Subunit c protein might lead to a depletion of cytoplasmic chaperones, which normally bind mitochondrial protein precursors, and could block their import into mitochondria, causing Subunit c and other mitochondrial proteins to form aggregates, or become degraded by cytoplasmic proteases. In *C. elegans*, chaperone depletion was observed after RNAi knock-down of *hsf-1*, the transcriptional regulator of genes involved in stress-inducible gene expression and protein folding homeostasis, resulting in developmental arrest, lethality, and sterility [53, 54, 55]. It is tempting to speculate that chaperone depletion underlies the Subunit c overexpression phenotype, but we cannot exclude that cytoplasmic Subunit c kills the worms by forming pores in the plasma membrane.

In *cln-3* triple mutant worms, Subunit c overexpression was expected to cause NCL-associated features, such as the lysosomal Subunit c accumulation observed in mammalian CLN3 models. In contrast, the presence of triple *cln-3* mutations did not enhance the lifespan and brood size and altered morphology of the Subunit c overexpression strain, regardless of the temperature and duration of the induction.

The lysosomal and mitochondrial staining patterns did also not differ. The most likely explanation would be that Subunit c overexpression does not result in the envisaged increase of mitochondrial Subunit c protein and the subsequent mitochondrial turnover necessary to saturate the lysosomal Subunit c degradation pathway. In conclusion, the combination of triple *cln-3* mutations and Subunit c overexpression does not seem to be suitable for genetic screens to isolate other genes involved in the lysosomal Subunit c degradation.
Induction of the Subunit c transgene might be useful, however, as an alternative strategy for laser-mediated cell ablation to physically terminate particular cells in order to examine the effects of absence of cells or tissues [56]. Genetically targeted cell disruption is more suitable for large numbers of animals and anatomically dispersed cells and presently can be accomplished by ectopic expression of the *ced-3* or *ced-4* cell death genes [57], a gain-of-function allele of the *egl-2* potassium channel gene [58], a dominant allele of the *mec-4* sodium channel subunit [59], and possibly by the *atp-9* overexpression described here.

Acknowledgements

E. coli strain DY380 was kindly provided by Donald Court. *C. elegans* vectors pPD48-78 and pPD95-77 were kindly provided by Andrew Fire (Carnegie Institute of Washington, Baltimore, MD). Some strains were provided by the *C. elegans* Genetics Center, which is funded by the NIH National Center for Research Resources (NCRR). Antiserum against Subunit c was generously provided by Eiki Kominami and Jakub Sikora, and anti-GFP antibodies were generously provided by Wiljan Hendriks. We are thankful to Hans van der Meulen for performing the electron microscopy. This work was financially supported by the Center for Biomedical Genetics, the Batten Disease Support and Research Association, and the European Union, EU project NCL models (EU LSHM-CT-2003-503051).

References

[1] Hall NA, Lake BD, Dewji NN, Patrick AD. 1991. Lysosomal storage of Subunit c of mitochondrial ATP synthase in Batten's disease (ceroid-lipofuscinosis). Biochem J 275:269-72.

[2] Rapola J. 1993. Neuronal ceroid-lipofuscinoses in childhood. Perspect Pediatr Pathol 17:7-44.

[3] IBDC (The International Batten Disease Consortium). 1995. Isolation of a novel gene underlying Batten disease, CLN3. Cell 82:949-57.

[4] Yoshida M, Muneyuki E, Hisabori T. 2001. ATP synthase--a marvellous rotary engine of the cell. Nat Rev Mol Cell Biol 2:669-77.

[5] Palmer DN, Fearnley IM, Walker JE, Hall NA, Lake BD, Wolfe LS, Haltia M, Martinus RD, Jolly RD. 1992. Mitochondrial ATP synthase Subunit c storage in the ceroid-lipofuscinoses (Batten disease). Am J Med Genet 42:561-7.

[6] Yan WL, Lerner TJ, Haines JL, Gusella JF. 1994. Sequence analysis and mapping of a novel human mitochondrial ATP synthase subunit 9 cDNA (ATP5G3). Genomics 24:375-7.

[7] Jarvela I, Sainio M, Rantamaki T, Olkkonen VM, Carpen O, Peltonen L, Jalanko A. 1998. Biosynthesis and intracellular targeting of the CLN3 protein defective in Batten disease. Hum Mol Genet 7:85-90.

[8] Katz ML, Shibuya H, Liu PC, Kaur S, Gao CL, Johnson GS. 1999. A mouse gene knockout model for juvenile ceroid-lipofuscinosis (Batten disease). J Neurosci Res 57:551-6.

[9] Mitchison HM, Bernard DJ, Greene ND, Cooper JD, Junaid MA, Pullarkat RK, de Vos N, Breuning MH, Owens JW, Mobley WC, Gardiner RM, Lake BD, Taschner PE, Nussbaum RL. 1999. Targeted disruption of the Cln3 gene provides a mouse model for Batten disease. The Batten Mouse Model Consortium. Neurobiol Dis 6:321-34.

[10] Cotman SL, Vrbanac V, Lebel LA, Lee RL, Johnson KA, Donahue LR, Teed AM, Antonellis K, Bronson RT, Lerner TJ, MacDonald ME. 2002. Cln3(Deltaex7/8) knock-in mice with the common JNCL mutation exhibit progressive neurologic disease that begins before birth. Hum Mol Genet 11:2709-21.

[11] Pearce DA, Sherman F. 1998. A yeast model for the study of Batten disease. Proc Natl Acad Sci U S A 95:6915-8.

[12] De Voer G, Jansen G, van Ommen GJ, Peters DJ, Taschner PE. 2001. Caenorhabditis elegans homologues of the CLN3 gene, mutated in juvenile neuronal ceroid lipofuscinosis. Eur J Paediatr Neurol 5 Suppl A:115-20.

[13] Culetto E, Sattelle DB. 2000. A role for Caenorhabditis elegans in understanding the function and interactions of human disease genes. Hum Mol Genet 9:869-77.

[14] Jorgensen EM, Mango SE. 2002. The art and design of genetic screens: caenorhabditis elegans. Nat Rev Genet 5:356-69.

[15] White JG, Southgate E, Thomson JN, Brenner S. 1986. The Structure of the Nervous System of the Nematode *Caenorhabditis elegans*. Philos Trans R Soc Lond B Biol Sci 314:1-340.

[16] De Voer G, van der Bent P, Rodrigues AJG, van Ommen GJB, Peters DJM, Taschner PEM. 2005. Deletion of the *Caenorhabditis elegans* homologues of the CLN3 gene, involved in Juvenile Neuronal Ceroid Lipofuscinosis (JNCL), causes a mild progeric phenotype. J Inherit Metab Dis 28:1065-80.

[17] Lakso M, Vartiainen S, Moilanen AM, Sirvio J, Thomas JH, Nass R, Blakely RD, Wong G. 2003. Dopaminergic neuronal loss and motor deficits in Caenorhabditis elegans overexpressing human alpha-synuclein. J Neurochem 86:165-72.

[18] Cao S, Gelwix CC, Caldwell KA, Caldwell GA. 2005. Torsin-mediated protection from cellular stress in the dopaminergic neurons of Caenorhabditis elegans. J Neurosci 25:3801-12.

[19] Faber PW, Alter JR, MacDonald ME, Hart AC. 1999. Polyglutamine-mediated dysfunction and apoptotic death of a Caenorhabditis elegans sensory neuron. Proc Natl Acad Sci U S A 96:179-84.

[20] Link CD. 1995. Expression of human beta-amyloid peptide in transgenic Caenorhabditis elegans. Proc Natl Acad Sci U S A 92:9368-72.

[21] Nollen EA, Garcia SM, van Haaften G, Kim S, Chavez A, Morimoto RI, Plasterk RH. 2004. Genome-wide RNA interference screen identifies previously undescribed regulators of polyglutamine aggregation. Proc Natl Acad Sci U S A 101:6403-8.

[22] Parker JA, Arango M, Abderrahmane S, Lambert E, Tourette C, Catoire H, Neri C. 2005. Resveratrol rescues mutant polyglutamine cytotoxicity in nematode and mammalian neurons. Nat Genet 37:349-50.

[23] Stringham EG, Dixon DK, Jones D, Candido EP. 1992. Temporal and spatial expression patterns of the small heat shock (hsp16) genes in transgenic Caenorhabditis elegans. Mol Biol Cell 3:221-33.

[24] Epstein HF and DC Shakes. 1995. Methods in Cell Biology, *Caenorhabditis elegans:* Modern Biological Analysis of an Organism. San Diego: Academic Press.

[25] Brenner S. 1974. The genetics of Caenorhabditis elegans. Genetics 77:71-94.

[26] Link CD, Cypser JR, Johnson CJ, Johnson TE. 1999. Direct observation of stress response in Caenorhabditis elegans using a reporter transgene. Cell Stress & Chaperones 4:235-242.

[27] Lee EC, Yu D, Martinez de Velasco J, Tessarollo L, Swing DA, Court DL, Jenkins NA, Copeland NG. 2001. A highly efficient *Escherichia coli*-based chromosome engineering system adapted for recombinogenic targeting and subcloning of BAC DNA. Genomics 73:56–65.

[28] Mello C, Fire A. 1995. DNA transformation. In: Epstein HF, Shakes DC editors. Methods in Cell Biology. San Diego: Academic Press p 451-82.

[29] Sambrook, J., E.F. Fritsch and T. Maniatis. 1989 Molecular Cloning a Laboratory Manual. Cold Spring Harbor, New York: Cold Spring Harbor Laboratory Press.

[30] Claros MG, Vincens P. 1996. Computational method to predict mitochondrially imported proteins and their targeting sequences. Eur J Biochem 241:779-86.

[31] Williams BD. 1995. Genetic mapping with polymorphic sequence-tagged sites. Methods Cell Biol 48:81-96.

[32] Simon P. 2003. Q-Gene: processing quantitative real-time RT-PCR data. Bioinformatics 19:1439-40.

[33] Kominami E, Ezaki J, Muno D, Ishido K, Ueno T, Wolfe LS. 1992. Specific storage of Subunit c of mitochondrial ATP synthase in lysosomes of neuronal ceroid lipofuscinosis (Batten's disease). J Biochem 111:278-82.

[34] Cuppen E, van Ham M, Wansink DG, de Leeuw A, Wieringa B, Hendriks W. 2000. The zyxin-related protein TRIP6 interacts with PDZ motifs in the adaptor protein RIL and the protein tyrosine phosphatase PTP-BL. Eur J Cell Biol 79:283-293.

[35] WormBase web site, http://www.wormbase.org, release WS144, date 21/06/2005.

[36] Sebald W, Hoppe J. 1981. On the structure and genetics of the proteolipid subunit of the ATP synthase complex. In: Sanadi RR editor. Current topics in bioenenergetics. London: Academic Vol 12: p 2-65.

[37] Clokey GV, Jacobson LA. 1986. The autofluorescent "lipofuscin granules" in the intestinal cells of Caenorhabditis elegans are secondary lysosomes. Mech Ageing Dev 35:79-94.

[38] Heim R, Prasher DC, Tsien RY. 1994. Wavelength mutations and posttranslational autoxidation of green fluorescent protein. Proc Natl Acad Sci U S A 91:12501-4.

[39] Pendergrass W, Wolf N, Poot M. 2004. Efficacy of MitoTracker Green and CMXrosamine to measure changes in mitochondrial membrane potentials in living cells and tissues. Cytometry A 61:162-169.

[40] Arechaga I, Butler PJ, Walker JE. 2002. Self-assembly of ATP synthase Subunit c rings. FEBS Lett 515:189-93.

[41] Carrozzo R, Wittig I, Santorelli FM, Bertini E, Hofmann S, Brandt U, Schagger H. 2006. Subcomplexes of human ATP synthase mark mitochondrial biosynthesis disorders. Ann Neurol. 59:265-75.

[42] McGeoch JE, Guidotti G. 1997. A 0.1-700 Hz current through a voltage-clamped pore: candidate protein for initiator of neural oscillations. Brain Res 766:188-94.

[43] McGeoch JE, Palmer DN. 1999. Ion pores made of mitochondrial ATP synthase Subunit c in the neuronal plasma membrane and Batten disease. Mol Genet Metab 66:387-92.

[44] Sylvestre J, Vialette S, Corral Debrinski M, Jacq C. 2003. Long mRNAs coding for yeast mitochondrial proteins of prokaryotic origin preferentially localize to the vicinity of mitochondria. Genome Biol **4**:R44.

[45] Corral-Debrinski M, Blugeon C, Jacq C. 2000. In yeast, the 3' untranslated region or the presequence of ATM1 is required for the exclusive localization of its mRNA to the vicinity of mitochondria. Mol Cell Biol **20**:7881-92.

[46] Kloc M, Zearfoss NR, Etkin LD. 2002. Mechanisms of subcellular mRNA localization. Cell 108:533-44.

[47] Shav-Tal Y, Singer RH. 2005. RNA localization. J Cell Sci 118:4077-81.

[48] Ricart J, Izquierdo JM, Di Liegro CM, Cuezva JM. 2002. Assembly of the ribonucleoprotein complex containing the mRNA of the beta-subunit of the mitochondrial H+-ATP synthase requires the participation of two distal cis-acting elements and a complex set of cellular trans-acting proteins. Biochem J. 365:417-28.

[49] Kaltimbacher V, Bonnet C, Lecoeuvre G, Forster V, Sahel JA, Corral-Debrinski M. 2006. mRNA localization to the mitochondrial surface allows the efficient translocation inside the organelle of a nuclear recoded ATP6 protein. RNA. 12:1408-17.

[50] Margeot A, Blugeon C, Sylvestre J, Vialette S, Jacq C, Corral-Debrinski M. 2002. In Saccharomyces cerevisiae, ATP2 mRNA sorting to the vicinity of mitochondria is essential for respiratory function. EMBO J. 21:6893-904.

[51] Neupert W. 1997. Protein import into mitochondria. Annu Rev Biochem 66:863-917.

[52] Mokranjac D, Neupert W. 2005. Protein import into mitochondria. Biochem Soc Trans. 33:1019-23.

[53] Maeda I, Kohara Y, Yamamoto M, Sugimoto A.2001. Large-scale analysis of gene function in Caenorhabditis elegans by high-throughput RNAi. Curr Biol 11:171-6.

[54] Simmer F, Moorman C, van der Linden AM, Kuijk E, van den Berghe PV, Kamath RS, Fraser AG, Ahringer J, Plasterk RH. 2003. Genome-wide RNAi of C. elegans using the hypersensitive rrf-3 strain reveals novel gene functions. PLoS Biol 1(1):E12.

[55] Hajdu-Cronin YM, Chen WJ, Sternberg PW. 2004. The L-type cyclin CYL-1 and the heat-shock-factor HSF-1 are required for heat-shock-induced protein expression in Caenorhabditis elegans. Genetics 168:1937-49.

[56] Bargmann CI, Avery L. 1995. Laser killing of cells in Caenorhabditis elegans. In: Epstein HF, Shakes DC editors. Methods in Cell Biology. San Diego: Academic Press p 225-50.

[57] Shaham S, Horvitz HR. 1996. Developing Caenorhabditis elegans neurons may contain both cell-death protective and killer activities. Genes Dev 10:578-91.

[58] Weinshenker D, Wei A, Salkoff L, Thomas JH. 1999. Block of an ether-a-go-go-like K(+) channel by imipramine rescues egl-2 excitation defects in Caenorhabditis elegans. J Neurosci 19:9831-40.

[59] Harbinder S, Tavernarakis N, Herndon LA, Kinnell M, Xu SQ, Fire A, Driscoll M. 1997. Genetically targeted cell disruption in Caenorhabditis elegans. Proc Natl Acad Sci U S A 94:13128-33.

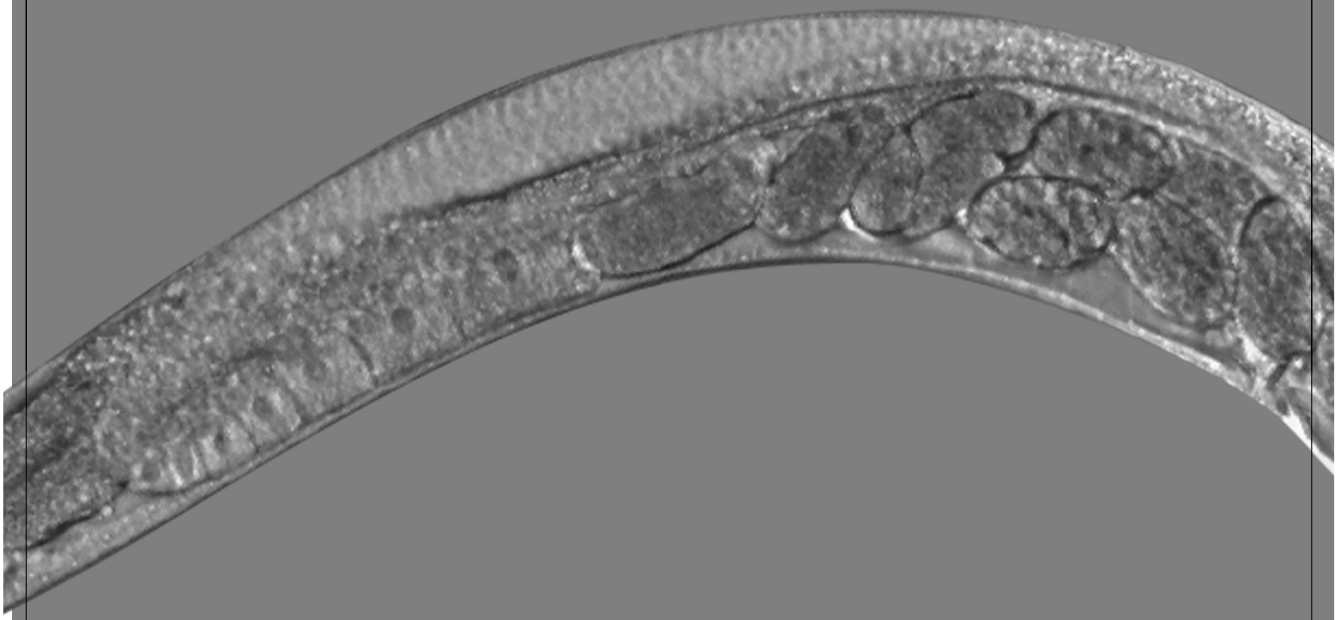

CHAPTER 6
Discussion

Part of the following section is derived
from De Voer and Taschner (in press), and Phillips *et al.* (2006)

Discussion

In this thesis I describe the analysis of the *cln-3* genes of the nematode *Caenorhabditis elegans*. Humans carrying mutations in both alleles of the *CLN3* gene suffer from a severe childhood neurodegenerative disorder, the lysosomal storage disease juvenile neuronal ceroid lipofuscinosis (JNCL). The etiology of JNCL is unknown, and no cure exists for this disease. My investigation of the function of the CLN3 homologues of this relatively simple model organism was expected to lead to additional insight into the processes in which the CLN3 protein is involved, since other studies of worm homologues of proteins involved in neurodegenerative disorders have proven useful (Chapter 2).

The *cln*-3 genes

C. elegans is the only model organism with three CLN3 homologues, designated *cln-3.1*, *cln-3.2*, and *cln-3.3*. The presence of three CLN3 homologues in *Caenorhabditis briggsae*, a nematode species closely related to *C. elegans* suggests that the three genes have evolved before the separation of the two species, some 100 million years ago (Stein *et al.*, 2003). Assuming that the genes result from ancient duplications of a common ancestor, their genomic sequences have diverged beyond recognition, but the encoded protein sequences show considerable homology (Chapter 3). The degree of conservation across their complete protein sequences suggests that none of the genes is a pseudogene, which is expressed but has lost most of its original function, as was shown for the *elt-4* gene (Fukushige *et al.*, 2003). The biological reason for the existence of multiple *cln-3* genes in the worm is unknown.

The *cln*-3 worm models for juvenile NCL

JNCL worm models with single *cln-3.1*, *cln-3.2*, or *cln-3.3* deletions were generated from the original mutants isolated from the deletion mutant libraries by out-crossing six times into wild type background to remove additional mutations (Chapter 4). Since the *cln-3* single mutant models had a wild type appearance, which might be caused by redundancy, they were crossed to generate three double and one triple *cln-3* mutant models. The *cln-3* triple mutant animals were viable and superficially displayed wild type behavior and normal morphology, indicating that the *cln-3* genes are not essential for life under standard laboratory conditions. Comparison of the life span of the different models to wild type worms suggested the *cln-3.1* mutant has a shorter life span than wild type worms, while *cln-3.2* and *cln-3.3* single mutants have a normal life span. This effect becomes more prominent in the *cln-3* triple mutant when *cln-3.2* and *cln-3.3* are also deleted. The *cln-3.2* single mutant has a decreased brood size compared to wild type. The brood size of the *cln-3* triple mutant is decreased more prominently

than that of the *cln-3.2* single mutant, even though the other single mutants do not have a significantly decreased brood size. To detect functional aberrations, the *cln-3* triple mutants have been investigated extensively, using assays for correct neuronal function and response to a diversity of external cues, such as temperature, touch, presence of other worms, mating behavior (Chapter 4, unpublished results). The integrity of the *cln-3* triple mutant nervous system was investigated using GFP which was expressed from the *unc-119* promoter in neuronal cells and was similar to wild type in all of the tests. Electron micrographs of *cln-3* triple mutant neurons did not reveal altered morphology or the presence of lysosomal storage material. The *cln-3* triple mutants could not be distinguished from wild type worms after staining with organelle or compound specific fluorescent dyes, Lysotracker Red, Acridine Orange, and Nile Red to assess whether lysosomes, acidic organelles and lipid content, respectively, were altered. We had hoped for robust mutant phenotypes useful for genetic screens to elucidate the genetic pathways the *cln-3* genes are involved in. The absence of sufficiently robust phenotypes prompted us to investigate the expression of the *cln-3* genes in order to be able to focus our phenotypical analysis of the *cln-3* mutants.

Expression patterns and profiles

The expression patterns of the *cln-3* genes have been analyzed by generating transgenic worms carrying one of the *cln-3* promoters driving the expression of the green fluorescent protein (GFP) gene. In fact the reporter constructs were generated such that the third exon of each *cln*-3 gene was fused, in frame, to the GFP gene. The green fluorescent signal in the transgenic worms at different points during their life cycle and at different locations indicated that these genes differ in their temporal and spatial expression patterns. Additional aspects of *cln-3* protein function could be inferred from co-regulated genes that were identified by combining datasets of 553 microarray experiments, generating a gene-expression map with "mountains" of co-regulated genes (Kim *et al.*, 2001). The genes that constitute a mountain have resembling expression profiles, which may indicate similar protein function.

Expression of the *cln*-3.1 gene

Expression of *cln-3.1* was restricted to cells of the intestine and GFP fluorescence was first observed in transgenic "comma-stage" embryos, and this expression lasted throughout larval and adult life stages in both hermaphrodite and male transgenic worms (Chapter 4). The *cln-3.1*::GFP fluorescence suggests *cln-3.1* expression in intestinal cells designated int2 to int8, while the most anterior and posterior segments of the intestine remained negative. The development of the intestinal tract and the expression of many intestinal proteins requires the regulation by GATA transcription factors (Maduro and Rothman, 2002, Pauli *et al*, 2006). Multiple GATA consensus sequence binding sites could be identified in the *cln-3.1* promoter region, indicating that the expression of *cln-3.1* could be regulated by GATA transcription factors (de Voer unpublished results). The *cln-3.1* gene is present in mountain 24 on the gene-

expression map. This suggests the cln-3.1 protein has a role in amino acid metabolism, lipid metabolism, or fatty acid oxidation, since expression profiles of genes encoding proteins functional in those processes are grouped together in mountain 24.

Expression of the *cln*-3.2 gene

The *cln-3.2* gene is expressed in cells of the hypoderm only in adult worms of both sexes. A different expression pattern of *cln-3.2* was described in the Wormbase database (Wormbase website). This expression pattern was obtained with a GFP reporter construct regulated by the putative promoter that was assumed to be located immediately upstream of the coding sequence. Since *cln-3.2* is located in an operon the sequence regulating *cln-3.2* expression is not located directly upstream the coding sequence, and this alternative expression pattern may not reflect *cln-3.2* expression (Blumenthal and Gleason, 2003). In the gene-expression map *cln-3.2* is grouped in mountain 2, which is enriched in proteins functional in the germline or oocyte, suggesting CLN-3.2 has a function in those tissues. The decreased brood size of *cln-3.2* mutants is in accordance with this position in the gene-expression map (Chapter 4).

Expression of the *cln*-3.3 gene

Expression of *cln-3.3* was detected in the intestinal muscle cells and hypoderm of adult hermaphrodite and male worms and also in posterior diagonal muscle cells of males. The *cln-3.3* gene is grouped in mountain 19, suggesting CLN-3.3 has a function in amino acid metabolism, lipid metabolism, or processes in which cytochrome P450 is involved. Except for co-expression of the *cln-3.2* and *cln-3.3* genes in hypodermal cells of adult worms, each of the *cln-3* genes is not expressed at detectable levels in all cells. It should be noted that this does not indicate that the *cln-3* genes are not expressed, but merely that expression levels in other cell types (neurons) are likely to be below the detection threshold of GFP by fluorescence microscopy. This could be circumvented by using another technique for expression analysis, such as RNA *in situ* hybridization. However, the nematode has a cuticle as an outer layer, which is difficult to permeabilize, thus worm morphology may not be optimally retained when the worm is prepared so that the RNA probe can reach all cells. Moreover, the GFP reporter constructs allow the fluorescence to be observed in live transgenic animals throughout their life cycle, without the need to synchronize worm cultures or fixing them.

Are the *cln*-3.2 and *cln*-3.3 genes part of operons?

Apart from the number of CLN3 homologues, the nematode also differs from other model organisms in the organization and regulation of some of its genes. *C. elegans* is one of the few multi-cellular eukaryotic organisms in which genes can be organized in an operon, a gene structure used by many bacteria for coordinated gene expression (Blumenthal and Gleason, 2003). This means that a single promoter is used to generate one transcript for a group of consecutive genes. In worms this polycistronic transcript is subsequently processed into separate transcripts for each gene by *trans-*

splicing to specific spliced leader sequences, for instance SL2. The question, whether in *C. elegans* the gene products of operons are functionally related or just linked to ensure coordinated temporal expression, cannot be answered unequivocally in all cases and remains a topic of investigation and discussion. The two *cln-3.2* and *cln-3.3* genes have closely located upstream genes and may therefore be organized in operons.
In accordance with this, *cln-3.2* was found to be trans-spliced to a SL2 spliced leader, but *cln-3.3* is associated to an SL1 spliced leader. However, we can not completely exclude that *cln-3.3* and its upstream gene, *ZC190.2*, are members of an operon, as the putative *cln-3.3* promoter-GFP fusion construct failed to cause GFP fluorescence in transgenic nematodes (De Voer *et al.*, unpublished results), whereas transgenic worms containing a larger upstream sequence including the *ZC190.2* promoter and gene in front of the *cln-3.3* promoter-GFP fusion did show GFP fluorescence (Chapter 4). Since both reporter constructs contain an in-frame fusion of GFP to the first three exons of *cln-3.3* and thus are partial translational reporter constructs (Boulin *et al.*, 2006), the GFP fluorescence from the longer one can only be caused by the presence of additional *cis*-acting elements. Currently, it remains unclear whether the *ZC190.2* promoter drives also the *cln-3.3* expression or whether *cis*-acting elements overlapping the *ZC190.2* coding region are responsible for the observed expression pattern.
The *cln-3.2* gene is the fourth in an operon also containing *erm-1*, *dnj-4*, and *dhs-1*. The first gene, *erm-1*, encodes a protein with homology to ezrin, radixin, and moesin proteins of the ERM family of cytoskeletal linkers, and is involved in organism development and positioning of cell-cell contacts (Van Furden *et al.*, 2004). ERM proteins have diverse roles in cell architecture, cell signaling and membrane trafficking (Louvet-Vallee, 2000), and have recently been shown to be important for actin assembly by phagosomes, which may facilitate their fusion with lysosomes (Defacque *et al.*, 2000). This gene is expressed from the two-cell stage onward throughout the entire life of the worm in epithelial cells lining the luminal surfaces of intestine, excretory canal, and gonad, whereas the *cln-3.2* gene was expressed in the hypoderm of adult worms (Chapter 4). This difference in expression between genes in the same operon could be caused by common errors in operon transcription, of which the probability decreases with increasing distance between the operon genes, or their mRNAs may be subject to differential mRNA destabilization (Lercher *et al.*, 2003). Expression patterns of the other operonic genes, *dnj-4*, *dhs-1*, have not been reported, and RNAi knockdown of these genes did not result in obvious phenotypes (Wormbase website). Therefore, the function of these genes can only be derived from protein sequence homology. The DNJ-4 protein has both chaperone and heat shock protein domains, which could indicate a role in protein folding. The DHS-1 protein has dehydrogenase and reductase domains and may have a function in metabolism of short chain alcohols. Although a role of ERM proteins in lysosome-phagosome fusion potentially connects it functionally with CLN-3.2, it is unclear whether a functional relationship exists between *cln-3.2* and the other genes in this operon.

No autofluorescent storage material in *C. elegans cln-3* triple mutants

In *C. elegans cln-3* triple mutant worms, storage of autofluorescent lipopigments, one of the hallmarks of NCL, could not be detected, probably due to the short life span of the worms. Therefore, an attempt was made to increase the amount of lipopigments in the *cln-3* triple mutant worm model by overexpressing the main component of the storage material found in Batten disease patients, the hydrophobic Subunit c of the mitochondrial ATP synthase (Haltia *et al.*, 1973, Hall *et al.*, 1991, Palmer *et al.*, 1995, Palmer *et al.*, 1992). The only homolog to the human *ATP5G1* gene encoding Subunit c in C. elegans is *atp-9*. Overexpression of this worm homolog was deleterious to wild type animals, causing overall structural impairment, increased transparency, and near paralysis (Chapter 5). On electron micrographs of worms overexpressing Subunit c, damaged mitochondria could be observed, which is in accordance to the loss of mitochondrial staining with Mitotracker Red seen in these animals. A mild Subunit c overexpression in a *cln-3* triple mutant background allowed the worms to survive, but did not result in an obviously different phenotype compared to mild Subunit c overexpression in a wild type background. Perhaps repetitive short overexpression pulses could induce increased turn-over rates of mitochondria whereby the amount of Subunit c in lysosomes could increase. Alternatively, targeting of Subunit c to the lysosomes could lead to increased Subunit c in the lysosomes.

In conclusion, with this study we have explored the potential of using the nematode *C. elegans* as a model organism to investigate JNCL. Knock-outs for each of the *cln-3* genes were generated and the expression patterns of the genes were studied. Although the expected neuronal phenotype was not found and mutant neurons appeared to be normal on electron micrographs, this does not mean that the model presented in this thesis is not useful. Additional analysis into gene function could be performed by doing microarray analysis. Investigation into the effects that overexpression of the *cln-3* genes would have was started and preliminary experiments have indicated an effect on mitochondrial labeling. Due to lack of time, this interesting finding was not pursued. These experiments, among others, may lead to a better understanding of the function of the *cln-3* proteins in *C. elegans* and may help to improve our understanding of Cln3 protein functions in other organisms. Ultimately, this may result in the development of treatments of JNCL patients.

References

Blumenthal T, Gleason KS. 2003. Caenorhabditis elegans operons: form and function. Nat Rev Genet. 4:112-20.

Boulin T, Etchberger JF, Hobert O. 2006. Reporter gene fusions, WormBook, ed. The C. elegans Research Community, WormBook, doi/10.1895/wormbook.1.106.1, http://www.wormbook.org.

Defacque H, Egeberg M, Habermann A, Diakonova M, Roy C, Mangeat P, Voelter W, Marriott G, Pfannstiel J, Faulstich H, Griffiths G. 2000. Involvement of ezrin/moesin in de novo actin assembly on phagosomal membranes. EMBO J. 19:199-212.

Fukushige T, Goszczynski B, Tian H, McGhee JD. 2003. The evolutionary duplication and probable demise of an endodermal GATA factor in Caenorhabditis elegans. Genetics. 165:575-88.

Van Furden D, Johnson K, Segbert C, Bossinger O. 2004. The C. elegans ezrin-radixin-moesin protein ERM-1 is necessary for apical junction remodelling and tubulogenesis in the intestine. Dev Biol. 272:262-76.

Hall NA, Lake BD, Dewji NN, Patrick AD. 1991. Lysosomal storage of Subunit c of mitochondrial ATP synthase in Batten's disease (ceroid-lipofuscinosis). Biochem J. 275:269-72.

Haltia M, Rapola J, Santavuori P, Keranen A. 1973. Infantile type of so-called neuronal ceroid-lipofuscinosis. 2. Morphological and biochemical studies. J Neurol Sci. 18:269-85.

Kim SK, Lund J, Kiraly M, Duke K, Jiang M, Stuart JM, Eizinger A, Wylie BN, Davidson GS. 2001. A gene expression map for Caenorhabditis elegans. Science. 293:2087-92.

Lercher MJ, Blumenthal T, Hurst LD. 2003. Coexpression of neighboring genes in Caenorhabditis elegans is mostly due to operons and duplicate genes. Genome Res. 13:238-43.

Louvet-Vallee S. 2000. ERM proteins: from cellular architecture to cell signaling. Biol Cell. 92:305-16.

Maduro MF, Rothman JH. 2002. Making worm guts: the gene regulatory network of the Caenorhabditis elegans endoderm. Dev Biol. 246:68-85.

Palmer DN, Fearnley IM, Walker JE, Hall NA, Lake BD, Wolfe LS, Haltia M, Martinus RD, Jolly RD. 1992. Mitochondrial ATP synthase Subunit c storage in the ceroid-lipofuscinoses (Batten disease). Am J Med Genet. 42:561-7.

Palmer DN, Bayliss SL, Westlake VJ. 1995. Batten disease and the ATP synthase Subunit c turnover pathway: raising antibodies to Subunit c. Am J Med Genet. 57:260-5.

Pauli F, Liu Y, Kim YA, Chen PJ, Kim SK.2006. Chromosomal clustering and GATA transcriptional regulation of intestine-expressed genes in C. elegans. Development. 133:287-95.

Phillips SN, Muzaffar N, Codlin S, Korey CA, Taschner PE, de Voer G, Mole SE, Pearce DA. 2006. Characterizing pathogenic processes in Batten disease: use of small eukaryotic model systems. Biochim Biophys Acta. 1762:906-19.

Stein LD, Bao Z, Blasiar D, Blumenthal T, Brent MR, Chen N, Chinwalla A, Clarke L, Clee C, Coghlan A, Coulson A, D'Eustachio P, Fitch DH, Fulton LA, Fulton RE, Griffiths-Jones S, Harris TW, Hillier LW, Kamath R, Kuwabara PE, Mardis ER, Marra MA, Miner TL, Minx P, Mullikin JC, Plumb RW, Rogers J, Schein JE, Sohrmann M, Spieth J, Stajich JE, Wei C, Willey D, Wilson RK, Durbin R, Waterston RH. 2003. The genome sequence of Caenorhabditis briggsae: a platform for comparative genomics. PLoS Biol. 1:E45.

De Voer G, Taschner PEM. Simple animal models, the nematode worm *Caenorhabditis elegans*, In: The neuronal ceroid lipofuscinoses, ed. Mole S, Goebel H, Williams R. IOS press Amsterdam, in press.

WormBase web site, http://www.wormbase.org, release WS172, date 060407.

CHAPTER 7

Summary

Summary

This thesis describes our exploration of the potential to use the nematode *C. elegans* as a model organism for juvenile neuronal ceroid lipofuscinosis (JNCL), the most common neurodegenerative genetically inherited disease of childhood. No treatment is available for this devastating lysosomal storage disorder, which is caused by mutations in the *CLN3* gene. In lysosomes of patients material with the characteristics of ceroid and lipofuscin accumulates and Subunit c of the mitochondrial ATP synthase (Subunit c) is the major component of this material. How mutations in *CLN3* lead to the neuronal symptoms, such as loss of vision, epileptic seizures, and dementia is unknown. Homologues of the CLN3 protein are being investigated in model organisms, such as baker's yeast *Saccharomyces cerevisiae* and mice, to elucidate the mechanisms by which these genetic lesions cause the symptoms. The research into the CLN3 homologues in these model organisms has proven useful as they have provided insight into the protein function at the molecular and organismal levels, respectively, but this has not resulted in a complete understanding of JNCL pathology. Therefore, the study of CLN3 homologues in relatively simple multicellular model organisms that have a nervous system would most likely complement research performed in other models. A model organism that has proven to be useful for research into proteins involved in neurodegenerative diseases is the nematode *Caenorhabditis elegans* and the data obtained with this model organism can be extrapolated to more complex organisms, such as humans (Chapter 2).

*C. elegans nema*todes have three proteins, designated CLN-3.1, CLN-3.2, and CLN-3.3, that are homologous to the human CLN3 protein (Chapter 3). For each of the genes that encode these proteins nematode knock-outs were generated (Chapter 3, 4). The *cln-3.1* deletion mutant has a slightly decreased life span compared to wildtype animals, and the *cln-3.2* deletion mutant has a little decrease in brood size (Chapter 4). Since no neurological or other robust phenotypes were present in the *cln-3* mutants, which could be due to redundancy, the mutations were combined into a triple mutant strain. This *cln-3* triple mutant is viable, indicating that the *cln-3* genes are not essential for nematode life under standard laboratory conditions. *Cln-3* expression analysis was performed using GFP reporter constructs to identify specific nematode life stages and cells or tissues on which the phenotypic analysis of the *cln-3* mutants could be focused (Chapter 4). The *cln-3.1* promoter regulated GFP expression in the intestine, *cln-3.2* was expressed in the hypoderm, and the *cln-3.3* reporter indicated expression in the intestinal muscle, male specific posterior muscle cells and hypoderm.

The *cln-3* triple mutant was thoroughly analyzed, but no neurological phenotype could be found and no stored material could be identified on electron micrographs of triple mutant nematodes. An explanation for the absence of accumulated materials could be the short life span of *C. elegans*. Therefore, transgenic nematodes were generated in

which Subunit c of the mitochondrial ATP synthase, the main component of the stored material in patients, was inducibly overexpressed and these transgenes were crossed into the *cln-3* triple mutant background (Chapter 5). Overexpression of Subunit c is deleterious to wildtype nematodes and appears to affect mitochondrial ultra-structure. The effect of Subunit c overexpression was not different in *cln-3* mutant nematodes. Perhaps, the overexpressed protein could be targeted to lysosomes or overexpression induction could be optimized to be able to observe differences between wildtype and *cln-3* triple mutant background.
Although a neuronal phenotype was not found, the nematode model presented here can be used for additional experiments, which may increase our understanding of the function of the *cln-3* genes.

Nederlandse samenvatting

In dit proefschrift wordt het onderzoek beschreven waarin wij de mogelijkheden verkend hebben om de nematode *C. elegans* te gebruiken als modelorganisme voor de ziekte juveniele neuronale ceroid lipofuscinose (JNCL). JNCL is de meest voorkomende neurodegeneratieve genetisch overerfbare kinderziekte. Voor deze verwoestende lysosomale stapelingsziekte, die veroorzaakt wordt door mutaties in het *CLN3* gen, is geen behandeling beschikbaar. In de lysosomen van patienten wordt materiaal opgehoopt dat zowel de eigenschappen van ceroid als van lipofuscine heeft en waarvan Subunit c van het mitochondriale ATP synthase het grootste deel vormt. Hoe mutaties in *CLN3* leiden tot neuronale symptomen als blindheid, epileptische aanvallen en dementie is onbekend. Om het pathofysiologische mechanisme, dat veroorzaakt wordt door deze mutaties en uiteindelijk tot het ziektebeeld leidt, te ontrafelen, werden homologen van het CLN3 eiwit door andere wetenschappers onderzocht in modelorganismen als *Saccharomyces cerevisiae* (bakkersgist) en muizen. Het onderzoek naar de CLN3 homologen in deze modelorganismen is waardevol gebleken omdat hierdoor het inzicht vergroot is in de functie van het eiwit op moleculair en organismaal niveau, respectievelijk. Maar dit heeft nog niet geleidt tot een volledig begrip van de pathologie van JNCL. Het onderzoek dat uitgevoerd is in deze modelorganismen zou kunnen worden aangevuld door de analyse van CLN3 homologen in een relatief eenvoudig multicellulair modelorganisme waarin een zenuwstelsel aanwezig is. De nematode *Caenorhabditis elegans* is een modelorganisme waarvan bewezen is dat het bruikbaar is voor het bestuderen van eiwitten die betrokken zijn bij neurodegeneratieve ziekten en waarvan de resultaten die ermee geboekt worden geëxtrapoleerd kunnen worden naar complexere systemen zoals mensen (hoofdstuk 2). In *C. elegans* zijn drie aan het humane CLN3 eiwit homologe eiwitten aanwezig, namelijk CLN-3.1, CLN-3.2, en CLN-3.3 (hoofdstuk 3). Van elk van de genen die coderen voor deze eiwitten zijn nematode knock-outs gegenereerd (hoofdstuk 3, 4). De *cln-3.1* deletie mutant heeft een licht afgenomen levensduur in vergelijking met wildtype *C. elegans* en de *cln-3.2* deletie-mutant heeft een kleine afname in de hoeveelheid nakomelingen (hoofdstuk 4). Aangezien er geen neurologische of andere robuuste fenotypen waargenomen werden in deze mutanten, zijn de deleties gecombineerd in één drievoudige mutanten stam. Deze *cln-3* triple mutant is levensvatbaar, hetgeen aangeeft dat de *cln-3* genen niet essentieel zijn voor het leven van de nematode onder standaard laboratorium condities. Om de specifieke levensstadia en cellen of weefsels te identificeren waar de fenotypische analyse op gericht zou kunnen worden, werd *Cln-3* expressie analyse uitgevoerd met behulp van GFP-reporterconstructen (hoofdstuk 4). De *cln-3.1* promoter reguleert expressie in de darm, *cln-3.2* komt tot expressie in de hypodermis en met de *cln-3.3* reporter werd expressie waargenomen in de darm spier, posteriore spiercellen die specifiek zijn voor de mannelijke *C. elegans* en hypodermis.

De *cln-3* triple mutant werd uitvoerig geanalyseerd maar er werd helaas geen neurologisch fenotype vastgesteld. Tevens werd geen gestapeld materiaal waargenomen met behulp van electronen microscopische opnamen van deze triple mutant beesten. Een verklaring voor de afwezigheid hiervan zou kunnen liggen in de korte levensduur van deze nematode. Daarom werden transgene *C. elegans* gegenereerd waarin Subunit c van het mitochondriale ATP synthase, de hoofdcomponent van het opgeslagen materiaal in patiënten, induceerbaar tot overexpressie zou kunnen worden gebracht. Een grotere hoeveelheid Subunit c zou wellicht tot een stapeling of een ander interessant fenotype kunnen leiden in de genetische achtergrond van de *cln-3* triple mutant (hoofdstuk 5). Overexpressie van Subunit c is even schadelijk voor zowel de wildtype als voor de *cln-3* triple mutant nematoden. Bij beide *C. elegans* stammen lijkt deze overexpressie te leiden tot aantasting van de mitochondriale ultra-structuur. Wellicht zou het eiwit dat tot overexpressie wordt gebracht naar lysosomen getarget kunnen worden of de inductie van de overexpressie zou kunnen worden geöptimaliseerd teneinde verschillen tussen wildtype en *cln-3* triple mutant achtergrond te kunnen waarnemen.
Alhoewel een neuronaal fenotype niet gevonden is, kan het nematode model dat hier gepresenteerd wordt gebruikt worden voor andere experimenten, waardoor de kennis van de functie van de *cln-3* genen zou kunnen worden vergoot.

Curriculum Vitae

Gert de Voer werd op 9 augustus 1973 geboren in Almelo. In 1992 behaalde hij het VWO diploma aan het Nienoordcollege te Leek, waarna hij in datzelfde jaar met de studie Biologie aan de Universiteit Leiden begon. Tijdens zijn studie liep Gert twee onderzoeksstages. De hoofdstage liep hij bij Moleculaire Microbiologie aan het Instituut Biologie Leiden, waarbij hij werd begeleid door dr. Guido Bloemberg. Een nevenstage liep hij bij het Laboratorio de Microbiologia aan de Universidade de Coimbra in Portugal. Tijdens deze stage werd hij begeleid door dr. Joey Marugg. In 1999 behaalde Gert het doctoraal in de Biologie. Op 3 januari 2000 begon hij als aio aan het werk dat in dit proefschrift beschreven is, onder begeleiding van dr. Peter Taschner, dr. Dorien Peters en prof. dr. Gert-Jan van Ommen, op de afdeling Humane Genetica van het Leids Universitair Medisch Centrum. Van 1 oktober 2005 tot en met 30 september 2007 is Gert werkzaam geweest als post-doc op het project "Analysis of the role of dSec16 in the organization of tER sites in *Drosophila* S2 cells" in de groep van dr. Catherine Rabouille van het Cell Microscopy Center, dat een onderdeel is van het Department of Cellbiology van het Universitair Medisch Centrum Utrecht. Vanaf 1 oktober 2007 is hij als Clinical Research Associate werkzaam bij Genzyme.

List of Publications

De Voer G, Ivan V, Spoorendonk K, Kondylis V, Rabouille C. *Drosophila* Sec16 controls the biogenesis of the tER sites upstream of the COPII machinery. Manuscript in preparation.

De Voer G, Peters DJ, Taschner PEM. Caenorhabditis elegans as a model for lysosomal storage disorders. Manuscript submitted.

De Voer G, de Keizer ROB, van der Bent P, van Ommen GJB, Peters DJM, Taschner PEM. Overexpression of Subunit c of the mitochondrial ATP synthase in *Caenorhabditis elegans* causes lethality by mitochondrial disruption. Manuscript submitted.

Phillips SN, Muzaffar N, Codlin S, Korey CA, Taschner PE, **de Voer G**, Mole SE, Pearce DA. 2006. Characterizing pathogenic processes in Batten disease: use of small eukaryotic model systems. Biochim Biophys Acta. 1762:906-19.

De Voer G, Rodrigues AJ, van der Bent P, van Ommen GJB, Peters DJM, Taschner PEM. 2005. Deletion of the *Caenorhabditis elegans* homologues of the CLN3 gene, involved in human Juvenile Neuronal Ceroid Lipofuscinosis (JNCL) causes a mild progeric phenotype. J Inherit Metab Dis. 28:1065-80.

De Voer G, Jansen G, van Ommen GJ, Peters DJ, Taschner PE. 2001. *Caenorhabditis elegans* homologues of the CLN3 gene, mutated in juvenile neuronal ceroid lipofuscinosis. *Eur J Paediatr Neurol*. 5 Suppl A:115-20.

Chin-A-Woeng TF, van den Broek D, **de Voer G**, van der Drift KM, Tuinman S, Thomas-Oates JE, Lugtenberg BJ, Bloemberg GV. 2001. Phenazine-1-carboxamide production in the biocontrol strain *Pseudomonas chlororaphis* PCL1391 is regulated by multiple factors secreted into the growth medium. *Mol Plant Microbe Interact*. 14:969-79.